

AD-A066 482

FOREIGN TECHNOLOGY DIV WRIGHT-PATTERSON AFB OHIO
STRENGTH OF REFRACTORY METALS. PART I, (U)
OCT 78 G S PISARENKO, V A BORISENKO

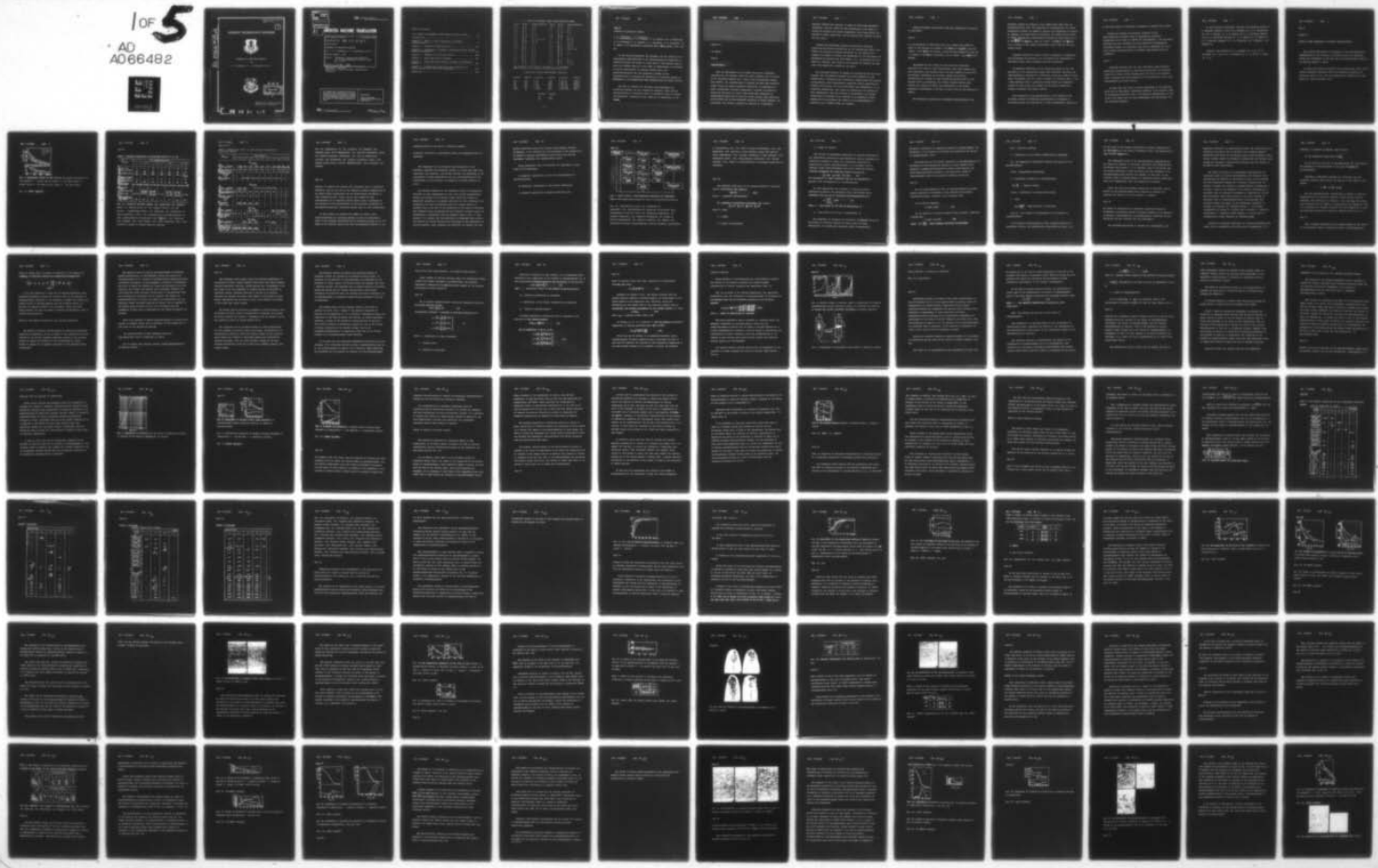
F/G 11/6

UNCLASSIFIED

FTD-ID(RS)T-1330-78-PT-1

NL

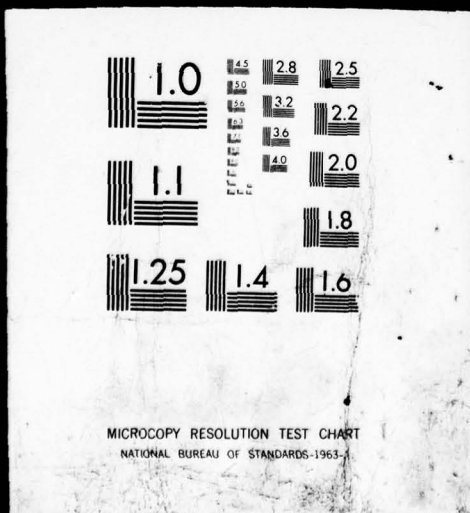
1 OF 5
AD
A066482



IFIED



AD
AO66482



AD-1066482

FTD-ID(RS)T-1330-78
PART 1 of 2

(1)

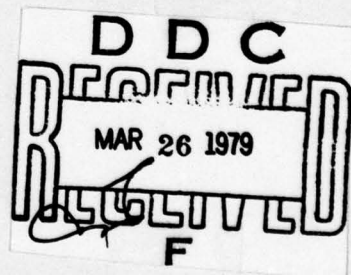
FOREIGN TECHNOLOGY DIVISION



STRENGTH OF REFRACTORY METALS

By

G. S. Pisarenko, V. A. Borisenko, et al.



Approved for public release;
distribution unlimited.

78 12 22 417

ACCESSION BY	
DSR	DATA SHEET <input checked="" type="checkbox"/>
SAC	DATA SHEET <input type="checkbox"/>
CHARACTERISTICS	<input type="checkbox"/>
IDENTIFICATION	
BY	
DISTRIBUTION/AVAILABILITY CODES	
DATA	AVAIL. AND W SPECIAL
A	

FTD- ID(RS)T-1330-78

UNEDITED MACHINE TRANSLATION

FTD-ID(RS)T-1330-78

4 October 1978

MICROFICHE NR: *FTD - 78-C-001361L*

CSC71299923

STRENGTH OF REFRACTORY METALS

By: G. S. Pisarenko, V. A. Borisenko, et al.

English pages: 745

Source: Prochnost' Tugoplavkikh Metallov,
Izd-vo "Metallurgiya," Moscow, 1970,
pp. 1-365.

Country of origin: USSR
This document is a machine translation.

Requester: FTD/TQTA

Approved for public release; distribution
unlimited.

THIS TRANSLATION IS A RENDITION OF THE ORIGINAL FOREIGN TEXT WITHOUT ANY ANALYTICAL OR EDITORIAL COMMENT. STATEMENTS OR THEORIES ADVOCATED OR IMPLIED ARE THOSE OF THE SOURCE AND DO NOT NECESSARILY REFLECT THE POSITION OR OPINION OF THE FOREIGN TECHNOLOGY DIVISION.

PREPARED BY:

TRANSLATION DIVISION
FOREIGN TECHNOLOGY DIVISION
WP-AFB, OHIO.

FTD- ID(RS)T-1330-78

Date 4 Oct. 1978

FIRST LINE OF TEXT

Table of Contents

U. S. Board on Geographic names Transliteration System.....	ii
Introduction.....	2
Chapter 1. Effect of Test Conditions on Strength Characteristics.....	8
Chapter 2. Elasticity Characteristics.....	143
Chapter 3. Dissipation of Energy in Refractory Metals During Repeated Deformation.....	233
Chapter 4. Hardness of Refractory Metals.....	293
Chapter 5. Short-Term Static Strength.....	387
Chapter 6. Creep and Stress-Rupture Strength of Refractory Metals.....	509
Chapter 7. Strength and Plasticity Under Conditions of Cyclic Variation in Stress and Temperature.....	600
References.....	722

U. S. BOARD ON GEOGRAPHIC NAMES TRANSLITERATION SYSTEM

Block	Italic	Transliteration	Block	Italic	Transliteration
А а	А а	A, a	Р р	Р р	R, r
Б б	Б б	B, b	С с	С с	S, s
В в	В в	V, v	Т т	Т т	T, t
Г г	Г г	G, g	У у	У у	U, u
Д д	Д д	D, d	Ф ф	Ф ф	F, f
Е е	Е е	Ye, ye; E, e*	Х х	Х х	Kh, kh
Ж ж	Ж ж	Zh, zh	Ц ц	Ц ц	Ts, ts
З з	З з	Z, z	Ч ч	Ч ч	Ch, ch
И и	И и	I, i	Ш ш	Ш ш	Sh, sh
Й й	Й й	Y, y	Щ щ	Щ щ	Shch, shch
К к	К к	K, k	Ь ъ	Ь ъ	"
Л л	Л л	L, l	Ы ы	Ы ы	Y, y
М м	М м	M, m	Ђ ъ	Ђ ъ	'
Н н	Н н	N, n	Э э	Э э	E, e
О о	О о	O, o	Ю ю	Ю ю	Yu, yu
П п	П п	P, p	Я я	Я я	Ya, ya

*ye initially, after vowels, and after ъ, ъ; е elsewhere.
When written as ё in Russian, transliterate as yё or ё.

RUSSIAN AND ENGLISH TRIGONOMETRIC FUNCTIONS

Russian	English	Russian	English	Russian	English
sin	sin	sh	sinh	arc sh	\sinh^{-1}
cos	cos	ch	cosh	arc ch	\cosh^{-1}
tg	tan	th	tanh	arc th	\tanh^{-1}
ctg	cot	cth	coth	arc cth	\coth^{-1}
sec	sec	sch	sech	arc sch	sech^{-1}
cosec	csc	csch	csch	arc csch	csch^{-1}

Russian	English
rot	curl
lg	log

Page 2.**STRENGTH OF REFRACTORY METALS.**

G. S. Pisarenko, V. A. Borisenko,
S. S. Gorodetskiy, B. A. Gryaznov, V. F. Dubinin, Yu. A. Kashtalyan,
V. V. Krivenyuk, V. N. Suderko, V. A. Strizhalo, V. T. Troshenko, Ye.
I. Uskov, V. K. Kharchenko. Publishing house "Metallurgy", 1970, 368
pp.

In the book are presented the procedure and the results of the experimental investigations of the physicomechanical properties of refractory metals and alloys on their basis in the various forms of power and thermal loading in the range of temperatures of 20-3000°C. Are given descriptions of original testing units. Are established the laws governing a change of the characteristics of strength and plasticity of refractory metals in dependence on the temperature-time, technological and other factors.

The book is intended for builders, metallographers and scientific workers, who are occupied by creation, tests and the application/use of refractory metals in different areas of science and technology. Illustration 297, table 42. of References of 230 titles.

Pages 3-4.

No typing.

Page 5.

INTRODUCTION.

With the development of the newest branches of technology (jet/reactive and nuclear) arose the large necessity for the alloys of the increased strength for a work at high temperatures (higher than 1000°C). The possibilities of applying the most heat-resistant nickel alloys are almost completely exhausted, in consequence of which considerably increased researchers' interest in refractory metals and the alloys on their basis whose heat resistance is considerably higher than in the best nickel alloys. From refractory metals widest use as heat-resistant materials is found tungsten, the molybdenum, the niobium, produced by industry in a sufficient

quantity. Rhenium and tantalum, in spite of their high mechanical properties, thus far cannot be used extensively as the basis of alloys for aviation and rocket engineering, since these metals are obtained in small quantities, and the reconstituted supplies of these metals are small.

Niobium and molybdenum, because of sufficient strength, plasticity and thermal conductivity at the temperatures higher than 1000°C, are distinct structural materials for jet engines and rockets. Is studied at present the possibility of the utilization of molybdenum and niobium with 1200-1400°C, i.e., as materials for the blades of turbines, nose cones of the aircraft and rockets and many other high-temperature assemblies and parts.

The increased interest in niobium is explained by the fact that together with satisfactory strength and creep strength at high temperatures it possesses good plasticity, comparatively low specific gravity/weight, high technological properties during perfecting by pressure and cutting, and also sufficiently good weldability. It is completely substantial, that oxides of niobium are not volatile at high temperatures. With the increase of temperature, the thermal conductivity of niobium is not lowered, as is observed in other metals, but it grows/rises; the values of the module/modulus of elasticity up to 1200°C barely are changed.

Niobium possesses sufficiently high heat resistance in interval of 700-1300°C.

Page 6.

So, in conditions of short-time tests for rupture with 700°C the limit of the strength of niobium is 647 MN/mm^2 (65 kg/mm^2), and with 1100°C - 225.6 MN/mm^2 (23 kg/mm^2); stress-rupture strength on base 100 h at 900°C is 137 MN/mm^2 (14 kg/mm^2), and at 1000°C - 83.4 MN/mm^2 (8.5 kg/mm^2).

Molybdenum and its alloys are also promising structural materials for a work at high temperatures, since they possess high heat resistance, good fatigue limit, the high modulus of elasticity. Furthermore, molybdenum has distinct thermal and electric characteristics. Because of high thermal conductivity and the low specific heat of molybdenum, the thermal stresses during rapid heating and cooling are small. The coefficient of the linear expansion of molybdenum to 50-70°C is lower than for the majority of steels.

The mechanical properties of molybdenum depend mainly on the

preceding working by pressure at the temperatures lower than the recrystallization ones. The properties of molybdenum and its alloys substantially affect the degree of strain, the temperature of working by pressure, the temperature of annealing, the surface finish value. At 1000°C hundred-hour stress-rupture strength of alloy Mo-0.5% Ti is $294 \frac{\text{MN}}{\text{m}^2}$ ($30 \frac{\text{kg}}{\text{mm}^2}$), while at 1100°C - $196 \frac{\text{MN}}{\text{m}^2}$ ($20 \frac{\text{kg}}{\text{mm}^2}$), i.e., it prove to be itself considerably higher than for the best nickel alloys.

Tungsten received at present smaller propagation in comparison with molybdenum and niobium. It is of interest for researchers as refractory metal, which possesses high heat resistance.

An essential deficiency in the refractory metals is low heat resistance at the temperatures higher than 400-600°C. Therefore the high-temperature utilization of refractory metals and alloys on their basis is possible only for a work in neutral or reducing agent or for a very momentary duty in oxidizing medium. Medium can completely consist of inert gases, for example of the helium closed-cycle turbine, connected with atomic reactor.

This monograph is the generalization of the results of the in-flight studies of different characteristics of strength of refractory metals and their alloys at high temperatures, carried out

by the large staff of Institute of problems of strength of AS UkrSSR.

Taking into account the specific character of the high-temperature strength tests of high-melting materials - temperature on the order of 3000°C and oxidizability - was thoroughly developed the test procedure and were created the corresponding experimental means. In connection with this in monograph the large place occupy the descriptions of original installations and test procedures.

Page 7.

Monograph contains also the vast information about different mechanical characteristics of high-melting materials, the obtained taking into account effect temperatures, the form of the stressed state, character and conditions/mode of the application of the load, time/temporary and other factors.

We hope that this book, in which, apparently, it is sufficient fully and are thoroughly illuminated questions of the strength tests of high-melting materials over a wide range of temperatures, it will prove to be useful both for the technologists and the builders and for scientific workers.

In the writing of monograph, took part the following authors: V. A. Borisenko (Chapter 4 and p. of 4 Chapters 5); S. S. Gorodetskiy (p. 1-3, 5, Chapter 1); V. P. Dubinin and V. V. Krivenyuk (Chapter 6); Yu. A. Kashtalyan (Chapter 2); V. N. Rudenko (p. 4, Chapter 1); G. S. Pisarenko (Chapter 3); V. K. Kharchenko (p. 3, Chapter 1 and Chapter 5).

Chapter 7 was written by E. A. Gryaznov (p. 1, 2), V. A. Strizhalo (p. 1, 2); to V. T. Troshenko (p. 1, 3) and Ye. I. Uskov (p. 1, 2).

Page 8.

Chapter I.

EFFECT OF TEST CONDITIONS ON STRENGTH CHARACTERISTICS.

The intense development of technology of the high-temperature investigations of the strength of refractory metals is impossible without the development of new ones and the perfection/improvement of the existing methods of tests.

In Soviet and foreign literature are published many works, which contain different information about the mechanical properties of refractory metals [1-7]. Some physicomechanical properties of these metals are given in Tables 1 and 2.

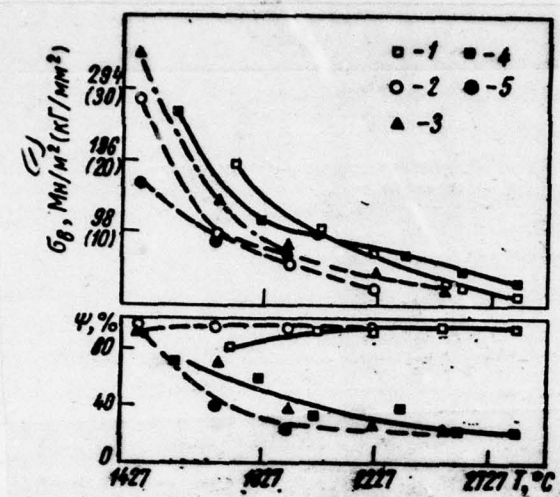


Fig. 1. Temperature effect on the strength and plastic properties of the tungsten: 1 - poured (on our data); 2 - the same [162]; 3 - cermet [165]; 4 - the same (on our data); 5 - the same [162].

Key: (1) - MN/m^2 (kg/mm^2) -

Page 9.

Table 1. Physical properties of refractory metals [1, 3, 5].

(2) Свойства	(1) Группы периодической системы						
	V A			VI A			VII A
	V	Nb	T _g	Cr	Mo	W	Re
(3) Плотность, г/см ³	6,1	8,7	16,6	7,19	10,2	19,3	21,02
(4) Температура плавления, °C	1900	2468	2996	1860	2622	3380	3140
(5) Кристаллическая решетка	O. ц. к. ⁽⁶⁾	O. ц. к. ⁽⁶⁾	O. ц. к. ⁽⁶⁾	O. ц. к. ⁽⁶⁾	O. ц. к. ⁽⁶⁾	O. ц. к. ⁽⁶⁾	Гексагональная ⁽⁷⁾
(8) Коэффициент линейного расширения, $\alpha \cdot 10^{-6}$	8,3	7,1	6,6	6,47	5,0	4,3	6,70
(9) Температура рекристаллизации, °C	800	1040	1250	900	1050	1100	1500
(10) Модуль упругости, ГН/м ² (кГ/мм ²)	150 (15 000)	160 (16 000)	192 (19 200)	250 (25 000)	332 (33 200)	415 (41 500)	470 (47 000)
(11) Твердость, ГН/м ² (кГ/мм ²)	—	2,0—2,5 (200—250)	1,25—3,50 (250—350)	—	2,0—2,5 (200—250)	3,5—4,0 (350—400)	—
(12) после деформации	—	—	—	—	—	—	—
(13) после отжига	0,64 (64)	0,75 (75)	0,450—1,25 (45—125)	1,0 (100)	1,4—1,85 (140—185)	2,0—2,5 (200—250)	2,74 (274)
(14) Поперечное сечение захвата тепловых нейтронов, барн/ат.	4,98	1,15	21,3	3,1	2,4	19,2	86,0

Key: (1). Groups of periodic system. (2). Properties. (3). Density, g/cm³. (4). Melting point, °C. (5). Crystal lattice. (6). BCC [O.ts.k. - bodycentered cubic]. (7). Hexagonal. (8). Coefficient of linear expansion, $\alpha \cdot 10^{-6}$. (9). Temperature of recrystallization, °C. (10). Module/modulus of elasticity, H/m² (kg/mm²). (11). Hardness, H/m² (kg/mm²). (12). after strain. (13). after annealing. (14). Cross section of capture of thermal neutrons, Barn/at.

Pages 10-11.

Table 2. Temperature effect on some physical properties of refractory metals.

(2) Свойство	(3) Температура, °C										
	20	730	1230	1530	1730	2030	2230	2530	2830	3030	3230
(3) Вольфрам											
Мощность излучения, вт/см ² (ккал/см ² · ч)	—	0,602 (0,55)	5,52 (4,6)	14,41 (12,6)	24,04 (21,6)	47,2 (42,3)	69,8 (41,4)	117,6 (105,3)	185,8 (166,5)	245,4 (220,5)	318 (286)
Удельное электросопротивление, мкм · см	5,49	24,93	40,36	50,05	56,67	66,9	73,9	84,7	95,8	103,3	111,1
Коэффициент термического расширения, $\frac{l_t - l_{20}}{l_{20}}$	—	3,2	5,7	7,5	8,8	10,8	12,4	14,8	17,2	18,9	20,7
Скорость испарения, мкг/см ² · сек	—	—	$1,69 \cdot 10^{-16}$	$3,6 \cdot 10^{-11}$	$1,4 \cdot 10^{-8}$	$7,8 \cdot 10^{-6}$	$7,6 \cdot 10^{-4}$	$7,4 \cdot 10^{-2}$	3,0	24	—
(3) Молибден											
Мощность излучения, вт/см ² (ккал/см ² · ч)	—	0,55 (0,49)	6,30 (0,56)	—	20 (18)	39 (36)	58 (55)	100 (89)	—	—	—
Удельное электросопротивление, мкм · см	5,2	23,9	38,2	47,3	53,5	62,5	68,9	78,2	—	—	—
Коэффициент термического расширения, $\frac{l_t - l_{20}}{l_{20}}$	—	5,7	8,6	10,2	11,3	—	—	—	—	—	—
Теплопроводность, вт/см · град (ккал/м · ч · град)	—	0,76 (0,68)	0,91 (0,82)	1,0 (0,88)	1,05 (0,94)	—	—	—	—	—	—
(2) Тантал											
Мощность излучения, вт/см ² (ккал/см ² · ч)	—	—	—	13,3 (11,9)	21,6 (19,4)	—	—	105,5 (94,9)	167,4 (14,7)	214,5 (20,4)	—
Удельное электросопротивление, мкм · см	14,6	49	66	71	80	87	—	—	108,7	—	—
Скорость испарения, мкг/см ² · сек	—	—	—	—	$1,6 \cdot 10^{-6}$	$3 \cdot 10^{-3}$	0,66	14	—	68	—
(2) Ниобий											
Мощность излучения, вт/см ² (ккал/см ² · ч)	—	—	6,4 (5,8)	11,4 (10,3)	18,5 (16,6)	—	67 (60)	130,6 (117,5)	—	—	—
Удельное электросопротивление, мкм · см	14,6	42,4	52,0	—	—	—	—	—	—	—	—
Теплопроводность, вт/см · град (ккал/м · ч · град)	0,145 (0,125)	0,182 (0,156)	0,209 (0,18)	0,234 (0,210)	0,238 (0,205)	—	—	—	—	—	—

Key: (1). Temperature, °C. (2). Property. (3). Tungsten. (4). Radiated power, W/cm² (kcal/cm²·h). (5). Specific resistance, $\mu\Omega\cdot\text{cm}$. (6). Thermal-expansion coefficient. (7). Rate of evaporation, $\mu\text{g}/\text{cm}^2\cdot\text{s}$. (8). Molybdenum. (9). Specific resistance, $\mu\Omega\cdot\text{cm}$. (10). Thermal conductivity, W/cm·deg (kcal/m·h·deg). (11). Tantalum. (12). Niobium.

Page 12.

However, to compare test results with literature data is completely difficult, even in the case of the identical chemical compositions of the metals being investigated and the technological procedures of their production (Fig. 1) used. One of the reasons for this nonconformity of the obtained results should count a difference in the procedure of the determination of the mechanical properties of high-melting materials, especially during tests at high temperatures.

In this chapter is examined the effect of vacuum, inert, carbon-containing and oxidizing medium, and also the deformation rates to the strength characteristics of refractory metals and on the basis of the obtained results are made recommendation relative to the

conditions/modes of the tests of refractory metals.

Similarity conditions of experiments during the mechanical tests of materials.

The comparison of the mechanical characteristics of the materials, measured with different methods of heating and under test conditions, are difficult, and becomes doubtful the legitimacy of the utilization of these experimental data for generalizations and the establishment of the criteria of strength and bearing capacity of parts.

The specific character of the mechanical tests of high-melting materials at high temperatures is such, that without comprehensive taking into account of the factors, which affect the indices of mechanical properties, is possible obtaining not only difficultly the comparable, but also contradictory data. To compare results is possible only in the case of the similarity of the tests of materials with identical found properties and with identical relative errors of measurement, in conformity with the diagram, given to Fig. 2. From diagram it is evident that the similarity of experiment must include the identity of initial material and technology of the manufacture of specimen/samples, their geometry and conditions of loading, and also

heating conditions taking into account time/temporary factors.

Furthermore, it is necessary for the evaluation of the authenticity of results to analyze experimental errors taking into account instrument, systematic and computational errors.

During mechanical tests is necessary the observance of three forms of the similarity:

- a) geometric (similarity of form and size/dimensions of specimen/samples).
- b) mechanical (similarity of the loading conditions).
- c) physical (similarity of ambient conditions) [5].

Page 13.

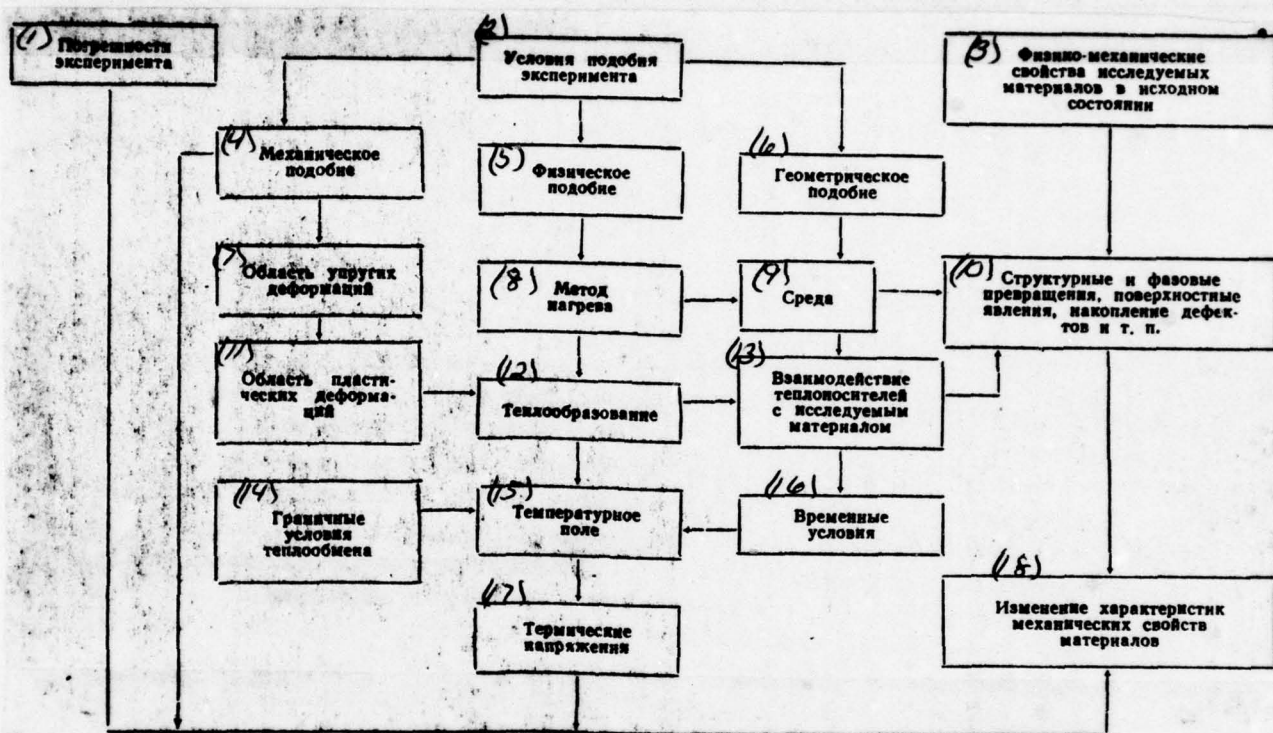


Fig. 2. Basic factors, which determine similarity of experiment during high-temperature mechanical tests of high-melting materials.

Key: (1). Experimental errors. (2). Conditions of experiment. (3). Physicomechanical properties of materials being investigated in initial state. (4). Mechanical similarity. (5). Physical similarity. (6). Geometric similarity. (7). Region of elastic deformations. (8). Method of heating. (9). Medium. (10). Structural and phase transformations, surface phenomena, accumulation

of flaws/defects, etc. (11). Zone of plastic deformation. (12). Heat generation. (13). Reaction of heat-transfer agents with material being investigated. (14). Secondary conditions of heat exchange. (15). Temperature field. (16). Time/temporary conditions. (17). Thermal stresses. (18). Change in characteristics of mechanical properties of materials.

Page 14.

The geometric similarity of the specimen/samples of identical form is satisfied by the condition

$$\frac{r_1}{r_2} = K^a, \quad (1.1)$$

where G - geometric characteristic.

K - relation of significant dimensions, for example:

$$\frac{F_1}{F_2} = K^2; \quad \frac{V_1}{V_2} = K^3; \quad \frac{W_1}{W_2} = K^3; \quad \frac{l_1}{l_2} = K^1,$$

where F - area.

V - volume.

W - moment of resistance.

I - moment of inertia.

The criteria of mechanical similarity are usually determined by the differential equations of thermoelasticity and are expressed the conditions according to which for a mechanical similarity in geometrically similar specimen/samples it is necessary that at congruent points specimen/samples would have identical stresses, identical mechanical and identical thermal strains [6]:

$$\frac{P}{\alpha^2} = \text{idem}; \quad \frac{\sigma}{\epsilon E} = \text{idem}; \quad \frac{\alpha T}{\epsilon} = \text{idem}. \quad (1.2)$$

The consequence of these conditions must be the similarity of specific work of deformation of specimen/samples.

At high temperatures the strength of refractory metals, substantially affects the deformation rate. This effect can be considered with the aid of following relationship/ratio [7]:

$$n = \left| \frac{\lg \frac{\sigma_1}{\epsilon_1}}{\lg \frac{\sigma_2}{\epsilon_2}} \right|_{\alpha, T} = \text{idem}, \quad (1.3)$$

where σ_1 - flow stress at the rate of deformation $\dot{\epsilon}_1$;

σ_2 - flow stress at the rate of deformation $\dot{\epsilon}_2$.

The observance of geometric and mechanical similarity during the utilization of different methods of heating does not cause difficulties. To considerably complexly ensure thermophysical

similarity (similarity of temperature fields in specimen/sample, the similarity of the processes of reacting the medium with the surface of specimen/sample, etc.).

The conditions of the thermal similarity of specimen/samples are determined by the differential equations of heat transfer which establish a communication/connection between time/temporary and three-dimensional/space changes in the temperature fields of specimen/sample under the appropriate boundary conditions.

Page 15.

For the high-temperature tests of specimen/samples in vacuum, thermal similarity is possible, if are observed the following relationship/ratios, recorded in the criterial form:

a) for the ray heating:

$$T = f(Ki, x, Fo); \quad (1.4)$$

b) for heating by internal sources of heat (contact, induction, cathode-ray):

$$T = \varphi(Ki, x, Fo, Po), \quad (1.5)$$

where $Ki = \frac{q(\tau)l}{\lambda \Delta t}$ - heat exchange criterion of Karpichev;

$q(r)$ - heat-flux density;

λ - coefficient of the thermal conductivity of material;

Δt - the temperature differential between the heater and the specimen/sample;

$x = \xi/l$ - dimensionless coordinate;

l - significant dimension of specimen/sample;

$Fo = \frac{\alpha t}{\beta}$ - fourier number;

$a = \lambda/c\gamma$ - coefficient of thermal diffusivity;

τ - time.

$Po = \frac{q(xy)R}{\lambda l_0}$ - the criterion of Pomerants;

$q(x, y)$ - the density of distribution of heat sources in specimen/sample.

In the steady conditions/mode of heat exchange criterion Fo approaches infinity, and dimensionless temperature for zero, i.e.,

for the state of the thermal equilibrium of system, characteristic for the majority of the types of mechanical tests, the dependences of form $T_i=f(F_0)$ degenerate.

The temperature field of the specimen/sample, deformed during ray heating in furnace, is virtually staticrary, and during heating by internal heat sources - it is unsteady, since in the second case the initial conditions of heat generation and heat exchange in the specimen/sample being deformed are changed. In this case, in the strained volume of specimen/sample, is disturbed initial temperature field and, consequently, also the properties of material.

Thus, the full/total/complete similarity of experiment during heating of the specimen/sample being deformed by external and internal heat sources it is not possible to achieve.

Page 16.

The degree of satisfaction of similarity conditions during the utilization of different methods of heating depends on the properties of material, size/dimensions of specimen/sample, conditions of heat generation and heat exchange with the environment.

The disturbance/breakdown of thermal and, consequently, also

mechanical similarity can substantially change the characteristics of plasticity and service life of material. From external physical conditions great value has the medium. Common media (technical argon, helium, vacuum) contain in different concentration the residual gases (oxygen and nitrogen), which actively interact with the surface of the metals being investigated.

The effect of medium on the mechanical characteristics of refractory metals is studied insufficiently. The criteria, which characterize the identity of the effect of media, can be obtained from the dimensional analysis and π -theorem. Assuming that the reaction of medium and surface of specimen/sample at temperature T for time τ leads to the formation of the defect (contaminated or purified) layer of material by thickness δ , identical are counted such conditions, under which relation to the area (volume) of defective layer to common/general/total cross-sectional area (strained volume) are equal. As the determining parameters of process, are selected the following values: k - the surface concentration of gases; τ - holding time in medium; D - diffusion coefficient; γ - specific surface energy; P - acting load; l - characteristic linear dimension of specimen/sample.

Besides the parameters indicated, on diffusion processes great effect has the temperature and contact area. Consequently, it is

necessary to introduce parametric type criteria:

- a) the homologous temperature: $\Theta = \frac{T}{T_{\infty}}$;
- b) the factor of the form of specimen/sample K_θ - the ratio of the perimeter of outline/contour to the basic dimension of specimen/sample.

Utilizing a dimensional analysis and π -theorem, find the following criteria, which ensure the identity of the effect of the medium:

$$\pi_1 = \frac{M^2}{P}; \quad \pi_2 = \frac{D_t}{P}; \quad \pi_3 = \frac{U}{P}.$$

For the specimen/samples, manufactured according to identical technology from one material, specific surface energy γ must be identical. The coefficient of diffusion D for low impurity contents also virtually does not depend on concentration [8]. Therefore γ and D it is possible to consider constants for this temperature of tests and similarity conditions to define as function from r , l , k , P .

Page 17.

Thus, reliable comparison and the generalization of the results of the mechanical tests of refractory metals in high-temperature

range, at steady state of heating is possible, if is retained the constancy of following criteria and communication/connections:

$$\Phi \left(\frac{r_1}{r_2}, K_\phi, \frac{P}{\sigma l^2}, \frac{\sigma}{sE}, \frac{\sigma T}{\varepsilon}, \frac{\lg \frac{\sigma_1}{\sigma_2}}{\lg \frac{\dot{\sigma}_1}{\dot{\sigma}_2}}, \theta, \frac{M^2}{P}, \frac{D\tau}{l^2}, \frac{\eta l}{P} \right) = \\ = \text{const.}$$

It is most difficult to carry out the thermal similarity whose disturbance/breakdown changes the stressed state of the material of specimen/sample. Therefore it is necessary to examine the thermal and stressed state of specimen/samples with the different methods of heating, the physical nature of the processes, which take place during heating, and also the effect of medium and deformation rate on strength during heating.

Effect of the method of heating on the strength properties.

The method of heating specimen/sample can affect the mechanical properties of materials, if the processes of heat generation and heat exchange do not provide adequate temperature fields in the strained volume, is caused the formation of the flaws/defects of crystal lattice or damage of the physical properties of the materials being investigated.

The physical nature of heating specimen/samples by different methods substantially is distinguished. During ray heating the falling/incident to the surface of specimen/sample emission/radiation is absorbed and energy of electromagnetic vibrations is transformed into heat. In metal are induced the forced oscillations of the free electrons which create the powerful wave reflected; therefore the electromagnetic waves penetrate inside metal at insignificant depth and in essence are reflected from its surface. The higher the electroconductivity of metal, the higher its reflectivity [9]. For refractory metals the basic spectrum of radiant flux is absorbed by the surface layer of metal 0.2-0.3 μm in thickness [10]. The propagation of heat flux is determined by the thermal diffusivity of material.

Made of all methods of heating specimen/samples by internal heat sources in physical nature and the character of heat generation is most close to ray cathode-ray heating.

Its application/use is most expedient during the high-temperature tests of materials in vacuum.

Let us examine some specific special feature/peculiarities of cathode-ray heating.

Page 18.

The processes, which appear during the electron bombardment of the surface of metal, differ somewhat from those, that they accompany luminous absorption. Electron, unlike photon, has a wavelength of the same order as the parameters of crystal lattice ($2.72\text{--}2.85\text{\AA}$) of refractory metals. Therefore electron is proved to be strictly localized and creates the field, very similar to the field of point charge. Approaching the electron of atom, outer electron is changed it into state with higher energy.

The energy loss by electrons is maximum at certain distance from the surface of metal. Depth of penetration of electrons with energy 10-40 keV, specific by formula B. Shenlanda, does not exceed $4 \mu\text{m}$ for the refractory metals of "large quarter" [10].

The comparison of the threshold energy of atomic displacement from the assembly of crystal lattice and energy, transferred by the driving/moving electron, shows that kinetic energy of the electrons, which bombard the surface of refractory metals with accelerating voltages indicated, must not cause radiative damage of the type "vacancy-interstitial atoms" and it will be in essence converted into thermal energy.

The physical essence of contact and induction heating is following. During the imposition of external electric field, the electrons in the material of specimen/sample are misaligned in the direction of field, appear the electron waves and together with them - electric current. The imperfections of crystal lattice of technical metals and alloys and the thermal oscillations of atoms cause scattering the electron waves, the causing electrical resistance, and in specimen/sample is separated thermal energy according to the law of Joule-Lenz.

The energy levels of heat-transfer agents in the cases in question are such, that a change in the physical properties of material or the appearance in it of radiation flaw/defects during the conversion of one form of energy into another, is highly improbable. Therefore a change in the mechanical characteristics of materials with electric heating is determined, apparently, not by the process of energy conversion in the strained volume, but by its consequence-nonuniformity of temperature field and by the thermal stresses in the specimen/sample being deformed.

It is known that the flat/plane temperature field does not cause stresses, if it stationary has heat sources, arranged/located only out of the outline/contour of region [11] in question. These conditions are satisfied for the external ray heating of solid specimen/sample

and, in the first approximation,, for electron-beam heating.

Other methods of electric heating create the temperature fields, calling the thermal stresses in specimen/sample. The greatest temperature differential in specimen/sample appears at the constant bulk density of heat release q_0 .

Page 19.

For a circular specimen/sample stationary temperature field are determined from the formula

$$\Delta T(r) = \frac{q_0}{4\lambda} (r_0^2 - r^2), \quad (1.6)$$

thermoelectric stresses - according to following formulas [15]:

$$\left. \begin{aligned} \sigma_r &= \frac{\alpha E}{1-\mu} \frac{r^2 - r_0^2}{4(r_0^2 - r^2)} \Delta T(r); \\ \sigma_\theta &= \frac{\alpha E}{1-\mu} \frac{3r^2 - r_0^2}{4(r_0^2 - r^2)} \Delta T(r); \\ \sigma_z &= \frac{\alpha E}{1-\mu} \frac{2r^2 - r_0^2}{2(r_0^2 - r^2)} \Delta T(r), \end{aligned} \right\} \quad (1.7)$$

where α - coefficient of linear expansion.

μ - Poisson ratio.

E - modulus of elasticity.

Utilizing an equation of heat balance, it is represented $\Delta T(r)$ depending on the temperature of the surface of specimen/sample T_0 , of the parameters of emission/radiation and properties of the material:

$$\Delta T(r) = \frac{e_t \epsilon_0}{2\lambda} T_0^4 \frac{r_0^2 - r^2}{r_0}. \quad (1.8)$$

where e_t - emissivity factor of the surface of specimen/sample.

ϵ_0 - radiation coefficient of blackbody.

λ - coefficient of the thermal conductivity of material.

r_0 - radius of specimen/sample.

A maximum temperature differential will be observed on the axle/axis of the specimen/sample:

$$\Delta T(r)_{r=0} = \frac{e_t \epsilon_0 r_0}{2\lambda} T_0^4. \quad (1.9)$$

Let us substitute (1.8) in (1.7):

$$\left. \begin{aligned} \sigma_r &= \frac{\alpha E}{1-\mu} \frac{r^2 - r_0^2}{8r_0} \frac{\epsilon_0}{\lambda} T_0^4; \\ \sigma_\theta &= \frac{\alpha E}{1-\mu} \frac{3r^2 - r_0^2}{8r_0} \frac{\epsilon_0}{\lambda} T_0^4; \\ \sigma_z &= \frac{\alpha E}{1-\mu} \frac{2r^2 - r_0^2}{4r_0} \frac{\epsilon_0}{\lambda} T_0^4. \end{aligned} \right\} \quad (1.10)$$

Page 20.

Great in absolute value value have tangential and longitudinal stresses with $r=r_0$:

$$\sigma_t = \frac{\alpha E}{1-\mu} \frac{r_0}{4} \frac{\sigma_{t0}}{\lambda} T_0^4. \quad (1.11)$$

According to formula (1.11), the thermal stresses with the contact electric heating of specimen/samples are proportional to the fourth degree of the temperature and, therefore, during the utilization of this method must be the limitedly maximum value of temperature. Let maximum permissible be the thermal stresses of value

$$\sigma_t \leq K \sigma_{app}, \quad (1.12)$$

where σ_{app} - apparent elastic limit; $K \ll 1$.

On formula (1.11) it is possible to find the maximum permissible temperature of heating specimen/sample when $q_v=\text{const}$:

$$|T_0| \leq \sqrt[4]{\frac{1-\mu}{\alpha E} [\sigma_t] \frac{4K}{r_0 \sigma_{app}}}. \quad (1.13)$$

Value $[T_0]$ can be raised, if is establishinstalled around specimen/sample the sheet reflectors and to decreased the heat of sink from its surface. The increase of the permissible temperature at the same thermal stresses it is possible to attain, by utilizing

induction heating.

During heating of specimen/samples by high-frequency currents, the density of distribution internal heat sources depends substantially on current frequency and temperature (Fig. 3).

With the increase of the heating temperature, the temperature differential over the section/cut of specimen/sample is increased and its maximum value can be calculated according to the following formula:

$$\Delta T_1(r)_{r=0} = \frac{\sigma_{max}}{2\lambda} T_0^4 \frac{1 + \frac{1}{120} \left(\frac{r_1}{\Delta}\right)^4 + \frac{10^{-3}}{307} \left(\frac{r_2}{\Delta}\right)^6}{1 + \frac{1}{24} \left(\frac{r_1}{\Delta}\right)^4 + \frac{10^{-3}}{23} \left(\frac{r_2}{\Delta}\right)^6}, \quad (1.14)$$

where Δ - depth of penetration of currents.

The given dependences make it possible to correctly select the geometric dimensions of specimen/samples, method and the conditions/modes of heating for the stage of uniform deformation or brittle decomposition of material. With the advent of microcracks and localization of strain (necking) occurs the redistribution of the density of heat sources whose values during contact and induction heating sharply are distinguished.

For contact electric heating during tests for elongation of the direction of normal stresses and vector of current, they coincide (Fig. 4a).

Page 21.

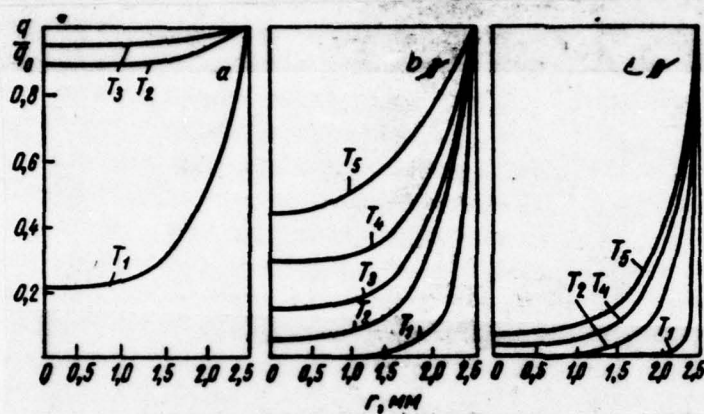


Fig. 3. Relative change in specific power in section/cut of tungsten specimen/sample during induction heating: a) $f=10^4$ Hz; b) $f=10^6$ Hz; c) $f=3 \cdot 10^5$ Hz; $T_1=0^\circ\text{C}$; $T_2=727^\circ\text{C}$; $T_3=1227^\circ\text{C}$; $T_4=1727^\circ\text{C}$; $T_5=2527^\circ\text{C}$.

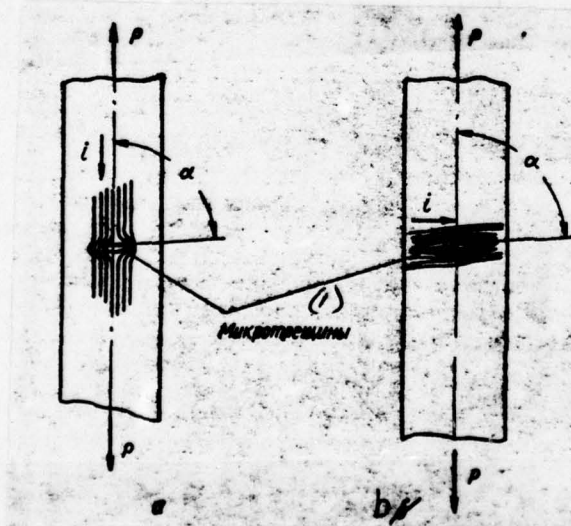


Fig. 4. Orientation of microcracks with respect to vector of current

during heating: a) contact; b) induction.

Key: (1). Microcracks.

Page 21.

Microcracks usually are formed in the plane, perpendicular to axis of dilatation [12]: at the apex/vertexes of cracks, occurs the concentration of current density. These zones during contact resistance heating are superheated and maximum local voltages relax. Resistance to development of crack grows and with a common/general/total increase in the accumulated flaw/defects the development of the crack of critical dimension can begin later, than during heating in furnace, i.e., the service life of specimen/samples can grow/rise. This is possible, if the velocity of propagation of crack is low, and the rate of relaxation is great.

During the induction heating of specimen/sample, the orientation of microcracks and the sense of the vector of current coincide (Fig. 4b).

The effect of the superheating of the apex/vertex of crack will

be minimum and in the case of plastic materials it will not at all influence the results of mechanical tests. Large role plays also the stressed state which can contribute the development of crack (elongation, shift/shear) or its "curing" (compression).

In the case of contact electric heating, the localization of strain leads to the superheating of the neck of specimen/sample, since in this zone sharply grows/rises the isclatable specific power:

$$P = \gamma_e \left(\frac{U}{l} \right)^2. \quad (1.15)$$

where γ_e - the specific conductivity of material at this temperature.

U/l - the voltage drop per unit of the length of specimen/sample.

The superheating of specimen/sample in neck intensifies the concentrated strain, suppresses the effects of the superheating of the apex/vertexes of microcracks and can considerably change in the characteristics of material.

For induction heating is characteristic the absence of the superheating of specimen/sample up to its decomposition. This conclusion is instituted on following considerations. The average specific power during induction heating is determined by the formula

$$P = \frac{8\rho_t H_0^2}{r \cdot \Delta} F, \quad (1.16)$$

where H_0 - magnetic field strength on the surface of specimen/sample;

$F = \psi\left(\frac{r}{\Delta}\right)$ - the function the graph by which is represented in Fig.

5;

r - radius of specimen/sample.

If is accepted H_0 , ρ_t and Δ as constants, then of the curve/graphs of equation (1.16) will take the form, shown on Fig. 6.

Page 23.

Function has a maximum in range of values $r/\Delta = 1.4-2.1$, and its value descends during the decrease of the radius of specimen/sample. Furthermore, the strain of specimen/sample, with the constant size/dimensions of inductor, leads to the decrease of initial magnetic field strength H_0 on the surface of specimen/sample, in consequence of which the heat release in the zone of necking also decreases, i.e., there will not be superheating in the zone of the concentrated strain.

The experimental works of Grant [13], of Harper [14] and of

Other researchers confirm the absence of the specific effect of induction heating (during its specific conditions/modes) on the mechanical characteristics of materials in comparison with ray heating in resistance furnace.

The effect of cathode-ray heating on the characteristics of strength and plasticity of refractory metals was checked during installation "Electron".

To testing subjected to sheets from tantalum and niobium the welded joints of sheets from the molybdenum alloy Tsm2A.

Figure 7 shows the temperature dependence of strength and plasticity of annealed cermet tantalum. The mechanical property of metal, heated in vacuum by ray and cathode-ray method, they are little distinguished in the range of mean temperatures. With the increase of the temperature of testing the value of the strength characteristics in the case of cathode-ray heating, somewhat lower than during ray heating, is retained the exponential dependence of the strength of tantalum on temperature. The comparison of the hardness of specimen/samples before and after high-temperature tests in vacuum gave identical results for both of methods of heating.

Analogous results are obtained also for the temperature

dependence of the strength of the annealed laminated niobium.

The analysis of the obtained dependences made it possible to assume that certain softening during cathode-ray heating causes not strictly the electron bombardment of the surface of specimen/sample, but the which associates it degassing, decontamination of metal.

Were carried out mechanical weld tests from the molybdenum alloy TSM2A, which, as is known, have considerable contaminations in the zone of the weld. Welds were made by argon-arc welding, their surface was clean, without undercuts and traces of oxidation. The results of the tests, carried out during the ray heating of specimen/samples in argon and cathode-ray - in vacuum, are given to Fig. 8. The strength characteristics in both cases of heating are virtually identical, and plasticity indices ($T > 1200^{\circ}\text{C}$) substantially are distinguished. The decomposition of the welds during ray heating occurs predominantly in the zone of the slack of weld, and with cathode-ray - in heat-affected zone.

Page 24.

Because of this the plasticity of the specimen/samples, tested during ray heating, remains low, and with cathode-ray - continuously it is

increased with the increase of temperature.

These results confirm the assumption about the possibility of softening as a result of degassing (decontamination) material during cathode-ray heating, which facilitates in essence an increase of the characteristics of plasticity. However, specific effect on mechanical properties metals in vacuum cathode-ray heating (accelerating voltages to 20 kV), apparently does not exert itself. Therefore it is possible to use during the short-time strength tests and plasticity, thermal and low-cycle fatigue of materials, and also during the tests of creep and stress-rupture strength on small bases at superhigh temperatures.

It must be noted that at the insufficient frequency of the scanning of electron beam over the surface of specimen/sample in the strained volume of material are possible the thermal pulsations, and as consequence, thermal fatigue and the corresponding reduction in the mechanical characteristics of material.

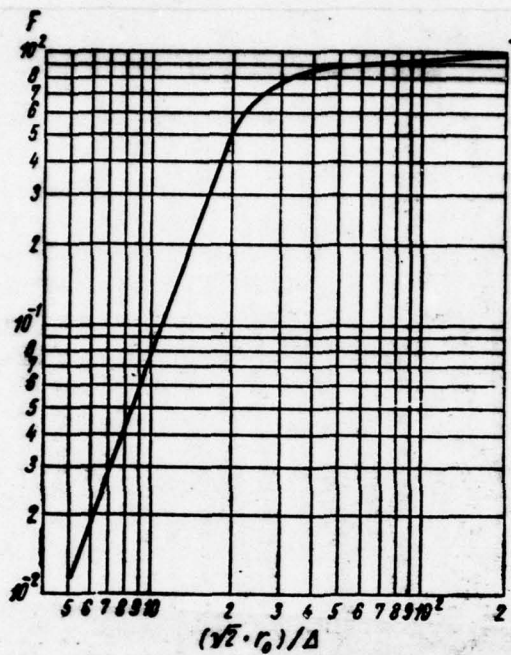


Fig. 6. Dependence of function F on the value of relation the radius of specimen on the depth of penetration of current.

Page 25.

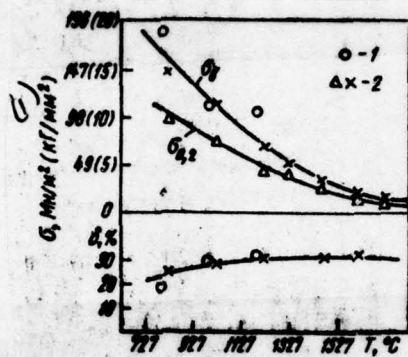
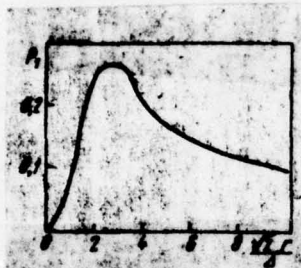


Fig. 6. Dependence of specific power, which separates in specimen/sample during induction heating, on radius of specimen/sample.

Fig. 7. Strength and plasticity of annealed tantalum depending on temperature: 1 - ray heating; 2 - cathode-ray heating.

Key: (1) • MN/mm² (kg/mm²).

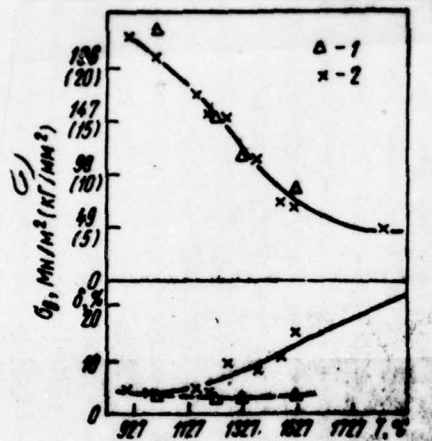


Fig. 8. Strength and plasticity of welded joints of alloy TSM2A depending on temperature: 1 - ray heating; 2 - cathode-ray heating.

Key: (1) - MN/m^2 (kg/mm^2).

Page 26.

For example, work [15] shows, that the scanning of electron beam with frequency 20-60 Hz causes the surface damage of specimen/sample, and the electron bombardment with high energy contributes to formation and the motion of point defects. An increase in the frequency of the scanning of electron beam to 3000 Hz made it possible to obtain the

identical microstructures of surface and mechanical characteristics during the ray and cathode-ray heating of tungsten.

The investigations of mechanical properties with the application/use of cathode-ray heating it is carried out somewhat, and data insufficient for final conclusions; however, it is possible to confirm that during the nonstationary systems of heating to the high temperatures in vacuum this method has the irrefutable advantages before other methods of heating.

Effect of medium on strength indices.

The mechanical properties of refractory metals at high temperatures, as is known, depend on medium, the time of heating, technological special feature/peculiarities of the production and many other factors [16, 17].

Let us examine, which effect on the strength indices of refractory metals exerts the change in the properties of the surface layers of specimen/sample, which depends on depth of vacuum, and also from the form of the medium: inert, that carbon-contains and oxidizing. It is necessary to note that at the temperatures more than 1200°C role of such factors as centering of specimen/samples during

tests, accuracy of the measurement of strain, load and the temperature is less essential, than at the RCCM and relatively low temperatures: 200-700°C. These questions are illuminated in sufficient detail in specialized literature [5, 6, 18, 19]; we on them be stopped will not be. Let us note only that during pursuance of research the factors indicated calculated in proportion to technical capabilities and depending on objectives of mission.

The strength properties of refractory metals as a result of their sensitivity to oxidation usually are determined in inert medium or in vacuum. The degree of the decontamination of inert gases, the depth of vacuum and inleakage into vacuum system significantly affect the strength and deformation characteristics both during prolonged ones and during short-time tests.

For example, during testing of the stress-rupture strength of niobium in the range of temperatures of 600-700°C was reveal/detected an increase in the oxygen content in material from 0.04% to 0.20% in connection with the fact that in the camera/chamber was maintained the dynamic vacuum (see [61]). The results of short-time tests in the medium of inert gases and in vacuum were distinguished.

In work [20] is investigated the strength of the niobium of cathode-ray remelting and tantalum in vacuum 6.65 dyn/m^2 ($5 \cdot 10^{-3}$ torr); the duration of heating specimen/samples to testing temperature was 30 min. The given in this work data show that the limit of the strength of niobium in the range of temperatures of $700-1000^\circ\text{C}$ is not virtually changed and is approximately 392 MN/m^2 (40 kg/mm^2). However, the mechanical characteristics of the niobium of cathode-ray remelting are considerably below. This confirm both results of our investigations and the data other authors [21]. It is obvious, in this case [20] occurred the saturation of metal by residual oxygen and nitrogen of air, which were being contained in test chamber.

It should be noted that the tests of niobium and tantalum generally undesirably to conduct at a pressure are higher than 1.33 sn/m^2 (10^{-4} mm Hg). If testing are subjected to especially pure refractory metals, then sometimes "washes" test chamber, after filling it with helium or argon, and then they conduct the repeated pumping out of the vacuum system of testing unit. A similar operation contributes to the decrease of the effect of gases on the properties of tested material.

In work [22] are generalized the results of the number of investigations and the conclusion is made that during mechanical

tests of refractory metals in vacuum deterioration in the material of specimen/sample is dissolved residual oxygen, contained in the medium of test chamber, and it strengthens it.

Therefore tests frequently are conducted "gradually" [20, 23]: to 700-900°C in the medium of argon, at the higher temperatures - in vacuum (Fig. 9).

It is necessary to note that even during short-time tests in argon or at dynamic vacuum such factors as duration of the preliminary check rate of climb of the temperature, the holding time in the heated state, the velocity of testing, significantly is determined the depth of the saturation of material by gases and is affected strength characteristics. However, in the procedures of short-time high-temperature tests [4, 24-26] are recommended the time of heating specimen/samples and the stabilizing holding from several minutes to half-hour, while work [25] gives the properties of niobium and molybdenum, obtained during tests in the medium of argon, the specimen/samples heating at a rate of 30-50 deg/s, and the stabilizing holding was 10-20 s.

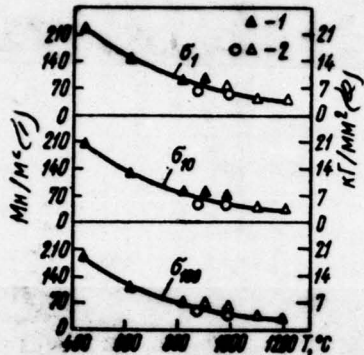


Fig. 9. The stress-rupture strength of niobium [31]: 1 - argon; 2 - vacuum.

Key: (1). MPa/m². (2). kg/mm².

Page 28.

Thus, by comparing the strength characteristics of refractory metals, it is necessary especially to thoroughly analyze test conditions.

The enumerated above factors play the significant role during the tests of refractory metals in the deformed nonannealed state. heating to the temperatures of recrystallization, i.e., to 800-1000°C

(for tungsten to 1400°C), with holding 20-30 min, as a rule, it leads to removal/taking of peening and stabilization of properties (to decrease of the scatter of the values of experiment). In the temperature range of recrystallization, mechanical properties strongly depend on the time of the determination of material in the heated state.

For the full/total/complete recrystallization of tantalum after cold strain with reduction 40% at temperature of 1350°C, is necessary the holding 14 min, and at 1400°C sufficient 3.5 min [1].

Minute holding at the temperatures, which considerably exceed the temperatures of recrystallization, lead to intense grain-growth. An increase in the duration of the holding of material at these temperatures, for example, to 5 min or to 10-15 min causes the small additional softening of material.

From foregoing it follows that the effect of inert medium, degree of dynamic vacuum is developed not only with prolonged ones, but also during short-time high-temperature tests. Consequently, it is necessary critically to be related to the results, obtained during the tests during which the delay time arbitrarily was changed within relatively wide limits, which sometimes is required for solving the special problems.

The test work the work-hardened refractory metals at the temperatures of recrystallization and several higher with different holding specimen/samples in the heated state, as a rule, it leads to the essential scatter of experimental data, and also impedes the comparison of the obtained results.

Effect of inert medium and vacuum.

The effect of inert medium and vacuum on the mechanical properties of refractory metals under the short-time effect of load was studied for niobium, molybdenum and tungsten. From these metals, as is known, most actively it interacts with medium the niobium, for which were carried out most thorough investigations.

The rods of cermet niobium subjected to two-fold cathode-ray remelting in the institute of the electric welding im. E. O. Paton.

Page 29.

Ingot 70 mm in diameter and 150 mm in length contained 0.002% O₂ and 0.004% N₂; it were rolled in the cold to sheets 7 and 1 mm in

thickness. The degree of strain for the sheets with a thickness of 1 mm composed ~95%.

For a comparison the strength indices were determined for cermet molybdenum in the form of sheets and rods, and also for the poured tungsten of vacuum-arc melting. The metals indicated contained on the average from 0.02 to 0.03% O₂ and N₂ (the chemical composition was given in Table 3).

As inert medium was utilized technical argon, which contained ~0.005% O₂ and ~0.05% N₂, without drying and special decontamination.

Determining mechanical characteristics was conducted during installation VTU-2V, consisting of testing machine SZF-1, working chamber, the system of vacuuming with pumps VN-2MG and N1-S2, heating system (in the packets of which enter bunchers ROT-25/0.5 transformer OSU-40 and heater with the system of shields), and also tools for measuring of temperature, strain and for the control of the work of the installation (in detail installation VTU-2V is described in Chapter V). Argon was supplied to the test chamber, pre-evacuated to 1.33 N/m² (10⁻² mm Hg) through the special four-way vacuum tap/crane. On the achievement of atmospheric pressure argon the tap/crane was covered and system they again evacuated, after which the

camera/chamber was charged by argon to overpressure 0.49-0.98 bar
atm(gage)
0.5-1.0 MN/m² (0.5-1 atm) and they began heating of specimen/samples.

Tests in vacuum were conducted at pressure 1.33 ^{SN} dyn/m² (10^{-4} mm Hg), inleakage into system was approximately 0.1 μ l/s.

Flat/plane specimen/samples were cut from sheet along direction of rolling, circular specimen/samples obtained by the machining of the molding/bars (form of specimen/samples was shown on Fig. 10). The velocity of the loading of specimen/samples on the average was 1-2 mm/min.

When conducting of specific tests, was utilized the ray heating of specimen/samples, since it is most widely common in the practice of mechanical tests. The average speed of stepped heating was 20-40 deg/min, continuous (rapid) heating - to 200 deg/min and more.



Fig. 10. Specimen/sample for mechanical tests.

Page 30.

Table 3. The chemical composition of the investigated refractory metals.
[graphic reads left to right]

(1) Наименование материала	(2) Содержание				
	Ре	Си	Nb	Al	Ti
(3) Вольфрам литой (вакуумно-дуговой плавки)	0,0035	0,002	—	—	—
(4) Вольфрам металлокерамический (кованный)	0,01	0,01	0,008	—	—
(5) Вольфрам литой (легированный)	—	0,002	—	—	—
W - 27% Re	—	—	—	—	—
Молибден литой (6)	—	—	0,001	0,001	—
Ниобий металлокерамический (7)	0,025	—	—	—	(7) До 0,1
Ниобий литой (8) (вакуумно-дуговой плавки)	—	—	—	—	—
Ниобий литой (9) (электронно-лучевой плавки)	0,02	—	—	—	0,01
Гантал литой (10) (электронно-лучевой плавки)	0,002	—	—	—	~0,003
BM-1	—	—	—	—	0,15
BN-2	—	—	—	—	—
Тантал (литой, (вакуумно-дуговой плавки)	0,002	—	—	—	—
Nb - 5% Mo . . .	0,073	—	—	—	0,14
Nb - 7% Mo . . .	0,1	—	—	—	0,05
Nb - 9,8% Mo . . .	0,03	—	—	—	0,03
Nb - 7% Mo - 10% Ti	0,028	—	—	—	10,0
Nb - 12% W . . .	0,028	—	—	—	0,005
Nb - 16% W . . .	0,02	—	—	—	0,05
Nb - 23% W . . .	0,007	—	—	—	0,048
Nb - 16% W - 1% Zr	0,02	—	—	—	0,05
Nb - 16% W - 0,5% Re	0,02	—	—	—	0,05

Page 31.

Tables 3 continued.

примесей, % (по массе)				
Ts	W	Nb	Zr	Cr
—	(13) Ochosa	—	—	—
—	.	—	—	—
—	.	0,02—0,05	—	—
—	.	—	—	—
—	—	—	—	—
—	—	(13) Основа	—	—
—	—	.	0,05	—
0,1	—	.	—	—
(13) Основа	—	0,003	—	—
0,01	0,6	—	0,1	0,003
—	—	96,05	—	3,8
—	—	0,003	—	—
0,62	—	(13) Основа	—	—
0,53	—	.	—	—
(5) До 0,1	—	.	0,03	—
0,60	—	.	—	—
0,40	12,5	.	0,02	—
1,0	16,0	.	0,05	—
0,30	23,1	.	0,06	—
0,50	—	.	1,07	—
0,50	—	.	—	—

Page 32.

Tables 3 continued.

[graphic reads left to right]

Наименование материала	Содержание			
	P	Si	Mo	Re
(14) Вольфрам литой (вакуумно-дуговой плавки)	0,002	0,01	—	—
(15) Вольфрам металлокерамический (кованный)	—	0,02	0,04	—
(16) Вольфрам литой (легированный)	0,002	—	0,06	—
W — 27% Re	—	0,008	—	—
Молибден литой (17)	—	—	Основа	—
Ниобий металлокерамический (18)	—	До 0,09	—	—
Ниобий литой (19) (вакуумно-дуговой плавки)	—	—	—	—
Ниобий литой (20) (электронно-лучевой плавки)	—	—	—	—
Тантал литой (21) (электронно-лучевой плавки)	—	—	—	—
ВМ-1	—	—	Основа	—
ВН-2	—	—	3,8	—
Тантал (литой, (вакуумно-дуговой плавки)	—	—	—	—
Nb — 5% Mo . . .	—	0,1	—	—
Nb — 7% Mo . . .	—	0,07	7,0	—
Nb — 9,8% Mo . . .	—	До 0,1	9,8	—
Nb — 7% Mo — 10% Ti	—	0,078	7,0	—
Nb — 12% W . . .	—	0,078	—	—
Nb — 16% W . . .	—	До 0,1	—	—
Nb — 23% W . . .	—	0,04	—	—
Nb — 16% W — 1% Zr	—	0,06	—	—
Nb — 16% W — 0,5% Re	—	0,007	—	0,50

Page 33.

Table 3 continued.

upmecen. % (no mass)					
C	O ₂	N ₂	H ₂	S	Pb
0,045	0,015	—	0,003	0,0012	—
0,015	—	—	—	—	—
0,035	0,013—0,017	—	0,002	0,006	—
0,035—0,045	—	—	—	—	—
~0,02	0,002	~0,001	~0,001	—	—
0,14	0,007	—	—	—	—
0,01	0,0045	0,01	<0,001	—	—
0,03	0,001	0,004	—	—	—
0,02	0,0005	0,002	0,0001	—	—
0,008	—	—	—	—	—
~0,05	<0,03	<0,04	—	—	—
0,02	0,005	0,002	0,001	—	—
<0,01	0,006—0,018	0,002—0,006	0,001	—	0,01
<0,01	0,005	0,003	0,001	—	0,003
0,003	0,003	0,001	0,001	—	—
0,013	0,006	0,004	0,001	—	—
0,03	0,004	0,002	0,001	—	—
0,011	0,011	0,002	5·10 ⁻⁴	—	—
0,02	0,013	0,003	0,001	—	—
0,018	0,005	0,003	0,001	—	—
0,018	0,005	0,003	0,001	—	—

Key: (1). Designation of material. (2). Impurity content, o/o (throughout mass). (3). Tungsten cast (vacuum-arc melting). (4). Tungsten cermet (forged). (5). Tungsten cast (alloyed). (6). Molybdenum cast. (7). Niobium cermet. (8). Ic. (9). Niobium cast (vacuum-arc melting). (10). Niobium cast (electron-beam melting). (11). Tantalum cast (electron-beam melting). (12). Tantalum (cast), (vacuum-arc melting). (13). Basis. (14). Tungsten cast (vacuum-arc melting). (15). Tungsten cermet (forged). (16). Tungsten cast (alloyed). (17). Molybdenum cast. (18). Niobium (cermet. (19). Niobium cast (vacuum-arc melting). (20). Niobium cast (electron-beam melting). (21). Tantalum cast (electron-beam melting). (22). Tantalum (cast, (vacuum-arc melting).

Page 34.

Temperature measured with thermocouples of the type KhA and PP whose joints are tightly contacted with the surface of specimen/sample in its middle part, for a check was utilized the optical pyrometer.

The gradient of the temperature in the cross section of circular specimen/samples during heating with different rates determined with the aid of the calibration specimen/sample, which had internal hole

2.5 mm in diameter for the input/introduction of additional thermocouple.

The velocity of the achievement of the assigned/prescribed temperature during stepped heating proved to be very low; for example, for the heating of specimen/sample to 1200°C, it was required by 30 min. This conditions/mode of heating it is reasonable to apply only during relatively low-temperature tests to the temperatures of recrystallization.

The conditions/mode of rapid heating makes it possible to obtain the assigned/prescribed temperature of specimen/sample in vacuum after 4-5 min at the average speed of heating 100-200 deg/min. (It must be noted that the rapid temperature rise in vacuum without the preliminary training of test chamber leads to pressure increase in it. The effect of medium on the heating time to the assigned/prescribed temperatures illustrates Fig. 11. Corrected values of the temperature, measured by the internal thermocouple of calibration specimen/sample).

The preliminary heating of furnace space and specimen/sample during 10-15 min with 200-300°C led to the decrease of the oscillation/vibrations of temperature on working section, temperature balance over the cross section of specimen/sample, and also to

DOC = 78133002

PAGE *2* 56

accelerated removal of gas made of test chamber; the average speed of heating was 200 deg/min and more.

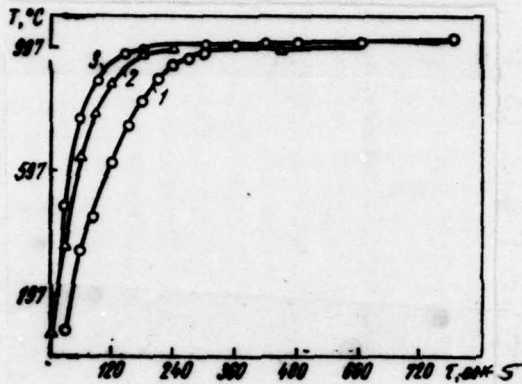


Fig. 11. The time of heating specimen/samples in different media (on internal thermocouple): 1 - vacuum 1.33 sn/m^2 (10^{-4} mm Hg); 2 - argon; 3 - helium.

Page 35.

Figures 12 shows the temperature distribution over the cross section of circular calibration specimen/sample during rapid temperature rise with the preliminary heating of furnace space and without it.

During heating of laminated specimen/samples 0.5-1.0 mm in thickness a difference in the temperatures over section/cut can be disregarded and counted that the temperature of specimen/sample is identical in all its points and is equal to the temperature of surface. Measurements showed that in this case it is possible to heat specimen/sample to testing temperature after 2-3 min [at pressure

1.33 sn/m² (10⁻⁴ mm Hg)].

For conducting short-time static tests for elongation, is proposed the following conditions/code of heating:

- 1) the slow increase of temperature during 10-15 min to 200-300°C;
- 2) rapid temperature rise to the assigned/prescribed values in vacuum during 2-5 min (in inert medium not more than 1-3 min);
- 3) holding at the assigned/prescribed temperature of 3-5 min in vacuum.

During the tests of the flat/plane and circular specimen/samples of niobium of cathode-ray remelting, made holding before the loading: 3, 10, 20, 30 and 60 min with 800, 1000 and with 1100°C, at prerecrysallization temperature, and also at the temperatures of beginning and end of the recrystallization.

A change of the limit of strength and elongation per unit length of laminated niobium in dependence on delay time before loading during tests in argon is represented in Fig. 13: in vacuum - in Table 4. In table and on graphs are given arithmetic mean values of results not less than five tests (for holding 30 and 60 min - three tests).

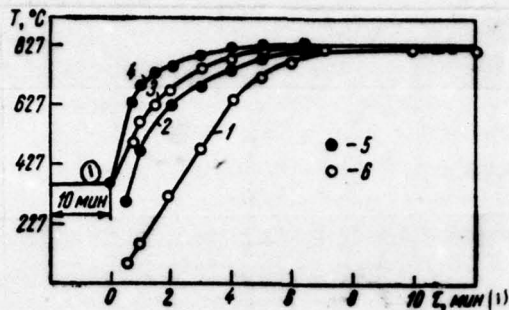


Fig. 12. The effect of the preliminary heating of electric furnace (10 min) on the temperature distribution over the section/cut of circular calibration specimen/sample during tests in vacuum 1.33 s^{-2} ($1 \cdot 10^{-4} \text{ mm Hg}$): 1, 2 - without heating; 3, 4 - with heating during 10 min; 5 - thermocouple on the surface of specimen/sample; 6 - thermocouple within specimen/sample.

Key: (1) . min.

Page 36.

Tests in argon showed that the limit of strength with 800°C somewhat falls with an increase in the duration of holding, that, apparently, it is possible to explain by partial relieving of stresses, caused by preceding cold working of material. At 1000°C increase in the holding to 30 min led to the increase of ultimate strength from 138 MN/m^2 (14 kg/mm^2) to 177 MN/m^2 (18 kg/mm^2).

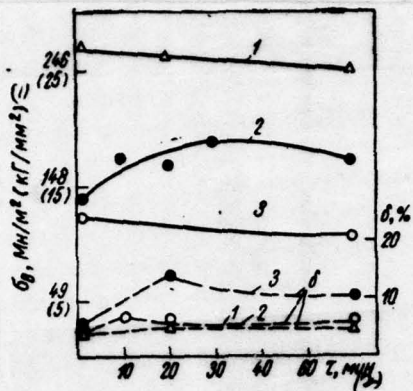


Fig. 13. The dependence of the limit of strength and elongation per unit length of laminated niobium on the duration of the holding of specimen/samples in the heated state during tests in argon: 1 - 800°C; 2 - 1000°C; 3 - 1100°C.

Key: (1) - MPa/mm^2 (kg/mm^2). (2) - min.

Table 4. Effect of holding before loading on the results of the high-temperature tests of niobium in vacuum [$p=1.33 \text{ sn/m}^2$ ($1 \cdot 10^{-4} \text{ mm Hg}$) the leakage of $0.1\text{-}0.2 \mu\text{l/s}$].

(1) Temperature, °C	(2) Время, мин	(3) $\sigma_{B, \text{ MN/m}^2}$ (kg/mm^2)	δ, %
1000*	5	148,0 (15,0)	7
	20	98,1 (10,0)	20
1100**	5	206,0 (21,0)	17
	20	143,0 (14,5)	16
1450***	5	123,0 (12,5)	—
	20	57,4 (3,8)	55

1. Sheet.

2. Rod 3 mm in diameter.

Key: (1). Temperature, °C. (2). Holding, min. (3). MN/m² (kg/mm²).

Page 37.

At the same time during tests in vacuum, as can be seen from Table 4, ultimate strength with an increase in the delay time to 20 min was decreased to 98.1 MN/m^2 (10 kg/mm^2).

The increase of the limit of strength with indicated 1000°C of the evidently, caused by the saturation surface layers of specimen/sample by residual gases, which are contained in argon. As

is known, oxygen and nitrogen even with content of 0.005-0.007% form the brittle phases of implementation on boundaries of the grains of BCC metal and thereby they change its mechanical properties. Figures 4 shows the dependence of the limit of the strength of niobium from the temperature at different oxygen concentrations [27]; an increase in oxygen concentration from 0.001 to 0.02% leads to considerable increase in strength at 500°C.

The saturation by residual gases of the surface layers of niobium during testing in argon was judged by a change of the microhardness in different points of the cross section of specimen/samples after testing. The results of measurements are represented in Fig. 15 and 16. The original value of microhardness was 1350 MN/m² (135 kg/mm²). The most intense saturation of material occurred with 1000 and 1100°C and to holding 20 min in argon. The depth of saturation with 1000°C varied from 0.1 mm after holding 3 min to 1.0 mm after 30 min. The volume of the material, saturated by gases, after holding 20 min at 1000°C composed ~50% of entire volume of the working section of flat/plane specimen/sample, and after 3 min - only 10-15%.

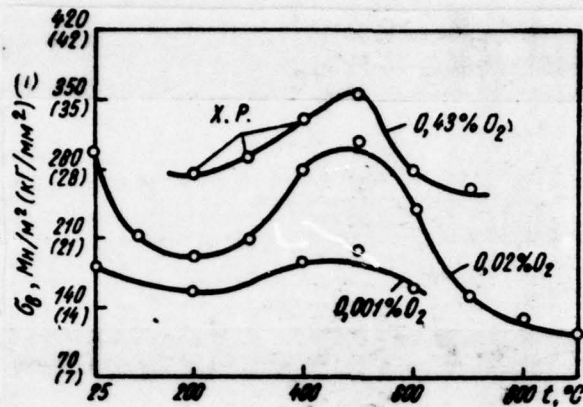


Fig. 14. The dependence of the limit of the strength of niobium from the temperature at different oxygen concentrations [27]: Kh. R. - brittle failure.

Key: (1) - MN/m² (kg/mm²).

Page 38.

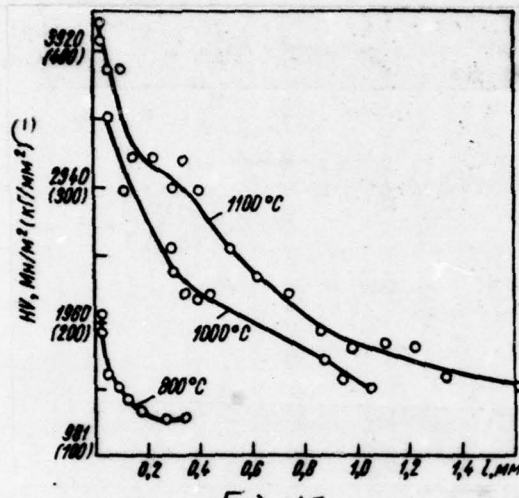


Fig. 15.

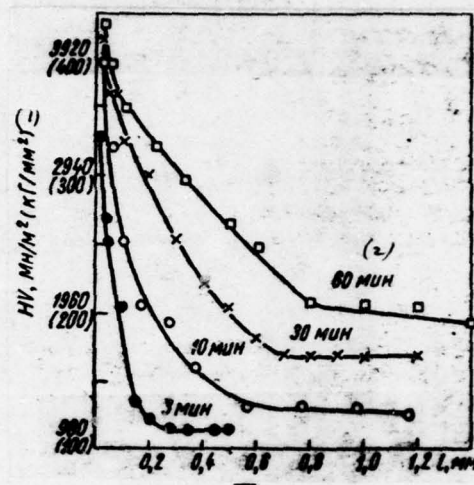


Fig. 16.

Fig. 15. Change in microhardness in cross section of specimen/samples of niobium after testing in argon at different temperatures with holding before loading 20 min.

Key: (1) - HV, MN/mm² (kg/mm²).

Fig. 16. Change in microhardness of nickel in depth of cross section after testing in argon with 1000°C with different holding before loading.

Key: (1) - HV, MN/mm² (kg/mm²).

Page 39.

The analysis of the microstructure of specimen/samples after testing with 1000°C showed (Fig. 17) that in the central zone of specimen/sample begins the recrystallization, whereas on surface it is braked due to saturation by residual gasses.

One should note (see Fig. 13) that the duration of holding with 1100°C exerts on the characteristics of strength and plasticity of laminated niobium the smaller effect than at 1000°C that, apparently, it is caused by the more intense saturation of material by residual at 1100°C gases.

The discovered laws will agree with the literature data on the effect of oxygen, nitrogen and other gases on the strength of niobium [21, 22].

The effect of the composition of protective medium on the results of the test of the specimen/samples of laminated niobium is represented in Fig. 18. The values of ultimate strength in the range of the temperatures from 800 to 1100°C at the duration of holding to 3 min are identical during tests in vacuum and argon.

The results of the test of niobium in forevacuum 6.65 N/m²

DOC = 78133002

PAGE 28 66

(5×10^{-2} mm Hg) testify against the effects of the residual gases:
ultimate strength is increased.

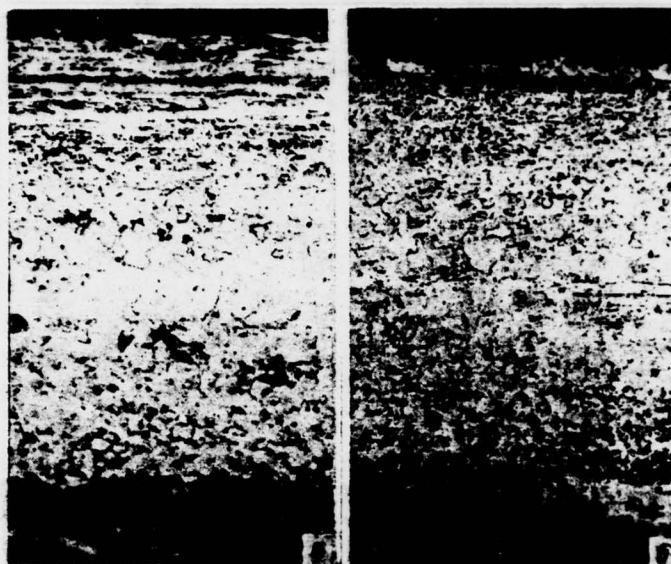


Fig. 17. Microstructure of niobium (x100) after testing in argon: a) 1000°C 30 min; b) 1100°C 20 min.

Page 40.

Thus during the high-temperature tests of niobium (or tantalum) in argon with short-time holding (1-3 min) before loading the saturation of the surface of specimen/samples by residual gases does not insignificantly and virtually affect test results. An increase in the duration of holding more than 5 min contributes to the considerable saturation of tested material by gases and leads to a change in its mechanical properties.

The effect of the delay time of specimen/samples in the heated state on their mechanical properties during testing in argon and vacuum was studied also for the molybdenum, obtained by the method of powder metallurgy.

The results, presented in Fig. 19, attest to the fact that with 800 and 1100°C values of ultimate strength barely depend on delay time. This is explained by the fact that the molybdenum, unlike niobium, is not virtually saturated by gases. On the surface of specimen/samples, is formed the fine/thin oxide film which is cracked in the process of deformation. Cracks on the working section of specimen/sample are well noticeable after testing with 1100°C.

After testing in argon with 1000°C with holding from 10 to 60 min, they observed a small increase in the microhardness on the surface of laminated molybdenum specimen/samples ~2950 MN/m² (300 kg/mm²) [hardness in the middle of specimen/sample was equal to initial, i.e., 2500 MN/m² (254 kg/mm²)].

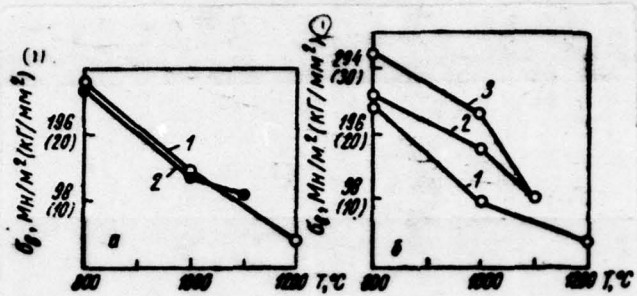


Fig. 18. The temperature dependence of the limit of the strength of molybdenum during testing in different protective media: a) 3 min, b) 20 min; 1 - vacuum $1.33 \text{ sn/m}^2 (10^{-4} \text{ mm Hg})$; 2 - argon; 3 - forevacuum $6.65 \text{ N/m}^2 (5 \cdot 10^{-2} \text{ mm Hg})$.

Key: (1). $\text{MN/m}^2 (\text{kg/mm}^2)$.

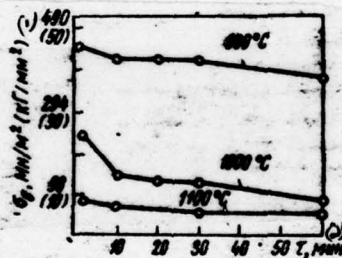


Fig. 19. Dependence of limit of strength of molybdenum from holding time before loading during tests in argon.

Key (1). $\text{MN/m}^2 (\text{kg/mm}^2)$. (2). min.

Changes in the microhardness of the specimen/samples of molybdenum in the depth of cross section after testing in vacuum did not observe (Fig. 20).

The decrease of the limit of the strength of molybdenum with 1000°C with an increase in the delay time to 10 min (see Fig. 19), apparently caused by the development of recrystallization.

Molybdenum testings in vacuum 1.33 sn/m^2 (10^{-4} mm Hg), carried out in circular specimen/samples 3 mm in diameter, they showed, that an increase in the delay time before loading leads to the decrease of the values of ultimate strength and the increase of plasticity (Table 5).

Form of fracture of specimen/samples also depends on the holding time. (In the process of tests specimen/samples photographed with the aid of special photographic attachment). During the deformation of molybdenum after holding 5 min at 1450°C on the surface of specimen/sample in the zone of neck, observed small small cracks; fracture was fibrous.

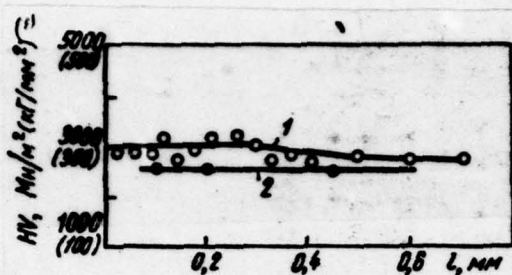


Fig. 20. A change in the microhardness in the depth of the cross section of the specimen/samples of molybdenum after the testing: 1 - in argon with $t=1000^{\circ}\text{C}$; 2 - in vacuum $1.33 \text{ sn/mm}^2 (10^{-4} \text{ mm Hg})$ with $t=1100^{\circ}\text{C}$.

Table 5. Effect of the duration of holding on the mechanical properties of cermet molybdenum during tests in vacuum ($p=10^{-4}$ torr).

Длительность выдержки, мин перед нагреванием при 1450°C	(1) σ_b , MN/mm² (kg/mm²)	(2) K
3 20	200.0 (14) 98.1 ($\times 10$)	30 45

Key: (1). Delay time, min before loading with 1450°C . (2). MN/mm^2 (kg/mm^2).

Page 42.

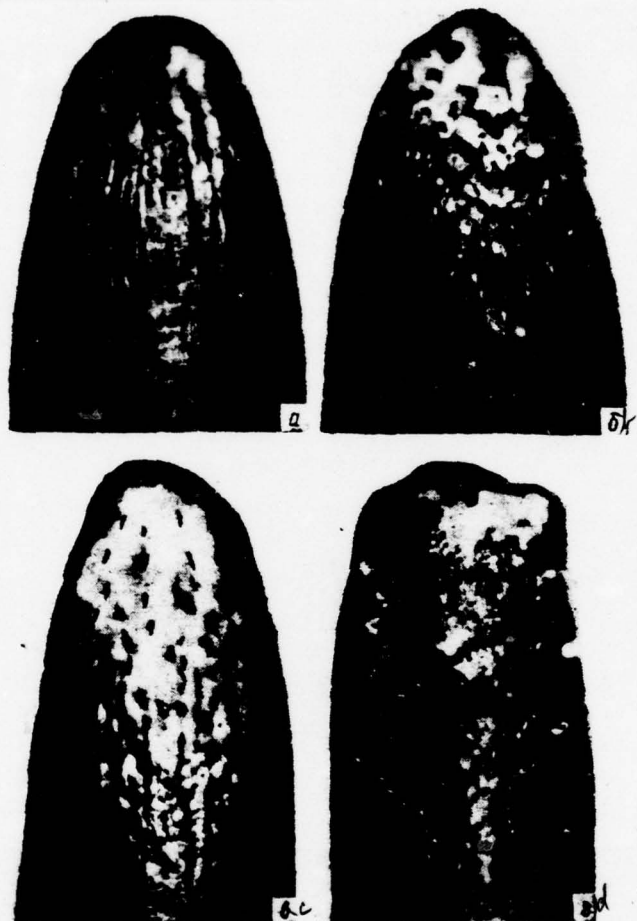


Fig. 21. Form of fracture of specimen/samples of molybdenum after testing in argon:

Время испытания до разрушения	(1) Температура испытания	
	1200°C	1400°C
5 мин	•	•
20 мин	•	•

Key: (1). Testing temperature. (2). Time of test to destruction. (3). min.

Page 43.

After holding 20 min at the same temperature over the surface of specimen/sample in the zone of maximum strain, were spread sufficiently large cracks. At 1400°C development of cracks occurs avalanche-type and they occupy almost entire working section of specimen/sample (Fig. 21).

Macrofissures were developed analogously in the process of the deformation of cermet niobium, while on the surface of the niobium of the cathode-ray remelting of cracks it was not.

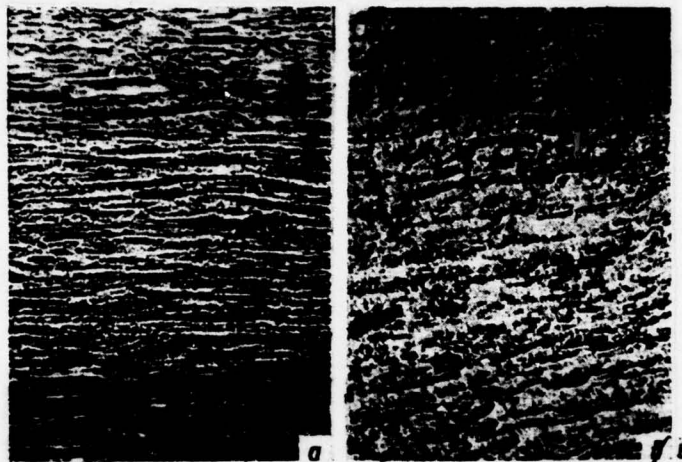


Fig. 22. Microstructure of the specimen/samples of tungsten (x200) after testing in vacuum with 1500°C with holding before the loading: a) 5 min; b) 20 min.

Table 6. Effect of the duration of holding on the mechanical properties of the poured forged tungsten during tests in vacuum [$p=1.33 \text{ sn/m}^2 (1 \cdot 10^{-4} \text{ mm Hg})$].

Температура испытания, °C	(1) Выдержка, мин	(2) σ_{B} , $\text{Mn/m}^2 (\text{kg/mm}^2)$	(3). %
1500	5	314 (32)	10
	20	246 (25)	11
1700	5	114 (11,6)	40
	20	108 (11,0)	42

Key: (1). Testing temperature, by °C. (2). Holding, min. (3). MN/m^2 (kg/mm^2).

Page 44.

The results, presented in Table 6, show that an increase in the delay time from 5 to 20 min at testing temperature by 1500°C leads to a reduction in the limit of the strength of the poured tungsten. This is caused by the development of recrystallization (Fig. 22). At the higher temperatures of the duration of holding, does not exert so noticeable an effect on the strength of tungsten.

Effect of the carbon-containing medium.

When conducting of mechanical tests, fairly often are utilized carbon-graphite materials as the heating elements of high-temperature furnaces. This leads to the fact that at high temperatures appears the carbon-containing medium and occurs the diffusion saturation of the surface of tested metal by carbon, and also the formation of carbide films.

In the literature there are data [4, 21, 23] on the reaction of refractory metals with carbon, and also on the effect of carbon on the properties of the refractory metals, heated in furnaces with graphitic cell/elements [21, 26].

According to these data, the intense saturation of refractory metals by carbon begins from 1400°C, in this case, are formed fine/thin carbide films, in essence on boundary/interfaces to grain boundaries. Further increase of temperature to 1700-2000°C causes the intensification of diffusion processes, which leads to the considerable carbidizing of the surface of material. It was also shown, that the oxygen content in the refractory metal, heated in vacuum furnace with graphitic cell/elements, noticeably is decreased, beginning from 1300°C. The phenomenon indicated is explained by the course of the reducing reaction of formation of carbon monoxide in the course by which oxygen is eliminated from metal.

Mordayk [23] considers that as a result of the diffusion of vapors of carbon from graphitic heater in tested material is formed the eutectic the melting point of which is considerably lower than for a base metal. Therefore the temperature range of tests in furnaces with graphitic cell/elements is limited, maximum temperature for tungsten equal to 2000°C, for molybdenum - 1700°C, for niobium - it is still below. The saturation of metal by carbon occurs at lower temperatures; however, it is assumed [23], that the occurring with this carbidizing insignificantly affects strength.

In the work of Marmer [26] is made the conclusion about the possibility of applying the graphitic heaters in vacuum furnaces for the melting of refractory metals.

By form, the literature data on the effect of heating in furnaces with graphitic cell/elements to the high-temperature mechanical properties of high-melting materials bear contradictory character.

Page 45.

For explaining the degree of this effect in the institute of the problems of the strength of AS UkrSSR, were carried out the mechanical tests of refractory metals during heating in furnaces with graphitic and tungsten cell/elements.

Chemical composition of the investigated materials is given in Table 7.

Hardness HV was measured at room temperature, after holding 10 sec at the assigned/prescribed temperature.

The strength characteristics and the plasticity of materials were determined during installation with the ray heating of specimen/sample.

were utilized tungsten and graphitic heaters with the volume of the furnace space $V=30 \text{ cm}^3$, heating was realized/accomplished in the medium of technical argon (0.006% N₂, 0.003% O₂, $<0.01\%$ CO₂) and in vacuum 3.99 mN/m^2 ($3 \cdot 10^{-5} \text{ mm Hg}$).

The character of a change of the hardness of the surface of the specimen/samples of molybdenum and tantalum as a result of reacting of material and gaseous medium, depending on the heating temperature, they illustrate Fig. 23 and 24.

The analysis of the results of measurements showed that temperature dependence $HV=f(T)$ for commercially pure molybdenum is virtually identical for short-time heating in pure argon and in vacuum.

Table 7. The chemical composition of the materials, used during the analysis of the effect of the carbon-containing medium on strength.

Материал	(2) Содержание элементов, %				
	Al	Fe	Si	Mg	Mn
Ниобий . . . (3)	~0,003	1,0	0,3	0,002	0,001
Тантал . . . (4)	—	0,01	0,005	0,001	—
Молибден . . . (5)	—	>0,1	0,05	0,003	0,001
Вольфрам . . . (6)	—	0,01	0,03	0,001	—
Сплав ЦМ2А (7)	—	0,01	0,05	0,001	—

Материал	(2) Содержание элементов, %					
	Ta	Tl	Nb	Sn	Cr	C
Ниобий . . . (3)	>0,03	0,07	Ост.	—	—	0,014
Тантал . . . (4)	Ост.	>0,1	0,05	0,001	0,01	0,016
Молибден . . . (5)	—	—	—	—	0,008	—
Вольфрам . . . (6)	—	—	—	0,001	0,001	0,016
Сплав ЦМ2А (7)	—	—	—	—	0,001	0,017

Key: (1). Material. (2). Content of cell/elements, o/o. (3). Niobium.
(4). Tantalum. (5). Molybdenum. (6). Tungsten. (7). Alloy TsM2A.

Page 46.

Tantalum absorbs oxygen and nitrogen, which are contained in technical argon, and because of this its hardness grow/rises (see Fig. 24). Temperature dependence of adsorption of oxygen by tantalum is subordinated to parabolic law, beginning from 480°C [22], adsorptions of nitrogen - from 800°C [27], moreover rate constant

continuously is increased with increase of temperature. The decrease of the adsorption of nitrogen becomes noticeable, beginning from 1500°C.

Carbon from graphitic heater binds residual oxygen, which is found in argon, creates reducing agent, saturates the surface of specimen/sample. The strengthened/hardened action/effect of carbon is proved to be greater than nitrogen and oxygen. Analogous data are interlocked in [22].

The effect of carburization was checked during the tests of specimen/samples by unidirectional tension in the medium of argon. The results of determining the temperature dependence of strength and plasticity of molybdenum are given to Fig. 25, tantalum - to Fig. 26.

The characteristics of high-temperature strength of molybdenum in the cases of the graphitic and metallic heater (see Fig. 25) almost coincide; however, the characteristics of plasticity prove to be themselves considerably above during heating of specimen/sample in the carbon-containing medium. This tendency more visually is developed in the temperature dependence of the mechanical properties of tantalum (see Fig. 26).

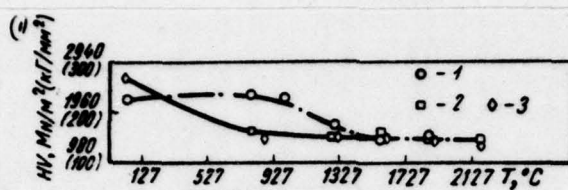


Fig. 23. A change of the hardness of molybdenum after 10 min of heating in different media: 1 - graphitic heater; 2 - technical argon; 3 - vacuum 1.33 MN/m^2 ($1 \cdot 10^{-5} \text{ mm Hg}$).

Key: (1). HV, MN/m² (kg/mm²).

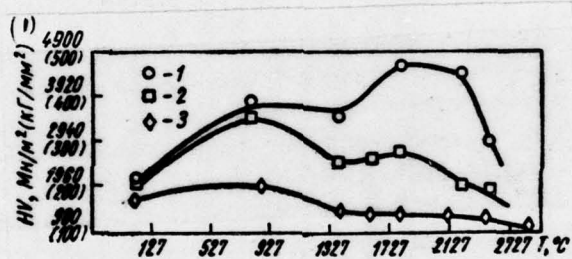


Fig. 24. Change of hardness of tantalum after 10 min of heating in different media (designation - see Fig. 23).

Key: (1). HV, MN/m² (kg/mm²).

Page 47.

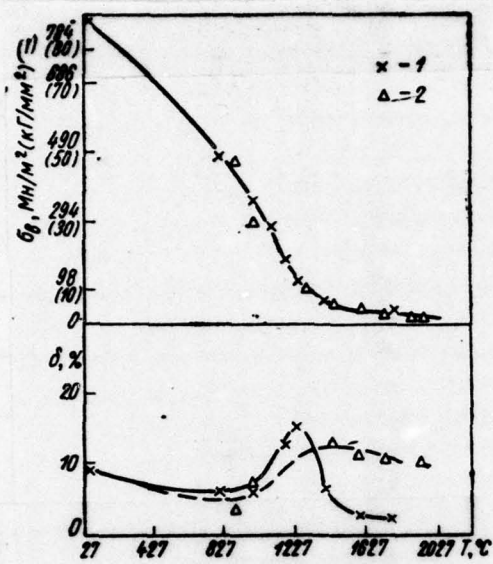


Fig. 25.

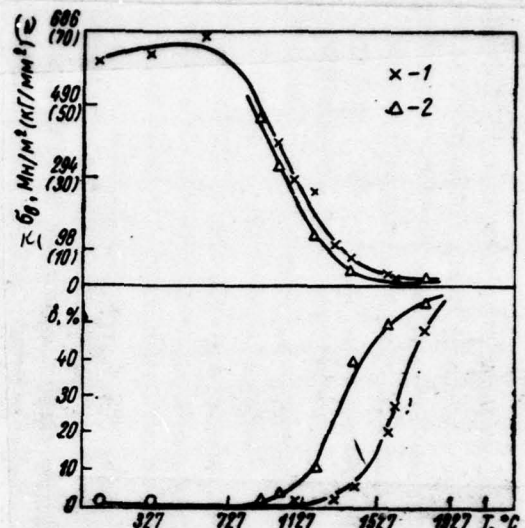


Fig. 26.

Fig. 25. Dependence of strength and plasticity of laminated molybdenum on temperature: 1 - metallic heater; 2 - graphitic heater.

Key: (1) - MN/m² (kg/mm²).

Fig. 26. Dependence of strength and plasticity of laminated tantalum on temperature (designation - see Fig. 25)..

Key: (1) - MN/m² (kg/mm²).

Page 48.

The effect of the increase of plasticity can be explained by the bonding of oxygen, dissolved in the surface layers of metal, during reaction with carbon. The thickness of the restored/reduced layer during short-time tests is insignificant, and therefore on the strength characteristics reducing agent has smaller effect.

A sharp increase of the plasticity of molybdenum and tantalum when $\frac{T}{T_{m\alpha}} \geq 0.4$ that observed in the presented curve/graphs, usually bind with the recrystallization, during which is remove/taken technological strengthening of cold-rolled material. Analogous effects were reveal/detected during the investigation of the temperature dependence of the mechanical properties of other refractory metals.

The laminar spectral analysis of the specimen/samples, tested in graphitic heater with 1600°C, showed that the surface layers of material (not deeper than 50 μm) contain carbon 5-8 times more than center.

The metallographic analysis of the annealed niobium also testifies to the diffusion penetration of carbon into the surface layers of specimen/sample (Fig. 27).

The results of determining the characteristics of strength and plasticity of the laminated tungsten, tested in metallic and graphitic heaters in the medium of argon, are represented in Fig. 28 and 29. For tungsten is confirmed previously discovered effect of the increase of plasticity and decrease of the strength of refractory metals during the utilization of graphitic heater [28].

From given data it follows that the intense saturation of refractory metals by carbon occurs at 1600-1800°C. Carburizing begins at the temperatures higher than 1200-1300°C. The utilization of graphitic cell/elements leads to a change in mechanical characteristics of refractory metals even during short-time tests; these heaters one ought not to apply at temperatures higher than 1200°C.

Graphitic cell/elements successfully can be utilized for heating of specimen/samples made of high-melting carbides and other oxygen-free compounds.

The investigated materials contained a considerable quantity of interstitial impurities which impeded the development/detection of the effect of the saturation of metal by the cell/elements of furnace atmosphere.

DOC = 78133002

PAGE -37 85

The effect of initial impurity/admixtures was investigated for annealed cermet tantalum during testing in vacuum with the utilization of a metallic heater.

Page 49.

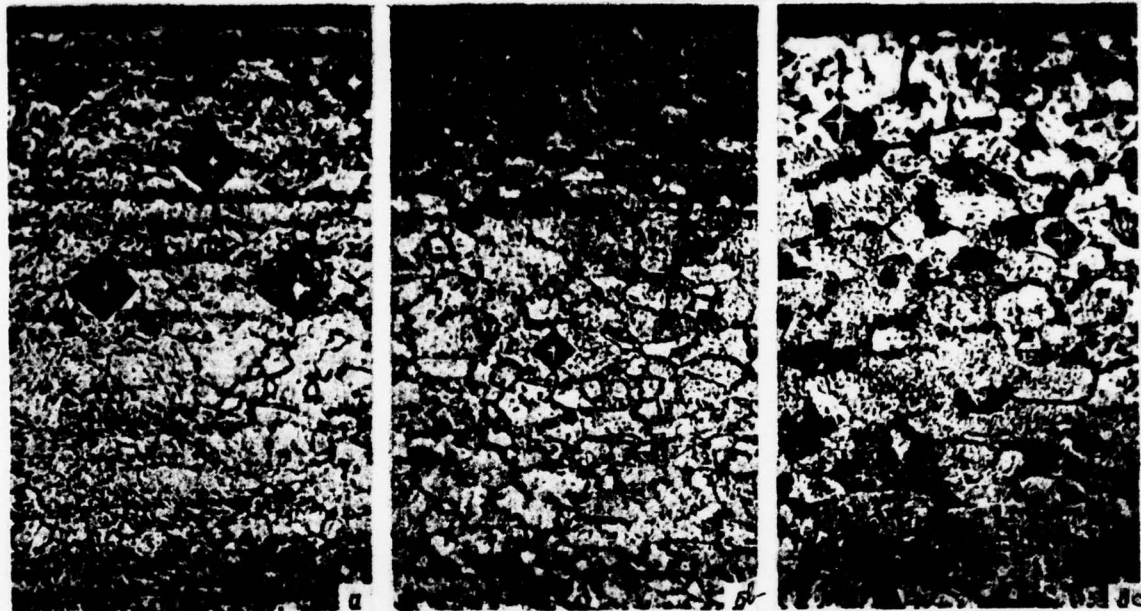


Fig. 27. Microstructure of annealed niobium (x500) after 10 min of heating in graphitic heater: a) 900°C; b) 1200°C; c) 1800°C.

Page 50.

[Conditions/mode of the annealing: $t=1380^{\circ}\text{C}$, $\tau=1$ h, $p=10^{-4}$ torr, hardness after annealing $HV=1176-1275$ cf MN/mm^2 ($120-130$ kg/mm 2)].

The temperature dependence of the mechanical properties of annealed tantalum is shown on Fig. 30.

The range of temperatures of 200-600°C they observed the stabilization of strength and reduction in the plasticity of tantalum, which, apparently, is caused by strain aging [27].

The analyses of the effect of the carbon-containing medium on the mechanical properties of refractory metals were carried out also for the pre-carbidized molybdenum. Specimen/samples made of laminated molybdenum of technical purity/finish 0.5 mm in thickness subjected to diffusion saturation by carbon. For this, were assembled the piles of four specimen/samples whose nose sections are insulated by packing from molybdenum.

Diffusion saturation by carbon was conducted in the chucks, filled with graphitic grist (or lamp black). (Procedure of saturation is in detail presented in work [29].) Chucks were fed into Tamman furnace and they heated to 1450°C with holding 1 h. As a result on the working section of specimen/sample, were obtained surface films Mo₂C with thickness 0.02-0.03 mm, closely fitted to basis. During heating to 1600°C with the holding 1 h of film in specimen/samples, they had thickness 0.12 mm. Figures 31 gives the typical microstructures of specimen/samples with diffusion carbide coating. For comparative tests part of the initial specimens of molybdenum

they annealed at 1450°C for 1 h in vacuum 13 sn/m² (10⁻⁵ mm Hg).

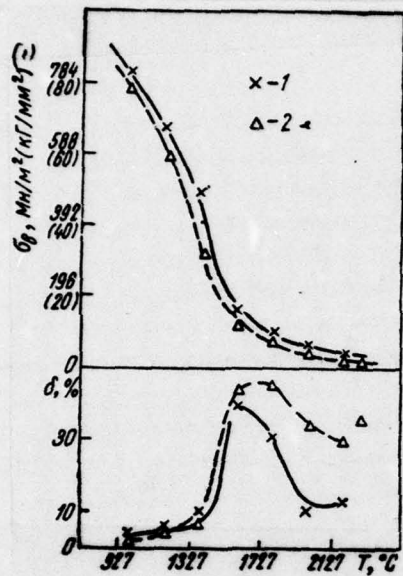


Fig. 28. Dependence of strength and plasticity of laminated tungsten on temperature (designation - see Fig. 25).

Key: (1) - MN/m² (kg/mm²).

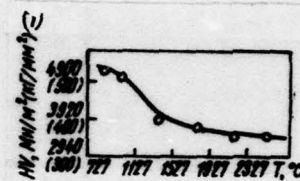


Fig. 29.

Fig. 29. Change of hardness of laminated tungsten after holding 10 min in graphitic heater.

Key: (1) - HV, MN/m² (kg/mm²).

Page 51.

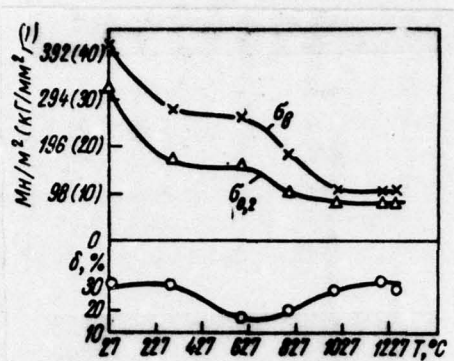


Fig. 30. Dependence of strength and plasticity of annealed tantalum on temperature.

Key: (1). M_N/m^2 (kg/mm^2).

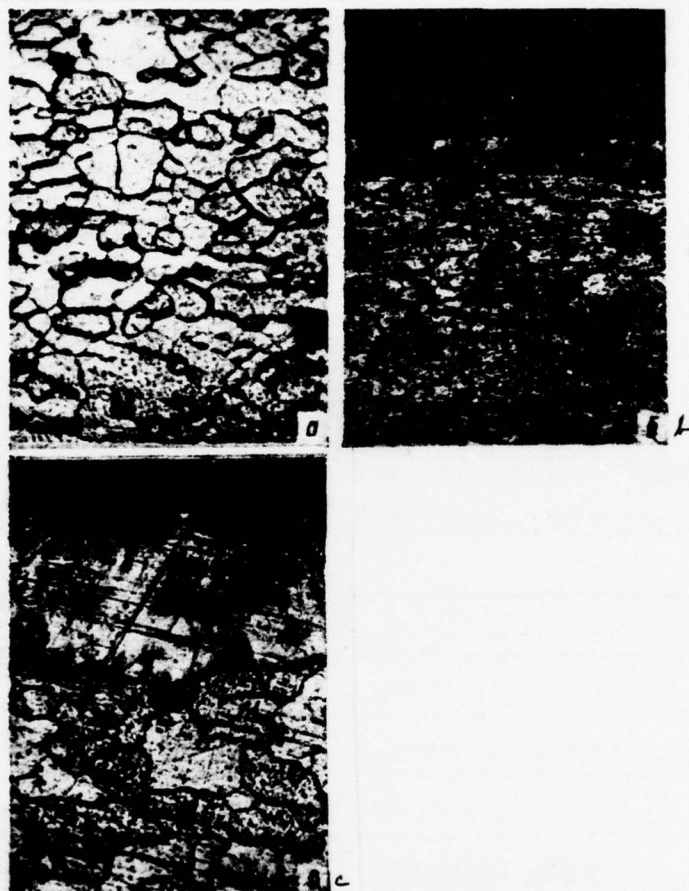


Fig. 31. Microstructure of specimen/samples of molybdenum with coating Mo_2C of various thickness: a) annealed at 1450°C for 1 h in vacuum; b) film approximately 0.03 mm in thickness; c) the same, ~0.12 mm x200.

The results of the strength tests of the annealed and covered with carbide film molybdenum are given to Fig. 32. From these data it is evident that the strength of molybdenum with carbide film 0.02-0.03 mm at 1200-1400°C by 10-15% is higher than the strength of the annealed molybdenum; with further increase of temperature, this difference is decreased. An increase in the thickness of the film Mo_2C up to 0.1 mm leads to reduction in the strength and the sharp decrease of plasticity. An increase in the plasticity of specimen/samples with film ~0.03 mm with 1600°C can be explained by certain decarbonization of the surface layer of specimen/sample at this temperature (tests are carried out in vacuum).

In the process of deformation, occurred disturbance of the continuity of material, at the working section of specimen/sample, appeared the cross cracks (Fig. 33). They were spread over an entire surface of specimen/sample.

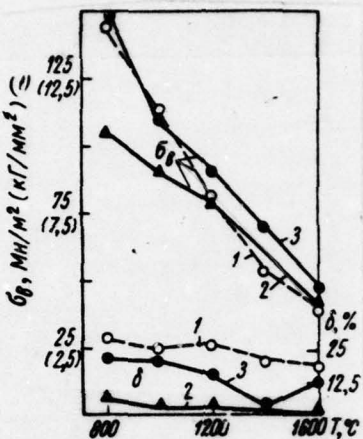


Fig. 32. Temperature dependence of limit of strength and plasticity of molybdenum: 1 - after annealing with 1450°C, for 1 h; 2 - with coating Mo_2C with thickness ~ 0.12 mm; 3 - the same, 0.03 mm.

Key: 1(1). MN/m^2 (kg/mm^2).

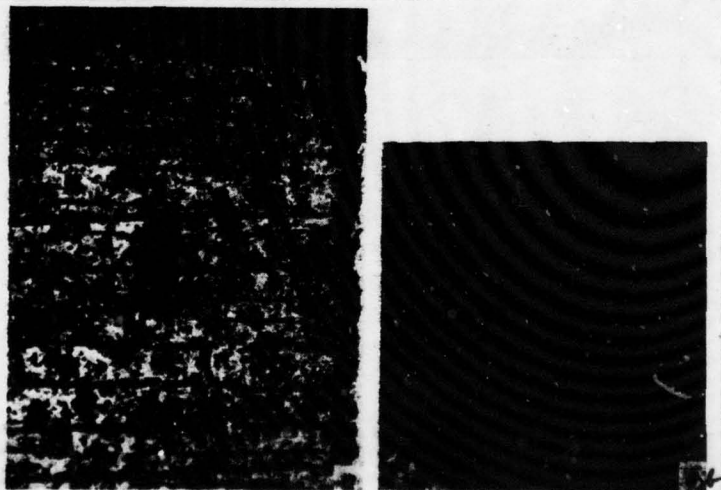


Fig. 38. Appearance of specimen/sample of molybdenum with coating

AD-A066 482

FOREIGN TECHNOLOGY DIV WRIGHT-PATTERSON AFB OHIO
STRENGTH OF REFRACTORY METALS. PART I, (U)
OCT 78 G S PISARENKO, V A BORISENKO

F/G 11/6

UNCLASSIFIED

2 OF 5
AD
AD66482

FTD-ID(RS)T-1330-78-PT-1

NL





0.03 mm in thickness after testing with 1000°C: a) x15; b) x350.

Page 53.

The separate strips of brittle film were moved on the plastic basis of specimen/sample. It must be noted that the cracks appeared at the initial stage of deformation, into the depth of material, they were not spread and, as can be seen from curve/graph in Fig. 32, on strength noticeable effect is did not had.

Thus, low-plasticity surface film up to 0.03 mm in thickness several increases ultimate strength and noticeably it descends the value of the elongation per unit length of molybdenum. Carbide films by thickness ~0.12 mm contain sufficiently many large flaw/defects in the form of inclusions and pores (see Fig. 31), moreover the volume, occupied with brittle film, composes ~50% of the volume of specimen/sample and therefore thick film is had more noticeable effect on the strength indices and plasticity.

The obtained results will agree well with the literature data on the behavior of brittle surface films on stainless steel and titanium [29].

Effect of oxidizing medium.

In recent years considerably increased the interest in the analysis of high-melting materials under conditions, maximally approaching operational ones, in particular in oxidizing medium at the unsteady thermal conditions and pressures.

For conducting such experiments, is created the installation, which makes it possible to conduct research in the specific routines of a change in the temperature and pressure oxidizing medium [30].

Installation consists of vacuum chamber, system of heating specimen/sample, which loads the systems also of the regulator of the conditions/modes of a change in the pressure (Fig. 34).

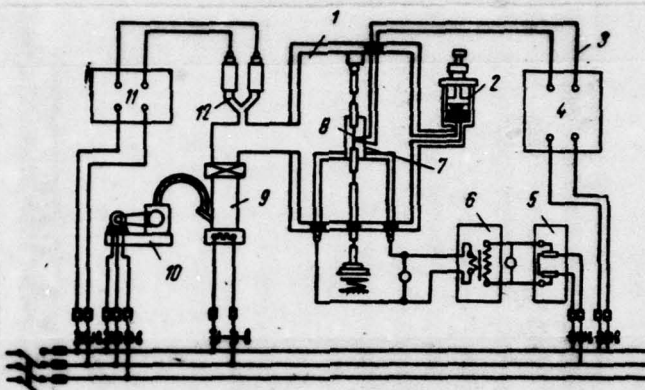


Fig. 34. The installation diagram for the analysis of the effect of temperature and oxidizing medium on strength refractory metals.

Page 54.

Vacuum chamber 1 is covered by the flap, packed by rubber packing. In the upper part of the rear wall, is arranged/located the connecting piece, which connects the camera/chamber with 9 types diffusion pump H1-C2. The forevacuum provides 10 types fore pumps RVN-20. Vacuum is measured with the aid of the manometric lamps of 12 types LT-2 and LN-2 and of 11 types vacuum gauges VIT-1A.

Test specimen is heated to the assigned/prescribed radiation temperature from laminated heater 7 (manufactured from the same refractory metal, as the specimen/sample which is fastened to the copper water-cooled shoes, attached at the ends of copper current

inlets. The clearance between the ends of heater is arranged/located against inspection window in cap/cover, which makes it possible to control the process of specimen/sample testing.

The temperature of specimen/sample is regulated according to predetermined program with the aid of control instruments and voltage regulator 5 of type RNC-250/10, voltage from which is supplied to 6 types step-down transformer OSU-40.

Temperature is measured by platinum or tungsten-rhenium thermocouple 3 and potentiometer 4 of type EPP-09M.

Specimen/sample they load, after filling with water the container which is suspend/hung to the thrust/rod, connected with lower movable capture.

Specimen/sample with 8 has the size/dimensions of working section/cut 5x1 mm and common/general/total length 65 mm, it is fastened to captures by tungsten pins. The axiality of load is provided with the aid of the special centering device.

For maintenance in the camera/chamber of the necessary pressure level oxidizing medium or for changing it by given program there is developed the special regulator of vacuum conditions/modes 2, which

DOC = 78133002

PAGE ~~49~~ 97

is represented in Fig. 35.

As the basis of its construction/design, is placed the principle of the operation of vacuum flow regulators [31], used in industrial vacuum systems.

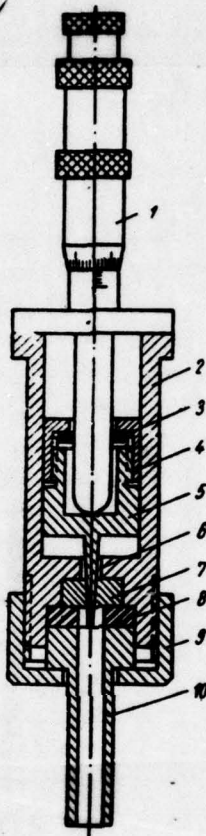


Fig. 35. Device for the batching of a quantity of air in the camera/chamber.

Page 55.

Within cylindrical housing 2, is moved in vertical direction needle 6, grooved together with insert 5 of tool steel. Insert is connected dismountable/release with cap/cover 4, by freely sponsor on

disk 3 which is rigidly connected with micrometer 1. Needle in the form of frustum with apex angle 6 deg and the diameter of basis/base 3 mm tightly enters in saddle 7, manufactured from lead. The site of the joint of saddle with regulator housing is packed with the aid of rubber packing by 8, branch 10, employe it is simultaneous for the connection of regulator with vacuum chamber of installation, and adapter nut 9.

Micrometer makes it possible to conduct the preliminary calibrating of the entering the camera/chamber air flow, and also the rate of pressure increase through predetermined program in dependence on range of needle. This is especially important when is required strict reproducibility of the cycle of unsteady vacuum conditions/mode.

With the aid of the described installation was studied the effect of oxidizing medium and temperature on the bearing capacity of the laminated molybdenum of the mark/brand МБН and laminated niobium. (By the bearing capacity of material was understood the load, in reference to the unit of the original cross-sectional area of specimen/sample, which the latter is able/held during this steady or unsteady vacuum- temperature state without decomposition). Research were conducted with 1000, 1100, 1200, 1500 and by 1800°C. Pressure in the camera/chamber was measured from 1.33 MN/m² to 98 kN/m² (10⁻⁵ to

760 mm Hg).

During steady states of tests the specimen/sample was age/held during 10 min at appropriate temperature and a pressure, and then was loaded and was carried to failure.

The findings on a change of the bearing capacity of laminated molybdenum in dependence on the degree of evacuation/rarefaction and temperature of testing are represented in Fig. 36.

The character of curves attests to the fact that a reduction in the bearing capacity of laminated molybdenum is proportional to temperature and pressure. In the range of pressures $1.33 \text{ MN/m}^2 - 1.33 \text{ daN/m}^2$ ($10^{-5}-10^{-1}$ mm Hg) the bearing capacity of molybdenum virtually remains constant/invariable for all values of temperature accepted. Further pressure increase leads to the intensification of oxidation processes, cross size decrease in connection with volatility of generating oxides and as consequence, to a considerable reduction in the bearing capacity.

In the curves (see Fig. 36) are noticeable the characteristic critical points, which correspond to the pressure whose excess at this temperature substantially affects the bearing capacity of molybdenum. For example, at 1500°C characteristic is the point, which

DOC = 78133002

PAGE ~~53~~ /101

corresponds to pressure 1.33 daN/m^2 (10^{-1} mm Hg); for 1200°C - 1.33 H/m^2 (1 mm Hg).

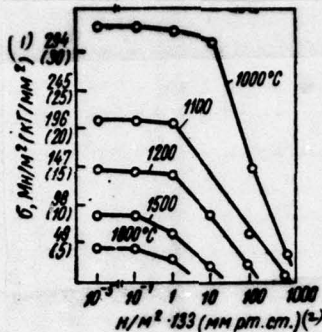


Fig. 36. Effect of temperature and pressure on the bearing capacity of molybdenum.

Key: (1) - MN/m² (kg/mm²). (2) - (mm Hg).

Page 56.

The process of high-temperature oxidation especially violently proceeds at the pressure, close to atmospheric; in this case, intensely is vaporized trioxide of molybdenum, open/disclosing to air access to the virtually unprotected surface of metal. Is decreased the section/cut of specimen/sample and its bearing capacity. So, at 1200°C and a pressure 13 kN/m² (100 mm Hg) it comprises 19% of bearing capacity in vacuum at the same temperature.

The most essential reason for catastrophic decomposition

during the oxidation of molybdenum is the appearance of a liquid phase - low-melting ($t_{m\text{in}}=795^\circ\text{C}$) trioxide of molybdenum. Test specimens failed themselves in lower part, where drained melted trioxide of molybdenum.

At atmospheric pressure the specimen/sample completely burned during 10 min with 1100°C .

The oxidation of molybdenum decreases its plasticity, which most is noticeable at 1500°C . With pressure increase from 10^{-1} to 133 N/m^2 (1 mm Hg) the elongation per unit length of specimen/samples at the temperature indicated descends from 33.3% to 6.4%, i.e., 5.5 times. The dependence of the plasticity of laminated molybdenum on pressure for two temperatures of testing is represented in Fig. 37.

For niobium, unlike molybdenum, the characteristically original increase of bearing capacity with pressure increase to 13.3 N/m^2 (10^{-1} mm Hg). Further increase in the pressure leads to a reduction in the bearing capacity of niobium; however, the negative effect of oxidation processes manifests itself to considerably smaller degree, than in the case of molybdenum. The bearing capacity of molybdenum specimen/sample after 10 min at atmospheric pressure and temperature of 1200°C is in effect equal to zero, while for the niobium, which was being found under analogous conditions, it composes 9% of its

bearing capacity with 1.33 mN/m^2 (10^{-5} mm Hg) and by 1200°C , or 62% of its maximum bearing capacity for this temperature [i.e. with $p=13.3 \text{ N/m}^2$ (10^{-1} mm Hg)].

The graph/diagrams of the dependence of the bearing capacity of laminated niobium on pressure are represented in Fig. 38.

The presence of maximum to curve $\sigma-p$ for niobium, apparently, should explain by the fact that the strengthened/hardened action/effect of interstitial impurities - oxygen and nitrogen, occurs before their specific concentrations higher than which begin the processes, which lead to the decrease of bearing capacity. It is known that among refractory metals the niobium is sensitive to the effect of oxygen and nitrogen.

Page 57.

Work [21] shows, that an increase in the oxygen content and nitrogen in niobium leads to its strengthening, moreover the effect of oxygen is predominating.

The strengthened/hardened action/effect of interstitial impurities was also revealed/detected by Frank [22]. Samples from the niobium alloy F-48, exposed/persistent for 0.5 h in air with 1090°C ,

during the subsequent tests proved to be stronger than the specimen/samples, which were not being subjected to oxidation.

The established/installation in our works laws governing a change of the bearing capacity of niobium in oxidizing medium confirm previously findings on the strengthened/hardened action/effect of interstitial impurities. Furthermore, tests at different temperatures and pressures and the corresponding to them oxidizing media made it possible to reveal/detect the existence of certain critical pressure whose excess causes a reduction in the bearing capacity. This critical pressure corresponds to the specific temperature interval of tests and specific delay time of specimen/samples at the assigned/prescribed temperature. For the time/temporary basis of tests (10 min) accepted in temperature range 1000-1500°C for niobium critical ones one should count pressure order 13.3 N/m^2 (10^{-1} mm Hg), that corresponds to the maximum value of the bearing capacity (see Fig. 38).

Increasing under certain conditions the bearing capacity of niobium, interstitial impurities even in insignificant quantities negatively affect its plasticity. A reduction in the plasticity is connected with the embrittlement of niobium as a result of the diffusion of oxygen even at very low partial pressures.

DOC = 78133002

PAGE ~~50~~ / 106

With pressure increase from 1.33 MN/m^2 (10^{-5} mm Hg) to 13.3 N/m^2 (10^{-1} mm Hg) the elongation per unit length of specimen/samples after holding with 1200°C is reduced from 35.2 to 22.3%.

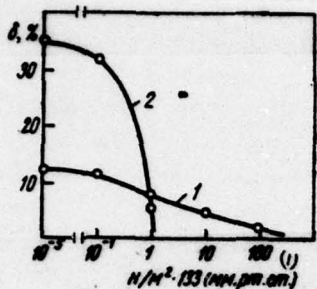


Fig. 37.

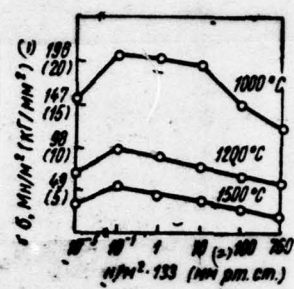


Fig. 38.

Fig. 37. The effect of pressure on the plasticity of the molybdenum:
1 - 1200°C; 2 - 1500°C.

Key: (1). (mm Hg).

Fig. 38. Effect of temperature and pressure on bearing capacity of niobium.

Key: (1). MN/m² (kg/mm²). (2). (mm Hg).

Page 58.

The dependence of the plasticity of niobium on pressure with 1200 and 1500°C predstavlena in Fig. 39.

The most complete representation of the laws governing a change

of the bearing capacity and plasticity of refractory materials under conditions of high-temperature oxidation can be obtained, if is considered the dependence of the intensity of the processes of corrosion on the stressed state of material. For this purpose, was studied the effect of the preliminary loading of specimen/samples under conditions of oxidizing medium for their bearing capacity under the following conditions: $t=1500^{\circ}\text{C}$; $p=133 \text{ N/m}^2$ (1 mm Hg); $r=10 \text{ min}$, $\sigma_1^0=0$; $\sigma_2^0=0.3\sigma_y$; $\sigma_3^0=0.6\sigma_y$, where σ^0 - stress of preliminary loading; σ_y - conditional bearing capacity.

The results of this investigation are represented in Fig. 40. As can be seen from graphs, initial load considerably intensifies oxidation processes, as a result of which descends the bearing capacity of materials.

Although the laws governing a change in the strength characteristics of molybdenum and niobium have specific special feature/peculiarities [presence of the zone of catastrophical oxidation and the sharp reduction in the plasticity with 1500°C and $p=133 \text{ N/m}^2$ (1 mm Hg) for molybdenum, the presence of the maximum of strength to curve $\sigma-p$ for niobium], nevertheless there is a common/general/total for both of metals tendency toward softening under the effect of oxidizing medium. In the range of low partial pressures on surface of both of metals, are formed the fine/thin

xide films, which possess high adhesive properties and shielding ability. With an increase in the oxygen pressure more intensely diffuses to interface the metal - oxide. The generating on the surface of molybdenum layer of tricxide of molybdenum melts and escapes, so that further oxidation occurs/flows/lasts rapidly, with the loss of the mass of specimen/sample.

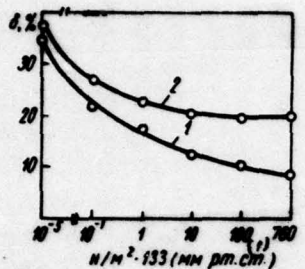


Fig. 39.

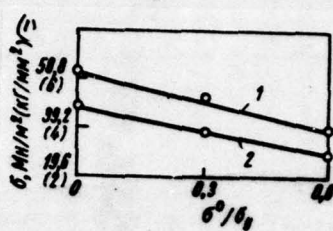


Fig. 40.

Fig. 39. The effect of pressure on the plasticity of the niobium: 1 - 1200°C; 2 - 1500°C.

Key: (1) - (mm Hg).

Fig. 40. Effect of preliminary holding under load on bearing capacity: 1 - molybdenum, 2 - niobium.

Key: (1) - σ , MN/m² (kg/mm²).

Page 59.

Oxides of niobium are not volatile components. However, the thickening of oxide layer leads to its cracking and peeling under the action/effect of compressive stresses.

For both of metals, the pressure increase leads to the loss of

the adhesive and shielding properties of oxide films, and also to the loss of the ability of films to absorb mechanical load. This, apparently, and is caused a reduction in the bearing capacity of molybdenum and niobium with $p > 13.3 \text{ N/m}^2$ (10^{-1} mm Hg).

Effect of the deformation rate on the strength properties.

In the institute of the problems of the strength of AS UKSSR, is developed the procedure of the investigation of the mechanical properties of high-melting materials taking into account the combined action of temperature and deformation rate it is created experimental installation IP-02 [32, 33], that makes it possible to change the deformation rate within the limits of $10^{-3} - 10^{-1} \text{ s}^{-1}$.

Accuracy/precision of measurement and recording the amounts of effort/force and strain - 3c/o.

Installation IP-02 is equipped with the devices, which make it possible in the process of tests to realize/acccmplish an automatic recording of stress-strain diagrams in coordinates $p-\Delta l$. The measuring mechanisms of recording mechanism possess minimum inertness.

Since the realization of the autcmatic recording of stress-strain diagram at high temperatures ($> 2200^\circ\text{C}$) with fixation of

a change in the length only of working section of specimen/sample is connected with extremely great difficulties, on the majority of the existing installations the strain of specimen/sample usually is measured according to displacement of active clamp, which is connected with considerable errors. In our installation used special device [32, 33], which makes it possible to continuously measure the strain of the working section of specimen/sample. Displacement of the levers, abut against the recesses of working section, is transferred to the indicator with which is connected spring bracket with resistance strain gauges. Signal from strain gauges enters the strain measuring station, and then the potentiometer of the type EPP-09M. Analogously is converted signal from force gauge (indicator of dynamometer DS-02). System makes it possible with high accuracy/precision to record/write the stress-strain diagram, limited by size/dimensions 270x270 mm.

With the aid of the developed installation were determined the characteristics of strength of some high-melting materials in the flat/plane specimen/samples which were cut lengthwise from the sheets, rolled with reduction 95% without the subsequent heat treatment. Tests were conducted at temperatures from 20 to 1600°C and the deformation rates from 10^{-4} to 10^{-1} s^{-1} [32].

The results of investigations are represented for commercially pure molybdenum in Fig. 41, for alloy VM-1 in Fig. 42, for commercially pure niobium in Fig. 43, for alloy VN-2 in Fig. 44. Data for an alloy on the basis of molybdenum with 0.50% Ti and 0.50% Zr are given to Fig. 45. Graphs are constructed for the average test values of 4-5 specimen/samples under identical conditions.

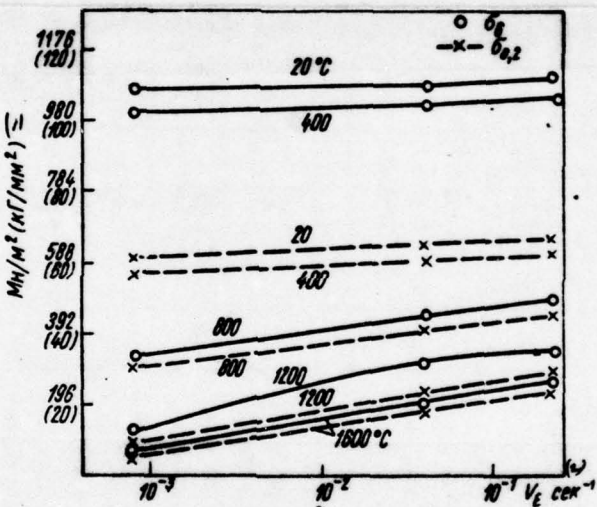


Fig. 41. Effect of temperature and deformation rate on mechanical properties of molybdenum.

Key: (1) - MN/m^2 (kg/mm^2). (2) - s.

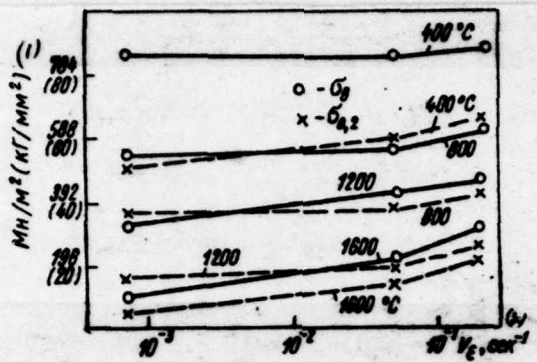


Fig. 42. Effect of temperature and deformation rate on mechanical properties of alloy VM-1.

Key: (1). MN/m^2 (kg/mm^2). (2). s.

Page 51.

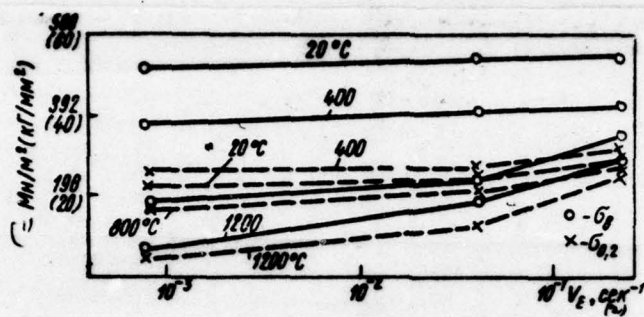


Fig. 43. Effect of temperature and deformation rate on mechanical properties of niobium.

Key: (1) - σ MN/m^2 (kg/mm^2).

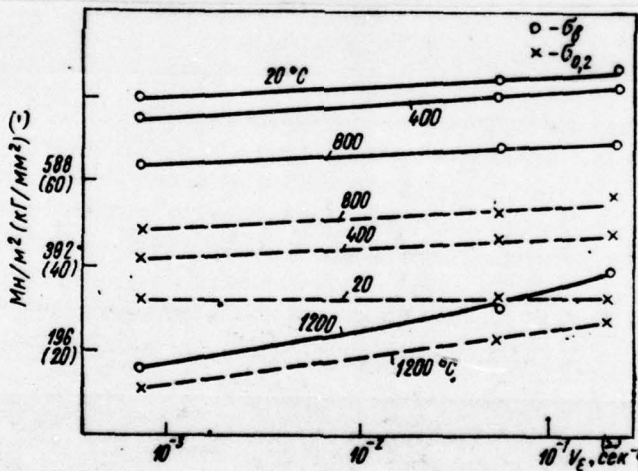


Fig. 44. Effect of temperature and deformation rate on mechanical properties of alloy VN-2.

Key: (1) - σ MN/m^2 (kg/mm^2).

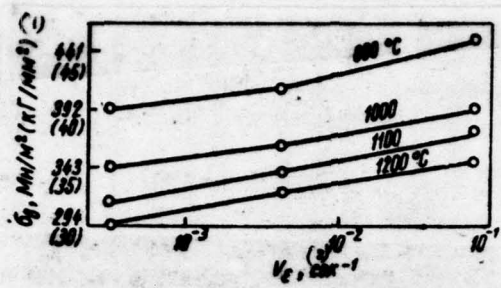


Fig. 45. Effect of temperature and deformation rate on the limit of the strength of alloy TSM-2A.

Key: (1) - MN/m^2 (kg/mm^2). (2) - s.

Page 62.

The analysis of the obtained results shows that in the range of temperatures of 20-400°C limits of the strength of the tested materials with an increase in the deformation rate grow/rise insignificantly. Beginning from the temperatures of order (0.35-0.50) $T_{m,n}$, an increase in the deformation rate leads to more essential increase in strength, in this case, is decreased a difference in the values of the limits of strength and yield; the dependence of strong properties on the deformation rate for alloys is developed to a lesser degree than for pure metals.

The obtained dependences of mechanical characteristics on temperature and deformation rate can be presented analytically:

$$\sigma_{T,v} = \sigma_0 e^{-\alpha(T-T_0)^2} + KT \lg \frac{v}{v_0}. \quad (1.17)$$

where $\sigma_{T,v}$ - ultimate strength at data to the temperature and the deformation rate; σ_0 - ultimate strength under the standard conditions of testing; α - coefficient of thermal softening; T - testing temperature; T_0 - room temperature; $T_{m,n}$ - melting point; K - coefficient of deformation strengthening; $K=K_1$ with $T < 0.4 T_{m,n}$; $K=K_2$ with $T > 0.4 T_{m,n}$; v - a deformation rate; v_0 - deformation rate under the

standard conditions of testing.

The proposed equation in mathematical form expresses assertion about the fact that the strength of metal at any values of temperature and deformation rate in essence is determined by the competing development of the processes of the strengthening, caused by plastic strain, and thermal softening.

Estimation of error in the measurements during mechanical tests.

The functional dependence between four parameters: by voltage/stress σ , strain ϵ , temperature T and time τ - is not single-valued.

Since it is impossible to obtain the solution of the equation

$$f(\sigma, \epsilon, T, \tau) = 0 \quad (1.18)$$

in general form, the role of separate factors is studied experimentally and finds the limiting conditions, which are dangerous ones for the work of construction/design.

During the study of the mechanical properties of material, it is necessary to determine the stresses and state of strain in point. However, local measurements to conduct is difficult; therefore the tendency is to create the uniform stressed state in volume.

Page 63.

For this reason for testing for elongation (compression) they give more correct information about the mechanical properties of material, than bend and twisting.

A classical single-factor experiment of type $\sigma=f(\epsilon)$ without taking into account of a change in parameters T and r is permissible only for normal temperatures. With the increase of testing, temperature the mechanical properties of materials substantially are changed as a result of the thermal activation of structural processes. Consequently, errors of measurement of effort/force and strain must depend on the temperature of tests, duration of the measurement and other factors.

In the general case a full/total/complete error of measurement is determined by the reaction of the following five factors:

- 1) the object of measurement;
- 2) experimenter's subjective data;

3) measuring instrument;

4) the method of measurement;

5) the environment, in which occur/flow/lasts the measurement.

Each factor introduces the appropriate error into the obtained results of measurements, and when selecting of optimum measuring circuit it is necessary to consider its partial contribution.

Errors, as a rule, are caused by the imperfection of means and methods of measurement and are subdivided into systematic, accidental and errors.

Systematic errors during repeated measurements remain constants or are changed according to the specific law. The reason for systematic measuring errors in many instances is known, then it is possible to determine by calibrating and to eliminate from the result of the measurement by the introduction of correction. Calibrating can be realized/accomplished by a method of substitution, by a method of the compensation error on sign, by a method of symmetrical observations and by other methods [34].

It must be noted that the undetected systematic error dangerous by accidental. The presence of random errors decreases the

authenticity of the result of measurement, the presence of systematic ones - makes it inaccurate ones.

The correct liberation/isolation of the errors, which check the accuracy of measurement, makes it possible to expediently plan experiment. If process is controlled by systematic error, then sufficient to conduct several precise experiments and to eliminate systematic error; if accidental - the is admissible utilization of less precise measuring circuits, but is necessary larger number of experiments, their statistical interpretation.

It is necessary to also distinguish static and dynamic errors. Dynamic error during the measurement of unsteady processes is determined in essence by the accuracy/precision of equipment, by oscillatory and inertia links [35].

Page 64.

As the criterion of the dynamic resolution of tools, is utilized the passband of frequencies, i.e., the range of the frequency spectrum of the measured value which is reproduced with the permissible relative errors.

In order to fulfill measurement in the required frequency range

necessary to correctly select the dynamic characteristics of the links of metering circuit.

For example, during the utilization as sensors of elastic cell/elements with strain gauges is necessary the observance of inequality [36]:

$$\omega_0 > (8 + 10)\omega, \quad (1.19)$$

where ω_0 - natural frequency of elastic system; ω - frequency of the process (highest harmonic component) being investigated.

During static tests the dominant role they play instrument/tool and systematic errors in direct measurements of temperature, strain and load from which are calculated resultant errors in the mechanical characteristics. Are examined below basic forms and the sources of errors.

For measuring the temperature, predominantly are utilized the thermocouples and the optical pyrometers, which make it possible to record local temperatures.

The capacities of temperature by the metallic thermocouples, used in industry, compose 1600°C in air and 2000°C in vacuum and inert medium.

The sources of errors of measurement of the temperature of specimen/sample are:

- a) the presence of thermal contact resistance between the thermojunction and the surface of specimen/sample;
- b) heat withdrawal in thermocouples;
- c) a change in TEMF in the thermocouples as a result of reaction with medium.
- d) calibration error of thermocouple;
- e) the errors, which depend on the method of measurement (direct estimation or compensating);
- f) meter error.

A total error of measurement of temperature can be presented in the form

$$\epsilon_t = \sqrt{\epsilon_1^2 + \epsilon_2^2 + \epsilon_3^2} . \quad (1.20)$$

where ϵ_1 - a relative calibration error of thermocouple ($\epsilon_1 \sim 1\%$);

ϵ_2 - a relative instrument error in tcel $\epsilon_2 = \frac{\Delta_2}{Kt}$;

Δ_2 - absolute instrument error

$K = \Delta\% / \Delta t$ - sensitivity index of thermocouple;

$\Delta\%$ - increase of TEMP with an increase in the temperature by value Δt .

t - temperature of tests;

e_s - the systematic error.

Page 65.

The total error of measurement in optical pyrometry depends on the following factors:

a) the measured value of temperature;

b) calibration error of temperature lamp (standard of comparison).

c) the class of the precision of measuring instrument;

d) the accuracy/precision of the control of the filament of

temperature lamp.

- e) the accuracy of visual pyrometric measurements;
- f) the error, which appears during the introduction of light filter, error in the extrapolation.
- g) the ambient conditions of measurements, coefficient of blackness $\epsilon_1 = \epsilon(T)$; the method of heating, radiation absorption in medium and sight glasses.

In the more general view of an error of measurement of the temperature of specimen/sample, are corrected the instrument error in the pyrometer and the systematic error, determined by measuring conditions.

The instrument errors in the pyrometers, utilized in the practice of mechanical tests, are given in table 8.

Table 8. The instrument errors in the pyrometers.

(1) Тип пирометра	(2) Диапазон измеряемых температур, °C	(3) Пределы измерения, °C	(4) Ошибки допустимая погрешность		(6) Литера-тура
			(%)	(5) deg	
ОПЛИР-09	800—2000	800—1400 1200—2000	—	±20 ±30	[37]
ОПЛИР-017	1200—3200	1200—2000 1800—3200	—	±30 ±80	[37]
ОП-48	900—3000	900—2000 2000—3000	0,2 0,5	—	[38]
ОМП-019	900—4000	900—2000	—	±3	[39]
ФЭП-3	600—1800	600—1100 800—1300 900—1400 1000—1700 1100—1800	1,0	—	[39]
ЦЭП-3	1400—2800	3—5 полук-диапазонов по 250—450°C ⁽⁷⁾	1,0	—	[38]

Key: (1). Type of pyrometer. (2). Range of measured temperatures, °C.
 (3). Capacities, by °C. (4). Basic permissible error. (5). deg. (6). Literature. (7). 3-5 subregions, 250-450°C each.

Page 66.

All pyrometers with the disappearing filament are graduated on absolute to blackbody and they make it possible to determine only temperature brightness of radiating surface. For determining the actual temperature of specimen/sample, it is necessary to consider deviation from the conditions of blackbody for the surface of material; this correction in the majority of the cases is known only

approximately.

The error of measurement of temperature, connected with the inaccurate determination of the value of the emissivity of the surface of the material of specimen/sample $\epsilon_{\lambda, r}$, can be calculated according to the formula

$$\Delta T_1 = \frac{\lambda_0^4}{C_2} \frac{\Delta \epsilon}{\epsilon_{\lambda}} T^2, \quad (1.21)$$

where λ_0 - effective wavelength for the red light filter of pyrometer;

$\frac{\Delta \epsilon}{\epsilon_{\lambda}}$ - relative error of measurement in the emissivity;

T - real temperature of body.

If a relative error in the determination of the emissivity of the surface of specimen/sample $\frac{\Delta \epsilon}{\epsilon} \leq \pm 0.1$, then an error in computed value of correction for measured temperature brightness S_n is equal to:

$$\Delta T_1 \approx \pm 4.5 \cdot 10^{-6} S_n^2. \quad (1.22)$$

A subjective error in the compensation of the brightness of filament and specimen/sample depends on contrast threshold of human eye, i.e., on value

$$\frac{\Delta B}{B_0} = \frac{B_1 - B_0}{B_0}, \quad (1.23)$$

where B_1 - brightness of the filament of temperature lamp;

B_0 - brightness of background (surface of specimen/sample).

During measurements with common photometric accuracy/precision $\frac{\Delta B}{B_0} \approx 0.01$ with $\lambda = 0.65 \mu\text{m}$ the error for the compensation of brightness can be calculated according to the formula

$$\Delta S = \frac{\lambda}{C_2} \frac{\Delta E_{\lambda, r}}{E_{\lambda, r}} S^2, \quad (1.24)$$

where $\Delta E/E$ - relative error of measurement of the monochromatic luminous density of blackbody.

Page 67.

Set/assuming $\Delta E/E \approx 0.01$, we find

$$\Delta S = 0.5 \cdot 10^{-6} S^2. \quad (1.25)$$

Correction for radiation absorption in sight glass of test chamber they calculate according to the formula

$$\frac{1}{S_1} - \frac{1}{S} = \frac{\lambda_0}{C_2} \ln \frac{1}{\tau}, \quad (1.26)$$

where S_1 - the temperature brightness, measured after radiation absorption in sight glass;

S - the temperature brightness, measured to the passage of emission/radiation through sight glass;

τ - coefficient of the transmission of the glass:

$$\tau = \frac{16n^2}{(n+1)^4}, \quad (1.27)$$

where n - refractive index.

For the quartz glass $n=1.46$; in this case $\tau=0.93$ and
 $1/S_1 - 1/S \approx \Delta S_1 / S^2 \approx 3.3 \cdot 10^{-6}$. Consequently,

$$\Delta S_1 \approx 3.3 \cdot 10^{-6} S^2. \quad (1.28)$$

Allowance for radiation absorption in glass can considerably be changed during metal spraying of the material of heater to the surface of glass. From formulas (1.26) and (1.27), and also from table 8 it follows that errors of measurement of temperature by the optical pyrometer are increased proportionally to the square absolute temperature of specimen/sample.

The examined instrument/tool and systematic errors are statistically independent; therefore a total error of measurement of the temperature of the specimen/sample:

$$\Delta T = \sqrt{\Delta T_n^2 + \Delta T_i^2 + \Delta S^2}, \quad (1.29)$$

where ΔT_n - the instrument error in the optical pyrometer.

The method of measuring the strains in many respects determines size/dimensions and the form of specimen/samples, the construction/design of test chamber. The small size/dimensions of specimen/samples, the high module/moduli of elasticity, the presence

of medium and the large active region of heating considerably complicate the measurement of strain.

Usually utilize following methods of measuring the strain:

1. Contact methods of measurement with the aid of the extensometers of different construction/designs, fastened in specimen/sample.

Page 68.

The ends of the thrust/rods of extensometers derive/conclude from hot zone and with the aid of optical-lever systems and transformers are obtained a plausible increase for observation and recordings of the strain of specimen/sample.

2. Noncontact methcds of measuring strain of specimen/sample with the aid of optical-mechanical systems of type of cathetometers.

The contact methods of measurements make it possible to comparatively simply convert input signal - mechanical displacement/movement (thrust/rods of extensometers, active capture) - into convenient for a recording electric or mechanical output signal with a great increase. This principle is placed as the basis

of the majority of construction/designs for the automatic recording of diagrams load - strain at elevated temperatures. During the utilization of this measuring circuit, it is necessary to stabilize well temperature or to manufacture the account of the thermal strains of metering circuit.

The instability of the temperature of specimen/sample leads to errors in the recording of stress-strain diagram (Fig. 46) at the constant velocity of the deformation of specimen/sample v. Magnitude of error determines the inequality

$$(U_t - \alpha \frac{\Delta T}{\Delta t}) \leq 0. \quad (1.30)$$

where $U_t = \frac{\Delta T}{\Delta t}$ - rate of change in the temperature along the length of heated section; α - coefficient of the linear expansion of material.

Systematic errors of measurement of the strain of specimen/sample as a result of the elongation of the cell/elements of power circuit under load can be determined by calibrating (Fig. 47).

132

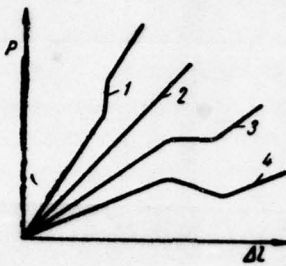


Fig. 46. Errors in the recording of stress-strain diagram during the oscillation/vibrations of the temperature of the specimen/sample: 1 - $\frac{v_{f^u}}{v} < 0$ - the speed of loading is increased during the decrease of the temperature of specimen/sample; 2 - $v=0$ - the temperature of specimen/sample is constant; 3 - $0 < \frac{v_{f^d}}{v} < 1$ - the speed of loading is decreased with an increase in the temperature; 4 - $\frac{v_{f^u}}{v} > 1$ - on diagram is record/fixed load.

Page 69.

Allowance is determined from the formula

$$\frac{\Delta l_{06\%} + \epsilon}{K_u} - \frac{\Delta l_0}{K_T} = \Delta l_n \pm \epsilon_1, \quad (1.31)$$

where $\Delta l_{06\%}$ - overall strain of power circuit, recorded to EPP; ϵ - confidence limit $\Delta l_{06\%}$ on the 10% level of significance; K_u, K_T - coefficients of an increase by EPP and the lever/crank extensometer TP, respectively; Δl_0 - strain of the working section of specimen/sample on TP; $\Delta l_n \pm \epsilon_1$ - correction and its confidence limit.

The results of calibrating installation "electron" are given to Fig. 48. The initial section of dependence $\Delta l_n=f(P)$ is approximated by parabola; it corresponds to the elastic deformation of links to the selection of clearances, to a change of the contact in the conjugate pairs, etc. With further increase in the load, is established/installled linear shape of the curve.

At the temperatures higher than 1700°C strains of specimen/samples are usually measured by optical, noncontact methods, i.e., by direct observations after changes in cross sections of the working section of specimen/sample.

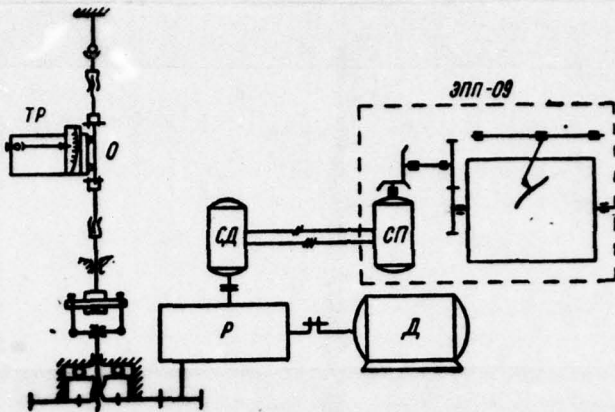


Fig. 47. Diagram of the determination of correction for the strain of the cell/elements of power circuit.

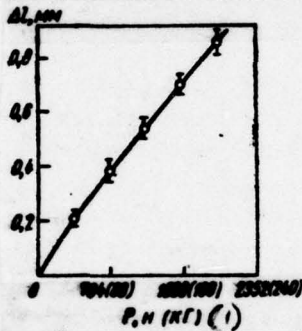


Fig. 48. Dependence of correction for strain of cell/elements of power circuit on load.

Key: (1) . kgf.

Page 70.

Errors in the noncontact method are caused by the following factors:

- 1) by the resolution of optical systems with long-distance objectives.
- 2) by the accuracy/precision of the sighting of locating surfaces of specimen/sample with the high brightness of hot body.
- 3) by the rate of the processes of the creep of the material of specimen/sample and relaxation of its stresses in the time of visual measurement at the high temperatures of testing.
- 4) by the difficulty of the transformation of input signal (strain) for automatic recording.

The measuring errors in essence are determined by the accuracy/precision of sighting which in turn, depends on useful magnification in duct and resolving power of observer's eye. Useful magnification in the duct G with the angular resolution of eye 1' they calculate according to the formula

$$r = \frac{D}{244}, \quad (1.32)$$

where D - a diameter of objective, mm.

The error for sighting is equal to:

$$m_s = \frac{60'}{2r}, \quad (1.33)$$

the permitted linear distance, or the linear error for sighting:

$$\Delta = m' f_o \quad (1.34)$$

where f_o - a focal length of objective.

The given dependences are valid at the average values of brightness to which corresponds contrast threshold of human eye 1,5-2 φ /c [40].

With the increase of temperature the intensity of the glow of specimen/sample is increased, appears the halo around locating surfaces, contrast deteriorates, the resolving power of eye sharply falls and a pointing error grows/rises.

The accuracy/precision of the installation of the crosshair depends also on the geometric form of bases. With the guidance/induction of filament to the edge of cylinder, the accuracy/precision of installation comprises 30-60", while with the cross coincidence of graduation marks, it is increased to 10".

An error of measurement of the strain of specimen/sample is increased also because of the displacement of the zero base, connected with the passive capture whose position is changed in the

process of loading and during the oscillations/vibrations of the temperature:

$$\Delta\sigma = \tau \cdot \dot{\epsilon}_t, \quad (1.35)$$

where τ - time of measurement; $\dot{\epsilon}_t = f(\sigma, T)$ - rate of transient creep.

The time of measurement depends on the subjective data of operator and varies over wide limits, $\tau=30-60$ s.

An error of measurement of load depends on the instrument instrument error, fluctuations of resistance of external power circuit, correct agreement of the range of measurement and value of load.

Page 71.

For common mechanical tests a relative error of measurement of load does not exceed 10% [41]. With the increase of the temperature of tests, this value can sharply grow/rise as a result of the considerable decrease of the strength of the heated materials. With light loads one should eliminate the mechanical resistance of external metering circuit, furnishing force gauge directly in test chamber. Thermostatically controlling force measurement and after matching the parameters of measuring circuit (elastic cell/element, strain gauge and recorder) with the value of load, it is possible to

attain the error of measurement whose values will not exceed the values of equipment error, i.e., ~1-1.5%.

If dynamometer is located out of test chamber, then total systematic error ΔP (connected with friction of stock/rod, external pressure on stock/rod during tests in vacuum, etc.) can be determined by recording the resistance to motion of stock/rod after the decomposition of specimen/sample.

Breaking load P is determined by the formula

$$P = P_D - \Delta P, \quad (1.36)$$

where P_D - reading dynamometer. Knowing a variation in the readings ΔP at different temperatures, it is possible to determine a relative error of measurement of load.

During the determination of yield point, the error in load measurement depends also on the accuracy of the measurement of strain and form of the function

$$P = f(\Delta l, T). \quad (1.37)$$

After determining errors in the direct measurements of load P , the strains of specimen/sample Δl , of its geometric dimensions before and after loading ($F_0, l_0; F_n, l_n$), find errors in the characteristics of strength ($\sigma_s, \sigma_{0.2}$) and of plasticity (δ, ψ).

Page 72.

In view of the fact that these characteristics represent the linear functions of several variables and their direct measurements are statistically independent variables, to the results of the measurements indicated correspond following values of relative root-mean-square errors:

a) a relative error in the determination of the stress:

$$\delta_s = \sqrt{\delta_p^2 + \left[\frac{\Delta P(\Delta l, T)}{P} \right]^2 + \delta_r^2}; \quad (1.38)$$

b) a relative error in the determination of the elongation per unit length:

$$\delta_e = \left(1 + \frac{1}{\epsilon}\right) \sqrt{\delta_{r_e}^2 + \delta_{r_s}^2}; \quad (1.39)$$

c) a relative error in the determination of the transverse contraction:

$$\delta_\nu = \left(\frac{1}{\nu} - 1\right) \sqrt{\delta_{r_\nu}^2 + \delta_{r_s}^2}. \quad (1.40)$$

where δ_s - relative errors in the direct measurements; $\frac{\Delta P(\Delta l, T)}{P}$ - relative error in the determination of load, which depends on the form of the function $P(\Delta l, T)$; δ_p - relative error for a strength measuring device in the measured range of loads.

The given formulas make it possible to select optimum procedure and the corresponding measuring means, to raise the accuracy of single measurements and, therefore, to decrease the scatter of

experimental data.

However, the scatter of the values of the mechanical properties of material in the specimen/samples being investigated, the deviations of the parameters of the conditions/modes of testing and error of measurement cause scattering experimental results. Therefore it is necessary to establish/install, which number of experiments is sufficient for conducting the objective analysis of the results of mechanical tests.

The number of necessary observations depends on the selected value of confidence coefficient α , of the permissible error δ and of the measure of the variability of mechanical characteristic. With a small number of observations, usually are used the distribution of Student and the calculation of number of experiments is performed on the formula

$$n = t_{\alpha}^2 \frac{s^2}{(\bar{x} - \mu)^2}, \quad (1.41)$$

where s^2 - empirical dispersion; $\Delta_{\mu} > |\bar{x} - \mu|$ - the upper limit of the error in determination of the actual value of mechanical characteristic μ from average selective x with the probability, not less α ; $\delta = \frac{\bar{x} - \mu}{s}$ - relative error in the estimation of the actual average value of the measured quantity according to selected data.

Utilizing table of values $\frac{t_{\alpha}}{\sqrt{n}}$ [42], it is easy to determine value n with the assigned/prescribed error δ and confidence coefficient α (table 9).

Page 73.

Further processing of the results of experiment is reduced to the determination of the confidence limits of the average value of the mechanical characteristic which with probability α connect the actual value of characteristic μ , i.e.,

$$P \left[\bar{x} - \frac{t_{\alpha} S}{\sqrt{n-1}} \leq \mu \leq \bar{x} + \frac{t_{\alpha} S}{\sqrt{n-1}} \right] = \alpha. \quad (1.42)$$

Having the equiprobable values of function at different points, it is possible to establish/install reliable correlative dependences [43, 44].

Table 9.

Values $\frac{t_n}{\sqrt{n}}$ for the assigned magnitudes δ and α .

$t = \frac{\bar{x} - \mu}{S}$	(1) Доверительная вероятность			
	0,90	0,95	0,99	0,999
1,0	5	7	11	17
0,5	13	18	31	50
0,4	19	27	46	74
0,3	32	46	78	127
0,2	70	99	171	277

Key: (1). Confidence probability.

Page 74.

Chapter 2.

ELASTICITY CHARACTERISTICS.

General information about elasticity characteristics of refractory metals.

At present refractory metals and alloys find a use in essence in the form of polycrystals. The elastic properties of separate crystal depend on crystallographic orientation. The polycrystalline aggregates, which consist of the disorderly oriented crystals, it is accepted to consider elastically isotropic.

The elastic behavior of isotropic body characterize the module/modulus of elasticity with elongation (Young's modulus) E , modulus of shear G , bulk modulus (bulk modulus) K , Poisson ratio μ . In the elementary formulation of Hooke's law, values E , G , K are the constants of proportionality between stress and tensile strain, displacement and the cubic compression:

$$\sigma = E\epsilon; \quad (2.1)$$

$$\tau = G\gamma; \quad (2.2)$$

$$p = K \frac{\Delta V}{V}. \quad (2.3)$$

Poisson ratio μ characterizes a change in the volume of body during strain. Elasticity characteristics are connected by the relationship/ratios:

$$G = \frac{E}{2(\mu + 1)}, \quad (2.4)$$

$$K = \frac{E}{3(1 - 2\mu)}. \quad (2.5)$$

Recently in industry they begin to apply the single crystals of refractory metals. The perfected crystal, being elastic are anisotropic, possesses several elastic constants. For example, cubic crystals have three elastic constants. The values of the elastic module/moduli of single crystal depend on direction and can be calculated according to the known values of elastic constants [45, 46].

The values of the moduli of elasticity characterize the strength of interatomic communication/connections in crystal lattice; therefore is possible the correlation between them and other physical quantities: heat of sublimation, melting point, enthalpy, the energy of the activation of diffusion and self-diffusion, root-mean-square deviation of atoms from position of equilibrium, characteristic

temperature, the coefficient of linear expansion, etc.

Page 75.

On this same reason the value of the module/modulus of elasticity depends on the position of cell/element in periodic system.

On Fig. 49 and 50 shown periodic change of the module/modulus of normal elasticity and shear modulus in dependence on the atomic number of cell/element [47]. The high values of the moduli of elasticity have the transition metals, especially those them them, the melting point of which exceeds 2500°C (cesium, rhenium, tungsten). It should be noted that the conformity between the values of the module/modulus of elasticity and melting point is observed not always. For example, maximum module/modulus has not tungsten, highest-melting cell/element, but cesium.

The value of the module/modulus of elasticity connected with the strength of interatomic communication/connections of material, in the case of perfect crystal must serve as the characteristic of its strength.

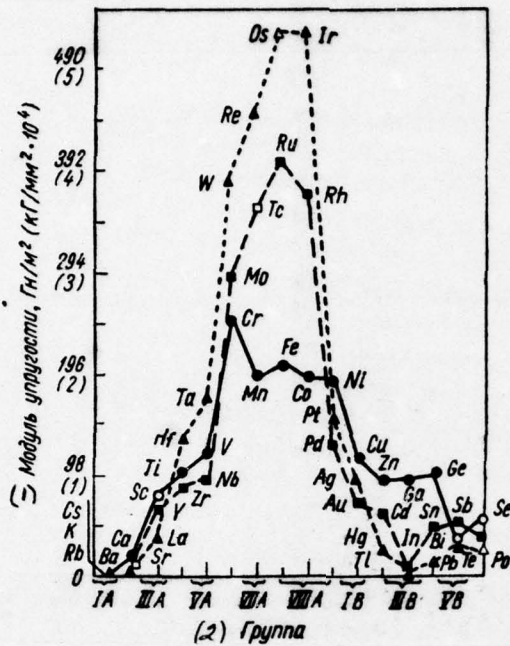


Fig. 49. Change of Young's modulus of transition metals in dependence on their position in periodic system.

Key: (1). Module/modulus of elasticity, ГН/м² (kg/mm² · 10⁴). (2). Group,

Page 76.

However, the strength of the real crystals much lower than theoretical value, determined by the forces of interatomic communication/connections, which is explained by presence in the crystal of a large number of flaw/defects: dislocation, the

boundaries of the grains, of interstitial atoms, etc.

A quantity of flaw/defects is determined to a considerable extent by the method of obtaining, by purity/firish and the state of metal.

Flaw/defects have certain effect also on the characteristics of elasticity. So, foreign atoms change the strength of interatomic communication/connections in the lattice of base metal, which produces change in the value of module/modulus. Is possible at present only the approximate estimate of the effect of the dissolved atoms on the bending characteristics of base metal; therefore necessary information on this question can be obtained only experimentally. Will be given below some data on the influence of impurity/admixtures and addition to elasticity characteristics of tungsten, molybdenum, niobium and tantalum.

The presence of pores in material can considerably change its elastic properties. The majorities of articles made of refractory metals obtain at present by the methods of powder metallurgy, they have residual porosity of approximately 2-3%.

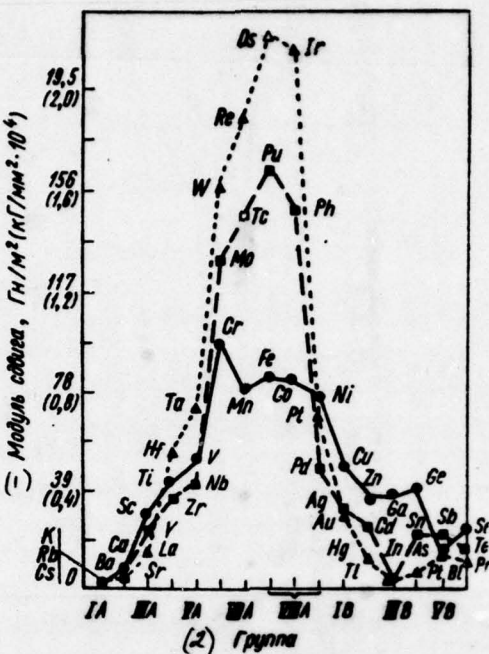


Fig. 50. Change of the modulus of shear of transition metals in dependence on their position in periodic system.

Key: (1). Modulus of shear, GN/mm^2 ($\text{kh/mm}^2 \times 10^4$). (2). Group.

Page 37.

Some parts possess special properties only because of the presence of pores in the material, from which they are made: oilless bearings, filters, etc.

The study of the effect of porosity on elasticity

characteristics of materials is carried out by many researchers. Theoretically this question for pure metals studied Mackenzie [48], Gatto [51], M. Yu. Bal'shin [49], and for a polyphase mixture - V. V. Skorokhod [50].

Mackenzie proposed the following expression for a module/modulus. the elasticity of the first gender of the porous bodies

$$\frac{E}{E_0} = 1 - 15p \frac{1-\mu}{7-5\mu} + Ap^2, \quad (2.6)$$

where p - porosity; A - experimental constant; E - modulus of elasticity of porous body; E_0 - modulus of elasticity of compact bdy; μ - Poisson ratio [it is assumed that $\mu(p)=\text{const}$].

To V. V. Skorokhod it proposed formulas for determining the moduli of elasticity of polyphase systems:

$$\sum_{(i)} \frac{3K+4G}{3K_i+4G} \cdot \frac{K_i}{K} p_i = 1; \quad (2.7)$$

$$\sum_{(i)} \frac{5(3K+4G)G_i p_i}{(9K+8G)G+8G_i(K+2G)} = 1. \quad (2.8)$$

where $i=1, 2, 3 \dots n$, n - a number of phases.

Kobal and Kingery[53] experimentally obtained the dependences of elasticity characteristics of oxide of aluminum on porosity; their data satisfactorily coincide with Mackenzie's theoretical dependences. The satisfactory conformity of experimental data to

expression (2.6) obtained Sh. N. Plyatt, Yu. M. Rapoport and E. T. Chefnus [54] also on aluminum oxide.

O. A. Chekhov and I. N. Frantsevich [52] studied the effect of porosity on the modulus of elasticity of the sintered iron. In Fig. 51 are noted them the data, and also the results, obtained by McAdam [55]. Extrapolation of the values of the modulus of elasticity to zero porosity gives the value, approximately equal to the modulus of elasticity of cast iron. Data will agree well with McAdam's empirical expression:

$$\frac{E}{E_0} = (1 - p)^m. \quad (2.9)$$

where m - an experimental coefficient.

I investigated the influence of porosity on modulus of shear and Pisces ratio [56].

Page 78.

Experiments were run in the specimen/samples made of porous iron, pressed from powder of the mark/brand AFZhMA and sintered in the medium of hydrogen with 1150°C for 3 h. Size/dimensions of the specimen/samples: diameter 8 mm and length 100 mm.

The value of module/moduli was determined according to the

measurements of the resonance frequencies of the cross and torsional vibrations. (This procedure is in detail presented in following paragraph). Findings are represented in Fig. 51. (Each point - result of the averaging of data, obtained in five specimen/samples).

With an increase in the porosity of specimen/samples, the Poisson ratio was decreased, moreover the character of its change in basic the same as for the moduli of elasticity and shear. Thus, assumptions [48, 54] about equality the Poisson ratio of porous and compact material are faulty ones. Extrapolation of findings to zero porosity gives $\mu \approx 0.27$, which corresponds to the given in the literature values of Poisson ratio for iron.

Of all external agencies the heating has most powerful effect on the value of the moduli of elasticity. With a temperature rise, is increased the amplitude of the oscillations of atoms around position of equilibrium and increase interatomic distances. They consider that with the increase of temperature by one degree of the value of module/moduli they are decreased by 0.030/c [46]. A change in the elasticity characteristics during heating of tungsten, molybdenum, niobium and tantalum is stated in following two paragraphs.

During the evaluation of mechanical effect on material, it is necessary to consider that expression (2.1)-(2.3) is described strain in the approach/approximation of ideal elasticity (model-spring).

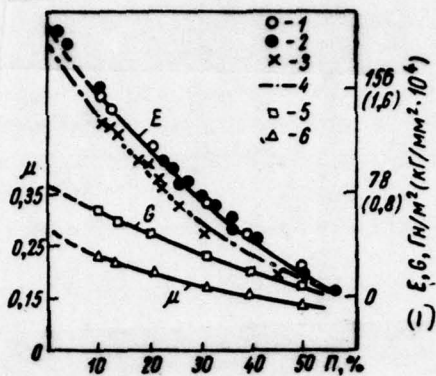


Fig. 51. The effect of porosity (P) on elasticity characteristics of the iron: 1, 5, 6 - their own data; 2, 3 - data [7]; 4 - data [10].

Key: 1) μ . $\text{GN/m}^2 (\text{kg/mm}^2 \cdot 10^4)$.

Page 79.

However, for real solids even with small tensions the characteristically inelastic behavior: phase lag of strain from stress (Fig. 52).

If solid is strained under adiabatic conditions, its temperature slightly is changed. With elongation it is reduced, while during compression it grows/rises. During the instantaneous application/appendix of tensile stress σ , the specimen/sample will be elongated to certain value ϵ_0 . (Fig. 53) and will lower its

temperature. At this moment its modulus of elasticity is determined by the tangent of the angle α of the slope/inclination of strain curve to the axle/axis of abscissas ϵ (see Fig. 53) and is unrelaxed, or adiabatic E_{ax} . In certain time the specimen/sample again of signs ambient temperature will be elongated to value AB. Now its modulus of elasticity will be determined by the tangent of angle β and will be relaxed, or isothermal E_m .

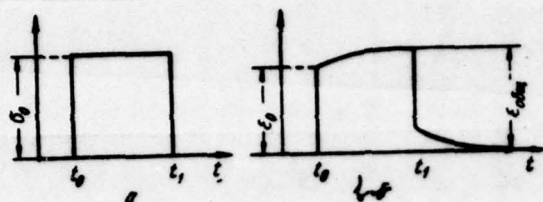


Fig. 52. Time/temporary dependences of the stress (a) and of strain (b) in the case of the inelastic behavior solid.

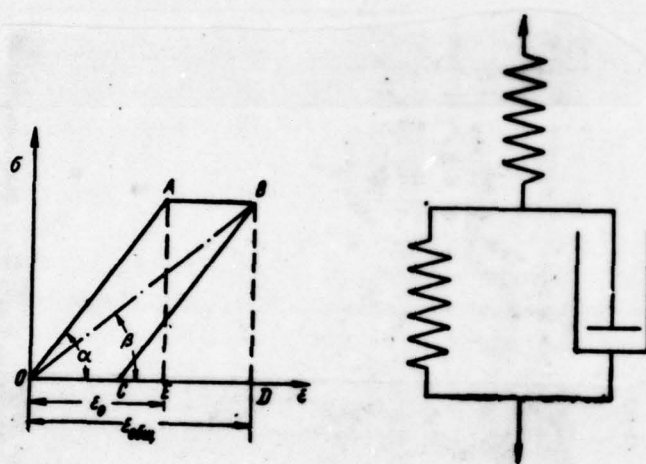


Fig. 53. Diagram of thermal relaxation.

Fig. 54. Mechanical analog of standard linear solid.

Page 80.

Communication/connection between these module/moduli is defined by the expression

$$\frac{E_{\text{ss}}}{E_{\text{st}}} = 1 - \frac{\alpha T E_{\text{ss}}}{\rho c_p} . \quad (2.10)$$

where α - a coefficient of linear expansion; T - absolute temperature; ρ - density; c_p - specific heat capacity at constant pressure.

For describing the inelastic behavior of metals, frequently is utilized the mechanical analog of the so-called standard linear solid (Fig. 54) [57]. Stresses and the strains of this body are connected by the relationship/ratio

$$\sigma + \epsilon_0 \dot{\epsilon} = M_p (\epsilon + \epsilon_0 \dot{\epsilon}), \quad (2.11)$$

where τ_{e-} - a relaxation time of stress under the condition of constant strain; τ_0 - time of the increase of strain with constant stress of up to value determined by stress level; M_p - relaxed modulus of elasticity.

The module/modulus, which corresponds to the conditions of the absence of relaxation, is called unrelaxed and is designated M_u .

Value

$$\Delta M = M_u - M_p, \quad (2.12)$$

is called the flaw/defect of module/modulus. The degree of the relaxation of module/modulus (flaw/defect of module/modulus) the definition

$$\Delta = \frac{M_u - M_p}{M_u}. \quad (2.13)$$

In the case of repeated deformation, the module/modulus will be unrelaxed in such a case, when the duration of cycle is less than relaxation time.

For the establishment of communication/connection between the stress and the strain in the standard linear body when these values periodically are changed in time, then they present in the form of the periodic functions of time and substitute in equation (2.11).

For fluctuations with angular frequency ω

$$\sigma(t) = \sigma e^{i\omega t}, \quad \epsilon(t) = \epsilon e^{i\omega t}. \quad (2.14)$$

After substitution (2.14) into equation (2.11) we have:

$$\sigma(1 + i\omega\tau_s) = M_p \cdot (1 + i\omega\tau_e). \quad (2.15)$$

Page 81.

From equation (2.15) it follows that between the relaxed and unrelaxed module/modulus there is the dependence

$$M_u = \frac{\sigma(\omega \rightarrow \infty)}{\epsilon(\omega \rightarrow \infty)} = \frac{\tau_e}{\tau_s} M_p. \quad (2.16)$$

After solving equation (2.15) relatively σ , we will obtain

$$\sigma = \frac{1 + i\omega\tau_e}{1 + i\omega\tau_s} M_p. \quad (2.17)$$

Q
Value M^* is called the complex modulus of elasticity.

$$M^* = \frac{1 + i\omega\tau_s}{1 + i\omega\tau_i} \quad (2.18)$$

The phase angle between the stress and the strain is determined by the dissipation of energy in the process of fluctuation.

The tangent of this angle is equal to the ratio of the apparent/imaginary and real parts of the complex module/modulus

$$\operatorname{tg} \varphi = \frac{I(M^*)}{R(M^*)} = \omega \frac{\tau_s - \tau_i}{1 + \omega^2 \tau_s \tau_i}. \quad (2.19)$$

Otherwise

$$\operatorname{tg} \varphi = \frac{\Delta M}{M} \frac{\omega\tau}{1 + \omega^2 \tau^2}, \quad (2.20)$$

where $\tau = \sqrt{\tau_s \tau_i}$, $M = \sqrt{M_s M_p}$.

They frequently consider that the dynamic modulus determines that part of the strain which is located in phase with stress, i.e.,:

$$M_d = M_p \frac{1 + \omega^2 \tau_s^2}{1 + \omega^2 \tau_s \tau_i}, \quad (2.21)$$

or

$$M_d = M_s \left(1 - \Delta \frac{1}{1 + \omega^2 \tau^2} \right). \quad (2.22)$$

Expressions for dynamic moduls (2.22) and the tangent of the phase angle between the stress and strain (2.20) are the symmetrical functions of product $\omega\tau$. The analysis of these expressions shows:

a) when $\omega \rightarrow \infty$ (high frequency) $M_d \rightarrow M_s$; $\operatorname{tg} \varphi \rightarrow 0$;

b) when $\omega \rightarrow 0$ (low frequencies) $M_d \rightarrow M_p$; $\operatorname{tg} \varphi \rightarrow 0$;

c) with $\omega\tau = 1$ the dissipation of energy will be maximum:

$$M_x = \frac{M_s + M_p}{2}$$

Change $\operatorname{tg} \phi$ and M_x in dependence on value ω is shown on Fig.

55.

Page 82.

The dissipation of energy is caused by different processes within solid, each of them possessing the proper time of relaxation. Therefore the dissipation of energy of body at separate frequencies reaches maximum values. The dependence of the dissipation of energy on the frequency of the loading (relaxation spectrum) of metals with 20°C [58-60] is represented in Fig. 56. With the increase of frequency, becomes less the height of peaks and, consequently, also the relaxation of the modulus of elasticity.

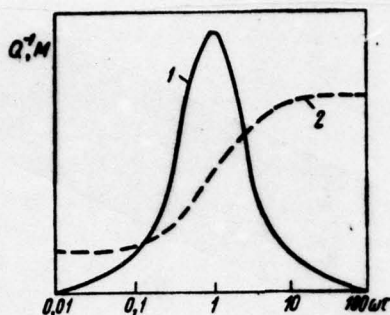


Fig. 55. The dependence of scattering energy and the dynamic modulus on the frequency: 1 - interstitial friction; 2 - modulus of elasticity.

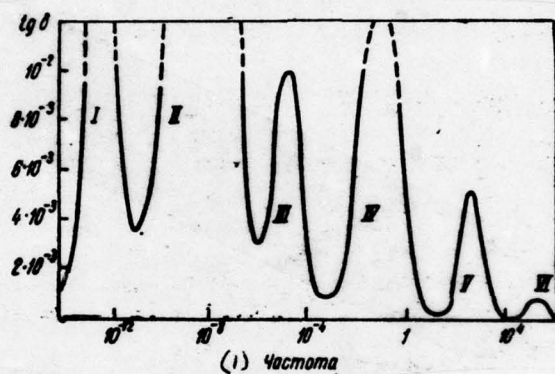


Fig. 56. Relaxation spectrum of metals with 20°C. Are shown the range of the dissipation of energy, caused: I - by presence of the pairs of atoms with different atomic radii; II - by viscous flow on grain boundaries; III - by viscous flow in the amorphous zones, formed by plastic deformation (bands of slip); IV - by diffusion of interstitial atoms; V - by cross thermal conductivity with the bend of specimen/sample; VI - by intercrystalline thermal conductivity.

Key: (1). frequency.

Page 83.

As the example of the temperature dependence of shear modulus Fig. 57 gives the curves G-T for mcnc- and pcly- crystal aluminum, obtained at frequency ~0.8 Hz [57]. The relaxation of the modulus of shear of polycrystalline specimen/sample, occurring at the temperatures higher than 470°K and reaching of several ten percent, is caused by viscous flow or grain boundaries.

The relaxation time of the processes, connected with the displacement/movement of atoms, depends substantially on temperature according to the equation:

$$\tau = \tau_0 e^{\frac{H}{RT}}, \quad (2.23)$$

where H - an energy of the activation of this relaxation process; R - universal gas constant; T - absolute temperature.

With the increase of temperature, the relaxation times are decreased and the peaks of relaxation spectrum are misaligned into the range of high frequencies. Consequently, for obtaining the values of the dynamic modulus, close to unrelaxed at high temperatures, measurement one should conduct at more possible high frequencies, i.e., by dynamic method. In principle method is based on the

velocities of propagation different wave modes in solid are determined by the elastic properties of body itself. The values of the moduli of elasticity it is possible to calculate according to the results of the measurements of the values, connected with the velocity of propagation of the elastic disturbance/perturbation: the time of its passage, frequency, from which is spread this disturbance/perturbation, and by its effect on the course of other phenomena.

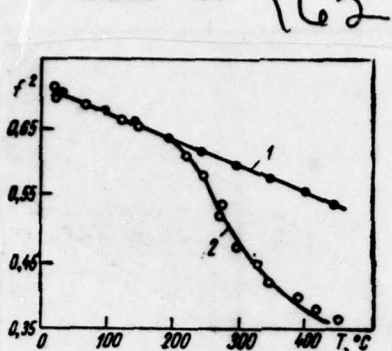


Fig. 57. The temperature dependences of shear modulus for single-crystal (1) and polycrystalline (2) aluminum (along the axis of coordinates is plotted the square of frequency, which is proportional to shear modulus).

Installations for determining of elasticity characteristics.

For measuring the moduli of elasticity of refractory metals and alloys by dynamic method at normal and high temperatures were developed resonance type installations УР-3, УР-5, УР-6 [30, 58, 59].

Resonance frequency f_{res} is connected with the natural frequency f_{cos} of specimen/sample by the dependence

$$f_{res} = f_{cos} \left(1 - \frac{\delta^2}{8\pi^2}\right), \quad (2.24)$$

where δ - a logarithmic decrement of fluctuations.

During small dissipation of energy in materials, for example with $\delta \approx 10^{-3}$, it is possible to count that $f_{res} \approx f_{eos}$. with an accuracy to 0.01c/o.

From the formula, which connects the natural frequency of specimen/sample with its geometric dimensions and weight, are determined the elasticity characteristics. For determining the module/modulus of elasticity E, are utilized longitudinal or transverse vibrations, while for determining the modulus of shear G, - torsional.

Are given below the basic formulas, which connect bending characteristics with the frequency of longitudinal, torsional and flexural vibrations. They are derived on the assumption that the specimen/samples have a form of stems with straight axle and constant along the length section/cut. By such is necessary satisfaction of condition $\lambda \gg d$, where λ - wavelength of the excited in specimen/sample vibration, and d - cross size/dimension of specimen/sample.

Longitudinal oscillations. The modulus of elasticity can be determined by the resonance frequency of the first form of the longitudinal oscillations of test sample with the aid of the expression:

$$E = 4l^2 \rho f_{sp}^2. \quad (2.25)$$

where ρ - material density of specimen/sample; l - length of specimen/sample; f_m - the resonance frequency of the first form of longitudinal oscillations.

As is known, during oscillations of a rod on the first (basic) form, is average along the length of rod the section/cut motionless, i.e., it is vibration node. This fact makes it possible to fasten during tests the mean section of specimen/sample, leaving its ends free.

The frequencies of the highest forms of the longitudinal oscillations of test sample differ from the frequency firstly of form into 2, 3, 4, 5 and so forth once, which makes it possible during measurements to differ the resonance frequencies of the longitudinal oscillations of specimen/sample from different interference.

Sometimes the test sample, in which are excited the oscillations of basic form, calls "half-wave", since fundamental frequency $f_m = \frac{c}{2l}$. $l = \lambda/2$.

Transverse vibrations. The modulus of elasticity can be also determined by the resonance frequencies of the various forms of cross oscillations of a rod.

Page 85.

In the case of the first form

$$E = \frac{4S}{l} \left(\frac{\pi^2}{4.76} f_m \right)^2. \quad (2.26)$$

where ρ - material density of specimen/sample; S - density of cross section; I - moment of inertia; l - length of specimen/sample; f_m - the resonance frequency of the first form of transverse vibrations.

For the experimental determination of the modulus of elasticity during transverse vibrations the specimen/sample is fastened at the nodes which with the first form are located at a distance 0.2241 from the ends of the specimen/sample.

Since the frequencies of the highest forms of transverse vibrations differ from the frequency of the first form into 2.76; in terms of 5.41; 8.94 and so forth once, sufficiently simply to determine the form of the oscillations of specimen/sample and it is possible to divide resonance frequencies and interference. If specimen/sample accomplishes cross and torsional vibrations simultaneously, the given relationship/ratio also can be utilized for the separation of the resonance frequencies of the cross torsional vibrations.

Torsional vibrations. Shear modulus can be determined by the

resonance frequency of the first form of the torsional vibrations:

$$G = 4\pi^2 f_{sp}^2 \quad (2.27)$$

where ρ - material density of specimen/sample; l - length of specimen/sample; f_{sp} - the resonance frequency of the first form of torsional vibrations.

In the case of the first form of torsional oscillations of a rod fixed (junction/unit) is its mean section. Therefore for fastening of specimen/sample during the wire suspensions, arranged located on its end/faces, it is necessary to utilize a wire of minimum thickness. (Otherwise the mass of wire can significantly influence the resonance frequency.)

The highest forms of the resonance frequencies of torsional vibrations differ from the first into 2, 3, 4 and 5 and so forth once.

Determining the moduli of elasticity at high temperatures, one should consider a change in the linear dimensions and density of specimen/sample during the heating:

$$l_t = l(1 + \alpha t); \quad (2.28)$$

$$d = d(1 + \alpha t); \quad (2.29)$$

$$\rho_t = \frac{\rho}{(1 + \alpha t)^3}, \quad (2.30)$$

where l_0, d_0, ρ_0 - length, diameter and density of specimen/sample at room temperature; l_t, d_t, ρ_t - the same parameters at the temperature of testing; α - coefficient of the linear expansion of the material of specimen/sample.

Page 86.

Taking into account relationship/ratios (2.28) - (2.30) the moduli of elasticity at high temperatures are determined from the following formulas:

a) during the longitudinal oscillations:

$$E_t = 4\rho l^2 f_{np}^2 (1 + \alpha t)^{-1}; \quad (2.31)$$

b) during transverse vibrations:

$$E_t = \frac{4\rho S}{l} \left(\frac{\pi l^2}{4,730^2} f_{np} \right)^2 (1 + \alpha t)^{-1}. \quad (2.32)$$

c) during the torsional vibrations:

$$G_t = 4\rho l^2 f_{np}^2 (1 + \alpha t)^{-1}. \quad (2.33)$$

From the developed by us installations of resonance type most perfected are УР-6; it is intended for measuring the module/modulus of elasticity and modulus of shear of high-melting materials at the temperatures to 2700°C in vacuum 0.0133 N/mm^2 (10^{-4} mm Hg) or in inert medium. Major advantage УР-6 consists in the fact that with the aid of this installation the moduli of elasticity and shear are measured in one and the same specimen/sample; this makes it possible with high

accuracy to calculate Poisson ratio.

The advantage indicated is reached because of the fact that the filaments of suspension transfer effort/force to cylindrical specimen/sample tangentially (Fig. 58). The longitudinal travel of one filament cause in specimen/sample cross and torsional vibrations, and with the aid of another filament is realized/accomplished recording the resonance frequencies of these oscillations. The measurement of the resonance frequency of transverse vibrations of specimen/sample makes it possible to calculate the module/modulus of elasticity E, and torsional vibrations - modulus of shear G.

1169

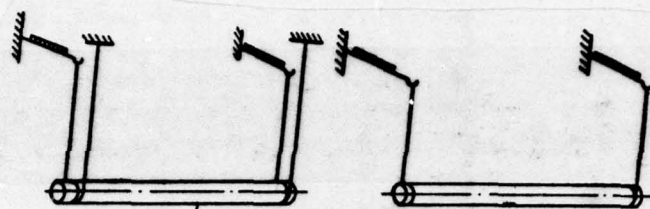


Fig. 58. Diagram of the suspension of specimen/sample during the determination of Young's modulus and displacement during installation up-6.

Page 87.

Block diagram **up-6** is shown on Fig. 59, is represented below the technical characteristic of the installation:

- | | |
|------------------------------------|---|
| (a) Образец | (h) Цилиндрический стержень длиной 80–120 мм, диаметром 7–8 мм |
| (b) Возбудитель колебаний | (i) Пьезоэлектрический |
| (c) Приемник колебаний | (j) Пластины из листового вольфрама толщиной 0,3–0,5 мм |
| (d) Нагреватель | (k) Термопары ВР5/ВР20 и пирометр |
| (e) Средства измерения температуры | (l) От комнатной до 2700°C |
| (f) Рабочий диапазон температур | (m) Вакуум 1,33 мк/m ² (10 ⁻⁵ мм рт. ст.) |
| (g) Среда | |

(a) Specimen/sample.

(b) Vibration exciter.

(c) Receiver of vibrations.

(d) Heater.

- (e) Means measuring the temperature.
- (f) Working temperature range.
- (g) Medium.
- (h) Cylindrical rod 80-120 mm in long, by diameter 7-8 mm.
- (i) Piezoelectric.
- (j) Plates from laminated tungsten 0.3-0.5 mm in thickness.
- (k) Thermocouples BP5/BP20 and pyrometer.
- (l) From room to 2700°C.
- (m) Vacuum 1.33 mN/m^2 (10^{-5} mm Hg).

High-temperature vacuum chamber design is shown on Fig. 60. It consists of vertical plate/slat and the cylindrical cap/hood, arranged/located horizontally.

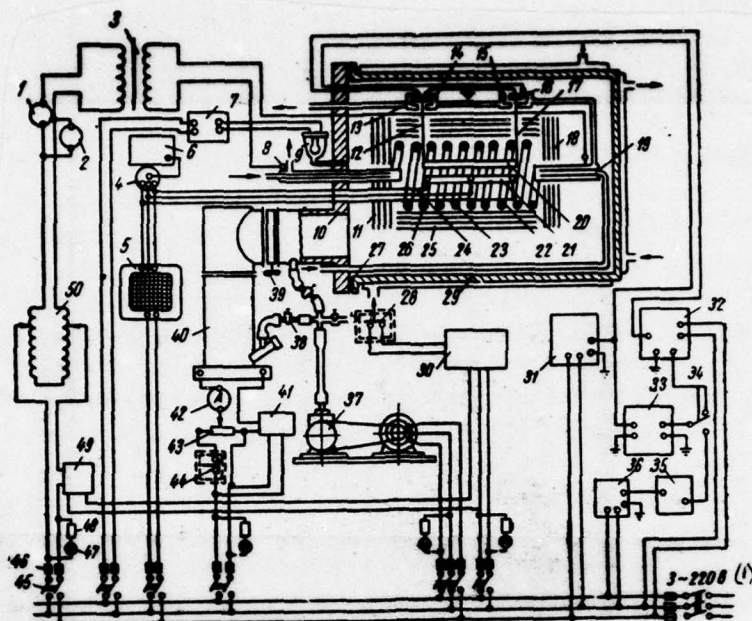


Fig. 59. Block-diagram of installation UP-6: 1 - ammeter of alternating current; 2 - voltmeter; 3 - transformer of the type OSU40x0.5; 4 - switch of thermocouples; 5 - electronic potentiometer of the type EPP-0.9; 6 - potentiometer of the type PP; 7 - vacuum gauge of type twisted-1; 8 - fixed current input; 9 - vacuum gauge lamps; 10 - plate/slab; 11, 18 - vertical shields; 12, 17 - wire suspensions; 13 - receiver of vibrations; 14, +5 - holders of exciter and receiver; 16 - vibration exciter; 19 - movable current supply; 20 - test specimen; 21 - control specimen/sample; 22, 23, 24 - thermocouple; 25 - horizontal shields; 26 - heater; 27 - packing layer; 28, 44 - relay of water pressure; 29 - cap/hood; 30 - MKU-48; 31 - master oscillator; 32 - amplifier; 33 - the cathode-ray

oscilloscope; 34 - single-pole switch; 35 - scaler; 36 - heterodyne wavemeter; 37 - fore pump; 38 - vacuum tap/crane; 39 - vacuum catch; 40 - diffusion pump; 41 - overload relay; 42 - ammeter; 43 - autotransformer; 45 - bipolar disconnection switch; 46 - fuse; 47 - signal lamp; 48 - resistance; 49 - contactor; 50 - bunchers
BOT-25/10.

Key: (1) - V.

Page 88.

Cap/hood can be abstract/removed on guides which provides free access to all internal assemblies of the camera/chamber and the light/lung exchange of specimen/samples. Most convenient for manufacture from high-melting materials cylindrical specimen/samples 6-8 mm in diameter and 80-100 mm in length (Fig. 61).

Test specimen is suspended during fine/thin metallic filaments in the working space of heater. Upper ends of the filaments are fastened to exciter and receiver of the vibrations which are establishinstalled on the water-cooled stand.

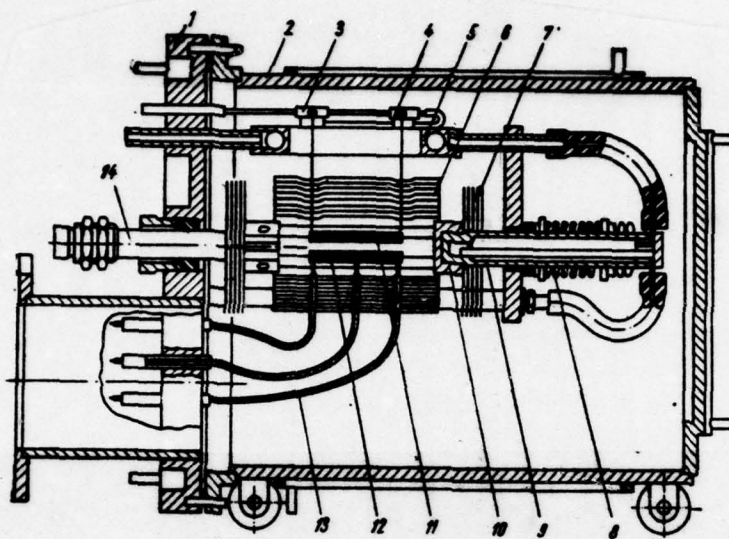


Fig. 60. High-temperature vacuum camera/chamber of installation up-6:
 1 - plate/slab; 2 - cap/hood; 3 - vibration exciter; 4 - receiver of vibrations; 5 - water-cooled table; 6 - horizontal shields; 7 - vertical shields; 8 - spring; 9 - movable current lead; 10 - holder for the plates of heater; 11 - test specimen; 12 - control specimen/sample; 13 - thermocouple; 14 - fixed current lead.

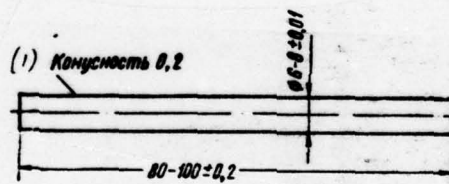


Fig. 61. Specimen/sample for determining module/modulus of normal elasticity and shear modulus.

Key: (1). Conicity.

Page 89.

Exciter and the receiver of vibrations are arranged equally (Fig. 62). Driver is plate from piezoceramics. This plate is attached by glass filament to holder. One of the conclusion/derivations of plate is grounded, and another conclusion/derivation approach/fits lead/duct from the master oscillator or amplifier. Holder at one end has a hook to which is fastened the filament, which supports specimen/sample; the opposite end of the holder is soldered to tube. The passing on tube water cools holder, preventing the superheating of piezoceramic plate.

By heater serve four tungsten plates 0.5 mm in thickness which with their ends are fastened to the molybdenum tips of current supplies. Movable current supply during the elongation of plates during heating is drawn down by spring.

Heater is encircled by shields from tungsten, molybdenum and nickel tin 0.2-0.3 mm in thickness. Horizontal shields are assembled of the cylinders, which are located one from another at a distance of 3-4 mm; vertical - of the flat sheets. Fastenings are made from tungsten and molybdenum. Nearest to heater sheets - tungsten;

remaining - molybdenum and rickel.

The device of horizontal shields makes it possible to easily establish/install specimen/sample, to realize/accomplish a delivery of thermocouples to control specimen/sample, and to also manufacture the measurement of the temperature of specimen/sample with pyrometer.

For determining the temperature of test specimen, are establishinstalled three tungsten-rhenium thermocouples of brand EPS/BR20; their joints are attached to middle and the end/faces of the control specimen/sample, arranged/located under test specimen.

During the work of the setting up of walls of the high-temperature camera/chamber, the stand, on which are establishinstalled the exciter and the receiver of vibrations, and also current supplies, intensely are cooled by running water.

176

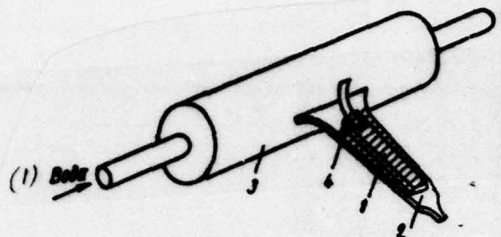


Fig. 62. The device of exciter and receiver of the vibrations: 1 - plate from piezoceramics; 2 - holder; 3 - water-cooled tube; 4 - conclusion.

Key: (1) water.

Page 90.

Vacuum in the camera/chamber they provide preliminary pump VN-2 and vacuum assembly VA-5-4. Feed is realize, acccmplished from the industrial net of alterrating current by voltage 220 V through gauging (ROT-25/10) and step-dcwn (OSU40/0.5) transformers.

During the operatcion of installation, it was noticed that during heating of specimen/sample to the temperature, exceeding 1700°C, for achievement by which was necessary considerable current, the circular parts of current supplies (nut, disk, etc.) are heated by eddy currents, and they also occur of focusing/induction high frequency current to lead/ducts frm receiver to amplifier. For purpose of eliminating these undesirable phenomena was developed the diagram of the feed of heater direct current (Fig. 63).

By the source of direct current serves motor generator AD 5000/2500 30 kW power. Output potential its smoothly is regulated frm 0 to 6 (or 12) V with the aid of two rheostats, connected in the circuit of the windings cf excitation. The cnditions/mode of heating

is controlled by the voltmeter and the kilammeter, connected in the target/purpose of heater.

For the modulus of elasticity during installation ~~up to 6~~, apply so-called "short" test samples ($\frac{l}{d} \approx 10$). By calculation according to formula (2.32), which does not consider shift/shear and the rotation of the cell/elements of rod, it is not possible to obtain a precise value of module/modulus. There are analytical methods the account of shift/shear and turn [60]; however, they require complex computations.

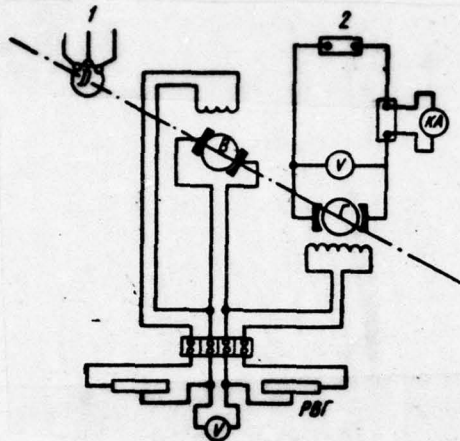


**Fig. 63. The diagram of heating specimen/sample by direct current in
UP-6;
installations up-6: 1 - 220 V, 50 Hz (from net); 2 - heater.**

Page 91.

Therefore during installation UP-1 [60] preliminarily for each specimen/sample was determined module/modulus according to the resonance frequency of longitudinal oscillations at normal temperature, obtaining precise values of module/modulus. Then for installation UP-6 was measured the resonance frequency of transverse vibrations of specimen/sample and was again designed the value of module/modulus. A difference in the obtained values was utilized as constant correction to the values of the modulus of elasticity, measured at high temperatures.

Elasticity characteristics of tungsten, molybdenum and their alloys in the range of temperatures of 20-2700°C.

Tungsten. In the literature most frequently is given the value of the modulus of elasticity of tungsten at normal temperature, published in 1948. by Kester[61], i.e., 40.7 E/m^2 ($4.15 \times 10^4 \text{ kg/mm}^2$). This value was obtained by measuring the resonance frequency of transverse vibrations of specimen/samples. The modulus of elasticity of cermet tungsten, determined by a similar method by M. G. Lozinskiy [62], render/showed equal to 386 E/m^2 ($3.94 \times 10^4 \text{ kg/mm}^2$). Other researchers' majorities, which conducted measurements in the specimen/samples of cermet tungsten of different porosity, were obtained the values of the modulus of normal elasticity from 344 E/m^2 ($3.50 \times 10^4 \text{ kgf/mm}^2$) to 412 E/m^2 ($4.20 \times 10^4 \text{ kg/mm}^2$).

We carried out the measurements of the modulus of elasticity of cermet tungsten of the mark/brand of VBN of the production of Moscow electric bulb plant (density 18.8 g/cm^3 [63]). Specimen/samples were prepared from rods 8 mm in diameter by machining external surface on grinding machine with the subsequent facing. Elastic modulus at room temperature render/showed equal to 386 E/m^2 ($3.95 \times 10^4 \text{ kg/mm}^2$). Extrapolation of the values of module/modulus to the zero porosity of dates value, the close of 407 E/m^2 ($4.15 \times 10^4 \text{ kg/mm}^2$).

The modulus of elasticity was determined also for the specimen/samples of poured tungsten [25, 64, 65]. (By melting in vacuum arc furnace with the consumable electrode 2 kg/h in velocity were obtained ingots 80 mm in diameter which were heated to 1400-1600°C and they strained with the degree of reduction 60-85%, and they annealed in vacuum). Specimen/samples were prepared by machining on lathe and by the subsequent grinding by the emery paper. The chemical composition of the specimen/samples of tungsten was following: 0.035% C; 0.006% S; 0.002% P; 0.002% Cu; 0.06% Mo; 0.02-0.05% Nb; 0.013-0.017% O₂; 0.002-0.004% H₂ (were shown percentages throughout mass).

The value of the modulus of elasticity, calculated in the resonance frequencies of specimen/samples, proved to be equal to 404 H/mm² ($4.12 \cdot 10^4$ kg/mm²).

In the literature there is much lesser than the information about the measurement of the modulus of shear of tungsten. On the data of Kester [61], its value with normal temperature is equal to 148 H/mm² ($1.51 \cdot 10^4$ kg/mm²). In the later works of value, are close this [66].

On data our measurements, the modulus of shear of cermet tungsten of the mark/brand of VRN with normal temperature is equal to 145 H/mm^2 ($1.48 \cdot 10^4 \text{ kg/mm}^2$), and for the poured tungsten 160 H/mm^2 ($1.63 \cdot 10^4 \text{ kg/mm}^2$). Kester gives for tungsten the value of Poisson ratio, equal to 0.30. This value is shown in [66], although, being it is calculated on the moduli of elasticity, the determined by Kester Poisson ratio of tungsten is proved to be equal to 0.37.

On measurement data by A. B. Lyashchenko, for tungsten $\mu=0.31$.

The value of Poisson ratio, calculated by us in the values of module/moduli for cermet tungsten of the mark/brand of VRN, is equal to 0.34, and for poured - 0.28. The value of the module/moduli of pulled tungsten wire depends to a considerable extent on the degree of reduction and temperature of annealing [3, 67]. The modulus of elasticity vary within the range of 147 H/mm^2 ($1.50 \cdot 10^4 \text{ kg/mm}^2$) to 372 H/mm^2 ($3.80 \cdot 10^4 \text{ kg/mm}^2$), while shear modulus - within limits from 137 H/mm^2 ($1.40 \cdot 10^4 \text{ kg/mm}^2$) to 177 H/mm^2 ($1.80 \cdot 10^4 \text{ kg/mm}^2$).

Wright [3] is in detail studied the elastic properties of single-crystal tungsten wire 0.9 mm in diameter. It established that the crystals of tungsten are almost completely elastic isotropic ones, differences in the elastic properties of crystals are very insignificant (less than 0.20%). On Wright's data, the modulus of

elasticity of the single-crystal tungsten wire equal to 386 H/m^2 ($3.94 \cdot 10^4 \text{ kg/mm}^2$), and modulus of shear - 150 H/m^2 ($1.53 \cdot 10^4 \text{ kg/mm}^2$).

Chalmers [68] gives the identical values of the modulus of elasticity of the single crystals of tungsten for directions [111] and [100], equal to 388 H/m^2 ($3.96 \cdot 10^4 \text{ kg/mm}^2$), and shear modulus, equal to 150 H/m^2 ($1.53 \cdot 10^4 \text{ kg/mm}^2$), and is made the conclusion that tungsten of elastic is isotropic.

By V. A. Dreshpak during installation UP-6 were determined elasticity characteristics of the single crystal of tungsten in test sample 7 mm in diameter and 73 mm in length with room temperature.

Single crystal was mechanically machined on plain grinding machine and polished by diamond disk. For removal/taking peening from the surface of test sample was removed layer 0.1 mm via chemical etching in the 30% solution of peroxide of hydrogen with the small addition of ammonia.

The longitudinal axis of specimen/sample, as it was established/installed from the Laue diffraction patterns, removed in molybdenum emission/radiation, composed the angle of 16 deg. with direction [100]. The modulus of normal elasticity of the single crystal of tungsten proved to be equal to 390 H/m^2 ($3.98 \cdot 10^4 \text{ kg/mm}^2$),

while shear modulus - 158 H/m^2 ($1.61 \cdot 10^4 \text{ kg/mm}^2$).

Page 93.

The calculated in the values of the moduli of elasticity Poisson ratio composed 0.24.

The modulus of normal elasticity of tungsten at elevated temperatures measured with the resonance method of Kester - to 800°C [61], M. G. Lozinskiy - to 1200°C [62], Braun and Armstrong [69] - to 2400°C by S. Impul'sn by the method of the value of module/modulus for tungsten were determined by Bernstein to 1200°C [70], but Lowry and Gonas - to 800°C [71]. The values of the modulus of normal elasticity of tungsten, obtained by different researchers coincide well in all studied temperature range (Fig. 64). Exception are only the results of work [63], in which even for normal temperature is obtained the value of the modulus of normal elasticity of tungsten more than 50.0 H/m^2 ($5.1 \cdot 10^4 \text{ kg/mm}^2$).

In our work were carried out the high-temperature measurements of the modulus of normal elasticity of the cermet and poured tungsten. Results are represented on Fig. 64 and Table 10.

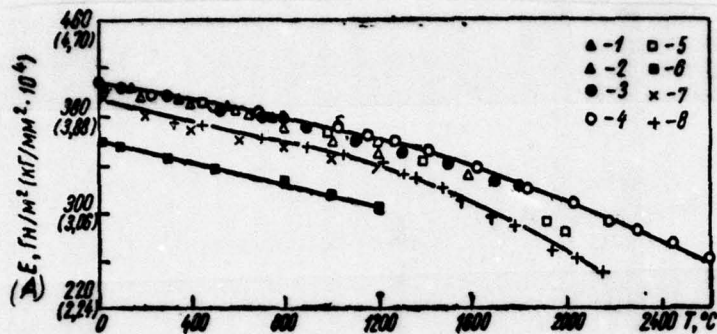


Fig. 64. Dependence of the modulus of normal elasticity of tungsten on temperature. Poured the tungsten: 1 - [61]; 2 - [70]; 3 - [71]; 4 - [65]; 5 - [25]. The cermet tungsten: 6 - [64]; 7 - [62]; 8 - [63].

Key: (A) - $E, \text{N/m}^2 (\text{kg/mm}^2 \cdot 10^4)$.

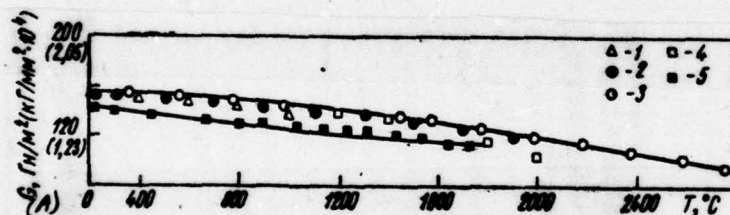


Fig. 65. Dependence of the modulus of shear of tungsten on temperature. Poured the tungsten: 1 - [70]; 2 - [71]; 3 - [65]; 4 - [72]. The cermet tungsten: 5 - [63].

Key: (A) - $G, \text{N/m}^2 (\text{kg/mm}^2 \cdot 10^4)$.

From the data obtained, it follows that the difference between the values of the moduli for cast and cermet tungsten which exists at normal temperature is also retained at high temperatures. At the same time, the nature of the temperature dependence of the tungsten modulus does not depend on the method of obtaining the metal. With an increase in temperature to 1500-1600° (which is **0.5 T_m**). The modulus of normal elasticity of tungsten is reduced first slowly and then more intensively. At high temperatures, tungsten retains a high modulus value; thus, at 2200°C modulus $E=255 \text{ MN/m}^2$ ($2.6 \cdot 10^4 \text{ kg/mm}^2$), i.e., higher than for steel at room temperature.

The shear modulus of tungsten changes with an increase in temperature similar to the modulus of normal elasticity (Fig. 65, Table 10).

Table 10. Dependence of tungsten elasticity characteristics on temperature.

(1) Temper- ature, °C	(2) Характеристики упругости металлоке- рамического вольфрама			(3) Характеристики упругости вольфрама электролугового переплава		
	(4) $E, \text{ГН}/\text{м}^2$ ($\text{kg}/\text{mm}^2 \cdot 10^{-4}$)	(5) $G, \text{МН}/\text{м}^2$ ($\text{kg}/\text{mm}^2 \cdot 10^{-4}$)	μ	(4) $E, \text{ГН}/\text{м}^2$ ($\text{kg}/\text{mm}^2 \cdot 10^{-4}$)	(5) $G, \text{МН}/\text{м}^2$ ($\text{kg}/\text{mm}^2 \cdot 10^{-4}$)	μ
20	388 (3,95)	145 (1,48)	0,34	404 (4,12)	160 (1,63)	0,26
100	385 (3,93)	143 (1,46)	0,34	400 (4,08)	159 (1,62)	0,26
200	380 (3,88)	141 (1,44)	0,34	396 (4,04)	157 (1,60)	0,26
300	376 (3,84)	139 (1,42)	0,35	393 (4,01)	155 (1,58)	0,27
400	372 (3,80)	137 (1,40)	0,35	389 (3,97)	154 (1,57)	0,26
500	368 (3,75)	135 (1,38)	0,35	385 (3,93)	152 (1,55)	0,27
600	363 (3,70)	133 (1,36)	0,35	381 (3,89)	150 (1,53)	0,27
700	349 (3,66)	132 (1,35)	0,35	377 (3,85)	148 (1,51)	0,27
800	354 (3,61)	131 (1,34)	0,34	374 (3,82)	146 (1,49)	0,28
900	350 (3,57)	129 (1,32)	0,35	370 (3,78)	145 (1,48)	0,28
1000	345 (3,52)	127 (1,30)	0,35	367 (3,74)	143 (1,46)	0,28
1100	341 (3,48)	125 (1,28)	0,35	363 (3,70)	141 (1,44)	0,28
1200	336 (3,43)	123 (1,26)	0,36	360 (3,67)	139 (1,42)	0,29
1300	331 (3,38)	122 (1,24)	0,36	355 (3,62)	137 (1,40)	0,29
1400	325 (3,32)	120 (1,22)	0,36	350 (3,57)	135 (1,38)	0,29
1500	314 (3,23)	117 (1,20)	0,34	344 (3,51)	133 (1,36)	0,29
1600	306 (3,12)	—	—	335 (3,42)	130 (1,33)	0,28
1700	295 (3,01)	—	—	328 (3,35)	127 (1,30)	0,28
1800	284 (2,90)	—	—	321 (3,28)	124 (1,27)	0,29
1900	274 (2,80)	—	—	314 (3,20)	122 (1,24)	0,29
2000	265 (2,70)	—	—	306 (3,12)	119 (1,21)	0,29
2100	255 (2,60)	—	—	298 (3,04)	116 (1,18)	0,29
2200	245 (2,50)	—	—	290 (2,96)	112 (1,14)	0,29
2300	—	—	—	283 (2,89)	110 (1,12)	0,29
2400	—	—	—	275 (2,81)	107 (1,09)	0,29
2500	—	—	—	268 (2,74)	104 (1,06)	0,29
2600	—	—	—	260 (2,66)	101 (1,03)	0,29
2700	—	—	—	253 (2,58)	— —	—

Key: (1). Temperature, °C. (2). Elasticity characteristics of cermet molybdenum. (3). Elasticity characteristics of molybdenum of cathode-ray remelting. (4). $E, \text{ГН}/\text{м}^2$ ($\text{kg}/\text{mm}^2 \cdot 10^{-4}$). (5). $G, \text{МН}/\text{м}^2$ ($\text{kg}/\text{mm}^2 \cdot 10^{-4}$).

The calculation of the Poisson ratio of tungsten in the values of module/moduli shows that μ barely is changed with the increase of temperature. Its values for the wide temperature range are given in Table 10.

All the examined results of measuring the moduli of elasticity of tungsten at high temperatures were obtained for polycrystalline specimen/samples. V. A. Dreshpak during installation UP-6 they determined the moduli of elasticity at high temperatures also for the specimen/sample of single-crystal tungsten. (The same specimen/sample which was used for measurements at normal temperature). The obtained by it values of the moduli of normal elasticity and shear of the single crystal of tungsten are represented on Fig. 66.

Comparison Figs. 64-66 shows that the temperature dependences of the moduli of elasticity of single crystal and polycrystal of tungsten somewhat are distinguished. The module/moduli of single crystal in all interval of temperatures of heating are decreased more evenly and it is less intense, than in the case of polycrystal.

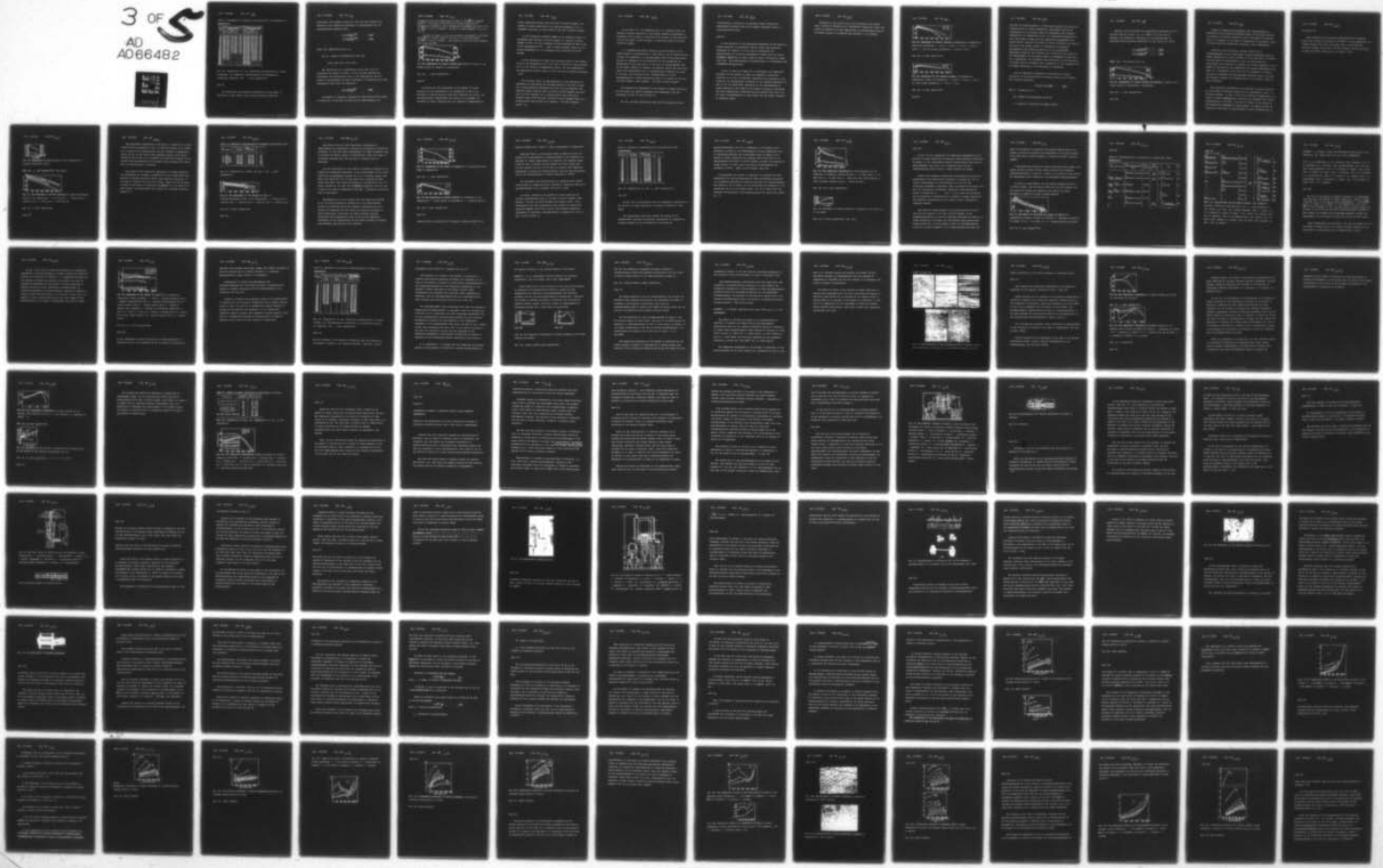
AD-A066 482 FOREIGN TECHNOLOGY DIV WRIGHT-PATTERSON AFB OHIO
STRENGTH OF REFRACTORY METALS. PART I, (U)
OCT 78 G S PISARENKO, V A BORISENKO
FTD-ID(RS)T-1330-78-PT-1

F/G 11/6

UNCLASSIFIED

NL

3 OF 5
AD
A066482



3 OF

AD

A066482

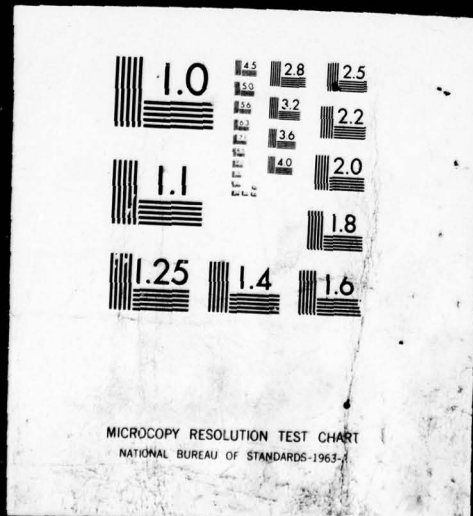


Table 11. Dependence of elasticity characteristics of molybdenum on temperature.

Tempera- ture, °C	(2) Характеристики упругости металлокерамического молибдена			(3) Характеристики упругости молибдена электроннолучевого переплава		
	(4) $E, \text{ГН/м}^2$ ($\text{кГ/мм}^2 \cdot 10^4$)	(5) $G, \text{ГН/м}^2$ ($\text{кГ/мм}^2 \cdot 10^4$)	μ	(4) $E, \text{ГН/м}^2$ ($\text{кГ/мм}^2 \cdot 10^4$)	(5) $G, \text{ГН/м}^2$ ($\text{кГ/мм}^2 \cdot 10^4$)	μ
20	323 (3,28)	121 (1,24)	0,32	322 (3,28)	119 (1,21)	0,35
100	315 (3,22)	120 (1,22)	0,31	318 (3,24)	118 (1,20)	0,35
200	311 (3,17)	118 (1,20)	0,32	314 (3,20)	116 (1,18)	0,35
300	306 (3,12)	116 (1,18)	0,32	310 (3,16)	114 (1,16)	0,36
400	300 (3,06)	114 (1,16)	0,31	306 (3,12)	112 (1,14)	0,36
500	294 (3,00)	112 (1,14)	0,31	301 (3,01)	111 (1,13)	0,36
600	290 (2,95)	110 (1,12)	0,31	297 (3,03)	110 (1,12)	0,35
700	282 (2,88)	107 (1,09)	0,32	292 (2,98)	108 (1,10)	0,35
800	276 (2,82)	105 (1,07)	0,31	288 (2,94)	106 (1,08)	0,36
900	270 (2,76)	103 (1,05)	0,31	284 (2,90)	105 (1,07)	0,35
1000	265 (2,71)	103 (1,03)	0,31	280 (2,86)	103 (1,05)	0,36
1100	258 (2,64)	98 (1,00)	0,32	275 (2,81)	101 (1,03)	0,36
1200	254 (2,59)	96 (0,98)	0,32	268 (2,74)	99 (1,01)	0,36
1300	248 (2,53)	94 (0,96)	0,31	263 (2,68)	96 (0,98)	0,36
1400	237 (2,47)	92 (0,94)	0,28	255 (2,60)	94 (0,96)	0,35
1500	222 (2,27)	— —	—	247 (2,52)	91 (0,93)	0,35
1600	208 (2,12)	— —	—	238 (2,43)	89 (0,91)	0,33
1700	193 (1,97)	— —	—	231 (2,36)	87 (0,88)	0,34
1800	177 (1,81)	— —	—	222 (2,21)	82 (0,84)	0,35
1900	163 (1,66)	— —	—	216 (2,20)	79 (0,81)	0,36
2000	— —	— —	—	208 (2,12)	75 (0,77)	0,38
2100	— —	— —	—	200 (2,04)	— —	—
2200	— —	— —	—	192 (1,96)	— —	—
2300	— —	— —	—	184 (1,88)	— —	—

Key: (1). Temperature, °C. (2). Elasticity characteristics of cermet molybdenum. (3). Elasticity characteristics of molybdenum of cathode-ray remelting. (4). —, Н/м^2 ($\text{кг/мм}^2 \cdot 10^4$).

Page 96.

For describing the temperature dependences of the moduli of elasticity of pure metals, were proposed different empirical

expressions. For example, Hayes into 1923 acre [67] proposed the formulas of the temperature dependence of module/moduli for the monocrystalline tungsten wires:

$$E_t = E_0 \left(\frac{T_{m1} - T}{T_{m1}} \right)^{0.263}; \quad (2.34)$$

$$G_t = G_0 \left(\frac{T_{m1} - T}{T_{m1}} \right)^{0.263}. \quad (2.35)$$

where T_{m1} — the melting point, °K.

E_0 , G_0 — values of module/moduli with 0°K.

E_t , G_t — the same, with $t=T^{\circ}\text{K}$.

The carried out by us computations showed that only the expression for modulus of shear G (2.35) provides satisfactory coincidence with experimental data at low temperatures. For the values of module/modulus E , good coincidence of calculation data with experimental ones gives the expression

$$E_t = E_0 \left(\frac{T_{m1} - T}{T_{m1}} \right)^{0.4}. \quad (2.36)$$

Molybdenum, as tungsten, possesses the high values of the moduli of elasticity. On the data of Kester [61], module/modulus E of

molybdenum with room temperature is equal to 329 MN/m^2 ($3.36 \times 10^4 \text{ kg/mm}^2$). The values of the modulus of normal elasticity of molybdenum, obtained by other researchers, are within the limits from 310 MN/m^2 ($3.16 \cdot 10^4 \text{ kg/mm}^2$) to 333 MN/m^2 ($3.3 \times 10^4 \text{ kg/mm}^2$) [1; 3; 61; 62; 64].

In work [1] given for the metalloceramic molybdenum is the value $E=312 \text{ MN/m}^2$ ($3.18 \cdot 10^4 \text{ kg/mm}^2$), and for the poured molybdenum - 317 MN/m^2 ($3.23 \cdot 10^4 \text{ kg/mm}^2$). The authors of work [72] also consider this value reliable.

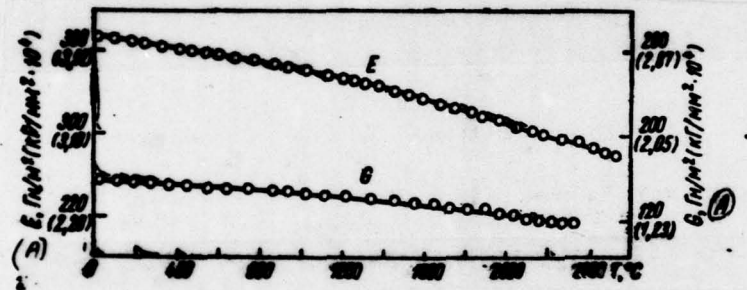


Fig. 66. Dependences of Young's modulus and modulus of shear of the single crystal of tungsten on temperature.

Key: (A). —, H/m^2 ($\text{kg/mm}^2 \cdot 10^4$).

Page 97.

We carried out the measurement of the modulus of normal elasticity of the molybdenum of the mark/brand of MRN of the production of Moscow electric bulb plant (density 10.2 g/cm^3). The specimen/samples, manufactured from rods 8 mm in diameter via machining on lathe, annealing were not subjected. Measurements at

normal temperature showed that $E=322 \text{ H/mm}^2$ ($3.28 \cdot 10^4 \text{ kg/mm}^2$). The modulus of normal elasticity of the poured molybdenum, on V. A. Dreshpak's data [65], is also equal to 322 H/mm^2 ($3.28 \cdot 10^4 \text{ kg/mm}^2$).

In the literature corrected values of the modulus of shear of molybdenum from 120 H/mm^2 ($1.23 \cdot 10^4 \text{ kg/mm}^2$), to 124 H/mm^2 ($1.27 \cdot 10^4 \text{ kg/mm}^2$) [72-74]. For the molybdenum of the mark/brand of MRN on data of our measurements $G=122 \text{ H/mm}^2$ ($1.24 \cdot 10^4 \text{ kg/mm}^2$), while for the poured molybdenum on V. A. Dreshpak's data $G=119 \text{ H/mm}^2$ ($1.21 \cdot 10^4 \text{ kg/mm}^2$).

In the literature are given the following values of the Poisson ratio of the molybdenum: $\mu=0.31$ [61] and $\mu=0.324$ [73]. The calculated by us in the values of module/moduli value, for the molybdenum of the mark/brand of MRN is equal to 0.32, and for the poured molybdenum - 0.35.

All corrected values of characteristics of the elasticity of molybdenum are determined for specimen/samples in the form of rods. For a polycrystalline molybdenum wire 0.5-1.0 mm in diameter were obtained values $E=250-292 \text{ H/mm}^2$ ($2.56 \cdot 10^4-2.98 \cdot 10^4 \text{ kg/mm}^2$) and $E=325 \text{ H/mm}^2$ ($3.32 \cdot 10^4 \text{ kg/mm}^2$); for a single-crystal wire 0.041 mm in diameter value $E=135-150 \text{ H/mm}^2$ ($1.38 \cdot 10^4-1.53 \cdot 10^4 \text{ kg/mm}^2$), while for a single-crystal wire 0.0365 mm in diameter - 179 H/mm^2 ($1.83 \cdot 10^4 \text{ kg/mm}^2$) [3].

On the data C. C. cf Aleksandrov and T. V. Ryzhovoy [74], the modulus of normal elasticity of the single crystal of molybdenum in direction [111] is equal to 294 H/m^2 ($3 \cdot 10^4 \text{ kg/mm}^2$), in the direction [110] of 313 H/m^2 ($3.2 \cdot 10^4 \text{ kg/mm}^2$), in direction [100] of 347 H/m^2 ($3.54 \cdot 10^4 \text{ kg/mm}^2$).

V. A. Dreshpak determined elasticity characteristics of the single crystal of molybdenum for a test sample 8 mm in diameter 90 mm in long. The manufacture of specimen/sample made of the grown single crystal of molybdenum and the definition of its orientation was manufactured in the same way as in the case of specimen/sample made of the single crystal of tungsten. As chemical etchant was used "aqua regia". The longitudinal axis of specimen/sample composed the angle cf 2-6 deg. with direction [111]. Module/modulus E of this specimen/sample at normal temperature proved to be equal to 285 H/m^2 ($2.91 \cdot 10^4 \text{ kg/mm}^2$), shear modulus - 104 H/m^2 ($1.06 \cdot 10^4 \text{ kg/mm}^2$).

You obtained the dependences of the modulus of normal elasticity for the cermet and poured molybdenum from temperature they were represented on Fig. 67 and in Table 11.

Our data coincide sufficiently well with the results of other

investigations, carried out by resonance method, whereas the measurements by pulse method give somewhat different results in high-temperature range.

Page 98.

In the character of the temperature dependence of the modulus of normal elasticity of molybdenum, much in common with analogous dependence for tungsten. In all range of temperature the module/modulus of the pured molybdenum is higher than for cermet, although a difference in their values is small. Afterward by 1300°C ($\sim 0.5 T_{\text{m}}$), an incidence/drop in module/modulus E of molybdenum with temperature is accelerated.

On Fig. 68 (see also Table 14) is represented the temperature dependence of the modults cf shear of molybdenus, constructed according to the data of different researchers and according to the results of our measurements. Character of the obtained dependence the same as for the temperature dependence of the module/modulus of normal elasticity. The values of the modulus of shear of molybdenum with high temperatures, determined by pulse method [75], just as in the case of module/modulus E, they differ from the values, obtained by resonance method.

DOC = 78133004

PAGE ~~17~~ 195

According to the carried out by us calculation, the Poisson ratio μ barely is changed in all investigated temperature range. The moduli of elasticity at high temperatures in specimen/sample made of the single crystal of molybdenum were measured V. A. Dreshpak.

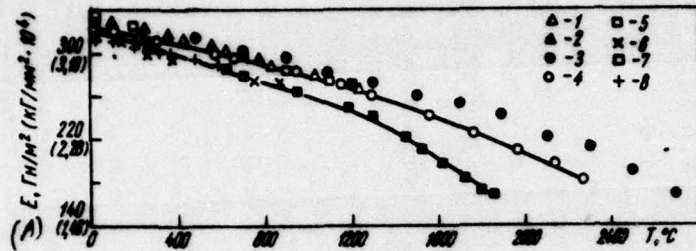


Fig. 67. Dependence of Young's modulus of molybdenum on temperature.

Scoured the molybdenum: 1 - [61]; 2 - [62]; 3 - [75]; 4 - [65]; 5 - [64]; 6 - [1]. The cermet molybdenum: 7 - [30]; 8 - [1].

Key: (A). E, H/m² (kg/mm² · 10⁴).

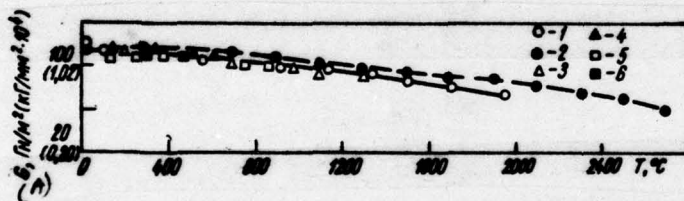


Fig. 68. Dependence of the modulus of shear of molybdenum on temperature. Poured the molybdenum: 1 - [65]; 2 - [75]; 3 - [4]; 4 - [1]. The cermet molybdenum: 5 - [1]; 6 - [30].

Key: (A). G, H/m² (kg/mm² · 10⁴).

Was used the specimen/sample, in which were measured the elasticity characteristics at normal temperature. Measurement data of the module/moduli of the single crystal of molybdenum with different temperatures are represented on Fig. 69. Temperature dependences E and G have much in common with the appropriate dependences for a single crystal tungsten. The moduli of normal elasticity and shear in the case of the single crystal of molybdenum are decreased approximately with identical intensity in all investigated temperature interval. The intensity of a reduction in the values of the module/moduli of the single crystal of molybdenum is less than for a polycrystal. For molybdenum this difference in the intensities is greater than for tungsten, what, apparently, is the consequence of the higher anisotropy of the elasticity of molybdenum.

For the temperature dependence of the modulus of normal elasticity of the polycrystalline molybdenum Touni [4] it proposed the following expression:

$$E_t = E_0 [1 - k(T - 273)], \quad (2.37)$$

where T - temperature °K.

E_0 - value of module/modulus with 0°K.

k - empirical coefficient ($k=0.0001-0.0002$).

Equation (2.37) describes well experimental dependence only on the first section curved, i.e., to 1300°C. As in the case of tungsten, the temperature dependences of the module/moduli of molybdenum better describe expressions of type (2.34) and (2.35):

$$E_t = E_0 \left(\frac{T_{m\bar{u}} - T}{T_{m\bar{u}}} \right)^{0.43}, \quad (2.38)$$

$$G_t = G_0 \left(\frac{T_{m\bar{u}} - T}{T_{m\bar{u}}} \right)^{0.43}. \quad (2.39)$$

where $T_{m\bar{u}}$ — the melting point, °K.

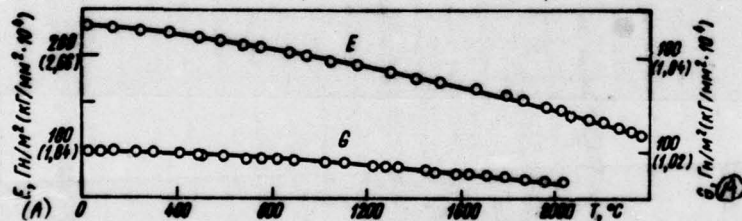


Fig. 69. Dependences of Young's modulus and modulus of shear of the single crystal of molybdenum on temperature.

Key: (A) —, $\text{N/mm}^2 (\text{kg/mm}^2 \cdot 10^6)$.

Page 100.

Alloys of tungsten and molybdenum. The characteristics of elasticity of the tungsten-molybdenum alloys of the vacuum electric arc melting of different composition have investigated we together with V. A. Dreshpak in the range of temperatures of 20-2700°C. Ingots of these alloys were plastically deformed at high temperatures.

Elasticity characteristics (average values for 2-3 specimen/samples) of all investigated tungsten-molybdenum alloys at normal temperature are given in Table 12. From these data it follows that the values of module/moduli E and G for each alloy are proportional to the content of tungsten. The linear dependence of the moduli of elasticity on the composition of tungsten-molybdenum alloys (Fig. 70) is explained by the fact that the parameters of crystal lattices of components are distinguished altogether only to 0.5%, and therefore tungsten and molybdenum form the continuous number of solid solutions.

The temperature dependences of the modulus of normal elasticity for the alloys of different composition are represented on Fig. 71, and shear modulus - on Fig. 72. With the increase of temperature, the moduli of normal elasticity of all alloys are decreased first slowly (approximately to 0.5 $T_{m\alpha}$), and then are faster. In the curves of the temperature dependence of shear modulus, the change of rate of reduction in the value of module/modulus is less noticeably than in

the curves E-T.

Were determined also elasticity characteristics of tungsten fusion with rhenium in interval of 20-2700°C. At room temperature for tungsten fusion from 27c/o (throughout mass) of Re E=403 H/m² ($4 \cdot 11 \cdot 10^4$ kg/mm²), G=154 H/m² ($1.57 \cdot 10^4$ kg/mm²), and the calculated in these two values Poisson ratio is equal to 0.30.

201

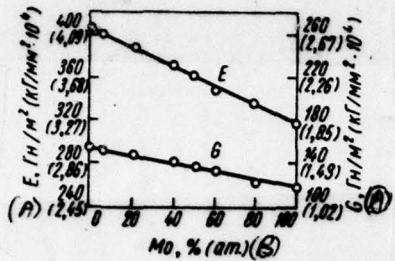


Fig. 70. Dependences of module/moduli on the composition of tungsten-molybdenum alloys.

Key: (A) - —, H/mm^2 ($\text{kg/mm}^2 \cdot 10^4$) - (B) - (at.) -

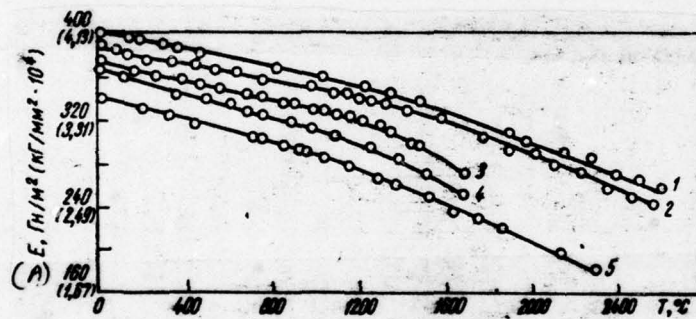


Fig. 71. The dependence of Young's modulus of tungsten-molybdenum alloys on the temperature: 1 - W+5.2% Mo; 2 - W+20.8% Mo; 3 - W+39.5% Mo; 4 - W+39% Mo; 5 - W+79.5% Mo.

Key: (A) - E, H/mm^2 ($\text{kg/mm}^2 \cdot 10^4$) -

The temperature dependences of the moduli of elasticity of alloy W-27% Re are represented on Fig. 73. From this figure it is evident that a change in the module/moduli with the increase of temperature occurs just as in the case of pure tungsten; however, with larger intensity. The latter, it is probable, is caused by the effect of the rhenium whose module/moduli are decreased during heating much faster, than the module/moduli of tungsten.

The curves of the temperature dependences of normal elasticity and displacement of tungsten, molybdenum and their alloys which were measured by dynamic resonance method, have identical character. In all cases is observed the bend with $0.5 T_{m}$. Since the law governing a change in the moduli of elasticity is observed for the majority of other metals, if measurements were carried out by dynamic resonance method [61].

Table 12. Elasticity characteristics of tungsten-molybdenum alloys.

(1) Состав сплавов, % (ат.)	(2) $E, \text{ГН/м}^2$ ($\text{кГ/мм}^2 \cdot 10^{-4}$)	(2) $G, \text{ГН/м}^2$ ($\text{кГ/мм}^2 \cdot 10^{-4}$)	μ
W	404 (4,12)	160 (1,63)	0,26
W - 52% Mo	401 (4,09)	157 (1,61)	0,27
W - 20,8% Mo	389 (3,97)	152 (1,55)	0,28
W - 39,5% Mo	374 (3,82)	147 (1,50)	0,27
W - 50,1% Mo	364 (3,72)	142 (1,45)	0,28
W - 60,1% Mo	350 (3,57)	139 (1,42)	0,26
W - 79,5% Mo	339 (3,46)	123 (1,28)	0,35
Mo	322 (3,28)	119 (1,21)	0,35

Key: (1). Composition of alloys, o/c (at.). (2). $G, \text{H/m}^2$
($\text{kg/mm}^2 \cdot 10^4$).

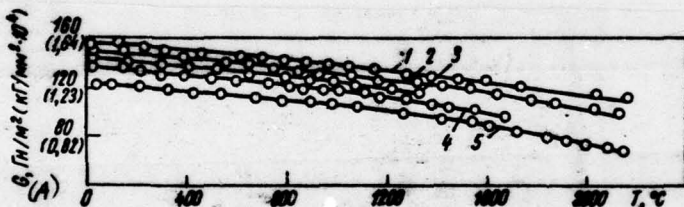


Fig. 72. The dependence of the modulus of shear of tungsten-molybdenum alloys on the temperature: 1 - W+5.2o/o Mo; 2 - W+20.8o/o Mo; 3 - W+39.5o/o Mo; 4 - W+50.1o/o Mo; 5 - W+79.5o/o Mo.

Key: (A). $G, \text{H/m}^2$ ($\text{kg/mm}^2 \cdot 10^4$).

The bends on of the curved temperature dependences of module/moduli can correspond to course in the material of relaxation processes. In this case during measurements on higher frequency, must be obtained the higher values of module/moduli, since the effect of relaxation processes with the increase of frequency must be decreased.

For the illustration of the effect of frequency indicated let us compare the temperature dependence of the module/moduli of the normal elasticity of molybdenum, obtained by us in a resonance manner ($f \approx 5$ kHz), with curved E-T for the same metal [62], obtained by pulse method ($f \approx 5$ MHz). Both these dependences are represented on Fig. 74. Curve, obtained at the more high frequency of testing, does not have a bend in the range of temperatures $0.5 T_{\text{max}}$, although its character also is curvilinear.

Consequently, it can be assumed that the bends when $\sim 0.5 T_{\text{max}}$ on of the curved temperature dependences of the module/moduli, obtained by resonance method for tungsten, molybdenum and their alloys, are connected with the course of relaxation processes at these temperatures. Apparently, in these processes actively participate grain boundaries, since on the curved temperature dependences of the module/moduli of the single crystals of tungsten and molybdenum such bends are not observed.

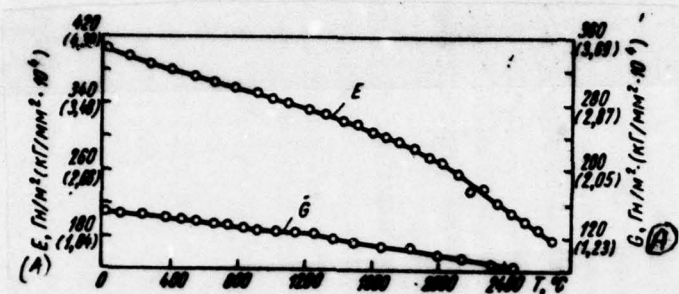


Fig. 73. Dependence of the moduli of elasticity of tungsten-rhenium alloy on temperature.

Key: (A). —, H/m^2 ($kg/mm^2 \cdot 10^4$).



Fig. 74. The dependence of Young's modulus of molybdenum on the temperature: 1 - pulse method of measurement; 2 - resonance method.

Key: (A) - E, H/m^2 ($kg/mm^2 \cdot 10^4$).

Page 103.

Characteristics of elasticity of tantalum, niobium, alloys on the

basis of niobium and a change in them in dependence on temperature.

Tantalum. There is only several works in which are given the results of the measurements of characteristics of the elasticity of tantalum. At normal temperatures for tantalum, are obtained values $E=175-187 \text{ H/m}^2$ ($1.78 \cdot 10^4-1.91 \cdot 10^4 \text{ kg/mm}^2$) [61, 76], $G=68.5 \text{ H/m}^2$ ($0.7 \cdot 10^4 \text{ kg/mm}^2$) [66] and $\mu=0.35$ [66]. As concerns the temperature dependences of elasticity characteristics, then are only measurement data of the module/modulus of normal elasticity to 1370°C .

You determined the characteristics of elasticity with higher temperatures for commercially pure tantalum of vacuum-arc melting in specimen/samples 8 mm in diameter and 90 mm in long.

At normal temperature the modulus of normal elasticity of tantalum render/showed equal to 176 H/m^2 ($1.79 \cdot 10^4 \text{ kg/mm}^2$), shear modulus - 705 H/m^2 ($0.72 \cdot 10^4 \text{ kg/mm}^2$), and Ecisscn ratio - 0.24. Measurements with high temperatures were conductn in vacuum with $p \leq 6.65-66.5 \text{ MN/m}^2$ ($5 \cdot 10^{-5}-10^{-4} \text{ mm Hg}$). The obtained temperature dependences of elasticity characteristics of tantalum are given to Fig. 75 and in Table 13.

Table 13. Elasticity characteristics of tantalum with high temperatures.

(1) Температура, °C	(2) $E, \text{ГН/м}^2$ ($\text{кг}/\text{мм}^2 \cdot 10^{-4}$)	(3) $\alpha, \text{ГН/м}^2$ ($\text{кг}/\text{мм}^2 \cdot 10^{-4}$)	
20	176 (1,79)	70,5 (0,72)	0,24
100	173 (1,76)	69,5 (0,71)	0,24
200	171 (1,74)	68,5 (0,70)	0,25
300	169 (1,72)	68,5 (0,70)	0,24
400	167 (1,70)	67,5 (0,69)	0,25
500	165 (1,68)	66,5 (0,68)	0,24
600	164 (1,67)	65,5 (0,67)	0,25
700	162 (1,65)	65,5 (0,67)	0,23
800	161 (1,64)	64,5 (0,66)	0,24
900	160 (1,63)	64,5 (0,66)	0,24
1000	158 (1,61)	63,5 (0,65)	0,24
1100	157 (1,60)	63,5 (0,65)	0,23
1200	156 (1,59)	62,7 (0,64)	0,24
1300	155 (1,58)	62,7 (0,64)	0,24
1400	153 (1,56)	61,8 (0,63)	0,24
1500	152 (1,55)	61,8 (0,63)	0,23
1600	150 (1,53)	60,8 (0,62)	0,23
1700	149 (1,52)	60,8 (0,62)	0,23
1800	148 (1,51)	59,8 (0,61)	0,23

Key: (1). Temperature, °C. (2). —, H/m^2 ($\text{kg}/\text{мм}^2 \cdot 10^{-4}$).

Page 104.

On Fig. 76, are represented also the temperature dependences of the modulus of normal elasticity of tantalum, obtained in other works.

The considerable difference between the values of the module/moduli, measured by different researchers, is explained by different degree of the contamination of tantalum by

impurity/admixtures, and also a difference in the methods of its obtaining. As early as 1955 measurements at normal temperature [76, 77] establishinstalled the considerable effect of oxygen on the modulus of normal elasticity of tantalum: with 0.1o/c (at.) of O₂ module/modulus E=176 H/mm² ($1.79 \cdot 10^4$ kg/mm²), and with the increase of oxygen content to 2.5o/c (at.) the value of module/modulus was increased to E=196 H/mm² ($2.0 \cdot 10^4$ kg/mm²) (Fig. 76).

We determined the modulus of elasticity of tantalum with high temperatures for the specimen/samples which preliminarily subjected to diffusion saturation by oxygen as follows. All specimen/samples were heated in air to 220°C, one of the batches were age/held at this temperature for 5 h, and another batch - for 10 h, after which was conducted the annealing of all specimen/samples in vacuum with 1200°C for 1 h.

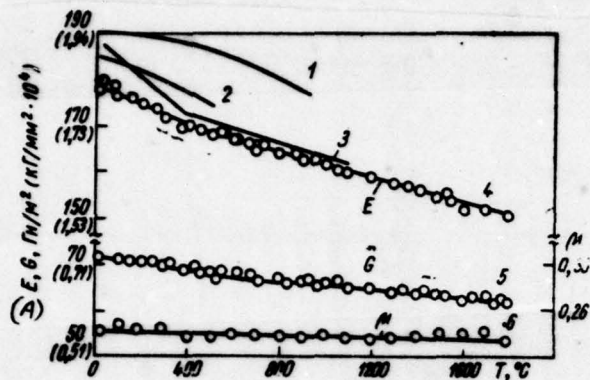


Fig. 75. The temperature dependences of characteristics of the elasticity of tantalum. Young's modulus: 1 - cn data [76]; 2 - on data [61]; 3 - on data [65]; 4 - their own data. Shear modulus: 5 - their own data. Poisson ratio: 6 - their own data.

Key: (A). E, G, H/m² (kg/mm²•10⁴). (B).

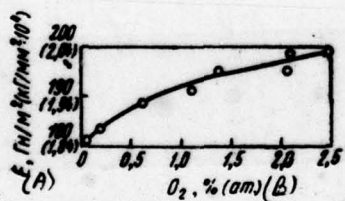


Fig. 76. Dependence of Young's modulus of tantalum on the content in it of oxygen.

Key: (A). E, H/m² (kg/mm²•10⁴). (B). (at.).

Page 105.

On Fig. 77, are represented the temperature dependences of the modulus of normal elasticity of tantalum, passed diffusion saturation by oxygen. In all investigated range of temperatures of the value of module/modulus, they prove to be themselves above for the specimen/samples which contain a larger quantity of oxygen.

Niobium. Are observed considerable disagreements as results of measurements of the mechanical properties of niobium [21, 72, 76, 78-85]. Disagreements are characteristic not only for the structurally dependent properties, such as apparitor of strength, but also for structurally independent properties, which include the moduli of elasticity. In Table 14 are given the literature data on elasticity characteristics of niobium at normal temperature for different purity/finish and the state of metal, measured by different methods.

The values of module/modulus E for niobium oscillate from 85 H/mm^2 ($8.7 \cdot 10^3 \text{ kg/mm}^2$) to 157 H/mm^2 ($1.6 \cdot 10^4 \text{ kg/mm}^2$). It was established/install [21] that the quenching increases the modulus of normal elasticity of niobium. For the deformed and recrystallized niobium $E=108 \text{ H/mm}^2$ ($1.1 \cdot 10^4 \text{ kg/mm}^2$), while for hardened/tempered $E=123 \text{ H/mm}^2$ ($1.26 \cdot 10^4 \text{ kg/mm}^2$). It is revealed/detected [76] that the

value of the modulus of elasticity of niobium depends also on the medium, in which are conductn the measurements. In air was obtained value $E=107 \text{ H/m}^2 (1.09 \cdot 10^4 \text{ kg/mm}^2)$, in vacuum $E=123 \text{ H/m}^2 (1.26 \cdot 10^4 \text{ kg/mm}^2)$.

I determined the modulus cf ncrmal elasticity of the compact and porous ($P=10\%$) cermet niobium, which contained the following impurity/admixtures: 0.25o/c Ta, 0.14o/o C, to 0.09o/o Si and 0.02o/o Fe. Measurements were ccnductn in the ncmannealed specimen/samples.

On data our measurements, for the compact niobium $E=103 \text{ H/m}^2 (1.05 \cdot 10^4 \text{ kg/mm}^2)$, and for porous $E=785 \text{ H/m}^2 (0.8 \cdot 10^4 \text{ kg/mm}^2)$. For the niobium of cathode-ray remelting, the mcdulus of normal elasticity is equal to $10 \text{ H/m}^2 (1.02 \cdot 10^4 \text{ kg/mm}^2)$.

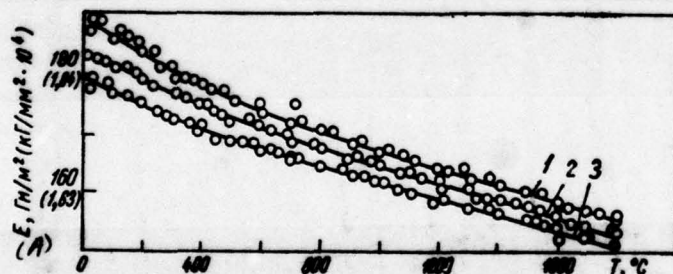


Fig. 77. The effect of saturation by oxygen on temperature dependences of Young's modulus of tantalum: 1 - diffusion saturation by oxygen, 10 h; 2 - the same, 5 h; 3 - commercially pure tantalum.

Key: (A). $E, \text{ H/m}^2 (\text{kg/mm}^2 \cdot 10^4)$.

Page 106.

Table 14. Characteristics of elasticity of rhenium with normal temperature.

(1) Чистота и состояние металла	(2) Метод измерения характеристик упругости	(3) $E, \text{Гн}/\text{м}^2$ ($\text{kG}/\text{мм}^2 \cdot 10^{-4}$)	(3) $\sigma, \text{Гн}/\text{м}^2$ ($\text{kG}/\text{мм}^2 \cdot 10^{-4}$)	μ	(4) Автор	(5) Год
—	(6) Динамический резонансный	157 (1,60)	58,8 (6,00)	0,35	(6a) В. Кестер [61]	1948
(7) Отожжен в вакууме в течение 1 ч при 1100°C	(5) Динамический импульсный	104 (1,06)	37,4 (3,82)	0,38	(9) М. Рейнольдс [79]	1953
99,95%; 1300°C	(10) отожжен при	(11) Статический	85 (0,87)	—	(12) К. Тоттл [80]	1957
99,9%; 1100°C	(10) отожжен при	(13) Динамический (в вакууме)	122 (1,25)	—	(16) Р. Бегли *	1959
(14) То же		(15) Динамический (на воздухе)	112 (1,15)	—		
—		(6) Динамический резонансный	—	41,5 (4,24)	(17) А. И. Дашковский, Е. А. Савицкий [83]	1960

Page 107

Table 14 (cont'd.)

(6)	(6)	Динамический резонансный	108 (1,10)	—	—	(19)	М. Г. Лозинский, Г. В. Захарова [21]	1961
(20)	(21)	Тот же	108 (1,20)	—	—	(25)		
(22)	" "		122 (1,25)	—	—	(26)	Д. Лаверти, Е. Эвенс [76]	1961
(23)	(24)	Статический	112 (1,15)	—	—	(27)		
—	—		110 (1,02)	—	—	(28)	Ф. Остерман [84]	1962
99,4%	(8)	Динамический импульсный	104 (1,06)	3,72 (3,80)	0,398	(29)		
—	(6)	Динамический резонансный	108 (1,10)	—	—	(30)	И. М. Недюха, В. Г. Черный [85]	1965
—	(21)	Тот же	108 (1,10)	—	—	(31)		
—	" "		92 (0,94)	—	—	(32)	Н. Д. Тарасов, Р. А. Ульянов [86]	1965
(31)	" "		110 (1,12)	—	—	(33)		
Отожжен в аргоне	" "					(34)	А. Б. Лященко [64]	1965
						(35)		
						(36)	П. Армстронг, Г. Браун [87]	1965
						(37)		
						(38)	В. А. Дреплик [65]	1967

Key: (1). Purity/finish and the state of metal. (2). Method of measuring elasticity characteristics. (3). —, E/m² (kg/mm²•10⁻⁴). (4). Author. (5). Year. (6). Dynamic resonance. (6a). V. Kester. (7). It is annealed in vacuum in course 1 h at 1100°C. (8). Dynamic pulse. (9). M. Reynolds. (10). it is annealed with. (11). Static. (12). K. Tottl. (13). Dynamic (in vacuum). (14). The same. (15). Dynamic (in air). (16). R. Begley¹.

FOOTNOTE 1. R T Begley. Wright and Development Center Techn. Rept.

WADC-TR-57. 344. March 1959, part II, p 192. ENDFOOTNOTE.

(17). A. I. Dashkovskiy, Ye. A. Savitskiy. (18). Deformed. (19). M. G. Lozinskiy, g. V. zaxarova. (20). Recrystallized. (21). The same. (22). Harden/tempered. (23). It is annealed at 1250°C. (24). Static. (25). D. Laverti, E. Evans. (26). F. Osterman. (27). I. M. Nedyukha, V. g. black/ferrous. (28). N. D. Tarasov, r. a. Ulianov. (29). A. B. Lyashchenko. (30). P. Armstrong, g. Braun. (31). It is annealed in argon. (32). V. A. Dreshpak.

Page 108.

The data on the modulus of shear of niobium it is considerably less than about the modulus of normal elasticity. However, among corrected values there are noticeable disagreements - from 38 ~~G~~N/m² ($3.88 \cdot 10^3$ kg/mm²) to 58.8 ~~G~~N/m² ($0.6 \cdot 10^3$ kg/mm²) and even to 86.5 ~~G~~N/m² ($8.8 \cdot 10^3$ kg/mm²) [1, 89]. At such values of shear modulus for niobium, is not fulfilled the known relationship/ratio between E, G and μ which it is correct for an isotropic material. On data our measurements, for the compact nichium $G=38.2$ H/m² ($3.9 \cdot 10^3$ kg/mm²).

Large disagreements are observed in the case of niobium also for the values of Poisson ratio. For compact nichium, according to our calculation, on measurement data of module/moduli, $\mu=0.35$.

On Fig. 78 and Table 15 gives the obtained by us temperature dependences of the module/moduli of compact mickium and niobium of electric arc remelting (T_c 1600°C), V. A. Dreshpak's data [65] for the niobium of cathode-ray remelting (T_c 2200°C), and also the temperature dependences of the modulus of normal elasticity of niobium, obtained by other researchers. Although almost all temperature dependences of module/modulus, obtained by different authors, differ from each other, it is possible to note that for a majority of them a characteristically very small change of the module/modulus in the range of temperatures from room to 1200°C.

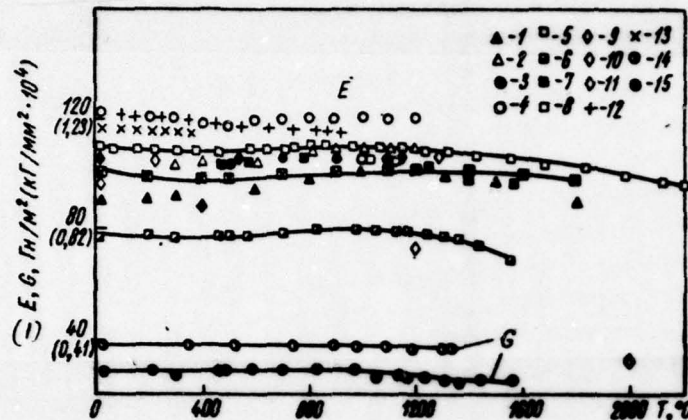


Fig. 78. Dependence of the moduli of elasticity of niobium on temperature. Young's modulus: 1 - [87]; 2 - niobium deformed [21]; 3 - niobium recrystallized [21]; 4 - niobium hardened/tempered [21]; 5 - niobium compact [30]; 6 - niobium porous [30]; 7 - niobium of electric arc remelting; 8 - niobium of cathode-ray remelting; 9 - [64]; 10 - [86]; 11 - [84]; 12 - testing in vacuum [76]; 13 - testing in air [76]. Shear modulus: 14 - niobium compact [30]; 15 - niobium porous.

Key: (1). E, G, H/m² (kg/mm² · 10⁴).

Page 109.

In this temperature interval the modulus of normal elasticity of niobium not only is not decreased as for the majority of metals, but

sometimes even somewhat grows/rises. Higher than 1200°C, according to data our research and the results, obtained V. A. Dreshpak, module/modulus is begun slowly to be decreased.

Measurements in compact specimen/samples also establish/installled that the modulus of shear of niobium during heating is changed analogously with the module/modulus of the elasticity (see Fig. 78).

Relative to cause of this peculiar change in the module/moduli of niobium with the increase of temperature are at present several points of view. In work [21] is assumed that similar behavior of niobium can be caused by the presence in it of interstitial impurities (mainly, oxygen). This assumption confirm saybolt's data [90] on a considerable increase of the solubility of oxygen in niobium in solid state with the increase of temperature.

Table 15. Dependence of elasticity characteristics of niobium on temperature.

(1) Temperatura, °C	(2) Характеристики упругости компактного ниобия			Модуль упругости E ниобия электродугового переплава (3)
	(4) $E, \text{ГН/м}^2$ ($\text{kG/mm}^2 \cdot 10^4$)	(4) $\sigma, \text{ГН/м}^2$ ($\text{kG/mm}^2 \cdot 10^4$)	μ	
20	103 (1,05)	38,2 (0,39)	0,35	110 (1,12)
100	103 (1,05)	38,2 (0,39)	0,35	109 (1,11)
200	103 (1,05)	39,2 (0,40)	0,31	109 (1,11)
300	103 (1,05)	39,2 (0,40)	0,31	109 (1,11)
400	103 (1,05)	39,2 (0,40)	0,31	108 (1,10)
500	103 (1,05)	39,2 (0,40)	0,31	108 (1,10)
600	104 (1,06)	39,2 (0,40)	0,33	108 (1,10)
700	104 (1,06)	39,2 (0,40)	0,33	109 (1,11)
800	105 (1,07)	39,2 (0,40)	0,34	109 (1,11)
900	105 (1,07)	39,2 (0,40)	0,34	110 (1,12)
1000	105 (1,07)	39,2 (0,40)	0,34	108 (1,10)
1100	104 (1,06)	39,2 (0,40)	0,33	108 (1,10)
1200	103 (1,05)	39,2 (0,40)	0,31	107 (1,09)
1300	102 (1,04)	38,2 (0,39)	0,33	107 (1,09)
1400	100 (1,02)	38,2 (0,39)	0,31	107 (1,09)
1500	98 (1,00)	—	—	106 (1,08)
1600	96 (0,98)	—	—	105 (1,07)
1700	—	—	—	104 (1,06)
1800	—	—	—	102 (1,04)
1900	—	—	—	101 (1,03)
2000	—	—	—	99 (1,01)
2100	—	—	—	98 (1,00)
2200	—	—	—	96 (0,98)

Key: (1). Temperature, °C. (2). Elasticity characteristics of compact niobium. (3). Module/modulus of elasticity E of niobium of electric arc remelting. (4). —, H/m^2 ($\text{kg/mm}^2 \cdot 10^4$).

Page 110.

With the increase of the modulus of elasticity with the increase of the content of oxygen in the analog of niobium - tantalum - testify

experimental data works [77], presented in Fig. 76.

The character of a change in the modulus of elasticity of niobium during heating Armstrong and Braun [87] explained, on the basis of the results, obtained in single-crystal specimen/samples. It was established that the temperature dependences of the modulus of normal elasticity of the single crystals whose longitudinal axis coincides with direction [100], fundamentally different, than for specimen/samples with the longitudinal axes, which coincide with directions [110] and [111] (Fig. 79).

For specimen/samples with orientation [100] with the increase of temperature the module/modulus is decreased, while for orientations [110] and [111] it grows/rises. The same researchers established that for the polycrystalline recrystallized niotium with the preferred orientation of grains [110] the character of the temperature dependence of the module/modulus very nearly the same as for a single crystal with axle/axis [110] (Fig. 80). On the basis of findings in work [87] the conclusion is made that the character of the temperature dependence of the modulus of elasticity of niobium is explained by the considerable elastic anisotropy of its crystals.

A. B. Lyashchenko : it assumed that the reason for the unusual behavior of the modulus of elasticity of nichium during heating is

the special structure of the electron shells of this metal.

FOOTNOTE 1. A. B. Lyashchenko. Author's abstract of candidate dissertation. IPM of AS UkrSSR, Kiev, 1965. ENDFOOTNOTE.

Since those given in the literature of the value of the modulus of elasticity of polycrystalline niobium at normal and high temperatures were obtained in specimen/samples with different structure and the not controlled/inspected composition, I undertook the attempt to estimate the effect of structure and interstitial impurity content (oxygen, nitrogen, carbon) on module/modulus of elasticity niobium over a wide range of temperatures.

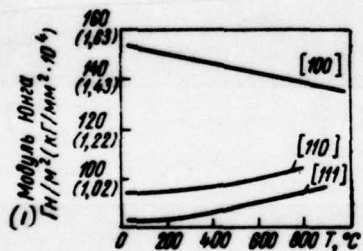


Fig. 79.

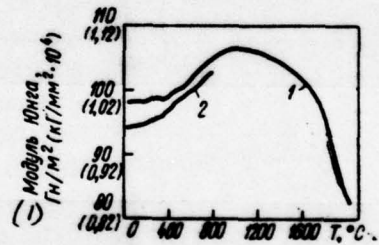


Fig. 80.

Fig. 79. The temperature dependences of Young's modulus of the single crystals of niobium.

Key: (1). Young's modulus R_n/m^2 ($\text{kg}/\text{mm}^2 \cdot 10^4$).

Fig. 80. The temperature dependence of Young's modulus of polycrystalline niobium with preferred orientation [111] (is curved 1), and the single crystal of the same orientation (curve 2).

Key: (1). Young's modulus, H/mm^2 ($kg/mm^2 \cdot 10^4$).

Page 111.

As initial material in all our investigations, was utilized the niobium of dual electron-beam melting. For explaining the effect of structure on the modulus of elasticity, were made the specimen/samples made of forged rods (degree of strain 95%) and the rolled in one direction band (degree of strain 65%).

The microstructure of these specimen/samples is shown on Fig. 81, and the results of their tests - for Fig. 82. To 600°C modulus of elasticity of specimen/samples of both of types barely is changed, at the higher temperatures in the case of forged specimen/samples, the module/modulus is reduced, but in the case of rolled - it is increased.

The temperature dependence of the modulus of elasticity of the rolled niobium is similar to dependence for a single crystal with axle/axis [110], obtained by Armstrong and Braun. The reason for this

resemblance consists in the fact that the preferred orientation of the structure of the rolled niobium is close to direction [110].

Some specimen/samples, manufactured from the rolled band, were subjected to recrystallization annealing (1 h with 1200°C). The temperature dependences of module/modulus for these specimen/samples differed little from analogous dependences for the nonannealed specimen/samples. The analysis of microstructure showed that in the annealed specimen/samples there are sections of deformation banding; analogous banding is they noted earlier.

FOOTNOTE 1. R T Begley. WADC-TR-57.344. March 1959, part II, p 192.

ENDFOOTNOTE.

The effect of nitrogen and oxygen on the module/modulus of elasticity of niobium was studied for the specimen/samples, manufactured from rod. For obtaining different degrees of saturation by oxygen these specimen/samples either annealed in vacuum 6.65 sn/m^2 ($5 \cdot 10^{-4} \text{ mm Hg}$) at 1150°C for 1 h (first batch), or they oxidized in air for 3 h with 600°C with the water quenching and the subsequent annealing in vacuum with 1150-1200°C for 3 h (third batch).

The temperature dependences of the modulus of elasticity of the specimen/samples of all three batches are represented on Fig. 83. The

more it is contained oxygen and nitrogen in nichium, the more noticeable descends the module/modulus with the increase of temperature to 300-400°C and the more intense it is increased with further increase of temperature.

The effect of carbon on the modulus of normal elasticity of niobium they investigated for the first time Kester and Rausher in 1948 [92]. They showed that an increase in the carbon content in niobium leads to an increase of the modulus of elasticity. In work [21] it is emphasized that the dependence of Kester and Rausher should consider good-quality, since their nichium was, apparently, insufficient pure ones.

DOC = 78133004

PAGE -46- 224

Pages 112 and 113.

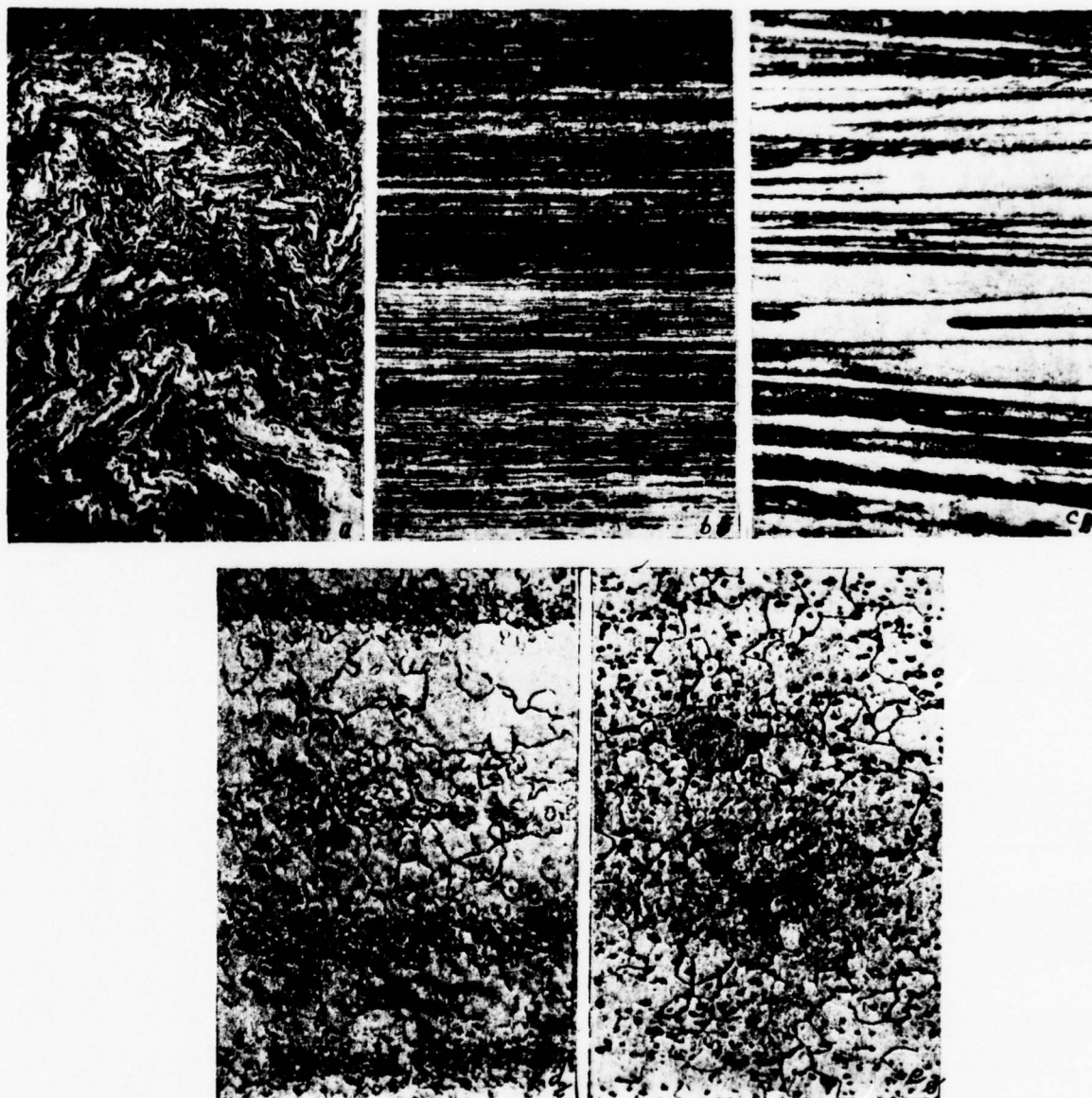


Fig. 81. Microstructure of the specimen/samples of niobium (x120): a) in the direction of forcing; b) in transverse direction; c) band

before annealing; d) hard after annealing; e) alloy Nb-0.10/oC.

Page 114.

Were obtained the temperature dependences of the modulus of elasticity of the niobium, containing 0.10/o C (Fig. 84).

Carbon inserted via the blending of the remelted molding/bars by carbide of titanium. With cathode-ray remelting titanium burned to the thousandths of percentage. Ingot were hammered in air with 1000°C to rod 12 mm in diameter with the degree of strain 95o/o. The specimen/samples, manufactured from this rod, experience/tested in the work-hardened and recrystallized states. The microstructure of the recrystallized specimen/sample is shown on Fig. 81.

As it follows from findings, carbon increases the module/modulus of the elasticity of niobium in the range of temperatures from room to 1000, 1000°C.

Further increase of the temperature in the case of the niobium, saturated by carbon, causes a sharper incidence/drop in the module/modulus, than for pure niobium.

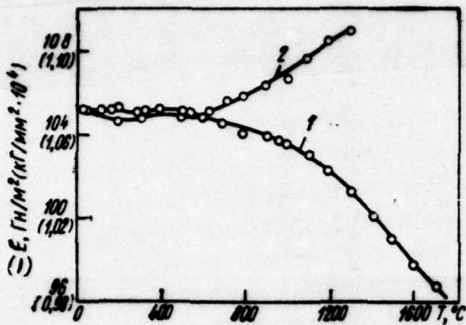


Fig. 82. The temperature dependences of Young's modulus for rolled (1) and forged (2) niobium.

Key: (1). E , H/m^2 ($kg/mm^2 \cdot 10^4$) .

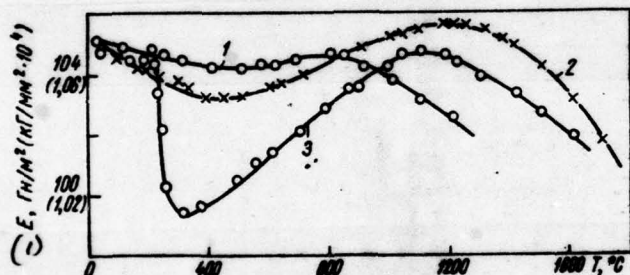


Fig. 83. The temperature dependences of Young's modulus of the niobium, which contains nitrogen and oxygen: 1 - annealing of 1150°C, 1 h; 2 - annealing of 1800°C, 1 h; 3 - oxidation in air of 600°C, 3 h, annealing of 1200°C, 3 h in vacuum.

Key: (1). E , ($H/m^2 \cdot 10^4$) .

Niobium fusions. The effect of the alloying of niobium with the small additions of chromium, rhenium, tungsten, molybdenum, tantalum, iridium, palladium, zirconium and titanium on the character of interatomic reaction investigated N. D. Tarasov, R. A. Ulianov Ya. D. Mikhaylov [86].

On Fig. 85, are represented to the dependence of the modulus of normal elasticity on the composition of alloys. As is evident, in essence are observed the laws, common/general/total for solid solutions. So, the alloying of niobium with chromium, rhenium by tungsten, molybdenum, tantalum, iridium and palladium, which have the higher modulus of elasticity, makes it possible to obtain the alloys, for which the value of module/modulus is higher than for niobium. The additions of zirconium and titanium whose module/moduli are close to the modulus of elasticity of niobium, lead to insignificant increase or the decrease of the modulus of elasticity of alloy in comparison with the module/modulus of niobium.

Table 16, comprised on of works [65, 78], give corrected values of the modulus of elasticity of niobium fusions, which contain several alloying cell/elements. From these data it follows that, although for the triple and quaternary alloys of niobium the

DOC = 78133004

PAGE -50- 228

dependence of the modults cf elasticity on form and quantity of alloying cell/elements is more complex than for binary alloys however the character of the effect of the alloying cell/elements on the module/modulus of elasticity is retained.

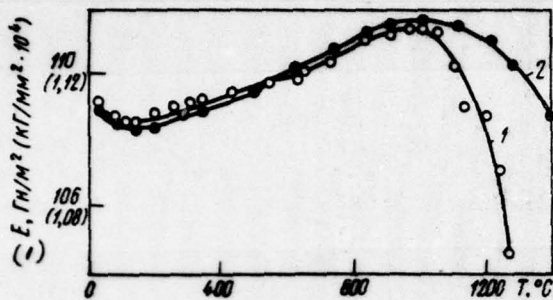


Fig. 84. The temperature dependences of Young's modulus of the niobium, which contains 0.1% C: 1 - not annealed; 2 - annealing of 1200°C, 1 h.

Key: (1). E, H/m² (kg/mm² * 10⁴).

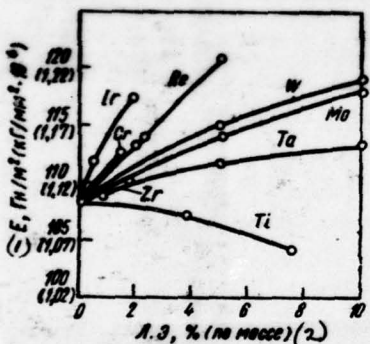


Fig. 85. Dependence of the modulus of elasticity of niobium fusions on the content of the alloying cell/elements (I, E).

Key: (1). E, H/m² (kg/mm² * 10⁴). (2). L.E., % (by weight).

Via alloying the modulus of elasticity of niobium can be considerably raised. So, for alloy Nb+15o/c W+5c/o Mo+1o/o Zr module/modulus $E=172 \text{ H/mm}^2$ ($1.76 \cdot 10^4 \text{ kg/mm}^2$), that almost 1.5 times it is higher than for unalloyed niobium. Consequently, there is a possibility to eliminate main disadvantage in the niobium alloys - low modulus of elasticity and to considerably expand the range of application of these alloys.

Table 16. Moduli of normal elasticity of some alloys of niobium.

(1) Состав сплава	(2) Температура, °C	(3) $E, \text{Н/м}^2 (\text{kg/mm}^2 \cdot 10^{-4})$
Nb + 15% W + 5% Mo + 1% Zr	20 1095	172 (1,75) 123 (1,25)
Nb + 15% W + 5% Mo + 5% Zr	20 1095	165 (1,68) 113 (1,15)
Nb + 10% Mo + 10% Ti	1095	59,5 (0,61)
Nb + 32,5% Ta + 0,75% Zr	20	113 (1,15)
Nb + 14% W + 2% Mo	20 1100	130 (1,33) 129 (1,32)
Nb + 14% W + 2% Mo + 0,83% HfC	20 1100	124 (1,27) 126 (1,29)

Key: (1). Composition of alloy. (2). Temperature, °C. (3). $E, \text{Н/м}^2 (\text{kg/mm}^2 \cdot 10^{-4})$.

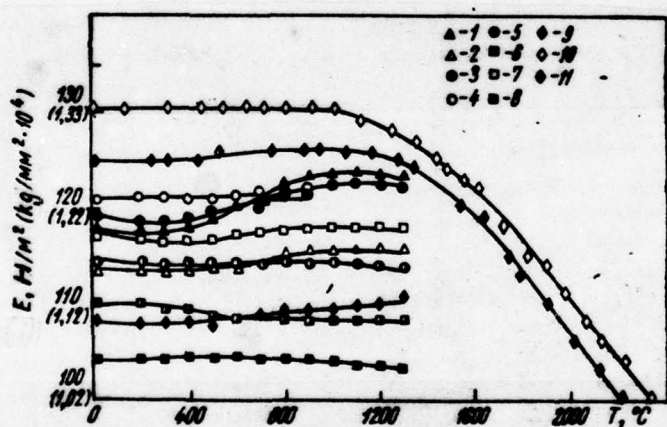


Fig. 86. The temperature dependences of Young's modulus in niobium fusions on data [86]: 1 - Nb+10% Mo; 2 - Nb+10% Ta; 3 - Nb+10% W; 4 - Nb+5% Re; 5 - Nb+2.3% Cr; 6 - Nb+7.6% Ti; 7 - Nb+2.0% Ir; 8 - Nb+1.78% Zr; 9 - Nb; on data [65]: 10 - Nb+14% W+2% Mo; 11 - Nb+14% W+2% Mo+0.83% HfC.

Page 117.

Works [65, 86] give the information about a change in the modulus of normal elasticity of niobium alloys during their heating. The temperature dependences of the moduli of elasticity of some alloys of the niobium, constructed according to data these works, are represented on Fig. 86, from which it follows that to 1300°C moduli of normal elasticity of all studied alloys are changed insignificantly, and with further increase of temperature, they descend.

Thus, for all investigated alloys the temperature dependences of the modulus of elasticity had in essence the same character as for the unalloyed niobium. This, apparently, is explained by the fact that the common/general/total content of the alloying cell/elements in each alloy was low (not more than 20c/o).

Page 118.

Chapter 3.

DISSIPIATION OF ENERGY IN REFRACORY METALS DURING REPEATED DEFORMATION.

Setting up for determining the actual dissipation of energy of cyclically deformed material over a wide range of temperatures.

Together with the traditional mechanical characteristics of materials, such as limits of strength, yield and durability, the elongation per unit length and transverse contraction, in machine-building practice increasingly more frequently appears the need for knowledge of other characteristics, also, first of all to the ability of material to absorb energy during repeated deformation.

Than are more energy losses in material during its repeated deformation, i.e., the higher the damping capacity of this material, the greater must be the dynamic strength of cell-elements,

construction/designs, manufactured from this material and which experience/test in the process of work the severe vibrations.

Therefore during the manufacture of the parts whose vibrations under actual conditions are unavoidable (such parts, for example, include the blades of different types turbines), frequently prove to be itself to advantageously select material with low endurance limit, but that possessing the increased internal dissipation of energy. This approach to the selection of materials for the class of parts indicated in practice completely itself justifies.

The need for data finding on the damping capacity of different class of structural materials, including high-melting, especially increased in recent years in connection with the development of the newest areas of technology, for which were characteristic the extreme parameters and the complexity of the power and thermal effects (high velocities and accelerations, high below temperatures, large pressure, etc.), which were being changed in time according to the specific law or having accidental character.

Unfortunately, at present in specifications to materials, as a rule, there are no damping characteristics. Existing in the literature knowledges about the dissipation of energy in materials, in the first place, is very few in number and, in the second place,

bear accidental character, since different authors determined the characteristics of scattering with the aid of different ones, the frequently insufficient perfected, methods, that does not make it possible to consider their results sufficiently correct ones.

Page 119.

This is why arose the imperative need for the development of procedure and the creation of setting up for studying the dissipation of energy for material during its repeated deformation under conditions of the optimum stressed state.

Since for the characteristic of vibration stability is of interest the actual dissipation of energy or high stress level, optimum test conditions one should consider those, by which in each unit volume of material are created identical cycle stress alterations (uniformly stressed state), and the great value of stresses will be close to endurance limit. Under such conditions, obviously, it is easy to determine the actual dissipation of energy in material on any stress level and to establish/install the dependence of the dissipation of energy on the amplitude of stress.

Taking into account an experiment in the investigations (among other things of our) in the range of the oscillations of elastic

systems the optimum procedure of the study of the dissipation of energy in the cyclically deformed material one should consider similar, which provides obtaining uniform extension - compression or repeating-alternating pure shear.

Such stressed states can be realized during the utilization of an oscillatory system with one degree of freedom, which is the mass, spring-mounted and capable of accomplishing longitudinal or torsional vibrations. Spring in this system is the tubular thin-walled specimen/sample of the material being investigated. Upper end of the specimen/sample is rigidly connected with the large mass, suspend/hung from fine/thin strings to ceiling beams (or to the special struts, connected with mounting). The target/purpose of this suspension is information to the negligible value of the leakage of energy into "foundation".

The schematic diagram of setting up for studying the actual dissipation of energy in high-melting materials is represented in Fig. 87, the general view of specimen/sample - in Fig. 88.

The working part of the specimen/sample of the tested material (see Fig. 88) presents the tube with length of 50 mm with mean diameter of 17 mm and wall thickness of 1 mm. Specimen/sample has the butt ends of the stepped section/cut, which are finished with cones.

One of the ends the specimen/sample is rigidly fastened in adapter with 3 (see Fig. 87), and the latter in turn, is fastened in plate/slab with 2, which it presents the mentioned above large mass and is suspend/hung from steel strings 1.

To the butt end of the specimen/sample, is rigidly connected load 7. To the lower end/face of load, is conducted electromagnet 9; at the end/faces of terminal load and the poles of electromagnet, are milled out the projections of identical form.

Page 120.

With the aid of one electromagnet, can be excited as longitudinal (vertical) vibrations of terminal load, during which entire material of specimen/sample will experience/test cyclic tensile strain - compression, so also the torsional vibrations of the same load, during which entire material of thin-walled specimen/sample will experience/test the cyclic deformation of pure shear. For exciting the longitudinal oscillations electromagnet are established so that the projections of the end/faces of load and electromagnet would coincide; for purpose of exciting torsional vibrations end/faces they misalign by certain angle relative to each other,

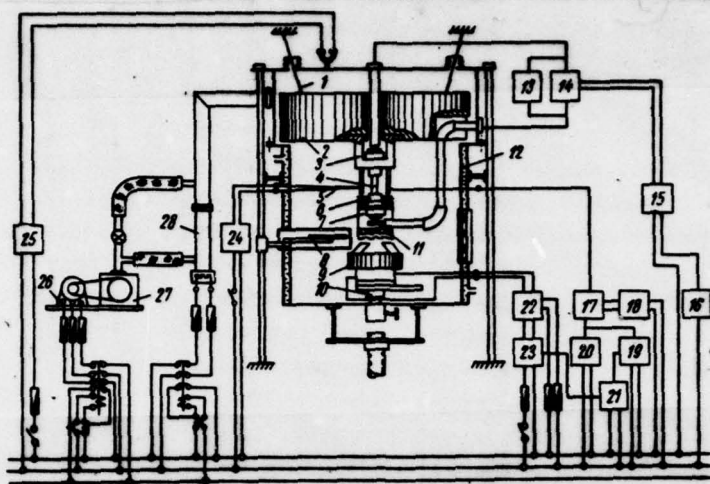


Fig. 87. The schematic diagram of setting up for the study of the dissipation of energy in cyclically deformed material in the uniform stressed state: 1 - steel filaments; 2 - plate/slab; 3 - adapter; 4 - specimen/sample; 5 - thermocouple Pt-PtRh; 6 - capacitance pickup; 7 - terminal load; 8 - microscope; 9 - electromagnet; 10 - directing mechanism; 11 - heater; 12 - vacuum chamber; 13 - voltmeter; 14 - transformer OSU-40; 15 - autotransformer RNO-250-10; 16 - ammeter; 17 - amplifier; 18 - power supply unit of amplifier; 19 - oscillosograph N-105; 20 - oscillosograph S1-1; 21 - relay MKU-48; 22 - amplifier TU-5-4; 23 - audiofrequency oscillator ZG-34; 24 - electronic potentiometer EPV2-11A; 25 - vacuum gauge VIT-1A; 26-28 - vacuum system.

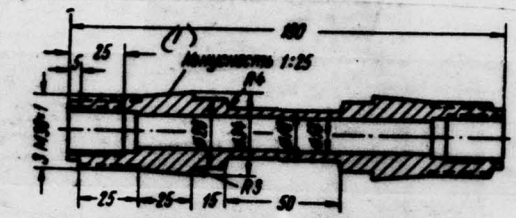


Fig. 88. Specimen/sample for studying dissipation of energy in material.

Key: 1) Conicity.

Page 121.

Electromagnet is fed from amplifier TU-5-3b, excited by a generator of the type ZG-12.

After the achievement of the assigned/prescribed amplitude of resonance oscillations, is manufactured the interruption of these vibrations and they record with the motion picture film of oscillograph the process of the free dying oscillations of terminal load.

Incl.

As the mechanical-electrical transformer is used capacitance pickup 6 (see Fig. 87), that presents not connected with specimen/sample plate which is fastened through the adapter to upper mass. A change in the capacity of sensor because of a change in the clearance between the fixed plate and the upper end/face of the oscillating load during longitudinal oscillations or because of a change in the area of the plate, covered by the projections of the end/face of terminal load during torsional vibrations, creates the electric signal which is reinforced and is recorded. The scale of vibrogram is determined with the aid of microscope, for this before cessation of oscillation, is measured their actual amplitude.

With the aid of this setting up it is possible to estimate the dissipation of energy according to resonance curve, and also according to skeletal/skeleton resonance curve, accurately by measuring the frequencies on different levels of resonance amplitudes with the subsequent recalculation according to the formulas, obtained on the basis of the theory of nonlinear vibrations with the utilization of the small parameter method.

For purpose of eliminating the errors, caused by oxide coating on specimen/sample and elements of construction/design, in the case

of tests at high temperatures, and in the case of low-temperature tests - with purpose of avoiding the icing of the cell/elements indicated, oscillatory system together with capacitance pickup and the electromagnet, establish/installled on directing mechanism, is placed in vacuum chamber 12 (see Fig. 87).

Vacuum chamber consists of two steel cylinders: upper, stationary, and lower, movable. Vacuum on the order of 1.83 mN/m² (10^{-5} mm Hg) creates the vacuum aggregate BA-05-4 together with an oil-vapor pump of the type N-5, rough vacuum - a fore pump of the type VN-2MG.

Setting up allows for measuring the dissipation of energy in materials over a wide range of temperatures.

In the case of experiments at the elevated temperatures (to 1700°C) in the cavity of specimen/sample is introduced with certain radial clearance the special-slimy heating element of resistance to 11 (see Fig. 87), that is thin-walled molybdenum tube. For providing uniform heating of specimen/sample, the heater has length, three times the exceeding length of the working part of the specimen/sample; furthermore, the thickness of the upper part of the heater 1.2 mm, and lower - 1 mm.

Page 122.

The basic assembly of setting up for high-temperature investigations is shown on Fig. 89, and heater - on Fig. 90.

Ecr measurements at the low temperatures in the cavity of specimen/sample instead of the heater, is introduced the cooler, which is tube with refrigerant - by liquid nitrogen or helium.

The described setting up makes it possible to determine with the high degree of accuracy of the characteristic of the dissipation of energy during cyclic deformation of material under conditions of the uniform stressed state.

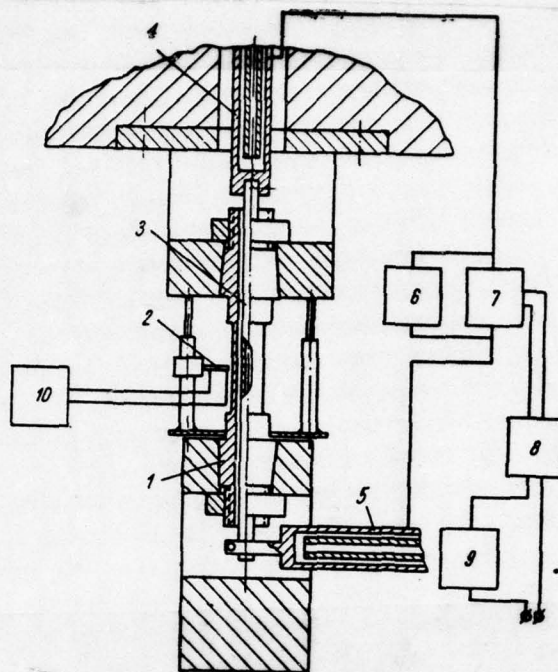


Fig. 89. The basic layout of setting up for investigation at high temperatures: 1 - specimen/sample; 2 - thermocouple; 3 - heater; 4, 5 - current conductors; 6 - voltmeter; 7 - transformer OSU-40; 8 - autotransformer RNO-250-10; 9 - ammeter; 10 - potentiometer.



Fig. 90. Heating element of setting up D-8.

Page 123.

Setting up is general purpose, since it makes it possible to vary the stressed state of the material being investigated, utilizing one and the same specimen/sample, and to also change over wide limits the temperature interval of tests.

Setting up for the study of the dissipation of energy in material during transverse vibrations at high temperatures.

During the study of the damping capacity of sheet materials, it is expedient to utilize transverse vibrations of the flat/plane specimen/samples, tested under conditions of pure bending.

Recommended well itself setting up D-7, making it possible to conduct this testing at the temperatures to 1500°C in vacuum to 1/33 mN/m² (10^{-5} mm Hg), in air, in neutral or any gaseous medium in the range of frequencies from 5 to 100 Hz [6].

The appearance of setting up D-7 is represented in Fig. 91, and

its schematic diagram is Fig. 92.

Setting up D-7 consists of the following basic systems: by oscillatory, the excitation of vibrations, heating, vacuum and optical (for recording and recording of the vibrations of specimen/sample). As can be seen from Fig. 91, the basis of setting up is welded mounting. The massive working plate/slab on which are mounted the basic assemblies of setting up, is established/installled on the mounting indicated in strictly horizontal position.

Oscillatory system includes the flat/plane specimen/sample being investigated (see 2b in Fig. 92 and Fig. 93a) with the connected to its butt ends loads (Fig. 93b). For decreasing the energy losses "into framing" oscillatory system is suspended/hung with the aid of fine/thin strings 2 of the molybderus wire and to the cross crosshead, which leans on box back traces 3.

To the decrease of losses in the places of the articulation of specimen/sample with loads contribute thickenings at the ends of the specimen/samples. The construction/design of the suspension of oscillatory system provides orientation and rigid holding of specimen/sample with the loads in the working space of the camera/chamber.

Suspension points of loads virtually coincide with the assemblies of the first form of the vibrations of system. During the excitation of vibrations by the pulse torque moment, applied to the loads at suspension points, at the ends of the specimen/sample are created variable torque, which ensure the conditions of the pure bending of the working part of the specimen/sample.

Loads consist (see Fig. 93) of three parts: upper, massive, middle, light and lower. In massive upper part with the aid of wedge clamps, are fastened the ends of the specimen/sample.

Page 124.

The middle part of the load is carried out by less massive for purpose of information to the minimum of the heat transfer from the heated specimen/sample to the lower part of the load, through which with the aid of electromagnets to specimen/sample is applied variable torque. In the lower part of each load, are milled out figure end/faces.

The system of the excitation of vibrations consists of two electromagnets, the generator of low frequencies, modulator, amplifier, collected of one block with detector. Electromagnets are mounted on two moving stands, arranged accurately under the

loads of oscillatory system. Stands can be turned around axle/axis, which makes it possible to establish/install the electromagnets prior to tests so that the projections on the end/faces of load and magnet core would be misaligned to certain angle.

During the supplying of electric pulse on coils in core, appears the magnetic flux,

which is closed through air gap between the projections of core and loads which attempt to stop one against another.

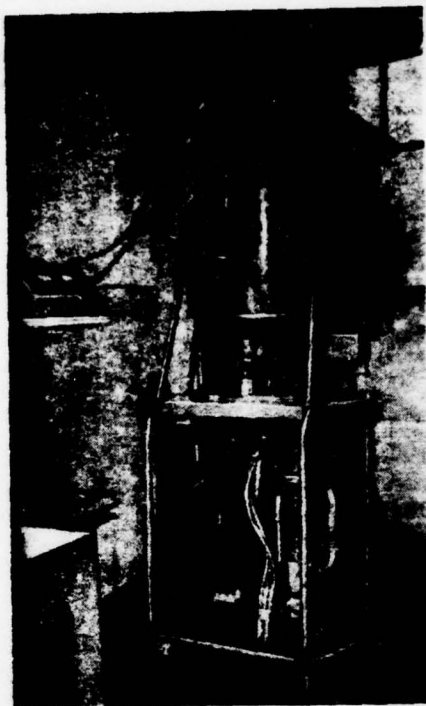


Fig. 91. The appearance of setting up D-7.

Page 125.

Horizontal components appearing in this case forces the creation in plane surface of load the torsional moment, which for a test specimen is bending.

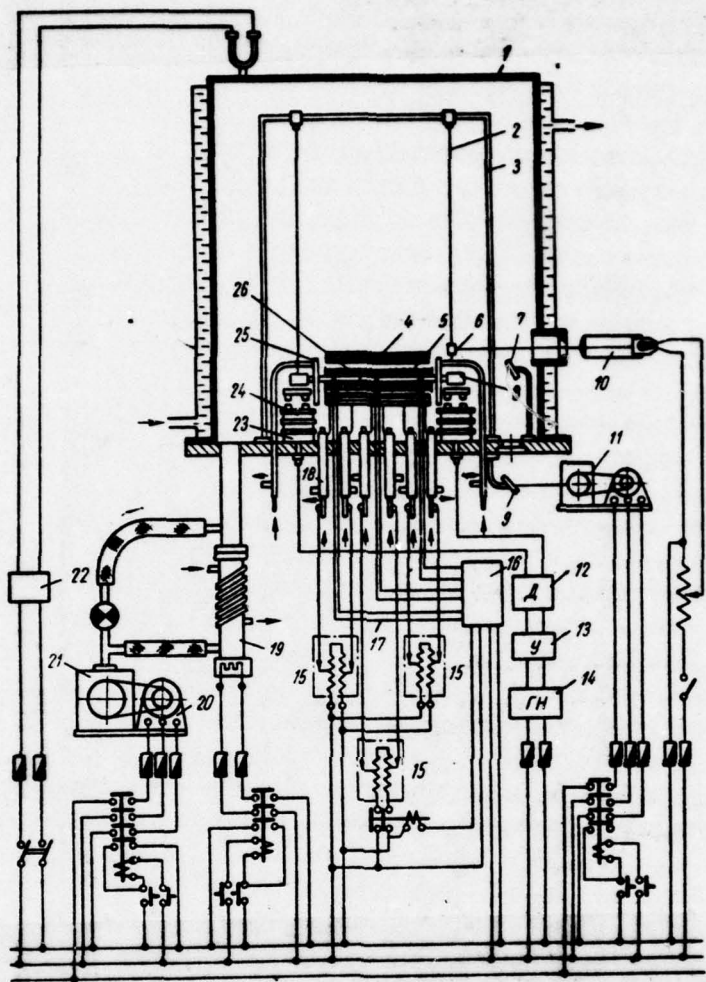


Fig. 92. The schematic diagram of setting up D-7: 1 - camera/chamber; 2 - filament of suspension; 3 - strut; 4 - shields; 5 - heater; 6, 7, 9 - mirror; 8 - loads; 10 - illuminator; 11 - recording mechanism; 12 - detector; 13 - amplifier; 14 - generator; 15 - RNO-10; 16 - EPP-09; 17 - thermocouple; 18 - current conductors; 19-21 - vacuum system; 22

- VIT -1; 23 - stands; 24 - electromagnets; 25 - shield; 26 - specimen/sample.

Page 126.

This torque/moment is changed in time with the natural oscillation frequency, selected with the aid of the master oscillator. Under the action/effect of the moment of load, are cyclically turned relative to suspension points and are caused transverse vibrations of specimen/sample. If suspension points and loads are sufficiently close to oscillation nodes, then the oscillating system is not virtually swung.

With the aid of the examined method of excitation oscillatory system is inserted into the resonance which on the achievement of the assigned/prescribed amplitude of oscillations they strip, breaking up the feed circuit of magnet windings.

The heating system of setting up consists of three-piece resistance furnace (Fig. 94), that makes it possible to heat specimen/sample to 1500°C, sealed current conductors, two autotransformers of the type RPO-250/10 and of the electronic

BQC = 78133005

PAGE 19 251

potentiometer EPP-09, which gauges the temperature in the sections of furnace. The temperature of specimen/sample is measured with the aid of three plate-platinum-rhodium thermocouples.

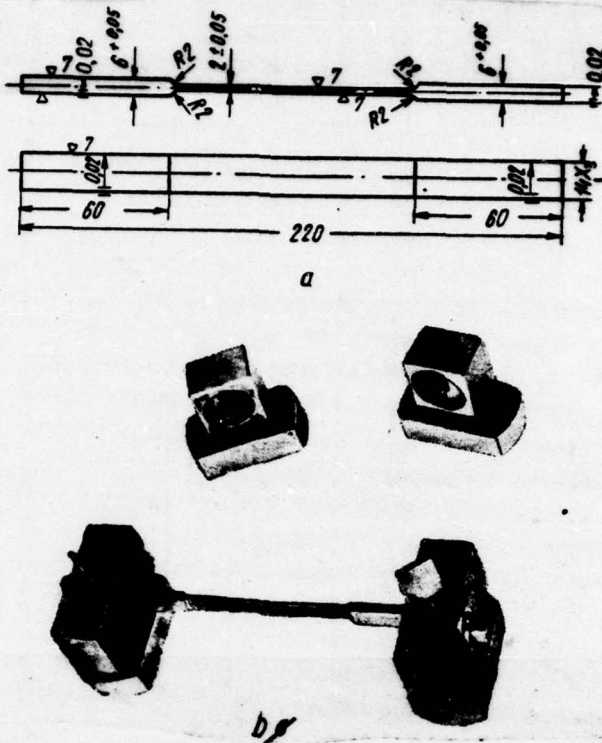


Fig. 93. Specimen/sample to setting up E-7: a) the drawing of specimen/sample; b) the general view of specimen/sample with loads.

Page 127.

Structurally furnace is designed in the form of three independent sections with the separate conclusion/derivations which are connected to the appropriate terminals of autotransformers.

Average section is included through the mercury switch of the gauging potentiometer EPP-09. The latter automatically disconnects average section from RNO-250/10 upon reaching of the temperature, equal to the temperature in extreme sections, and is included feed in the case of a temperature drop of midsection.

Heating system makes it possible to ensure the sufficient uniformity of heating along the length of specimen/sample; a difference in the temperatures of the ends of the working part of the specimen/sample and its center in air it does not exceed 10-15 deg, but in vacuum - 5 deg.

For protection from the radiation heating of the magnet windings, loads and other cell/elements in the zone, adjacent to the end-type part of the furnace, are establish/installled the chromated copper shields, water-circled.

The measures indicated ensured the continuous operation of setting up at high temperatures. It was establish/installled that during heating of working part to 1200°C the temperature of the lower part of the specimen/sample did not exceed 80-90°C, i.e., that value, with which the loads retain their magnetic properties. All elements of construction/design, with exception strictly of furnace, had temperature not higher than 60°C.

Setting up D-7 makes it possible to conduct tests in vacuum. Pumping out system consists of forepump VN-2MG for the creation of rough vacuum on the order of 1.33 MN/m^2 (10^{-2} mm Hg) and vacuum assembly VA-0.5-4 assembled with oil-vapor pump of type N-5, that ensure evacuation/rarefaction 13.3 MN/m^2 (10^{-6} mm Hg), the assembly of equipment for measuring of the vacuum and water-cooled vacuum camera/chamber.

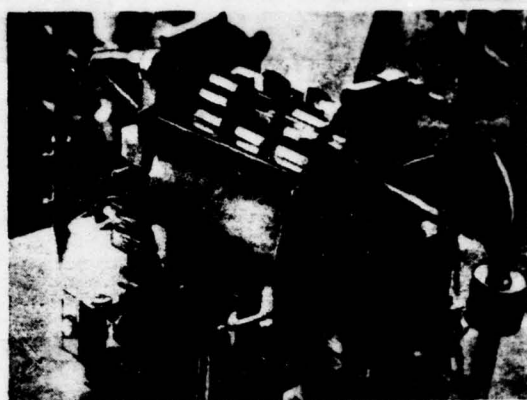


Fig. 94. The appearance of the electric furnace of setting up D-7.

Page 128.

In the camera/chamber there is inspection window with thermo-strong quartz glass which serves for observation after the work of furnace and the position of specimen/sample in the process of heating, and also for the input of the beam of illuminator into the camera/chamber. (For the conclusion/derivation of light ray serves analogous window in working plate/slab). Within the camera/chamber is located the bulb for illumination.

For recording the dying oscillations in setting up, is applied

the simple and reliable optical system, which ensures the recording of vibrations by light ray on photographic paper. In the system indicated enter the illuminator with long-focal-length lens and bulb, the batch of mirrors and recording mechanism.

Illuminator is long tube with the bulb which is equipped by device with gash 0.2 mm for the diaphragming of the luminous flux. The diaphragmed ray/beam, leaving illuminator, falls to the turned at an angle of 45 deg. mirror and - through inspection window - into the camera/chamber on the mirror which is fastened to one of the inertia loads near a node of the vibrations of system. After being reflected, ray/beam falls on another mirror, arranged located within the camera/chamber, which directs it to recording mechanism.

Recording mechanism (Fig. 95) includes cassette with photographic paper of the assembly of an automatic recorder of type K-4-51 and the drive of cassette, which consists of housing for the setting up of cassette and electrical mechanism MZR-1, equipped with additional miniature attachment with blocks for an increase in the range of the control of the rate of the drawing of photographic paper. For the exception/elimination of slippage, the blocks are established/installed between the epicyclic gear with gear ratio to 1:450 and electric motor, i.e. at high-speed step/stage.

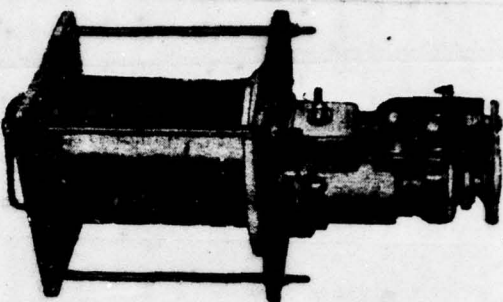


Fig. 95. The appearance of recording mechanism.

Page 129.

An electric motor of type MF-4 of direct current 15 V in power with nominal voltage 27 V and revolutions 1200 r/min in combination with reducer and attachment provides the infinitely variable control of the rate of the drawing of photographic paper from 10 to 300 mm/s.

The supply voltage of electric motor is regulated on the voltmeter of direct current within limits from 10 to 50 V with the aid of laboratory transformer LATR-1. This system makes it possible to easily select the optimum rate of the drawing of photographic paper for a frequency band 5-100 Hz and for materials with different fading.

During tests preliminarily was conducted calibrating the rate of the drawing of photographic paper in the function of stress on electric motor.

The ray/beam through the narrow gash in the wall of cassette falls to the driving/moving photographic paper.

Recording mechanism is establish/installled on the platform which can be fixed in any position after vertical displacement/movement. This adjustment makes it possible to acquire maximum of back-and-forth amplitudes on vibrogram at any amplitude value of the bending moment.

One of the major advantages of tests during setting up D-7 is the fact that during the measurement of the dissipation of energy in material are brought to minimum the external losses. So, torsional stress in the strings of the suspension of specimen/sample is 2-3 MN/m² (0.2-0.3 kg/mm²); therefore energy losses in the material of the strings, twisted at an angle of [redacted] 3-5 deg., are negligible.

Losses into framing are virtually excluded because of the introduction of thickenings at the ends of the specimen/sample, the

second moment of area of which is 30 times more than for the cross section of the working part of the specimen/sample.

Test work in vacuum makes it possible to eliminate losses into the environment whose effect on the dissipation of energy during the vibrations of flat/plane specimen/samples can be in certain cases very essential.

The thermocouples, introduced into working chamber of furnace, are not connected with the oscillating specimen/sample, which also eliminates possible additional losses.

The application/use of an optical recording system of vibrations does not require mechanical communication/connection between the oscillating specimen/sample and the recording mechanism.

The excitation of vibrations with the aid of alternating current eliminates the effect of magnetic field on the dissipation of energy.

Taking into account the specific character of conducting studies of the dissipation of energy in material during the utilization of setting up D-7, expediently in more detail to examine the test procedure with the aid of this setting up.

Page 130.

Procedure of the experimental studies of the dissipation of energy in a cyclically deformed material.

For the criterion of the damping capacity of material during experimental investigations, it is expedient to accept the logarithmic decrement of damping the vibrations of flat/plane specimen/samples. The basic advantages of this selection are relative simplicity of obtaining and sufficient for engineering practice accuracy/precision and the reliability of test results. Is presented below the recommended by us procedure of the determination of the decrement of vibrations with the aid of setting up D-7.

The resonance mode of vibrations are established with the aid of the master oscillator. Platform with recording mechanism they are set in such a position that the spread/scope of the amplitude of the oscillations of ray/beam on photographic paper would reach ~120 mm, after which is realize/accomplished the interruption of resonance. After several seconds before interruption is connected the recording.

During the treatment of its obtained thus vibrogram they divide not several sections by such form, in order to the difference between

the first and last/latter amplitude for each section of were approximately identical. In this case, they assume that on the section in question the decrement retains constant value, i.e., they assign the value of decrement indicated to average stress on this section.

In order to avoid errors in the accidental character, to the dependence of decrement on stress one should construct on the data of two -three vibograms, and for obtaining a large number of points select the covering each other sections of vibrogram.

Decrement is determined from the formula

$$\delta = \frac{1}{z} \ln \frac{a_0}{a_{0+z}}, \quad (3.1)$$

where z - a number of cycles on individual section;

a_0 and a_{0+z} - value of amplitude in the beginning and at the end of the selected section of vibrogram.

Stress is calculated from known formula for a bend on the edge of the specimen/sample:

$$\sigma = \frac{Eh}{l} \cdot \frac{\alpha}{2R}, \quad (3.2)$$

where E - modulus of elasticity;

h - thickness of specimen/sample;

l - length of working part;

R - total distance from mirror on the load to slit in the cassette of recording mechanism.

Page 131.

For the exception/elimination of the effect of air on the decrement of vibrations sequence indicated above of operations one should conduct in the connected vacuum system [$p < 1.33 \text{ N/m}^2$ (10^{-2} mm Hg)].

For decreasing the driving of the oscillatory system, consequence of which is undulation on vibrograms, it is necessary to accurately set the clearances between the end/faces of magnet cores and loads. (It is necessary to note that the swaying of specimen/sample does not influence the dissipation of energy in material and only somewhat impedes the treatment of vibrograms).

To the advantages of the used method of the recording of vibrations, one should relate the fact that all inaccuracies in setting up and fastening of specimen/sample easily are detected on vibrogram.

When conducting of calibrating thermocouple with the aid of fine/thin molybdenum wire, they fasten to test specimen at three points. The stress in sections they increase by step/stages with holding to 20 min until is establish/installled equilibrium temperature conditions. Stress controls by the voltmeter with the elongated scale, which with the aid of the three-position switch can be included in any section of furnace.

In order to eliminate a difference in the temperatures along the length of specimen/sample, in midsection are established approximately the same stress as in extreme ones, and this section is connected through the mercury switch EPP-09.

In the process of heating, the specimen/sample is elongated, this leads to the displacement of loads relative to the cores of magnets and, as a result, to the driving of loads. Therefore for the compensation the elongation of specimen/sample, one of the stands of magnets is equipped with the transmission with high gearing, which is given from the handle, brought out outside from the camera/chamber. Cranking in proportion to heating specimen/sample, experimenter attempts to reduce the driving of specimen/sample to minimum.

In work with heat-resistant alloys on nickel basis to 900-1100°C, is sufficient forevacuum on the order of 1.33 MN/m² (10^{-2} mm Hg). At this residual pressure is virtually completely eliminated the effect of air on damping of the vibrations of specimen/sample.

At the same time for a work with such metals as molybdenum, tungsten and niobium, at temperatures to 1200°C is necessary more high vacuum (created with the aid of vacuum assembly), since heating the metals indicated in air is accompanied by intense oxidation, especially beginning from 350-600°C.

At normal temperature vacuum assembly creates permission in camera/chamber on the order of 1.33 MN/m² (10^{-5} mm Hg). During heating to 1100-1200°C, the vacuum falls to 3.99 MN/m² (3×10^{-5} mm Hg).

Page 132.

Thus, the sequence of operations during testing can be presented as follows:

1. After setting up and batch of specimen/sample, are remove/taken the vibograms of vibrations in air with the normal temperature and the raised camera/chamber.

2. Camera/chamber is lower/cmited and is connected ^{vacuumation} A pump.

On the achievement of vacuum 1.33 N/m^2 (10^{-2} mm Hg) is connected vacuum assembly.

3. During permission 1.33 mN/m^2 (10^{-5} mm Hg) are record/written vibograms through every 100 deg (holding at each temperature must be of sufficient for obtaining two-three vibograms).

4. Are record/written vibograms in vacuum during cooling of specimen/sample. (Removal/taking vibograms during cooling pursues the target/purpose of obtaining the more full/total/complete data on the possible structural transformations, occurring in material at high temperatures and with considerable stresses).

5. Obtained vibograms are processed by method indicated above. Are plotted a curve of the dependences of the logarithmic decrement of vibrations on the average peak stress in the center section of the specimen/sample for different temperatures. The curves indicated serve as the initial material for plotting of the dependence of the logarithmic decrement of vibrations on the temperature at different stresses.

Results of the experimental investigations of the dissipation of energy in refractory metals.

As already mentioned, damping capacity is the important mechanical characteristic of high-melting materials. However, in the literature are absent the data on the attenuating properties of refractory metals at the high values of cyclic stresses and high temperatures. We carried out the investigation of the attenuating properties of molybdenum, tungsten and niobium, obtained by different methods during setting up D-7 according to the procedure, described in the preceding/previous paragraph.

The moduli of normal elasticity of the materials indicated in wide temperature interval were determined in assembly UP-6; the values of module/moduli for all materials being investigated were given in Tables 10, 11, 15, but the results of the analysis of the attenuating properties of the materials indicated were examined below,

Niobium. Specimen/samples were made of the rods of the niobium, obtained by cathode-ray remelting, and they were not subjected to preliminary heat treatment.

The dependences of the logarithmic decrement of vibrations on stress are given to Fig. 96 and 97.

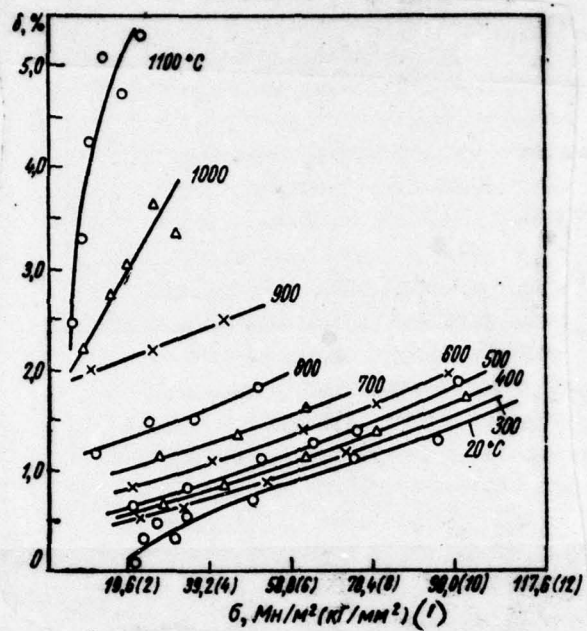


Fig. 96. Attenuating properties of nichium in the function of the stresses during heating in vacuum.

Key: (1). MN/m² (kg/mm²).

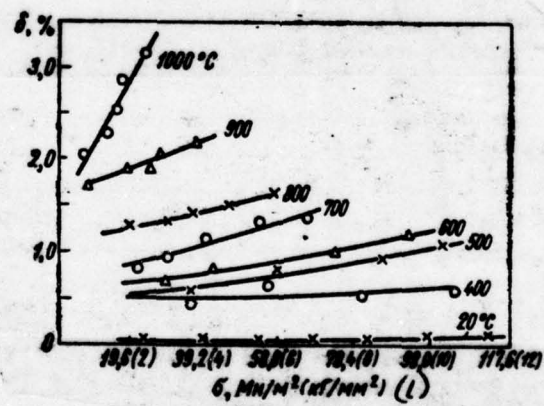


Fig. 97.

Fig. 97. Attenuating properties of niotium in function of stresses during cooling in vacuum.

Key: (1). MN/m² (kg/mm²).

Page 134.

From graphs it is evident that at temperatures from 20 to 1100°, is observed the clearly expressed tendency of an increase in the damping capacity of niobium with an increase in the stresses, moreover most sharply grows/rises decrement with 1100°C - from 2.5 to 5.8% (i.e. it is more than ^{two}₁ times) with an increase in the stress three times.

The analysis of the dependence of logarithmic decrement on the temperature at the fixed level of stresses [19.6; 58.8; 98.1 MN/m² (2; 6; 10 kg/mm²)] (Fig. 98) shows that with a temperature rise the damping capacity of niotium is increased. No anomalies in a change in the decrement depending on the temperature there were reveal/detected either during heating or during cooling of specimen/samples. With the increase of temperature from 20 to 800°C, logarithmic decrement grows/rises insignificantly, while, beginning from 900°C, the intensity of its growth becomes significant.

All experiments as a result of which were obtained the dependences $\delta=f(\sigma)$ and $\delta=f(t)$, were carried out in vacuum 1.33 MN/m^2 (10^{-5} mm Hg) at $20-900^\circ\text{C}$ and 2.66 MN/m^2 ($2 \cdot 10^{-5} \text{ mm Hg}$) at higher temperatures.

Thus, together with the sufficiently high characteristics of strength, plasticity and heat resistance mickium possesses the good attenuating properties.

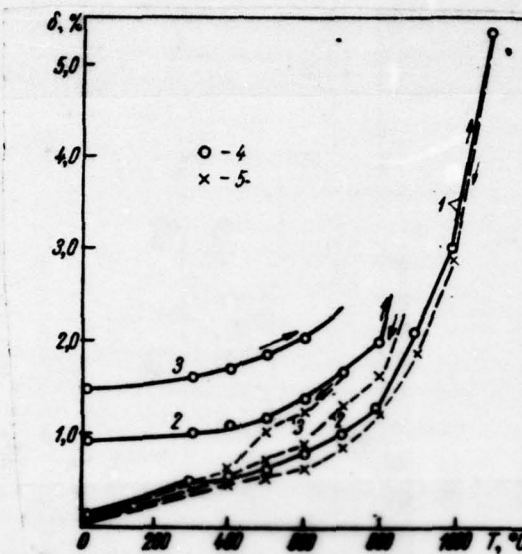


Fig. 98. The temperature effect on the dissipation of energy in the niobium: 1 - $\sigma = 19.6 \text{ MN/m}^2$ (2 kg/mm^2); 2 - $\sigma = 58.8 \text{ MN/m}^2$ (6 kg/mm^2); 3 - $\sigma = 98.1 \text{ MN/m}^2$ (10 kg/mm^2); 4 - heating; 5 - cooling.

Page 135.

The combination indicated makes this material with completely suitable ones for manufacturing the parts, working at high temperatures and cyclic loads.

Molybdenum. For the investigation of the attenuating properties of molybdenum we have made specimen/samples made of:

- 1) cermet molybdenum, deformed by rolling with the degree of reduction ~40%;
- 2) the cermet molybdenum, rolled with the same reduction and then annealed at 900°C for 1 h;
- 3) the molybdenum, which contains 0.2%, Ti and 0.005% C, obtained by common arc melting and deformed by rolling with degree reduction ~40%;
- 4) the alloy of the analogous composition, rolled with the same reduction and annealed at 900°C for 1 h.

The analysis of the results of tests (Fig. 99-111) makes it possible to make following conclusions.

1. For all tested specimen/samples is observed clearly expressed tendency of increase in decrement with increase in stress at all temperatures.
2. With temperature rise at constant stress, decrement also grows/rises, moreover for deformed molybdenum is observed sharp incidence/drop in decrement in range of temperatures of 300-800°C.

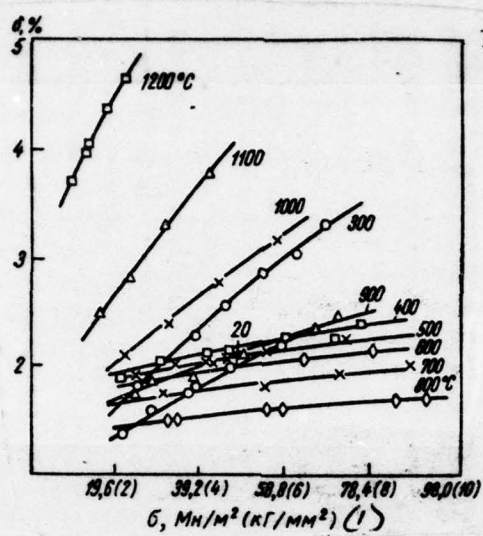


Fig. 99.

Attenuating properties of cermet molybdenum as a function stress
during heating in vacuum.

Key: (1). MN/m² (kg/mm²).

Page 136.

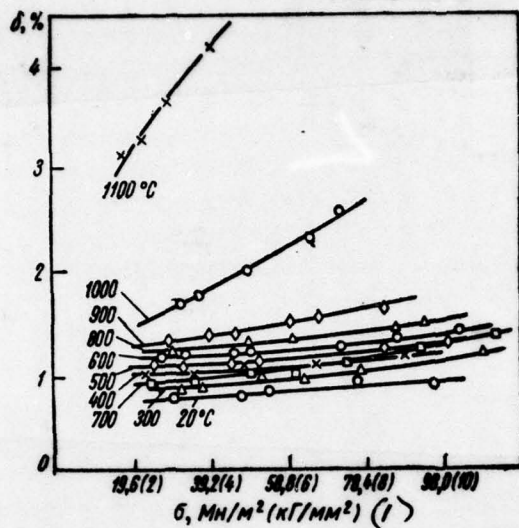
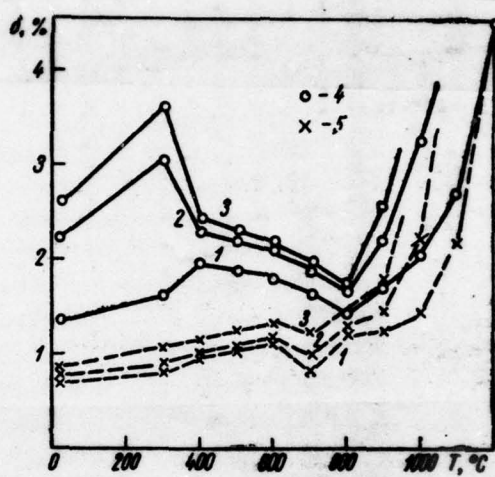


Fig. 100. Attenuating properties of cermet molybdenum as function of stresses during cooling in vacuum.

Key: (1). MN/m^2 (kg/mm^2).

Fig. 101. Temperature effect on dissipation of energy in deformed cermet molybdenum: 1 - $\sigma=19.6 \text{ MN/m}^2$ (2 kg/mm^2); 2 - $\sigma=58.8 \text{ MN/m}^2$ (6 kg/mm^2); 3 - $\sigma=78.5 \text{ MN/m}^2$ (8 kg/mm^2); 4 - heating; 5 - cooling.



Page 137.

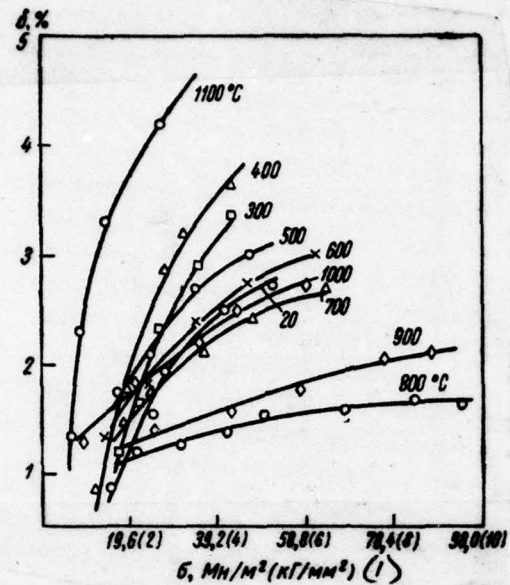


Fig. 102. Attenuating properties of poured molybdenum in function of stresses during heating in vacuum.

Key: 11) MN/m² (kg/mm²).

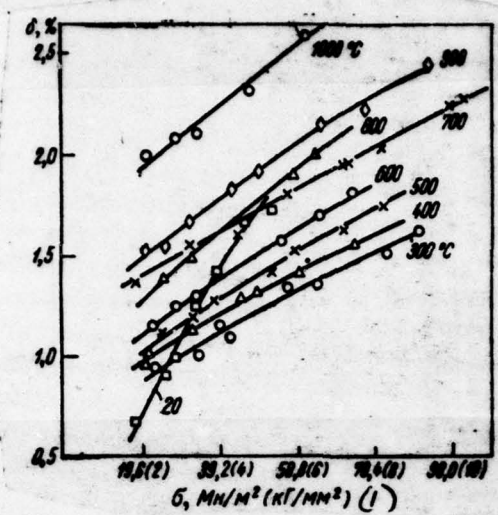


Fig. 103. Attenuating properties of poured molybdenum in function of stresses during cooling in vacuum.

Key: (1). MN/m² (kg/mm²).

Page 138.

During the analysis of the temperature dependences of the damping capacity of the poured and cermet molybdenum in the state of strain (see Fig. 101 and 104) it is noticeable that the good-quality picture of a change in the decrement to a temperature rise and stress is approximately identical. The same can be said about a change of

the decrement for the pcured and cermet molybdenum in the annealed state, is observed even the completely satisfactory quantitative conformity of attenuation characteristics for these two materials, which, however, can be accidental factor, since the impurity content in the specimen/samples of the cermet and pcured molybdenum is different. Taking into account this fact, subsequently we will not separately analyze curves, obtained for specimen/samples made of each material, but let us examine them together.

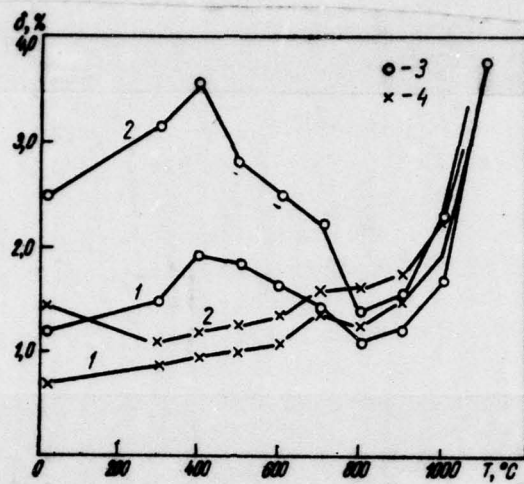


Fig. 104. The temperature effect on the dissipation of energy in the deformed pcured molybderum: 1 - $\sigma = 19.6 \text{ MN/m}^2$ (2 kg/mm^2); 2 - $\sigma = 39.2 \text{ MN/m}^2$ (4 kg/mm^2); 3 - heating; 4 - cooling.

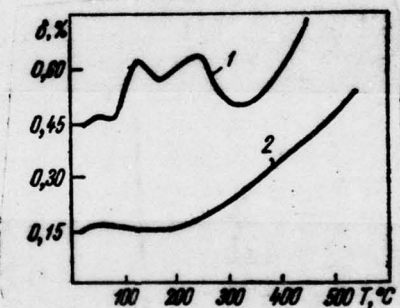


Fig. 105. Temperature effect on dissipation of energy in poured molybdenum at small amplitudes of strain ($\gamma < 10^{-5}$) and frequency 1 Hz: 1 - deformed; 2 - annealed (700°C , 1 h).

Page 139.

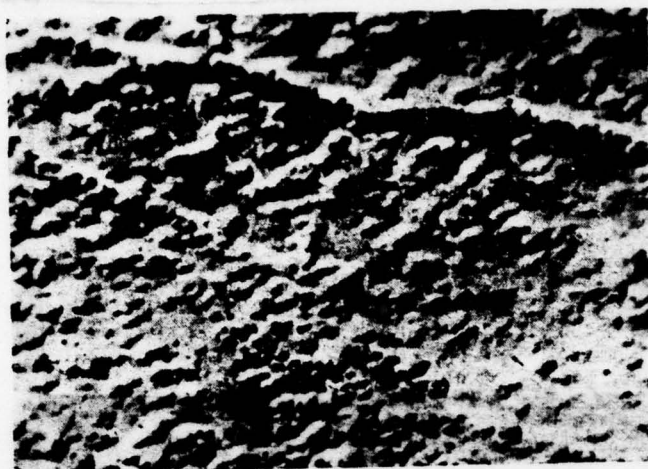


Fig. 106. Microstructure of poured molybdenum, annealed at temperature of 900°C (x9500).



Fig. 107. Microstructure of cermet molybdenum, annealed at temperature of 900°C (x3000).

Page 140.

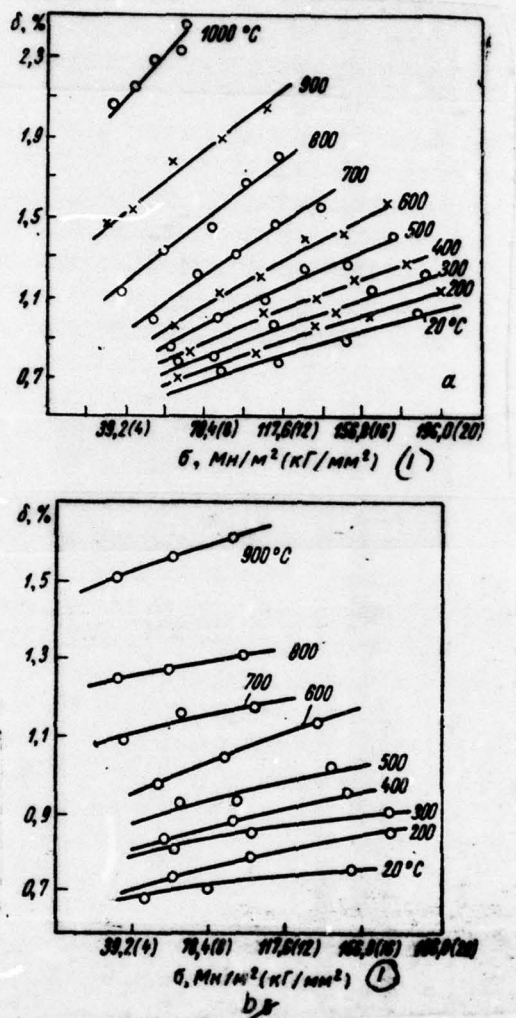


Fig. 108. Attenuating properties of annealed (900°C) powder molybdenum in function of stresses during heating (a) and cooling (b) in vacuum.

Key: (1). MN/m^2 (kg/mm^2).

Page 141.

Initially let us discuss the typical special feature/peculiarities of the behavior of specimen/samples made of the pcured and cermet molybdenum in state of strain. It is first of all necessary to note that the decrement of these specimen/samples with 20°C is considerably higher than for the specimen/samples of molybdenum, annealed after rolling. So, if with $\sigma=39.2 \text{ MN/m}^2$ (4 kg/mm^2) for deformed pcured molybdenum $\delta=2.5\%$, then with the same stresses the annealed pcured molybdenum it has $\delta=0.5\%$, i.e., is 5 times less. Analogous law is observed also for cermet molybdenum.

The increase of the value of logarithmic decrement for the deformed specimen/samples should explain by the intensification of the irreversible processes in material with a large number of flaw/defects, introduced by plastic deformation, and consequently, by an increase in the dissipation of vibrational energy.

The increase of temperature led to an anomalous incidence/drop in the decrement in interval of $400-800^{\circ}\text{C}$ for the specimen/samples of

the poured and cermet molybdenum, deformed by rolling. For explaining the nature of the processes, which take place at the temperatures indicated, were determined the values of the logarithmic decrement of vibrations depending on the temperature at small amplitudes of strain ($\gamma < 10^{-5}$).

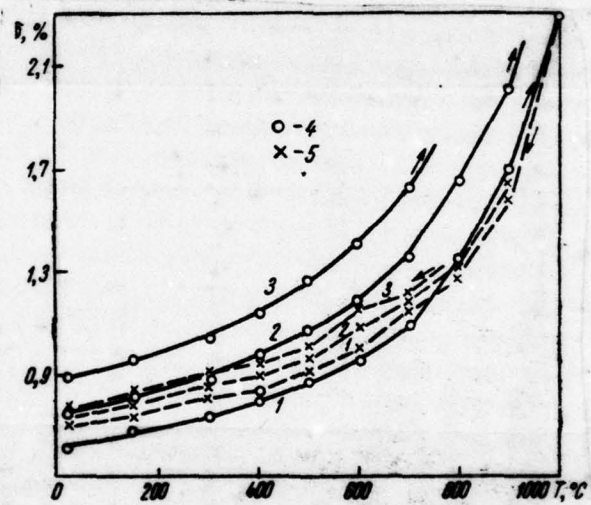


Fig. 109. The temperature effect on the dissipation of energy in the annealed powder molybdenum: 1 - $\sigma = 58.8 \text{ MN/m}^2$ (6 kg/mm^2); 2 - $\sigma = 98.1 \text{ MN/m}^2$ (10 kg/mm^2); 3 - $\sigma = 137 \text{ MN/m}^2$ (14 kg/mm^2); 4 - heating; 5 - cooling.

283

Page 142.

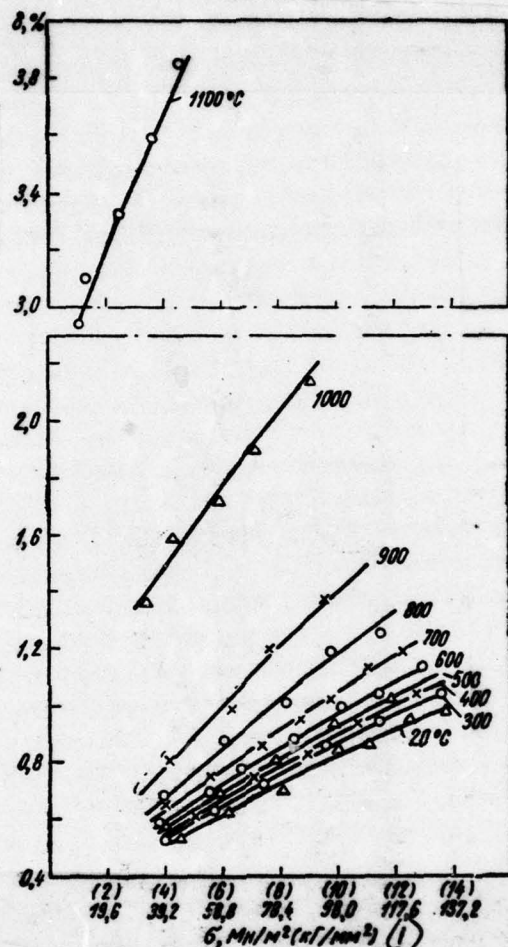


Fig. 110. Attenuating properties of annealed (900°C) poured molybdenum in function of stresses during heating in vacuum.

Key: (1) - MN/m² (kg/mm²) -

Page 143.

These tests were conducted with the aid of the torsion pendulum at frequency 1 Hz.

As can be seen from curve/graph in Fig. 105, with 130 and 250°C are observed the maximums of internal friction. In work [96] the increase of decrement with 130°C is connected with the migration of nitrogen atoms in solid solution under the influence of the applied stresses. The nature of maximum with 250°C they treat differently [96, 97, p. 123].

After the annealing of the specimen/samples of the deformed molybdenum with 700°C for 1 h, relaxation maximums disappear. This testifies to the course of the strain aging, connected with the liberation/isolation of interstitial impurities during the dislocations. (Analogous results were obtained for cermet molybdenum). Specifically, by strain aging one should, apparently, explain a reduction in the logarithmic decrement of the deformed molybdenum specimen/samples in the range of temperatures of 300-800°C.

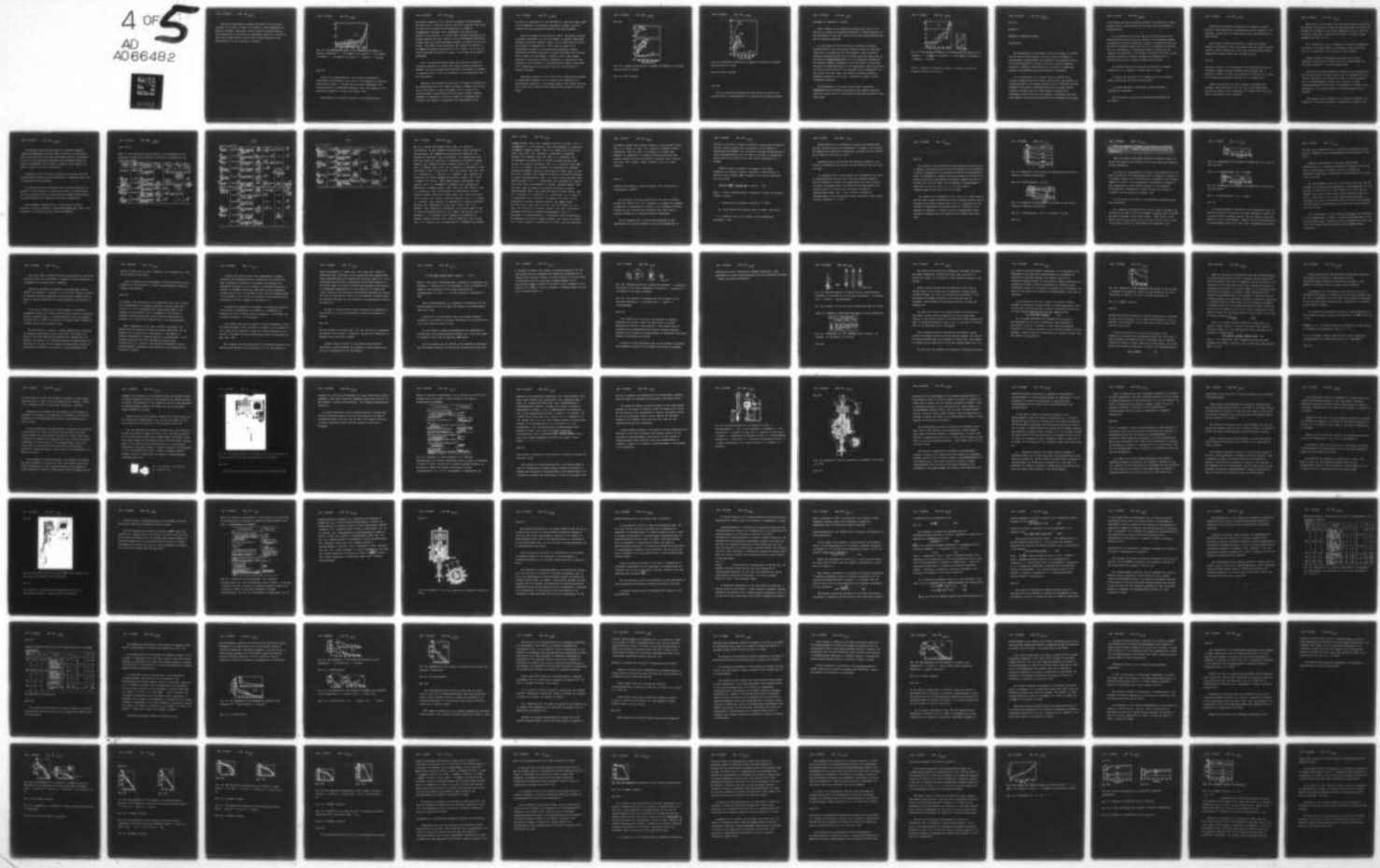
AD-A066 482 FOREIGN TECHNOLOGY DIV WRIGHT-PATTERSON AFB OHIO
STRENGTH OF REFRACTORY METALS. PART I-(U)
OCT 78 G S PISARENKO, V A BORISENKO
FTD-ID(RS)T-1330-78-PT-1

F/G 11/6

UNCLASSIFIED

NL

4 OF 5
AD
AD66482





Heating to temperatures is higher than 800°C, as can be seen from Fig. 99 and 102, it leads to an increase of the dissipation of energy in material. Apparently, this is caused by the fact that at high temperatures is decreased the dislocation density as a result of their mutual annihilation, which becomes possible because of the intensification of the processes of creeping.

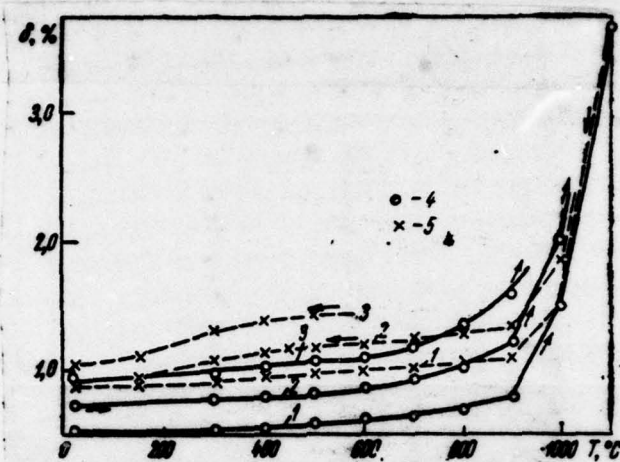


Fig. 111. The temperature effect on the dissipation of energy in annealed molybdenum: 1 - $\sigma = 39.2 \text{ MN/m}^2$ (4.0 kg/mm^2); 2 - $\sigma = 78.5 \text{ MN/m}^2$ (8 kg/mm^2); 3 - $\sigma = 118 \text{ MN/m}^2$ (12 kg/mm^2); 4 - heating; 5 - cooling.

Page 144.

Heating the specimen/samples of the deformed molybdenum to temperatures of 900-1200°C it must lead to the formation of polygonal sub-structure, which is retained during cooling. Apparently, this causes reduction of logarithmic decrement, which they observed in the experiments conducted (see Fig. 100 and Fig. 103).

The formation of polygonal structure in the process of the

preliminary annealing of the deformed molybdenum specimen/samples with 900°C for 1 h (see Fig. 106 and 107) led to the fact that during the tests of the annealed specimen/samples of arc-malcus incidence/drop decrement with a temperature rise they did not observe; on the contrary, it occurred the continuous increase of the damping capacity (see Fig. 108-111). In the investigated temperature interval which for cermet molybdenum composed 20-1000°C, and for that poured 20-1100°C, damping capacity, for example, for stress of 58.8 MN/m² (6 kg/mm²) grow/rose from 0.6 to 2.3% - in the case of cermet molybdenum and from 0.6 to 4% - in the case of the poured molybdenum.

Thus, the obtained results showed that cermet and poured the molybdenum possesses the sufficiently high attenuating properties together with the increased heat resistance, which makes it possible to recommend it for a work the conditions of high alternating loads and temperatures.

Tungsten. The attenuating properties of tungsten investigated at the temperatures from 20 to 1000°C in vacuum 1.33 MN/m² (10^{-5} mm Hg) and at 1100-1200°C in vacuum 2.66 MN/m² ($2 \cdot 10^{-5}$ mm Hg) in the specimen/samples, manufactured from the remelted cermet tungsten, subjected to deformation to rolling without the subsequent heat treatment. The results of experiments are represented in Fig.

112-114. For temperatures 20 and 300-500°C, is given the common curve of the dependence of logarithmic decrement on stress, since the values δ for the temperatures indicated virtually coincide.

With the increase of temperature to 600°C, the damping capacity noticeably grows/rises. So, for $\sigma=98.1 \text{ MN/m}^2$ (10 kg/mm^2) logarithmic decrement with 500°C composes 0.65%, and at 600°C value $\delta=1.25\%$. The increase of temperature to 1000°C does not lead to the considerable increase of the attenuating properties, whereas beginning from 1000°C logarithmic decrement grows/rise very intensely, and at 1200°C for $\sigma=58.8 \text{ MN/m}^2$ (6 kg/mm^2) $\delta=50\%$. This intense increase in the damping capacity, apparently, is explained by the beginning of the processes of recrystallizations which, accordingly [98], considerably are accelerated under the action/effect of external voltages.

Noticeable anomalies in the curves of the temperature dependence of logarithmic decrement did not observe, with exception of an insignificant reduction in the damping capacity with 1000°C (see Fig. 114), which can be caused by the course of the processes of strain aging,

Page 145.

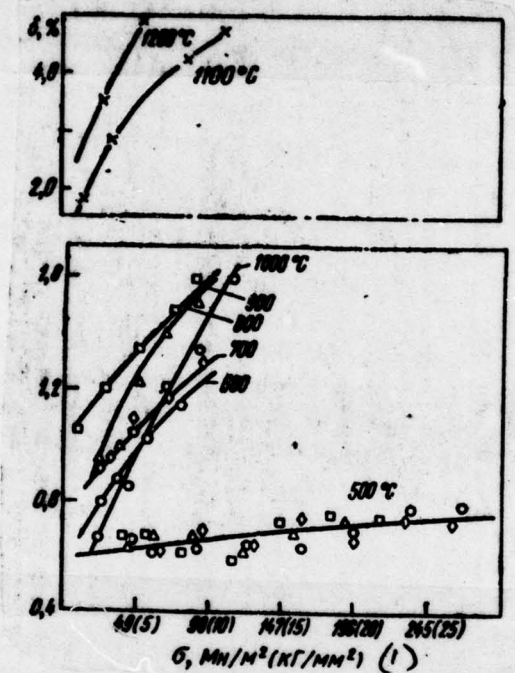


Fig. 112. Attenuating properties of tungster in function of stresses during heating in vacuum.

Key: (1) . MN/m² (kg/mm²) .

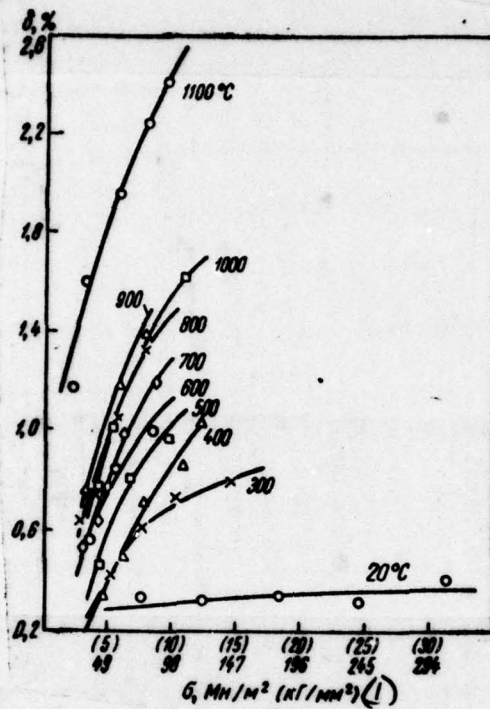


Fig. 113. Attenuating properties of tungsten in function of stresses during cooling in vacuum.

Key: (1) • MN/m² (kg/mm²).

Page 146.

For all investigated temperatures both during the heating and during cooling of specimen/samples is observed the sharply pronounced

dependence of decrement or stress.

Thus, tungsten in the investigated temperature range is not inferior to niobium and molybdenum according to damping capacity and can successfully be accepted itself for the same target/purposes that and the materials indicated.

In conclusion was made the attempt to compare the damping characteristics of the investigated materials under the comparable conditions: at temperatures and with stresses, which constitute identical portion/fraction from the melting point and yield point of the materials being investigated, i.e., at homologous temperatures and stresses. Figure 115 depicts to the dependence of logarithmic decrement on homologous voltage at the temperature, which constitutes 0.4 from the melting point of the materials being investigated. As can be seen from this graph, the highest attenuating properties possesses tungsten, by the lowest - molybdenum; niobium occupies intermediate position.

It is necessary to note that in the range of operating temperatures the attenuating properties of the studied refractory metals are higher than for the majority of most heat-resistant nickel base alloys.

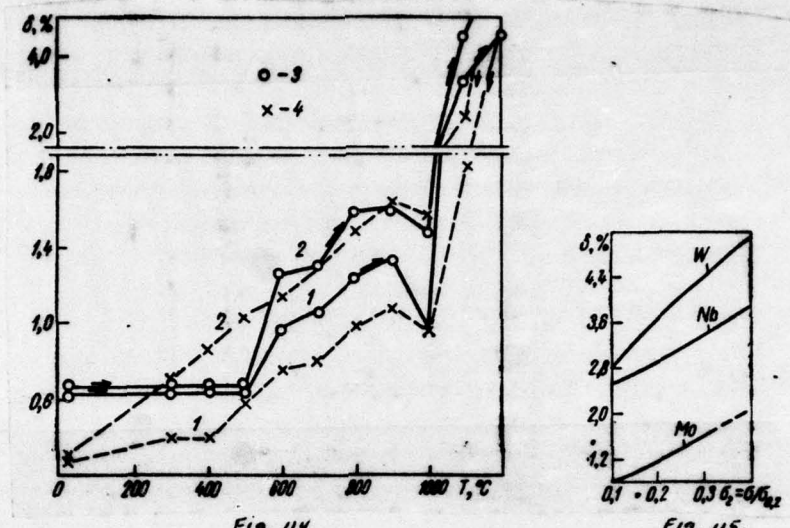


Fig. 114. The temperature effect on the dissipation of energy in the tungsten: 1 - $\sigma = 49 \text{ MN/m}^2$ (5 kg/mm^2); 2 - $\sigma = 98.1 \text{ MN/m}^2$ (10 kg/mm^2); 3 - heating; 4 - cooling.

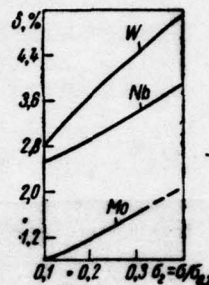


Fig. 115. Comparison of attenuating properties of refractory materials with homological temperature and stresses.

Page 147.

Chapter 4.

HARDNESS OF REFRactory METALS.

Generalities.

The measurement of the hardness of materials widely is utilized for the check of their quality, and also as one of methods of metallographic investigations. The scientific and practical value of this method consists in the fact that in the value of hardness, measured at different temperatures, it is possible to judge many important physicomechanical characteristics of materials.

It is real/actual, as it follows from the results of the numerous investigations (see survey in work [100]), the hardness of material depends on its crystal structure and is connected with many mechanical and physical characteristics, with the yield points, strength, fatigue, creep and stress-rupture strength; with compressibility and value of ionic radius; it correlates also with some magnetic and electrical properties. The measurement of hardness

is the simple, but highly sensitive method of the study of the aging, peening, return, recrystallization and other phase and structural transformations.

N. N. Davidenkov [99] showed that the hardness does not have special physical nature, being the measure of the averaged strength of materials to plastic deformation. However, it should be noted that the value of hardness depends not only on the properties of material, but it is determined to a considerable extent by method and the conditions of measurement. The values of hardness of one and the same material, measured by different methods, can substantially be distinguished and even possess different dimensionality.

The existing methods of measuring the hardness at elevated temperatures it is possible to divide into two groups:

- 1) static ones (methods of the indentation of tip, abrasion, mutual indentation, one-sided sclerification);
- 2) dynamic (methods of impression, elastic come-back, oscillation of pendulum).

The principles on which are instituted these methods, are well-known.

Scattering the results of measuring the hardness by dynamic methods at high temperatures is sufficiently great; therefore it is difficult to speak about the possibility of the wide utilization of these methods.

Were recently undertaken attempts to measure the dynamic hardness of materials at high temperatures with the method of elastic come-back (Shor's method) [101, 103]. The achieved/reached maximum temperatures compose 1800°C [102] and 2580°C [104].

Page 148.

However, in spite of the development of new experimental means and procedures, dynamic methods, including Shor's method, make it possible as before to obtain only qualitative evaluation of a change of the hardness of different materials in the heated state.

Widest use received the static methods of measuring the hardness. Among them both at low and at high temperatures prevail the methods of the indentation of indentor with tip in the form of ball/sphere, cone or pyramid.

The majority of the given in the literature results of measuring the hardness of metals and alloys at high temperatures (to 1650°C) is obtained by the method of the static indentation of tip in the form of correct tetrahedral pyramid with the angle of 136 deg. between opposite faces [62, 107-111].

M. M. Khrushchov [112] it recommends to accept the indentation of pyramid as the basic method of the hardness test of materials, since it is applicable to the materials of any hardness.

Without indentor is determined the hardness via mutual indentation and one-sided sclidification [18]. These methods are especially effective at very high temperatures.

The method of mutual indentation consists in the compression of two specimen/samples of tested material and the measurement of the obtained impression. Most convenient proved to be the cylindrical form of specimen/samples; however, it is possible to apply specimen/samples and another form. Are possible two methods of the arrangement of the specimen/samples: mutually perpendicular and parallel.

The method of mutual indentation is applied for measuring the hardness of refractory compounds at temperatures to 2100°C [113].

Ber hardness test from the method of one-sided flattening conical specimen/sample with the angle of 120 deg. at apex/vertex they flatten with the aid of flat/plane punch/male die, is measured the area of the flat/plane impression, which was being formed as a result of flattening. On the value of hardness, they judge by the ratio of load to the area of flattening.

Punch/male die for one-sided flattening must be made from the material whose hardness at high temperatures is knowingly higher than the hardness of test specimens.

The methods of mutual indentation and one-sided flattening are similar. To the advantages of last/latter method, one should relate its high productivity and the double smaller expenditure/consumption of specimen/samples (in comparison with mutual indentation).

The fundamental characteristics of the methods, used for measuring of static hardness at temperatures higher than 1000°C, with references to literary sources are given in Table 17.

Pages 149-152.

Table 17. The fundamental characteristics of the procedures of the measurement of the static hardness of materials at temperatures are higher than 1000°C.

(1) Авторы методики, год, работа	(2) Интервал температур, °C	(3) Метод определения (статической твердости или микротвердости)	(4) Среда для защиты от окисления	(5) Материал исследования	(6) Нагрузка к (кг)	(7) Время выдержки под нагрузкой
ГОСТ 2999—59	(8) Комнатная	(9) Твердость, вдавливанием алмазной пирамиды Виккерса	—	(10) Цветные металлы, черные металлы и сплавы	50 (5,0); 100 (10,0); 200 (20,0); 300 (30,0); 500 (50,0); 1000 (100,0)	30±2 сек; 10—15 сек
(12) Энгл И., Феллер И., 1936, [114] (16)	20—1860	(3) Твердость, вдавливанием конуса с углом 120° при вершине	—	W, Mo, Ni и сплавы	86 (8,6)	1 мин
Лозинский М. Г., Гудков Н. Т., Богданов Н. А., 1960 [62, 107, 224]	20—1300	(17) Твердость, вдавливанием алмазной и сапфировой пирамиды Виккерса	(18) Вакуум $1,33 \text{ мн}/\text{м}^2$ ($10^{-5} \text{ мм рт. ст.}$)	(19) Металлы, стали, твердые сплавы	2,5—100 (0,25—10), обычно	1—60 мин обычно
(21) Дамагала Р. Ф., Джонсон У. Р., 1961 [105]	20—1315	(22) Твердость, вдавливанием алмазной пирамиды	(23) Инертный газ	(24) Кремний	10 (1)	1 мин
(25) Вестбрюк Дж. Х., 1967 [125]	20—1500	(26) Микротвердость, вдавливанием сапфировой пирамиды Виккерса, инденторами разных типов	(27) Вакуум $2,66 \text{ см}/\text{м}^2$ ($2 \cdot 10^{-4} \text{ мм рт. ст.}$)	(28) Металлы, минералы, карбиды	60—80 (6—8)	—
(29) Губкин С. И., Тамилин Р. И., 1968 [106]	900—1450	(20) Твердость, вдавливанием микролитовой пирамиды Виккерса	(31) Расплав шлака	(32) Стали	0,2—9,0 (0,02—0,9)	—
					20 (2)	20 сек

299

Table 17 continued.

(33) Бетанчи А. И., 1958 [115]	20—1200	(34) Твердость, вдавливанием куска с углом 136° из сплава марки ЦМ-332	(35) Расплав шлака	(35) Стали, твердые сплавы	3750 (375)	(5) 1 мин
(36) Семчесен М., Торгерсон К. С., 1958 [110]	20—1650	(37) Твердость, вдавливанием сапфировой пирамиды Виккерса	(38) Вакуум или инертный газ	(39) W, Mo, Fe, сплавы	50 (5)	(10) 10 сек
(40) Бокучава Г. В., 1958 [225]	20—1300	(41) Микротвердость, вдавли- ванием алмазной пи- рамиды Виккерса	(42) Вакуум 1,33 см/м ² (1·10 ⁻⁴ м.м рт. ст.)	(42) Рубин, сапфир, карбид кремния	0,5—3 (0,05—0,3)	—
(43) Лозинский М. Г., Миртоворский В. С., 1959 [62, 229]	20—1300	(44) Микротвердость, вдавли- ванием сапфировой пирамиды Виккерса	(43) Вакуум 1,33 мн/м ² (10 ⁻⁵ м.м рт. ст.)	(43) Fe, стали	0,1—2 (0,01—0,2), обычно 0,5 1 (0,1)	(15) 1 мин
(45) Геммел Г. Д., прибор фирмы «Дюпон», 1959 [109]	20—1400	(46) Твердость, вдавливанием сапфировой пирамиды	(44) Вакуум 1,33 мн/м ² (10 ⁻⁵ м.м рт. ст.)	(44) Ниобий	10 (1)	—
(49) Вестбрук Дж. Х., 1960 [126]	—190+1500	(50) Микротвердость, вдавли- ванием сапфировой пирамиды Виккерса	(51) Вакуум	(52) Кварц, молибден, Ni—Al, TiC	0,05—10 (0,005—1)	2—60 сек обычно 15 сек
(53) Борисенко В. А., 1960 [58, с. 230, 121, 122, 130, 132, 133, 152]	20—1760	(37) Твердость, вдавливанием сапфировой пирамиды Виккерса	(45) Вакуум 1,33 мн/м ² (10 ⁻⁵ м.м рт. ст.)	(45) W, Mo, Ta, Nb и сплавы	10 (1)	(54) От 10 сек до 1 ч, обычно 1 мин
	20—2000	(55) Твердость, вдавливанием пирамиды Виккерса из алмаза, карбида бора и его сплавов	(56) или инертный газ	(57) Карбиды	10 (1)	(55) 1 мин
	1500—3000	(58) Твердость методом од- ностороннего сплю- щивания конического образца		(58) W, Mo, Nb	50 (5)	(15) 1 мин
(59) Иванов О. С. с со- трудниками, 1962 [111, 58 с. 230, 130]	20—1700	(37) Твердость, вдавливанием сапфировой пирамиды Виккерса	(46) 1,33 мн/м ² (10 ⁻⁵ м.м рт. ст.) вакуум	(60) сплавы ниobia	10 (1)	(59) 1 мин
(61) Шалочкин В. А., 1964 [226]	20—1760	(62) Твердость подобно [58, с. 230; 130], вдавли- ванием сапфировой пирамиды Виккерса			(63) макс. нагрузка 500 (50)	—
	1760—2500	(64) Методом односторонне- го сплющивания кони- ческого образца	(65) инертные газы и пары щелоч- ных металлов			

300

Table 17 continued.

(66) Кульбах А. А., Щавелин В. М., Макарычев Б. А., Годин Ю. Г., Евстюхин Н. А., 1965 [227, 228]	20—1600 1500—2800— 3000	(67) Твердость подобно [58, с. 230; 130] вдавлива- ием сапфировой пи- рамиды Виккерса (71) Методом одностороннего сплющивания кониче- ского образца	13,3—1,33 ми/м ² (68) вакуум 10^{-4} — 10^{-5} м.м рт. ст.	Mo, Ni, Cu	(68) От 5 (0,5) до 100 (10) через 50 н (0,5 кг)	От 40 сек и больше, (60)
(72) Писаренко Г. С., Скуратовский В. Н., Борисен- ко В. А., 1965 [119]	20—1760 20—2000	(73) Микротвердость, вдавли- ванием сапфировой пирамиды Виккерса (75) Вдавливанием пирамиды Виккерса из алмаза, карбида бора и его сплавов	(8) Вакуум 1,33 ми/м ² (10^{-5} м.м рт. ст.)	W, Mo, Nb (5) Карбиды	(74) От 0,05 (0,005) до 5,0 (0,5), обычно 0,5 (0,05) и 0,7 (0,07)	30 сек 1 мин, обычно 1 мин (5)
(76) Аткинс А. Г., Табор Д., 1965 [113]	900—2100	(77) Твердость методом вза- имного вдавливания	(27) Вакуум 1,33 си/м ² (10^{-4} м.м рт. ст.)		(78) До 250	—
(79) Кестер Р. Д., Моак Д. П., 1967 [230]	20—1900	(80) Твердость, вдавливанием пирамид Виккерса и Киупа из алмаза, кар- бида бора и карбида тантала	(81) Вакуум или инертный газ	(82) Бориды, окислы, карбиды	1,0 (0,1)— 25,0 (2,5), (3) чаще 10,0 (1,0)	20 сек (1)

Key: (1). Authors of procedure, year, work. (2). Range of temperatures, °C. (3) Method of determination (static hardness or microhardness). (4). Medium for protection from oxidation. (5). Material of experiment. (6). Load N (kg.). (7). Holding time under load. (8). Room. (9). Hardness, by indentation of Vickers' diamond pyramid. (10). Nonferrous metals, ferrous metals. (11). s. (12). I. Engl., I. Felmer, 1936, [114]. (13). Hardness, by indentation of cone with angle of 120° at apex/vertex. (14). and alloys. (15). min. (16). M. G. Lozinskiy, N. T. Gudtsov, N. A. Egdanov. (17). Hardness, by indentation of Vickers' diamond and sapphire pyramid. (18). Vacuum 1.33 MN/m² (10⁻⁵ mm Hg). (19). Metals, steels, hard alloys. (20). usually. (21). R. F. Damagal, U. R. Johnson. (22). Hardness, by indentation of diamond pyramid. (23). Inert gas. (24). Silicon. (25). J. H. Westbrook. (26). Microhardness, by indentation of Vickers' sapphire pyramid, indentors of equal types. (27). Vacuum 2.66 sn/m² (2•10⁻⁴ mm Hg). (28). Metals, minerals, carbides. (29). S. I. Gubkin, B. I. Tamlin. (30). Hardness, by indentation of Vickers' microlytic pyramid. (31). Fusion/melt of slag. (32). Steels. (33). A. I. Betaneli. (34). Hardness, by indentation of cone with angle of 136° of alloy of mark/brand 1sm-332. (35). Steels, hard alloys. (36). M. Semchisen, C. C. Torgerson. (37). Hardness, by indentation of Vickers' sapphire pyramid. (38). Vacuum or inert gas. (39). alloys. (40). G. V. Bokuchav. (41). Microhardness, by indentation of Vickers'

diamond pyramid. (42). Rubir, sapphire, carbide of silicon. (43). M. G. Ložinskiy, V. S. Mirctverskiy. (44). Microhardness, by indentation of Vickers' sapphire pyramid. (45). G. D. Gemmel, tool of firm "du Pont", 1959 [109]. (46). Hardness, by indentation of sapphire pyramid. (47). Niobium. (48). and. (49). J. H. Westbrook. (50). Microhardness, by indentation of Vickers' sapphire pyramid. (51). Vacuum. (52). Quartz, molybdenum. (53). V. A. Pisarenko. (54). From 10 s to 1 h, usually. (55). Hardness, by indentation of Vickers's pyramid from diamond, carbide of boron and his alloys. (56). or inert gas. (57). Carbides. (58). Hardness by method of one-sided flattening of conical specimen/sample. (59). C. S. Ivanov, with coworkers. (60). niobium fusions. (61). V. A. Shapochkin. (62). Hardness it is similar [58, p. 230; 130], by indentation of Vickers' sapphire pyramid. (63). max. load. (64). By method of one-sided flattening of conical specimen/sample. (65). inert gases and vapors of alkali metals. (66). N. A. Kul'takh, V. M. Shchavelin, E. A. Makarychev, Yu. G. Godin, N. A. Yevstyukhin. (67). Hardness it is similar [58, p. 230; 130] by indentation of Vickers' sapphire pyramid. (68). MN/m^2 vacuum 10^{-4} - 10^{-5} mm Hg. (69). From 5 (0.5) to 100 (10) through 50 n (0.5 kgf). (70). From 40 s it is more, usually 1 min. (71). By method of one-sided flattening of conical specimen/sample. (72). G. S. Pisarenko, V. N. Skuratovskiy, V. A. Borisenko. (73). Microhardness, by indentation of Vickers' sapphire pyramid. (74). From 0.05 (0.005) to 5.0 (0.5), usually 0.5 (0.05) and 0.7 (0.07). (75). By indentation

of Vickers' pyramid from diamond, carbide of boron and his alloys. (76). A. G. Atkins, D. Taber. (77). Hardness by method of mutual indentation. (78). To. (79). B. D. Kester, L. F. Moak. (80). Hardness, by indentation of pyramids of Vickers and Knoop from diamond, carbide of boron and carbide of tantalum. (81). Vacuum or inert gas. (82). Borides, oxides, carbides. (83). it is more frequent.

Page 153.

Procedure and settings up for the hardness test of materials at temperatures to 3000°C.

Up to present time the temperature of the tests of hardness reached only 1900°C [110, 114]. Therefore for studying the hardness of materials at temperatures to 3000°C, it was necessary to design settings up and to develop the procedures which would make it possible substantial to increase measuring temperature.

For the hardness test of high-melting materials at high temperatures, we utilized a method of the static indentation of

indentor in the form of correct tetrahedral pyramid with the angle of 136 deg. between opposite faces (according to GOST 2999-59) at temperatures of 20-2000°C and a method of one-sided solidification of conical specimen/samples with the angle of 120 deg. at apex/vertex, which proved to be convenient for even higher temperatures (to 3000°C).

Hardness number according to the method of the static indentation of pyramidal indentor (according to GOST 2999-59) is defined as mean pressure, MN/m² (kg/mm²), over area of indentation from the formula

$$HV = \frac{P}{F} = \frac{2P \sin \gamma}{\pi I^2} = 1,8544 \frac{P}{I^2} \text{ MN/m}^2 \text{ (kg/mm}^2\text{)} \quad (4.1)$$

where P - load on specimen/sample, transferred through the pyramidal indentor, Mn (kgf);

I - surface area of pyramidal impression, m² (mm²):

2γ - angle between the opposite faces of pyramid (136 deg.);

I - arithmetic mean of the lengths of two diagonals of impression, m (mm).

Impressions with the indentation of pyramid are geometrically similar; therefore during the measurement of hardness by this method are observed the conditions of mechanical similarity and test results do not depend on the value of load P .

Experimental data confirm that the hardness according to the method of implementing the pyramid does not depend on load with $P > 10$ N (1 kgf).

In accordance with the most widely used procedures of the study of high-temperature hardness and so that the obtained results it would be possible to compare with experimental data other authors, the load on specimen/sample, transferred through the pyramid, was accepted equal to 9.81 N (1 kgf), the time of holding of specimen/sample under load - 1 min, the time of holding of specimen/sample at the assigned/prescribed temperature before making the first impression - 3-5 min.

Page 154.

For testing of the correctness of the selection of the duration of loading, were carried out the tests of tungsten of the mark/brand of VRN and molybdenum of the mark/brand of MBN in the work-hardened state. The hardness are measured during the setting up of UVT by the method of the static indentation of pyramidal sapphire tip with 20 degrees, 940, 1310 and 1600°C and the holding of specimen/sample under load 10, 20, 30 s and 1, 2, 3, 5, 10 min. Load on specimen/sample in all cases is 9.81 N (1 kgf).

Test results are represented in Fig. 116 and 117. They attest to the fact that a sharp incidence/drop in the hardness proceeds with an increase in the time of loading from 10 to 30 s, moreover with the increase of temperature the absolute value of a reduction in the hardness is decreased. At 1600°C occurs the insignificant smooth decrease of hardness with the increase of the holding time under load.

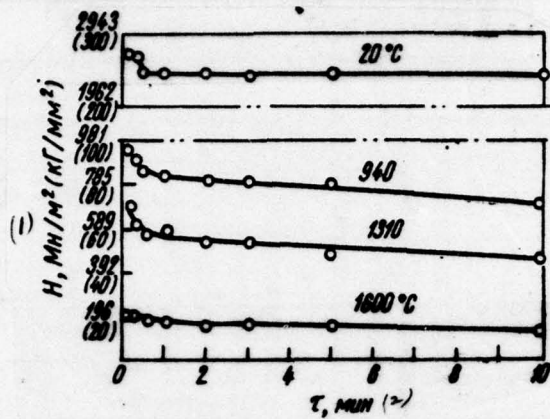


Fig. 116. Dependence of the hardness of molybdenum on the time of loading at different temperatures.

Key: (1). H, MN/m² (kg/mm²). (2) min.

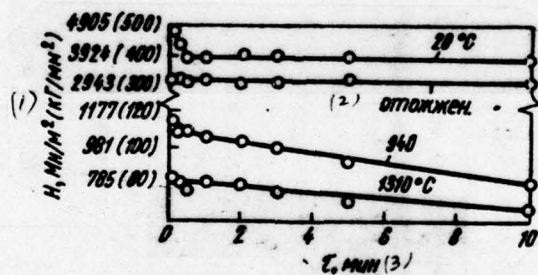


Fig. 117. Dependence of the hardness of tungsten on the time of loading at different temperatures.

Key: (1). H, MN/m² (kg/mm²). (2) it is annealed. (3) min.

With the subsequent increase in the duration of load from 30 s to 10 min, the hardness decreases monotonically for all temperatures.

Thus, the holding time under load must be selected taking into account the speed of the softening of the metal being investigated at testing temperature.

Are valid the propositions of a number of the authors [115, 116] about the need for the standardization of the duration of loading. It is obvious, standard time of holding must correspond to the monotonic segment of a curve of the time/temporary dependence of hardness at mean temperatures of this material testing. To this condition corresponds well temperature of 1600°C (average for interval of 20-3000°C) and the duration of loading 1 min.

As can be seen from Table 17, this duration of loading accept many researchers.

For explaining the effect of the value of load on hardness, are carried out the tests of the work-hardened molybdenum with 20 degrees and 1600°C and loads 1.962; 4.905; 6.867; 9.81; 14.715, 19.62; 29.43; 49.05 and 98.1 N (0.2; 0.5; 0.7; 1.0; 1.5; 2.0; 3.0; 5.0 and 10 kgf) (Fig. 118 and 119). The duration of loading is 1 min.

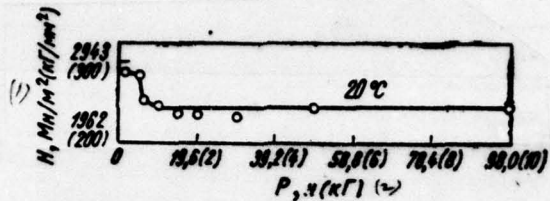


Fig. 118. Dependence of the hardness of molybdenum on the value of load with 20°C.

Key: (1). H, MN/m² (kg/mm²). (2). P, N (kgf).

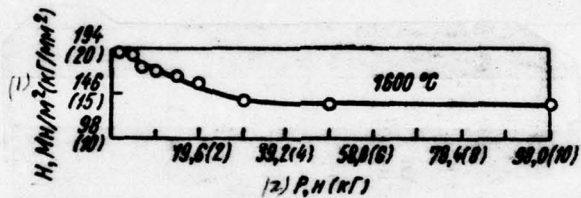


Fig. 119. Dependence of the hardness of molybdenum on the value of load with 1600°C.

Key: (1). H, MN/m² (kg/mm²). (2). P, N (kgf).

Page 156.

As already mentioned, according to many experimental data, the hardness according to the method of static indentation (indentor in the form of cone or standard pyramid) does not depend on load with $P > 9.81 \text{ N}$ (1 kgf) (macrohardness). However, during the measurements of the microhardness [$P < 9.81 \text{ N}$ (1 kgf)] were revealed deviations

from the law of similarity both to the side of increase and to the side of a reduction in the microhardness with the decrease of load [117].

Conducted investigations do not give single-valued answer/response to a question concerning how influences load on the value of microhardness; therefore, until now, there is no satisfactory explanation to dependence of microhardness on the value of load [120-126].

Data our experiments (see Fig. 118) attest to the fact that the hardness of the work-hardened molybdenum at room temperature with the decrease of load from 98.1 to 9.81 N (from 10 to 1 kgf) does not depend on the value of load. During further decrease of load from 9.81 to 1.962 N (from 1 to 0.2 kgf) the hardness grows/rises. In accordance with Fig. 118 transition from the range of macrohardness into the range of microhardness occurs with load, somewhat smaller 6.867 N (0.7 kgf).

It is interesting to trace, where is misaligned this transition at high temperatures. At 1600°C is observed its displacement to the side of higher loads - transition begins with $P \approx 29.43$ N (3 kgf) (see Fig. 119), during further decrease of load hardness smoothly grows/rises.

From given data it follows that for the observance of similarity conditions during the measurement of hardness at high temperatures it is expedient to increase loads on indentor.

Before the deposition of impression specimen/sample and the indentor was placed at a distance ~1-2 mm one from another are heated to identical radiation temperature from tape/strip tungsten heater. Thus, the maximum temperature of testing depends on the material of tip.

As the tip of indentor for the measurements of hardness at temperatures higher than 1100°C, utilize single crystals of synthetic corundum (sapphire Al_2O_3). I establish/installled that the sapphire tip works well to 1760°C, but already at somewhat higher temperature (~1800°C) occurs the flattening of tip.

The utilization of a method of static indentation for measuring of hardness at temperatures higher than 1760°C will require the search of new solid high-melting materials for manufacturing the indentor. The results of the specially conducted investigations will show that for the tests of the hardness of high-melting carbides at temperatures to 2000°C it is possible to utilize indentors from

carbide of boron B₄C, and also a number of other carbides [121, 122] and of alloys on their basis.

With an increase in the temperature, sharply grows/rises rate of evaporation of the materials of heater, specimen/sample, housing of indentor, heat shields.

Page 157.

For example, with an increase in the temperature from 1730 to 2530°C rate of evaporation of tungsten grows/rises 5,000,000 times (with $5.3 \cdot 10^{-8}$ to $2.7 \cdot 10^{-1}$ mg/cm²·h) [123]. Vaporization leads to the formation of the metallic film of condensate on the surface of indentor. This film introduces errors during the measurement of hardness and is caused the "grasping" of tip with specimen/sample.

Thus, temperatures on the order of 2000°C, apparently, are maximum ones for applying the method of static indentation. For the hardness test of materials at temperatures of 2000-3000°C, is necessary fundamentally different method of its measurement. It was established/installation that most satisfactory results gives application/use of a method of the one-sided flattening of conical specimen/samples, developed in the institute of the problems of the strength of AS UkrSSR.

However, the method of the static indentation of indentor possesses high accuracy/precision, productivity and requires the small consumption of material. For example, for obtaining the temperature dependence of the hardness of high-melting material in interval of 20-2000°C during the deposition of three impressions through every 100 deg is sufficient to have only one specimen/sample 8 mm in diameter 5 mm in high; the duration of this testing during our setting up of UVT composes not more than 6 h.

Therefore for measuring the hardness of high-melting materials in the range of temperatures of 20-3000°C, is recommended the combining of both of methods: static indentation - at 20-2000°C and one-sided flattening - at 1750-3000°C.

For hardness test from the method of static indentation, utilize the specimen/sample, having the form of cylinder 8 mm in diameter 5-7 mm in high, one of end/faces of which for testing according to the method of one-sided flattening additionally come with apex angle 120 deg. (Fig. 120).

For hardness test from the method of one-sided flattening at the elevated temperatures in the literature [18, 115, 124] usually is

given the schematic of testing (Fig. 121), which has a number of deficiencies and, obviously, is not suitable for high temperatures. First, specimen/sample has comparatively intricate shape and it is technologically difficult to manufacture from brittle material. In the second place, the tightly attached specimen/sample after heating to considerable temperature it is very difficult to recover from holder. During the utilization of the schematic indicated the testing unit will be unproductive, since it is not possible to design simple and reliable attachment for the exchange of specimen/samples directly in setting up.

In order to create simple, highly productive and convenient in work setting up, it will be necessary to change the schematic of testing.

Page 158.

The new schematic of testing (Fig. 122) does not have the enumerated deficiencies and it makes it possible to increase the temperature of hardness tests from 1850 to 3000°C.

Hardness number according to the method of the one-sided flattening of conical samples they determine as mean pressure over the area of indentation of the flattening:

$$H_c = \frac{P}{F} = \frac{4P}{\pi d^2} = 1,2732 \frac{P}{d^2}, \text{ MN/m}^2 \text{ (kg/mm}^2\text{)}, \quad (4.2)$$

where P - the load on specimen/sample, transferred by punch/male die, MN (kgf); F - surface area of the impression, which is generated as a result of the flattening of the conical apex/vertex of specimen/sample, m^2 (mm^2); d - the mean diameter of impression, m (mm).

Load on specimen/sample, P , transferred by punch/male die, are accepted equal to 49.05 N (5 kgf), the holding of specimen/samples under load 1 min.

Mellok [124, 127] established that the hardness, measured according to the method of one-sided flattening, with $P=4.905-49.05$ N (0.5-5 kgf) does not depend on load.

In the process of heating specimen/sample and punch/male die between them, also establish/install distance by 1-2 mm, which makes it possible to heat them to identical temperature.

For the hardness test of tungsten as the material of punch/male die, are applied carbides of tantalum and zirconium, and also alloy

of carbides of hafnium and tantalum in relationship/ratio 1:4. For the hardness test of molybdenum and niobium the punch/male die is prepared from tungsten. Figures 123 shows indentor (1) and two forms of punch/male dies with flat/plane polished end/face (2, 3). High-melting carbide compound in the form of small cylinders 8 mm in diameter and $\frac{16}{12-26}$ mm in high is fastened to tungsten holder with the aid of tungsten insert (3).

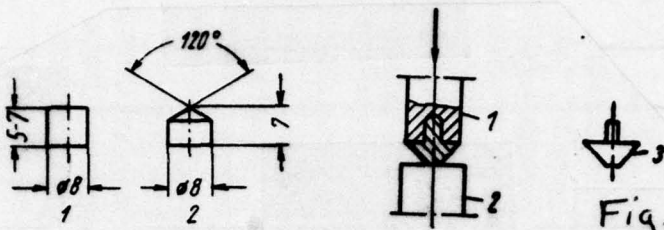


Fig. 121.

Fig. 120. Specimen/samples for testing the hardness: 1 - according to the method of the static indentation of indentcr; 2 - according to the method of one-sided flattening.

Fig. 121. The schematic of hardness test by the method of the one-sided flattening: 1 - punch/male die; 2 - anvil; 3 - specimen/sample.

Page 159.

The comparison of the data on the hardness of tungsten, molybdenum and niobium (tables 18) shows that at the high temperatures tungsten is approximately 3 times harder than the molybdenum and considerably harder than the niobium. Therefore tungsten can be utilized for manufacturing the punch/male dies during testing of molybdenum and niobium.

Figures 124 gives measurement data of the hardness of tungsten and molybdenum according to two methods. Each value of hardness,

DOC = 78133006

PAGE ~~13~~ 318

obtained with static indentation, presents average six - nine
measurements in three specimen/samples, but with one-sided flattening
- average two-three measurements.

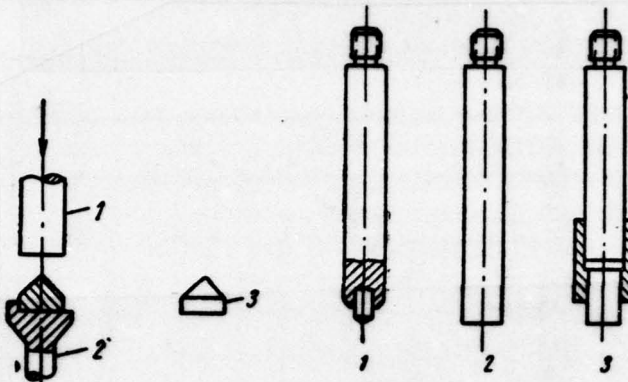


Fig. 123.

Fig. 122. The new schematic of testing conical specimen/samples according to the method of the one-sided flattening: 1 - punch/male die; 2 - stand; 3 - specimen/sample.

Fig. 123. Indentor (1) and two forms of punch/male dies (2, 3) used.

Tables 18. Hardness of some refractory metals at high temperatures.

(1) Температура, °C	(2) Твердость, MN/m ² (kg/mm ²)		
	(3) титан	(4) молибден	(5) ниобий
1560	525 (53,5)	172 (17,6)	102 (10,4)
1750	410 (41,8)	126 (12,9)	50,0 (5,1)
2000	167 (17,0)	65,7 (6,7)	10,8 (1,1)
2500	71,6 (7,3)	22,5 (2,3)	—
3000	46,1 (4,7)	—	—

Key: (1). Temperature, °C. (2). Hardness, MN/m² (kg/mm²). (3) tungsten. (4) molybdenum. (5) niobium.

The results of measuring the hardness via one-sided flattening and static indentation coincide well (Fig. 124). Let us try to explain how caused the coincidence of test results according to both methods.

Usually static hardness they characterize by the ratio of vertical load to the surface area of impression. Another method, proposed by Meyer, but those not obtained wide acceptance, is the calculation of hardness according to the projected area of impression. This hardness calls hardness according to Meyer and designate HM.

For tips in the form of the regular pyramid or cone with any apex angle, average contact pressure or, in other words, mean pressure on the lateral surface of the extruded by them impression is equal to hardness according to Meyer, i.e., to the ratio of vertical force to the projected area of impression.

Thus, hardness during its computation using Meyer's method acquires the physical sense of average contact pressure. The values of vickers hardness (HV) and according to Brinell (HB), the computed by surface area of impression, do not have physical sense [99, 118].

The fact that the hardness test according to Vickers and Brinell

will receive wide distribution, apparently, it is explained by the inadequacy of the theoretical substantiation of the methods of measuring the hardness accepted. For example, there is no full/total/complete solving of the problem of precise distribution of stresses and strains around the impressions of different forms. Furthermore, during the calculation of hardness is not considered the effect of the bulge of the surface of specimen/sample in the zone of impression.

It is possible to show that between the values of Vickers hardness and according to Meyer there is a relationship/ratio, which for the case of tip in the form of correct tetrahedral pyramid with the angle between opposite faces 136 deg. keeps the form

$$HV = HM \sin \frac{136^\circ}{2} = 0.9272HM. \quad (4.3)$$

Let us examine the effect of the bulge of the surface of specimen/sample in the zone of impression. This phenomenon is unavoidable, so it is possible to count that during plastic deformation the volume of material is not virtually changed. Strictly speaking, assertion about the invariability of volume is correct with high degree of approximation.

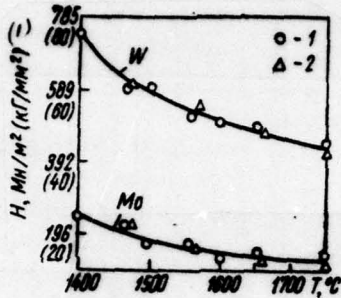


Fig. 124. Comparison of the temperature dependences of the hardness of tungsten and molybdenum, obtained by the methods of the static indentation of indentor (1) and of one-sided flattening (2).

Key: (1). H , MN/m^2 (kg/mm^2).

Page 161.

Usually during plastic deformation material density first increases, and then with an increase in the degree of deformation, it falls. A reduction in the density to 0.5% they observe after rolling with reduction 90%. [128].

Khedou and Johnson [131] based on the example of the indentation of pyramid they theoretically showed that the account of bulge noticeably decreases the value of hardness. For the hardness, calculated according to Meyer taking into account (HM_{corr}) and without taking into account of bulge (HM), is correct the relationship/ratio

$$HM_{\text{corr}} = 0.9428HM. \quad (4.4)$$

With the indentation of pyramid the material of specimen/sample is swelled upward along the faces of pyramid. Maximum bulge occurs near the middle of the sides of impression. Unlike the method of the indentation of the ball/sphere when bulge increases the diameter of impression and therefore to a certain extent it is considered during the routine calculation of hardness, during indentation test of pyramid the size/dimensions of the diagonals of impression are not virtually changed and, therefore, the existing methods of calculation of hardness Vickers and Meyer bulge are not completely considered. Calculation shows that the hardness according to Meyer, calculated with the aid of formulas (4.3) and (4.4) upon consideration of the effect of bulge with accuracy/precision 1.6c/c is equal to the value of vickers hardness, i.e.

$$HV = HM_{\text{av}}. \quad (4.5)$$

Thus, it is turned out that taking into account bulge the vickers hardness acquires the sense of average contact pressure. Therefore formula (4.1) for computing the vickers hardness can be recorded as follows [119]:

$$HV = 1.8544 \frac{P}{b^2} = 0.9272 \frac{2P}{b^2} = 0.9272HM = KHM. \quad (4.6)$$

where K - the coefficient, which considers the bulge and other phenomena (for example, friction), also, in the first approximation, equal to 0.9272.

During hardness test from the method of one-sided flattening, are measured the diameters of impressions with the full/total/complete account of bulge and the hardness it also acquires the physical sense of average contact pressure.

Consequently, the coincidence of the results of the test of hardness by the methods of indentation and one-sided flattening (see Fig. 124) is explained by the fact that in both cases was determined one and the same physical characteristic of material, not depending on the method of testing.

For studying the hardness of materials at high temperatures we have created two special settings tp: UVT [130]¹. and UVT-2 [152; 30, s. 7]².

FOOTNOTE 1. V. A. Borisenko. Author's Certificate No 161135. Bulletin of inventions and trade marks. 1964, No 4, p 47.

2. V. A. Borisenko. Author's Certificate No 179973. Inventions, specimen/samples and brands, 1966, No 6, p 45. ENDFOOTNOTE.

In the setting up of UVT, the hardness is measured in inert medium, while into UVT-2 - both in the inert medium and in vacuum. (There is an automated version of last/latter setting up - (UVT-2M).

Settings up are intended for the analysis of the hardness of materials in the range of temperatures of 20-3000°C by both methods (intervals of the application/use of each of the methods will be shown earlier).

For the protection of specimen/samples and heater from oxidation in the setting up of UVT, are utilized the purified inert gases (argon, helium) with overpressure 20 kN/m² (0.196 bar), which makes it possible to decrease (in comparison with high vacuum) the intense vaporization of the materials of the specimen/sample, heater and other parts. In installations UVT-2 and UVT-2M the hardness is measured in vacuum and medium of inert gases with overpressure to 78 kN/m² (0.78 bar).

As the material of radiation heater, was selected the tungsten. Was made the heater of special form (Fig. 125) without grooves and holes. The selection of this construction/design will ensure the stable operation of heater at temperatures, close to melting point of

tungsten; the reliability of electrical contact and fastening heater to current supplies; reducing to the minimum of the thermal stresses in heater; the possibility of the pyrometric check of the temperature of specimen/sample, indentor and heater, and also the reliable thermal screening of heater.

General view and the technical characteristic of the setting up of UVT are given respectively to Fig. 126 and into tables 19. The block diagram of the setting up of UVT is given to Fig. 127.

Tool for measuring the hardness is basic part of the setting up of UVT. Its schematic diagram is given to Fig. 128. Tool is placed into the steel water-cooled vacuum camera/chamber with double walls, which after pumping out preliminary pump of the type RVN-20 (through branch 9) is filled with the purified inert gas to the required overpressure. The camera/chamber consists of housing 2 and basis/base 1. In it are mounted basic nodes - system of heating, system of indentor, device of supply/feed and loading of specimen/samples, calibrating load, etc.



Fig. 125. Heater in settings up for hardness test.

DOC = 78133006

PAGE 23 329

Page 162

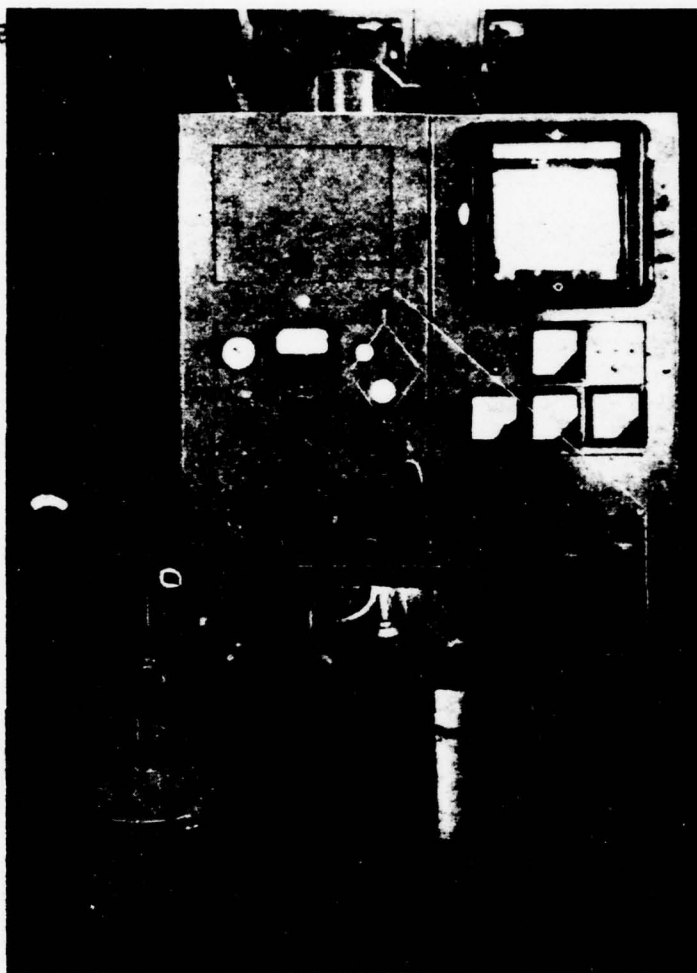


Fig. 126. The general view cf the setting up of UVT for hardness test
in inert medium in the range of temperatures cf 20-3000°C.

Page 164.

Heating system includes strip heater by 10, manufactured from

tungsten tin 0.3-0.5 mm in thickness, two copper water-cooled current conductor 4 with wedge clamps for fastening heaters and two piles of heat shields - vertical and horizontal - from tungsten molybdenum and nickel tin.

As already mentioned, heating specimen/samples is manufactured caused by emission/radiation from the strip heater of the special construction/design (see Fig. 125) in bore 20 mm diameter and 40 mm in height, manufactured from laminated tungsten 0.3-0.5 mm in thickness.

Tables 19. Technical characteristic of the setting up of UVT for the hardness test of materials in neutral media in the range of temperatures of 20-3000°C.

(1) Наименование параметров	(2) Технические данные
(3) Рабочий диапазон температур испытаний: а) по методу статического вдавливания стандартного пирамидального индентора б) по методу одностороннего сплющивания конического образца	20-2000°C До 3000°C
Измерение температур (4)	Термопарами и пирометрами
Регулирование и запись температуры (5)	Автоматическим потенциометром ЭПП-09
Рабочая среда: (6) инертные газы (аргон, гелий) с избыточным давлением	(14) 0,2 кГ/см ²
Рабочий диапазон нагрузок (7) Применимые выдержки под нагрузкой (8)	1,96-98,1 кН (0,2-10,0 кГ) От 10 сек до 1 ч (обычно 60 сек)
Размеры образцов: диаметр×высота (9) Регулировка величины смещения индентора (10)	8×(5+7) мм Главная, от 0 до 5 мм
Максимальное количество отпечатков, наносимое: а) на образце диаметром 8 мм б) по одной окружности	(21) Свыше 100 30 20×40 мм
Размеры вольфрамового нагревателя: внутренний диаметр×высота (11)	
Основное трансформаторное оборудование: (20) автотрансформатор силовой трансформатор	РНО-250-10 ОСУ-20/6
Вакуумное оборудование: (22) форвакуумный насос	PBN-20
Габаритные размеры установки: длина×ширина×высота (23)	1500×1160×2900 мм

Key: (1). Designation of the parameters. (2). Technical specifications. (3). Working temperature range of tests: a) according to method of static indentation of standard pyramidal indentor; b) according to method of one-sided flattening of conical specimen/sample. (4). To. (5). Measurement of temperatures. (6).

Regulating and recording of temperature. (7). Working medium: inert gases (argon, helium) with overpressure. (8). Operating range of loads. (9). Holding used under load. (10). Size/dimensions of specimen/samples: diameter x height. (11). Control of amount of displacement of indentor. (12). By thermocouples and pyrometers. (13). By self-balancing potentiometer of EPE-09. (14) kgf/cm². (15) 1.96-98.1 N (0.2-10.0 kgf). (16). From 10 s to 1 h (usually 60 s). (17). Smooth, from 0 to 5 mm. (18). Maximum quantity of impressions, applied: a) in specimen/sample 8 mm in diameter; b) in one circumference. (19). Size/dimensions of tungsten heater: bore diameter x height. (20). Basic transformer equipment: autotransformer; power transformer. ^{(21), Greater than,} (22). Vacuum equipment: fore pump. (23). Overall dimensions of setting up: length x width x height.

Page 165.

Entire cycle of manufacture and exchange of this heater occupies not more than 10 min.

Test specimen is established/installed in the camera/chamber in stand 13. Thermocouple 16 passes through drilling in stand and it concerns the basis/base of specimen/sample. With thermocouples 14 it is possible to measure the temperature of heater in two points. With

the aid of pyrometer the temperature of specimen/sample, indentor, table and heater is measured through window 3 with quartz glass.

The system of indentor consists of built in into mandrel/mount indentor 5, the holder of indentor 6 with the bellows seal, device for the control of the displacement of indentor and loading device. As the tip of indentor, utilize single crystals of artificial sapphire or the carbide insets (see pg. 158), built in into mandrel/mounts from pure molybdenum.

During testing according to the method of static indentation the axle/axis of the node of indentor they misalign relative to the axle/axis of specimen/sample, which allows via the rotation of specimen/sample around axle/axis after each implementation of indentor to apply to the surface of specimen/sample in circumference to 30 impressions.

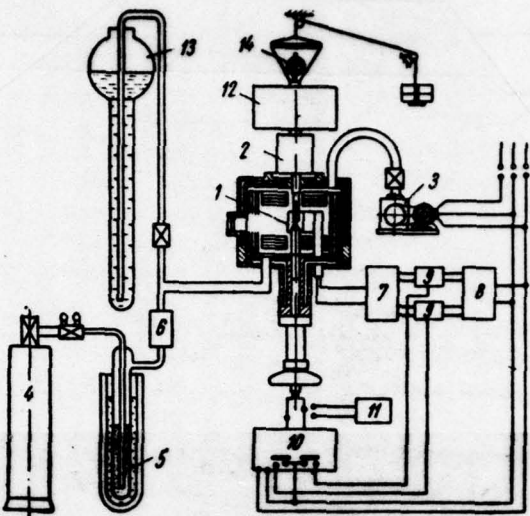


Fig. 127. The block diagram of the setting up of UVT: 1 - specimen/sample; 2 - tool of the measurement of hardness; 3 - fore pump RVN-20; 4 - cylinder of inert gas; 5 - purifier of inert gas; 6 - filters; 7 - single-phase transformer OSU-20/6; 8 - autotransformer RNO-250-10; 9 - contactors; 10 - electronic potentiometer EPP-09; 11 - control potentiometer; 12 - batch of loads; 13 - manostat; 14 - indicator.

Page 166.

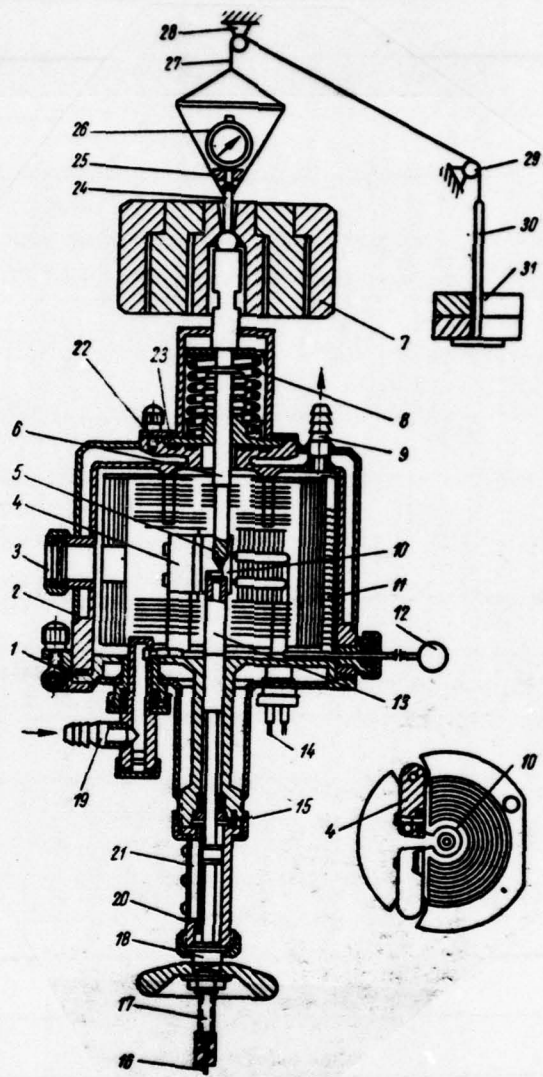


Fig. 128. Schematic of tool for measuring the hardness in the setting up of UVT.

Page 167.

The device of the displacement of the indentor includes disk by 23 with eccentric hole, to which is mounted the system of indentor and loads. Disk is placed into the circular deepening of housing 2 which is misaligned relative to the axle/axis of the camera/chamber and specimen/sample. Through invoice ring 22, disk is pressed against housing. (Circular sealing gaskets between disk and housing make it possible to change the amount of the displacement of indentor without stopping of the process of testing.).

The loading device consists of the batch of removable loads 7, which lean on ball bearing, and interchangeable gauged springs 8, which ensure the smooth loading of specimen/sample. The first load creates on indentor load into 9.81 N (1 kgf), and the second and the third (in sum with preceding/previous) - with respect 49.05 and 98.1 N (5 and 10 kgf).

The device of supply/feed and loading of specimen/sample consists of stand by 13, manufactured from tungsten or molybdenum, actuating screw 17, nut 18 and the insert of divider/denominator 20 with feather key 21. This device makes it possible to supply specimen/sample from the level of the upper area/site of the basis/base of the camera/chamber into heater, after heating to the

assigned/prescribed temperature to manufacture the loading of specimen/sample, to rotate specimen/sample for depositing on it the impressions in several circumferences, to derive/conclude specimen/sample made of furnace and to establish/install new specimen/sample.

At the work of setting up mancstat maintains in the camera/chamber of tool the constant overpressure inert gas which through the bellows seal is transferred to load system and therefore the latter must be calibrated. For this purpose through the hole in pin 24, which it passes through ball bearing and is rigidly connected with indentor, is passed caprone filament by 27. It is thrown through two block 28 and 29 on ball bearings and is attached to plate by 30, to which it is possible to place calibration loads 31. Above pin 24 on bracket 25, is placed the dial indicator 26 with scale value 0.002 mm.

The calibration system of load device makes it possible to establish/install and to check with high accuracy/precision any load [within the limits of 1.962-98.1 N (0.2-10 kgf)] which is applied to specimen/sample for depositing the impression. In this case, are considered all losses to friction in guides and in the bellows seal and their change during heating of the camera/chamber.

After the deposition of next impressions according to the method of static indentation, they turn actuating screw by 17 for the insert of divider/denominator 20 with feather key 21 in the new position (on $11^{\circ}50'$), determined by ball bearing clamping fixture 15, and is repeated the process of loading. If the circumference of specimen/sample, they will apply 30 impressions at different temperatures.

Page 168.

If it is necessary to apply to specimen/sample a larger quantity of impressions, with the aid of device for displacing the indentor, is establishinstalled its new position. To specimen/sample it is possible to apply additional impressions in several circumferences whose radii correspond to the values of the displacement of indentor. If impressions is placed at a distance 0.5 mm are from another [107], then to specimen/sample 8 mm in diameter it is possible to apply more than 100 impressions.

For testing the conical specimen/samples by the method of one-sided flattening according to the schematic, presented in Fig. 122, indentor with tip they replace by punch/male die with flat/plane end. The system of the control of the displacement of indentor is establishinstalled in the zero position, by which there is no

displacement of the axle/axis of indentor relative to the axle/axis of specimen/sample.

After testing specimen/sample by lowering of actuating screw they derive/conclude from furnace to the level of the upper area/site of basis/base and by pusher 12 they move into hopper 19. After this the process is repeated: they supply by pusher new specimen/sample made of magazine 11 to stand 13.

The device of the filling of the camera/chamber with inert gas carried out together with the valve of hopper 19 makes it possible to recover the tested specimen/samples without stopping of testing.

Setting up is equipped by the purifier, in which inert gas is passed through the activated carbon, cooled to the temperature of liquid nitrogen.

The constant overpressure inert gas in the working chamber of the tool of the measurement of hardness, created by manostat, makes it possible to retain the constancy of load in the process of testing. In the absence of manostat as a result of the increase of the temperature in the camera/chamber, will be heated inert gas and grow/rise its pressure (camera/chamber of vacuum is consolidated), which will lead to the decrease of load on specimen/sample.

Many high-melting alloys are intended for a work in vacuum. The maximum approach/approximation of test conditions to operating conditions requires the hardness test of these alloys in vacuum in the range of temperatures of 20-2000°C and, sometimes, in interval of -196-3000°C.

Settings up UVT-2 and of UVT-2M, developed into IPP of AS USSR, are intended for measuring the hardness of high-melting materials in vacuum and in the medium of inert gases in the range of temperatures of 20-3000°C.

General view and the short technical characteristic of settings up are given respectively to Fig. 129 and into Tables 20.

In settings up UVT-2 and of UVT-2M, the measurement of hardness is manufactured by the same methods, also, in the same temperature ranges, as in the setting up of UV1.

For measuring the hardness at temperatures to -196°C in the stand of tool, are establishinstalled the puddle and the specimen/sample they are placed directly in cooling liquid. The tip of indentor also is lower/committed into the cooling fluid.

Page 169.

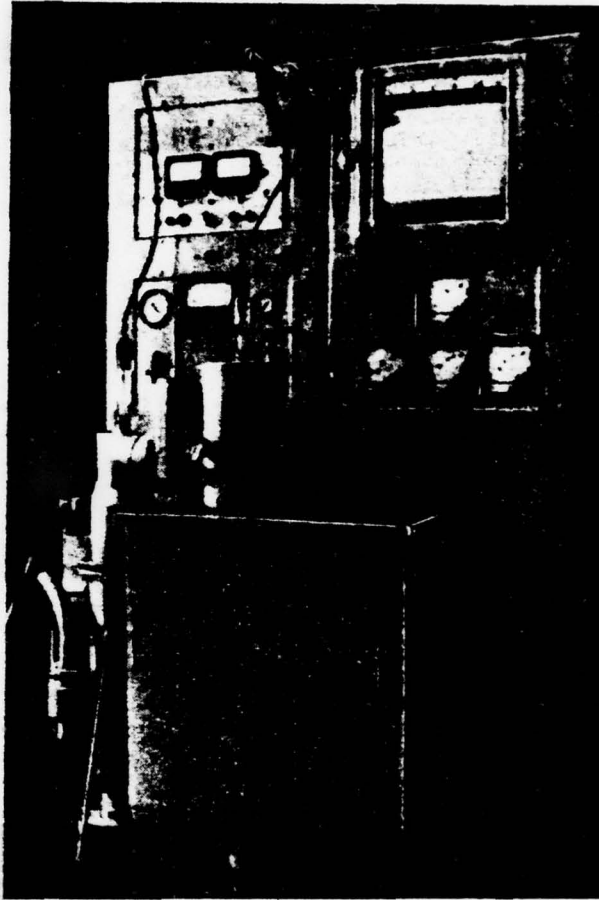


Fig. 129. The general view of setting up UVT-2 for hardness test in inert medium and vacuum at high temperatures.

Page 170.

The temperature of specimen/sample measures with the aid of thermocouples (chromel - Alumel, copper - constantan).

Setting up UVT-2 is characterized by from previously described setting up of UVT only possibility of work in vacuum.

Tool for measuring the hardness of setting up UVT-2 (Fig. 130) differs from a similar tool of the setting up of UVT in the fact that in the first the loading device is located within vacuum chamber and therefore manostat and the calibration system of load it is absent. More complex will become the control of the displacement of indentor with the aid of flexible shaft and gear drive.

Tables 20. Technical characteristic of the setting up of UVT-2M for the hardness test of materials in vacuum and neutral media in the range of temperatures of 20-3000°C.

(1) Назначение параметров	(2) Технические данные
(3) Рабочий диапазон температур испытаний: а) по методу статического вдавливания стандартного пирамидального индентора б) по методу одностороннего сплющивания конического образца Измерение температур 5	20-2000°C 4) До 3000°C
Регулирование и запись температуры 7	6 Термопарами и пирометрами ✓ Автоматическим потенциометром ЭПП-09
Рабочая среда: 9 а) вакуум б) среда инертных газов (аргона, гелия)	10) 1,33 мм/сек (1 · 10 ⁻⁵ мм рт. ст.) До 0,8 кГ/см ² (12) 4,905-9,81-49,05-98,1 кг (0,5-1,0-5,0-10,0 кГ) 8×(5+7) мм (16) Автоматическая, реле (18) времени 100
Рабочий диапазон нагрузок ступенями (11) Размеры образцов: диаметр×высота (13) Выдержка образца под нагрузкой (15) Максимальное количество отпечатков на плоском образце Максимальное количество образцов в магазине Расход воды (максимальный) (19a) (19) <	10 1,35 м ³ /ч (20)
Вакуумное оборудование: а) вакуумный агрегат б) форвакуумный насос	BA-05-1 PBH-20
Габаритные размеры установки: 621 длина×ширина×высота (23) Габаритные размеры дополнительного оборудования (насос PBH-20, баллон, автотрансформатор)	1530×1150×2250 мм 1500×500×1500 мм

Key: (1). Designation of the parameters. (2). Technical specifications. (3). Working temperature range cf tests: a) according to method of static indentation of standard pyramidal indentor; b) according to method of one-sided flattening of conical specimen/sample. (4). To. (5). Measurement of temperatures. (6). By

thermocouples and pyrometers. (7). Regulating and recording of temperature. (8). By self-balancing potentiometer of EPP-09. (9). Working medium: a) vacuum; b) medium of inert gases (argon, helium). (10) MN/m². (11). Operating range of loads by step/stages. (12). To 0.8 kgf/cm². (13). Size/dimensions of specimen/samples: diameter x height. (14) N. (15). Holding of specimen/sample under load. (16) kgf. (17). Maximum quantity of impressions on plane specimen/sample. (18). Automatic, time relay. (19). Maximum quantity of specimen/samples in magazine. (19a). Consumption of water (maximum). (20) m³/h. (21). Vacuum equipment: a) vacuum aggregate; b) fore pump. (22). Overall dimensions of setting up: length x ~~width~~^{width} x height. (23). Overall dimensions of accessories (pump RVN-20, cylinder, autotransformer).

DCC = 78133006

PAGE - 39 - 343

Page 171.

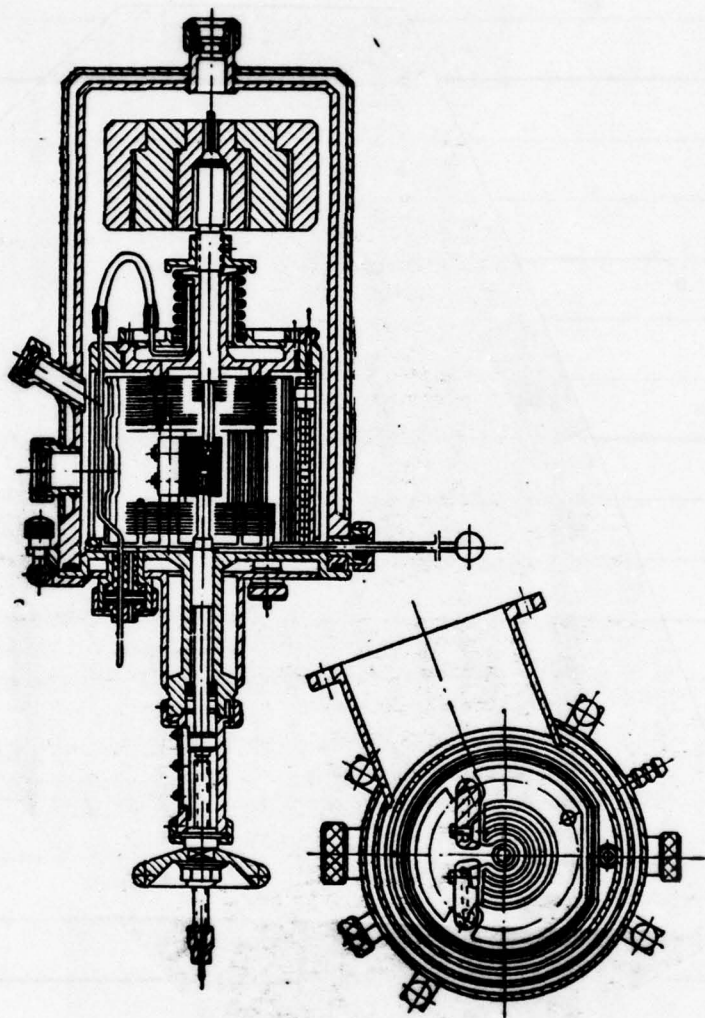


Fig. 130. Schematic of tool for measuring the hardness in setting up UVI-2.

Page 172.

The construction/design of the working chamber of the setting up of UVT-2M with the aid of special device provides the exchange of loads with the closed camera/chamber. Duration of the holding of specimen/sample under load is realized/accomplished by an adjustment of the special time relay. The lift of stand with specimen/sample can be manufactured by two speeds.

In the setting up of UVT-2M, the displacement of the axle/axis of indentor relative to the axle/axis of specimen/sample is established/installation on cam; therefore impressions will be applied on helix.

The temperature of specimen/samples at work during the settings up of UVT and UVT-2 in interval of 20-2000°C are measured with the aid of the thermocouples: platinum-rhodium-platinum (20-1600°C) and tungsten-rhenium VR5/20 (to 2000°C). Potentiometer EPP-09M1 provides recording and the automatic maintenance of the assigned/prescribed temperature with accuracy/precision $\pm 0.5^{\circ}\text{C}$. Furthermore, is provided for the possibility of the control of the measurements of the temperature of specimen/sample with the aid of galvanometer and the

movable potentiometer of the higher class of precision.

In installations of both of types the thermocouple (Fig. 128, 130), with the aid of which is measured and is regulated the temperature of specimen/sample, it passes through the hole in stand it touches the basis/base of specimen/sample. Thermoelectrodes are isolate/insulated from each other by ceramic tubes from Alundum, oxide of magnesium or carbonitride of boron, free ends are thermostatically controlled. In parallel is measured the temperature of specimen/sample, indentor, table and heater with the aid of the optical pyrometer of the type ОРРІР-09 and of color photoelectronic pyrometer ТСЕР-3.

During the tests of hardness in the range of temperatures of 2000-3000°C measurements of the temperature of specimen/sample are conducted with the aid of the optical pyrometer ОРРІР-017 and color photoelectronic pyrometer ^{ТСЕР} 3-3.

For the increase of the accuracy/precision of the measurement of high temperatures by pyrometers conduct the special calibrating:

- 1) through melting points of molybdenum and tantalum of high purity/finish;

2) through readings of the special calibration tungsten-rhenium thermocouple of VR5/20, which was graduated to temperature of 3000°C.

Specimen/samples for calibrating of pyrometers prepare the same size/dimensions and forms as for hardness test. At the apex/vertex of specimen/sample, is drilled cut the hole for the room of thermojunction. Specimen/sample was placed in stand 13 (see Fig. 128) together with the calibration thermocouple, sealed on top into hole and free from insulation/isolation on that section near the joint which was heated to the temperatures, exceeding 2000°C. The remaining sections of the electrodes of thermocouple insulate by ceramic tubes. Thus, hot end was shielded from emission/radiation by bore surfaces in specimen/sample.

Page 173.

During calibrating the specimen/sample is heated under the stepped conditions before melting. The real temperature of specimen/sample measures with the aid of thermocouple and control potentiometer; temperature brightness - by optical pyrometer OPPIR-017, color - with pyrometer IsFP-3.

A calibration thermocouple of the type VR5/20 was graduated on melting points of pure metals - nickel, platinum, chromium, vanadium, molybdenum and tantalum. Data, obtained during calibrating, attest to the fact that this thermocouple gives correct readings up to melting

point of tantalum of 3000° c only during the first heating. During subsequent heatings observe the deviations of readings of thermocouple from the calibration values thermo-emf.

Accuracy/precision of the hardness test of tungsten and molybdenum at high temperatures.

In the general case hardness H is the function of the applied load P , of the size/dimension of the obtained impression (diameter d or diagonal b), of the time of the application of load τ and of the absolute temperature of testing T :

$$H=f(P, b, \tau, T). \quad (4.7)$$

During the measurement of values P , b , τ and T are unavoidable the errors each of which gives the specific contribution to overall error for function H .

The hardness, determined on the method of the static indentation of standard tetrahedral pyramid at constant temperature T and the constant/invariable duration of loading τ , is connected with the value of load P and the size/dimension of the diagonal of impression b by the dependence

$$HV=\frac{2P_{\text{min}} \cdot \frac{136^{\circ}}{2}}{\mu^2}. \quad (4.8)$$

The hardness, determined according to the method of one-sided flattening, is connected with the value of load P and with a diameter

cf impression of d by dependence [133]

Page 173.

$$H_c = \frac{4P}{\pi d^2}. \quad (4.9)$$

The hardness of tungsten and molybdenum for the constant/invariable duration of loading τ depending on temperature is determined by expression [132, 133]

$$H = k_n H_0 e^{-\alpha_n T}, \quad (4.10)$$

and at the constant/invariable temperature T in dependence on the duration of loading τ - by expression [25, p. 121; 147]

$$H = a \tau^n, \quad (4.11)$$

where T - temperature, °K; H_0 - value of hardness with 0°K (it is obtained by the extrapolation of the low-temperature section of the curve of the dependence of hardness on temperature); $\alpha_n (\alpha_1, \alpha_2, \alpha_3)$ - temperature coefficients of hardness for different temperature ranges; $k_n (k_1, k_2, k_3)$ - constants for intervals indicated; a and n - constants, that depend on the nature of material.

If is substituted equations (4.8-4.11), into expression (4.7), then it will be obtained for two methods hardness test respectively:

$$HV = f \left(\frac{2P \sin 68^\circ}{b^2}, k_n H_0 e^{-\alpha_n T}, a \tau^n \right), \quad (4.12)$$

$$H_c = f \left(\frac{4P}{\pi d^2}, k_n H_0 e^{-\alpha_n T}, a \tau^n \right). \quad (4.13)$$

Known [144] that the maximum relative error for the function of

several independent variables is equal to the differential natural logarithm of this function:

$$\delta_H = \pm d[\ln f(P, b, T, \tau)], \quad (4.14)$$

moreover all terms in expression (4.14) are undertaken in the absolute value:

$$\delta_H = \pm \left(\frac{dP}{P} + 2 \frac{db}{b} + a_n dT + n \frac{d\tau}{\tau} \right). \quad (4.15)$$

After designating absolute errors ϵ (for relative errors is already selected designation δ), we will obtain the resultant expression for computing the maximum relative error in determination of the hardness:

$$\delta_H = \pm (\delta_P + 2\delta_b + a_n \epsilon_T + n\delta_\tau), \quad (4.16)$$

where $\delta_P = \frac{dP}{P}$ — relative measuring error of load; $\delta_b = db/b$ or $d(d)/d$ — relative measuring error of the size/dimension of impression; ϵ_T — the absolute error for measurement at temperature T; a_n — temperature coefficient of hardness for the appropriate interval of measurement; δ_τ — relative measuring error of the duration of loading at temperature T; n — high-speed/velocity hardness number at temperature T.

Page 175.

The results of computing the maximum relative errors in determination of the hardness of tungsten and molybdenum are given into Tables 21 and 22. It turned out that the values of these errors

at high temperatures are sufficiently low and that the greatest contribution in δ_H gives the measuring error of temperature (at 2500-3000°C). With an increase in the accuracy of the measurement of temperature, sharply is increased the accuracy/precision of hardness test. For example, if is increased the accuracy of the measurement of the temperature by 0.5%, the maximum relative error in determination of the hardness of tungsten at 3000°C it decreases almost by 30%.

Investigation of the hardness of tungsten, molybdenum and tantalum in the range of temperatures of 20-3000°C.

The hardness of refractory metals was determined with the aid of settings up UVT and UVT-2 according to the procedure, presented in the preceding/previous paragraph (see pg. 153).

The specimen/samples (see Fig. 120) for hardness test from the method of static indentation, they turned from rod; on sample prepared metallographic section. For testing the hardness according to the method of one-sided flattening specimen/samples they sharpen to cone on lathe with the subsequent processing of cone on grinding machine. If necessary the specimen/samples subject to heat treatment in vacuum.

The determination of the temperature dependence of hardness is conducted for the specific and constant/invariable duration of loading and with the value of load, corresponding to similarity conditions.

Hardness of tungsten. Experience/test the specimen/samples, manufactured from the forged rods of cermet tungsten of the mark/brand of VRN in as-received condition. (Sintered molding/bars by section/cut 10x10x400 mm machine in rotary forging machines without intermediate annealing to diameter 10 mm - reduction ~1 mm; then manufacture forging in machines with 1450°C - reduction ~0.5-0.3 mm, heating in hydrogen electric furnaces).

The common/general/total impurity content in tungsten does not exceed 0.15%. In the sum of impurity/admixtures, enter molybdenum, one-and-one-half oxides, oxides of silicon and calcium in the following quantities (it is not more): 0.02% R_2O_3 ; 0.005% NI; 0.015% CaO; 0.01% SiO_2 ; 0.04% Mo.

[Page 176.] Table 21. Maximum relative errors in determination of the hardness of tungsten.

Tempera- ture, °C	$\pm \delta p$, %	$\pm 2\delta_b$, %	$\pm n\delta_t$, %	(2) Способ измерения температуры	$\pm \epsilon_T$		a_n , %	$\pm a_{n\delta T}$, %	$\pm \delta H$, %
					%	град			
940	0,25	1,00	0,14	(3) Термопара ПП + потенциометр ПП (4) Термопара ПП + потенциометр ЭПП-09 (3) Термопара ВР5/20 + (4) потенциометр ПП (3) Термопара ВР5/20 + + потенциометр(4) ЭПП-09	0,47	4,4		0,30	1,69
1600	0,25	1,00	—	(3) Термопара ПП + потенциометр ПП (4) Термопара ПП + потенциометр ЭПП-09 (3) Термопара (4) ВР5/20 + + потенциометр ПП (3) Термопара ВР5/20 + + потенциометр(4) ЭПП-09	0,45	7,2		1,36	2,60
2000	0,25	1,00	—	(3) Термопара (4) ВР5/20 + + потенциометр ПП (6) Пирометр ОППИР-09	0,70	11,2	0,1890	2,12	3,40
2500	0,25	1,00	—	(6) Пирометр ОППИР-017 (5) (специальная тарировка)	1,00	16,0		3,02	4,30
3000	0,25	1,00	—	(6) Пирометр ОППИР-017 (5) (специальная тарировка)	0,70	14,0	0,1890	2,65	3,90
					1,50	30,0		5,70	7,00
					1,00	25,0		4,70	6,00
					1,50	37,5	0,1890	7,10	8,30
					1,00	30,0		5,70	7,00
					1,50	45,0	0,1890	8,50	9,80

Key: (1). Temperature. (2). Method of measurement of temperature.

(3). Thermocouple. (4) potentiometer. (5) (special calibrating).

(6). Pyrometer.

Page 177.

Table 22. Maximum relative errors in determination of the hardness of molybdenum.

(1) Темпера- тура, °C	$\pm \delta_P$, %	$\pm 2\delta_B$, %	$\pm n\delta_T$, %	(2) Способ измерения температуры	$\pm \epsilon_T$,		α_H , %	$\pm \alpha_H \epsilon_T$, %	$\pm \delta_H$, %	
					%	град				
940	0,25	1,00	0,086	(3)	(4)	0,470	4,4	0,216	0,95	2,30
				Термопара ПП + потенциометр ПП		0,700	6,6		1,43	2,77
				Термопара ПП + потенциометр ЭПП-09		1,000	9,4		2,03	3,37
				Термопара ВР5/20 + потенциометр ПП		0,450	7,2		1,55	3,00
1600	0,25	1,00	0,152	Термопара ВР5/20 + потенциометр ЭПП-09	(4)	0,700	11,2	0,216	2,42	3,80
				Термопара ВР5/20 + потенциометр ПП		1,000	16,0		3,45	4,80
				Термопара ВР5/20 + потенциометр ЭПП-09		0,700	14,0		3,02	4,30
				Пирометр ОППИР-09		1,500	30,0		6,5	7,80
2000	0,25	1,00	—	(5) Пирометр ОППИР-017 (5) (специальная тарировка)	(4)	1,000	25,0	0,216	5,4	6,70
						1,500	37,5		8,1	9,40

Key: The same as for Table 21.

Page 178.

The values of hardness for the annealed tungsten are obtained during testing in the cycling process of samples from 1750°C down to room temperature.

The temperature dependences of the hardness of tungsten in the range of temperatures of 20-3000°C are represented in Fig. 131.

The hardness both of the deformed and annealed tungsten with the increase of temperature from 20 to 300°C sharply falls. With further increase of temperature (to 1100°C) the hardness gradually decreases; the difference in the hardness of those work-hardened and annealed samples decreases insignificantly.

At 1100-1200°C (range of temperatures of the beginning of recrystallization) the difference in the hardness of the work-hardened and annealed tungsten rapidly is decreased. Apparently, so on of 1600°C is completed the recrystallization of processing, since the curves are drawn off at the value of hardness ~500 MN/m² (51 kg/mm²). At 1740°C, i.e., with 0.55T_{nn} again is observed the noticeable incidence/drop in the hardness, which, apparently, is connected with a change in the mechanism of deformation, with further increase of temperature, the hardness smoothly is decreased, reaching the values of 167 MN/m² (17 kg/mm²) so on of 2000°C, 71.6 MN/m² (7.3 kg/mm²) at 2500°C and 46 MN/m² (4.7 kg/mm²) at 3000°C.

Hardness of molybdenum. Tests are subjected to the

specimen/samples, manufactured from the forged rods of the cermet molybdenum of the mark/brand of MRN in as-received condition. (Sintered molding/bars 15x15x500 mm machine to diameter 10 mm in rotary forging machines with 1350-1400°C; heating in hydrogen electric furnaces, reduction ~1 mm for transition. Then is manufactured forging in machines at temperatures to 1200-1000°C).

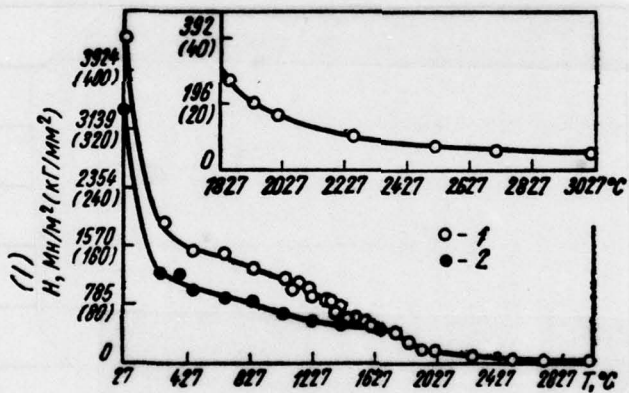


Fig. 131. The dependence of the hardness of tungsten on the temperature: 1 - work-hardened; 2 - annealed.

Key: (1) - H_v , MN/m² (kg/mm²).

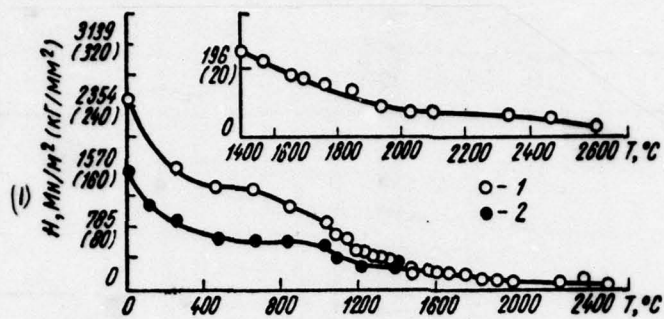


Fig. 132. The dependence of the hardness of molybdenum on the temperature: 1 - work-hardened; 2 - annealed.

Key: (1). $H, \text{MN/m}^2 (\text{kg/mm}^2)$.

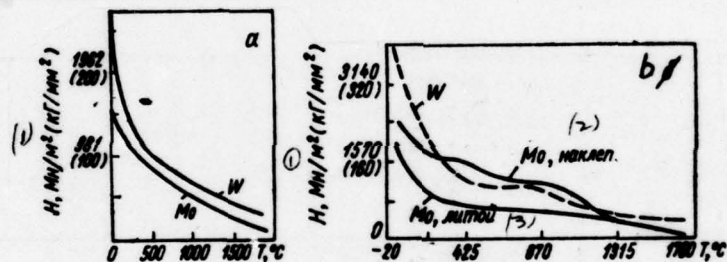


Fig. 133. The dependence of the hardness of tungsten and molybdenum on the temperature: a - on data [114]; b - on data [110].

Key: (1). $H, \text{MN/m}^2 (\text{kg/mm}^2)$. (2). peening. (3). poured.

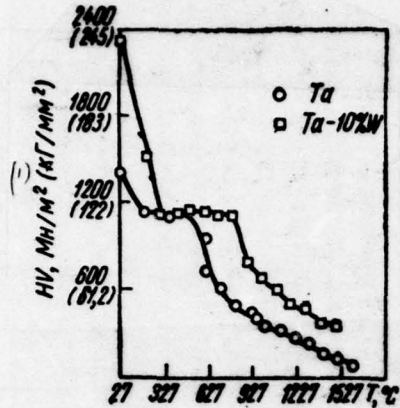


Fig. 134. Dependence of the hardness of tantalum and its alloy with tungsten on temperature.

Key: (1). HV, MN/mm² (kg/mm²).

Page 180.

The common/general/total impurity content does not exceed 0.10%. In the sum of impurity/admixtures, enter one-and-one-half oxides, nickel, oxides of silicon, calcium and magnesium in the following quantities (it is not more): 0.04c/c E_2O_3 , 0.02% Ni, 0.03% SiO_2 , 0.008% CaO+MgO.

The values of hardness for the annealed molybdenum are obtained during testing in the process of cooling samples from 1750°C to room.

The results of the investigation of the temperature dependence of the hardness of the deformed arc annealed molybdenum are represented in Fig. 132. Is observed a sharp incidence/drop in the hardness of molybdenum during heating from room temperature to 300°C, after which up to 1000°C hardness is decreased insignificantly, especially for the annealed material; with further increase of temperature to 1400°C, again occurs a noticeable incidence/drop in the hardness. The hardness of the deformed molybdenum at temperatures of 450-650°C twice exceeds the hardness of annealed molybdenum.

Higher than 1000°C begins the recrystallization of deformed molybdenum [134]. At 1400°C curves completely are drawn off at the value of hardness 240 MN/m² (24.5 kg/mm²).

In the course of further increase of temperature, the hardness smoothly is decreased, reaching the values of 66 MN/m² (6.7 kg/mm²) at 2000°C and 23 MN/m² (2.3 kg/mm²) at 2500°C.

For a comparison Fig. 133 gives the results of the hardness test of tungsten and molybdenum in the works Engl and Felmer [114] and Seachisen and Torgerson [110].

Hardness of tantalum. Investigation is carried out in the annealed specimen/samples made of the forged ingots of vacuum-arc

melting. Specimen/samples are annealed for 1 h in vacuum 1.33 MN/m^2 (10^{-5} mm Hg) at 1400°C . Experimental Data (Fig. 134) are obtained during testing in vacuum 1.33 MN/m^2 (10^{-5} mm Hg) during setting up UVT-2. The hardness of tantalum fusion with 10c/c W prove to be itself above the hardness of tantalum, beginning from 500°C in all investigated temperature interval (see Fig. 134).

Hardness of niobium and its alloys at temperatures of 20 - 2100°C .

Hardness of niobium. Are investigated the specimen/samples of cermet niobium, and also the poured niobium after single cathode-ray remelting and after vacuum-arc melting.

Cermet niobium (99.2c/c) contains the following impurity/admixtures: 0.25c/o Ta, 0.14c/o C, to 0.1c/o Ti, to 0.09c/o Si, 0.02c/o Fe.

Poured niobium after single cathode-ray remelting contains: 0.02c/o C, 0.01c/o N₂ and 0.001c/o O₂. (Gas analysis of cermet niobium carried out will not be).

Page 181.

Cermet niobium and by poured niobium after single cathode-ray

resolving they investigate during the setting up of UVT in the medium of the purified inert gases, the niobium of vacuum-arc melting is experience/tested during setting up UVT-2 in vacuum.

For measuring the hardness of niobium according to the method of one-sided flattening the punch/male die is prepared from tungsten.

The temperature dependences of the hardness of niobium are given to Fig. 135. Each point on graph corresponds to the average value of 9-15 measurements.

The analysis of test results will show that the cermet niobium is very contaminated. In the specimen/samples which experience/test in the range of temperatures of 20-1760°C, the impressions, plotted/applied at temperatures of 20-1500°C, partially disappear, apparently, as a result of the recrystallization of the deformed volume of metal and sealing off of impressions by the low-melting impurity/admixtures, which were being contained in niobium. During testing of cathode-ray niobium the disappearance of impressions they observe more rarely. Let us note that, accordingly [89, 135], the temperatures of the solidification of niobium fusions with by hydrogen, iron, oxygen, silicon and titanium are located in interval of 1300-1720°C.

After testing in different inert media, the mirror section of the specimen/samples of cermet and cathode-ray niobium of both of forms becomes matte. During specimen/sample testing of tungsten and molybdenum under the same conditions, mirror section on the surface of specimen/sample completely is retained. Section is retained also during specimen/sample testing of vacuum-arc niobium in vacuum.

In many instances on the surface of the specimen/samples of cermet niobium after testing of hardness with 1500-1760°C, observe the cracks on the perimeter of impressions.

362

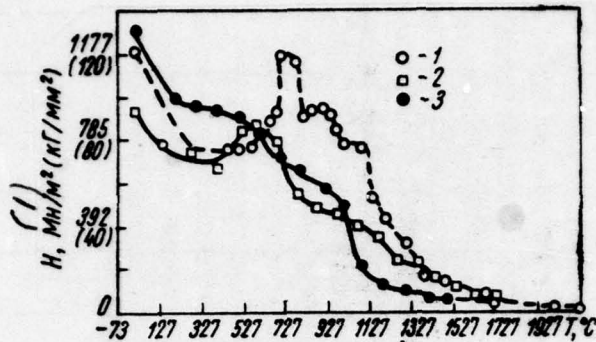


Fig. 135. The dependence of the hardness of niobium on the temperature: 1 - cermet; 2 - poured, after single cathode-ray remelting; 3 - poured, vacuum-arc.

Key: (1) - H , MN/m^2 (kg/mm^2).

Page 182.

In the range of temperatures of 20 - 1000°C , occurs the scatter of measurement data of hardness in different specimen/samples; however, the character of the curved temperature dependence of hardness with pronounced peaks of hardness is retained. At the higher temperatures of this scatter, it will not be noticed.

As is evident from curves in Fig. 135, the increase of the temperature of testing from 20 to 300°C is accompanied by a sharp reduction in the hardness. In interval of 300 - 560°C , hardness of

cermet niobium is not changed. With further temperature rise to curve for the poured cathode-ray niobium, is observed the peak of hardness with 600°C, and for cermet - two peaks: with 750 and 900°C.

As it will be shown below, the same two peaks are on the curved temperature dependence of the limit of the strength of the cermet niobium (see Fig. 179). For this same the material of the value of the module/modulus of elasticity with 460-1200°C, they will be above than at room temperature. The maximum value of the modulus of elasticity obtained in the range of temperatures of 800-1100°C. The increase of the modulus of elasticity of nichium in interval of 600-1200°C is noted also in works [21, 136].

With further increase of temperature, the hardness of niobium again is decreased. At the temperatures higher than 1350°C cermet and cathode-ray niobium have identical hardness. The hardness of cermet niobium reaches the values of 10.8 MN/m² (1.1 kg/mm²) at 2000°C and 7.85 MN/m² (0.8 kg/mm²) at 2120°C.

The special feature/peculiarities of the shape of the curve of the temperature dependence of the mechanical properties of niobium at temperatures higher than the room, apparently can be connected [137] with strain aging in the process of testing.

Hardness of niobium fusions. With the aid of setting up UVT-2, they investigate the annealed specimen/samples of the poured and forged niobium alloys. Annealing was carried out in vacuum 1.33 MN/m^2 (10^{-5} mm Hg) for 2 h for niobium fusions with molybdenum with 1250°C and for niobium fusions with tungsten with 1500°C . Hardness measures with the method of static indentation.

Temperature measures with a platinum-platinum-rhodium thermocouple.

In Fig. 136 are shown the temperature dependences of hardness for alloys Nb-Mo. The hardness of the investigated alloys sharply is decreased during heating from 20 to 300°C , moreover especially sharply of the ternary alloy, which contains 10% Ti.

With further increase of temperature, an incidence/drop in the hardness is retarded, especially it is strong for an alloy with 7% Mo during heating from 300 to $\sim 900^\circ\text{C}$.

The comparison of the temperature dependences of the hardness of alloys Nb - 7% Mo and Nb - 7% Mo - 10% Ti shows that the additional alloying with titanium sharply decreases the hardness of alloy at the high temperatures: at 910°C 2.7 times, at 1190°C 4.5 times, at 1500°C 3.6 times.

Page 183.

The investigation of the temperature dependences of the hardness of niobium fusion with 9.8c/c Mo, three meltings (24, 34 and 54), obtained from different raw material and with some differences in technology of melting, will show (Fig. 137) a considerable difference in the hardness of the specimen/samples of different meltings at temperatures from 20 to 1100°C.

Figures 138 shows the temperature dependences of the hardness of three alloys Nb-W. Curves these dependences are similar to curves for alloys Nb-Mo with the only difference, that for alloys Nb-W an incidence/drop in the hardness at temperatures is higher than 950°C somewhat less.

Introduction to alloy Nb-160/o W as addition 1o/o Zr will not change the hardness of alloy, but 0.5o/o Re - decrease its hardness at the temperatures lower than 1000°C (Fig. 139). The hardness of the investigated alloys Nb-W noticeably depends from composition only at relatively low temperatures (to 1000°C).

Figures 140-142 depicts the temperature dependences of the

hardness of alloys Nb-Mo and Nb-W in semilogarithmic coordinates. These dependences are described by the exponential expression of Ito-Shishokin (see Chapter V). The temperature dependences of the hardness of alloys Nb-Mo have two sections; the low-temperature sections of curves for binary alloys are finished at 1000°C, for a ternary alloy with 10% Ti, - at 700°C.

The curves of the temperature dependence of the hardness of alloys Nb-W have a bend with 800-1000°C.

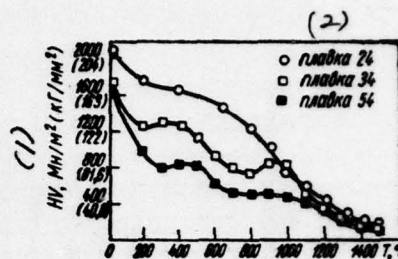
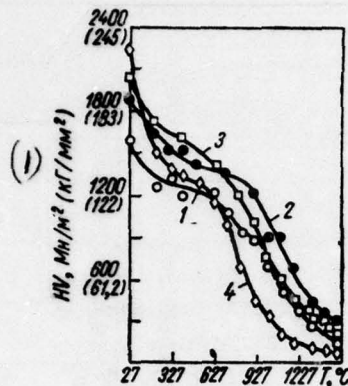


Fig. 137

Fig. 136. The dependence of the hardness of niobium fusions with molybdenum on the temperature (are shown percentages throughout mass): 1 - 50/o Mo; 2 - 70/o Mo; 3 - 9.80/o Mo; 4 - 70/o Mo+10/o of Ti.

Key: (1). HV, MN/m² (kg/mm²).

Fig. 137. Dependence of the hardness of nickelium fusion with 9.80/o Mo on temperature.

Key: (1). HV, MN/m² (kg/mm²). (2) melting.

Page 184.

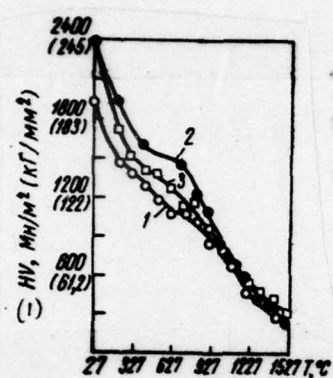


Fig. 138.

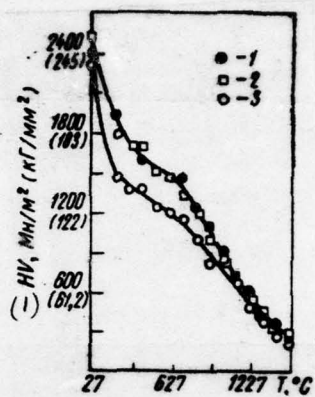


Fig. 139.

Fig. 138. The dependence of the hardness of niobium fusions with tungsten on the temperature (are shown percentages throughout mass):
 1 - 12c/o W; 2 - 16c/o W; 3 - 23c/c W.

Key: (1). HV, MN/m² (kg/mm²).

Fig. 139. The dependence of the hardness of niobium fusions on temperature (are shown percentages throughout mass): 1 - 16c/o W; 2 - 16c/o W+10c/o Zr; 3 - 16c/o W+0.5c/o Re.

Key: (1). HV, MN/m² (kg/mm²).

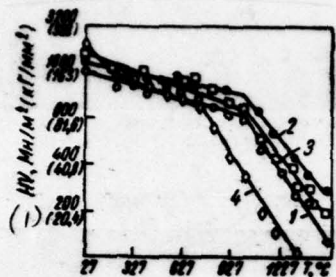


Fig. 140.

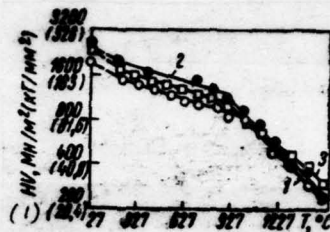


Fig. 141.

Fig. 140. The temperature dependences of the hardness of alloys
 Nb-Mo: 1 - 5o/o Mo; 2 - 7c/c Mo; 3 - 9.8o/c Mo; 4 - 7o/o Mo+10o/o
 Ti.

Key: (1) - HV, MN/m² (kg/mm²).

Fig. 141. The temperature dependences of the hardness of alloys
 Nb-W: 1 - 12o/o W; 2 - 16c/c W; 3 - 23o/c W.

Key: (1) - HV, MN/m² (kg/mm²).

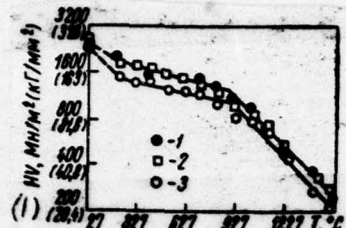


Fig. 142.

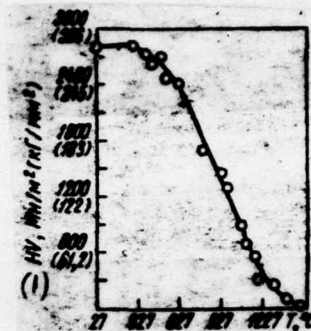


Fig. 143.

Fig. 142. The temperature dependences of the hardness of niobium fusions: 1 - 16% W; 2 - 16% W + 10% Zr; 3 - 16% W + 0.5% Re.

Key: (1). HV, MN/m² (kg/mm²).

Fig. 143. Dependence on the temperature of the hardness of niobium fusion from 25% (throughout mass) Zr.

Key: (1). HV, MN/m² (kg/mm²).

Page 185.

For niobium fusion with 25% Zr, is characteristic the tendency

toward the increased saturation by oxygen which in interval of 1100-1500°C is developed even in vacuum (Fig. 143). During testing of this alloy, the pressure in the camera/chamber of tool was 0.665 MN/m² ($5 \cdot 10^{-6}$ mm Hg) at 200°C, at 500°C - 1.06 MN/m² ($8 \cdot 10^{-6}$), at 655° - 1.33 MN/m² ($1 \cdot 10^{-5}$), at 1060°C - 2.0 MN/m² ($1.5 \cdot 10^{-5}$), at 1300°C - 2.2 MN/m² ($1.7 \cdot 10^{-5}$) and at 1500°C - 4.25 MN/m² ($3.2 \cdot 10^{-5}$) mm Hg). The mirror section of specimen/samples after testing became slightly matte. At temperature of 915°C, it was for the first time noticed, while during further heating continually was reinforced the reaction of alloy with indentor from sapphire. After testing of one specimen/sample, the indentor completely was broken.

The plotting of graphs in coordinates ln H-T°K shows (Fig. 144) that the temperature dependence of the hardness of alloy Nb - 25% Zr is also described by its - Shishokin's exponential expression. Curve has smooth bend at 927°C.

Investigation of the prolonged hardness of tungsten and molybdenum.

Experiments show that the prolonged high-temperature tensile tests lead to the results, which differ not only in quantitative, but also in a qualitative respect from the data which obtain with short-time tensile tests at high temperatures. Therefore the results of short-time high-temperature tensile tests cannot be placed as the

basis of the characteristic of the heat resistance of alloys.

At the same time the high duration of tensile tests does not make it possible shortly to accumulate sufficient material about the effect of composition and structure of alloys on their heat resistance. Furthermore, creep test with linear elongation insufficiently characterizes the subsequent behavior of metal in volumetrically stressed state [138, 139].

A. A. Bochvar [139] in 1947 proposed to apply the method of prolonged hardness as auxiliary accelerated method for studying the heat resistance of alloys at high temperatures.

In the process of the Guillary tests, occurs the decrease of stress level as a result of an increase in the size/dimensions of impression with constant load. This fact causes the gradual retarding/deceleration/delay of an incidence/drop in the hardness in time whose intensity depends on the nature of material. This artificially caused, but completely regular fading of an incidence/drop in the hardness makes it possible to sharply reduce the duration of tests.

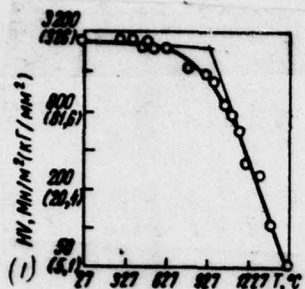


Fig. 144. The temperature dependence of the hardness of alloy Nb-Zr.

Key: (1). HV, MN/m² (kg/mm²).

Page 186.

As a result of the investigation of the heat resistance of A. A. Bochvar's aluminum alloys [139] it arrived at conclusion about the fact that on the dependence of hardness numbers on the time of loading aluminum alloys can be arranged in a series with the same sequence which occurs in the case of creep tests. The measurement of prolonged hardness, for temperatures is above at least $0.6T_c$ (T_c — the absolute temperature of solidus), although do not replace completely prolonged creep tests, it can reduce a quantity of latter and accelerate works on research are new refractory alloys.

I. L. Mirkin and D. Ye. Lifshitz [140], studying the hardness of

metals and alloys at temperatures to 650°C, they arrived at conclusion about the existence of the correlation between hot hardness and the stress-rupture strength, which for the specific type of alloys is linear. By V. E. Shishokin [141] he established that between the size/dimension of impression and period of loading there is a power dependency. Based on this, the authors of work [140] developed the method of the triple hot tests of hardness, with which the duration of holding under load in each subsequent testing is increased 10 times in comparison with preceding/previous. The shape of the curve, obtained the method three hot tests, most closely will agree with the data of prolonged heat resistance tests.

The method of prolonged hardness is insufficiently studied and therefore it gives the difficultly interpretive results. This, obviously, and is explained the fact that that unwinding during the years 1949-1950 discussions detected two basic opinions [18, 142].

Academician A. A. Bochvar and his school they assume that the method of prolonged hardness gives the results which at high and average/mean homologous temperatures ($0.6T_{m}$) qualitatively correspond to test data for stress-rupture strength and creep [140]. This assertion is experimentally confirmed by a series of tests of aluminum and copper alloys.

The opposite point expressed A. P. Gulyayev and Ye. S. Trusova [143]: "the method of prolonged hardness neither it is qualitative nor quantitatively do not characterize heat-resistant alloys". Main disadvantage in this method they see in the fact that with testing are changed both parameters from which it is possible to judge the heat resistance of material, and deformation, and stress. To this is added the difference in initial specific pressure, unavoidable for the alloys, which have dissimilar short-time hardness.

In spite of the deficiencies indicated and the absence of unified opinion about the advisability of testing the prolonged hardness, is continued study and the application/use of this method in metallographic investigations [62, 110, 138, 145, 146, 153-156].

Page 187.

The majority of researchers consider that according to the character of a change in the prolonged hardness it is possible to qualitatively estimate the heat resistance of metals and alloys, not inclined to aging or already aged [18, 62, 107, 138, 139, 146].

You carried out the measurements of the high-temperature prolonged hardness of refractory metals - tungsten and molybdenum of brands VRN and MRN. Specimen/samples were prepared from forged rods

and to heat treatment they did not subject to.

The prolonged hardness of the work-hardened tungsten and molybdenum were measured at temperatures 20, 940, 1310 and 1600°C in the installation UVI. Tests were conducted in the medium of purified helium by the method of the static indentation of sapphire indentor in the form of standard pyramid. Specimen/sample age/held under load during 10, 20, 30 s and 1, 2, 3, 5, 10, 30, 60 min. The temperature of specimen/sample measured with thermocouple KF5/20.

The primary data of creep during tensile test under constant load present curved strain - time (Fig. 145). Analogously during the tests of the prolonged hardness of primary is the curve of the dependence of the size/dimension of impression on time with constant load - curve of indentation. To Figs. 146 and 147, are given curved indentations for molybdenum and tungsten at different temperatures.

However, for the graphic representation of kinetics of indentation, more is frequently utilized curves hardness - time, since to each size/dimension of impression corresponds the specific hardness. To Figs. 116, 117 and 148, 149, are given the curves of the prolonged hardness of molybdenum and tungsten with holding to 10 min and to 1 h respectively.

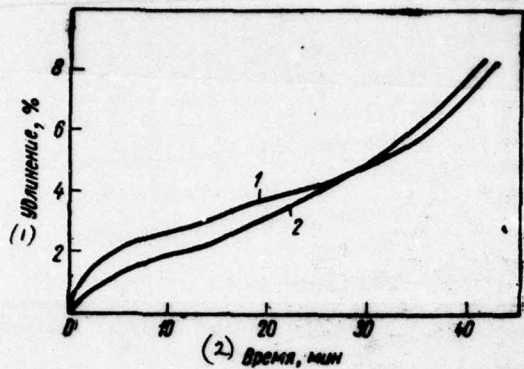


Fig. 145. Primary the curves of creep of molybdenum [150]: 1 - 7.2 MN/m² (0.7 kg/mm²) at 2250°C; 2 - 10.0 MN/m² (0.98 kg/mm²) at 2000°C.

Key: (1). Elongation, %. (2). Time, min.

Page 188.

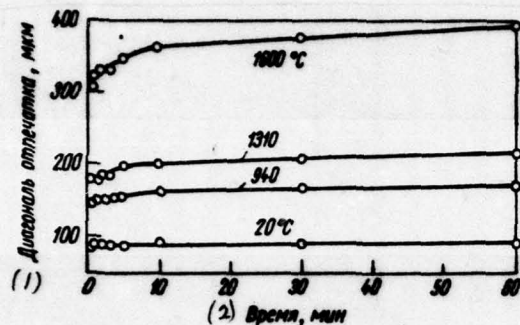


Fig. 146.

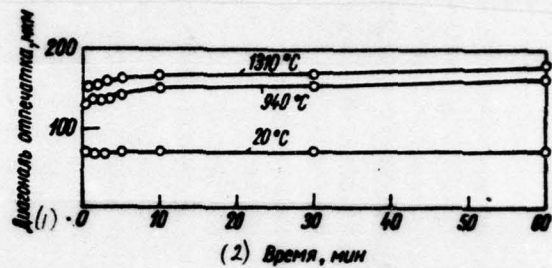


Fig. 147.

Fig. 146. Curve of indentations for molybdenum at different temperatures.

Key: (1). Diagonal of impression, μm . (2). Time, min.

Fig. 147. Curved indentations for tungsten at different temperatures.

Key: (1). Diagonal of impression, μm . (2). Time, min.

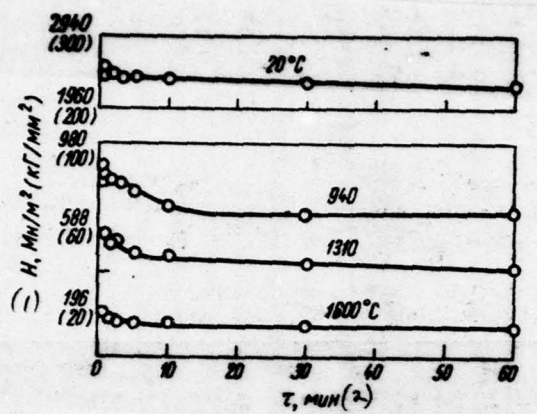


Fig. 148. Prolonged hardness of molybdenum.

Key: (1). H , MN/m² (kg/mm²). (2). min.

Page 189.

Outwardly curves of prolonged hardness and creep with elongation are analogs, but between them there is an essential difference, since the curve of creep characterizes a change in the strain with time, but the curve of the dependence of the size/dimension of impression on time such characteristic is not.

According to academician V. D. Kuznetsov's works [138], the first section in the curve of the indentation (see Figs. 146 and 147) - the region of the transient conditions of indentation - it does not characterize creep, unlike the first section in curve of creep with the elongation (see Fig. 145). The first section of the curve of indentation corresponds to the stress, which considerably exceeds

yield point; in time of the first period of indentation occurs the peening of metal.

In the second period of indentation, the diagonal of impression is changed with constant velocity - steady-state conditions/mode of indentation. An increase in the strain begins because of creep, since it occurs during long time under the effect of constant load.

As is evident on Figs. 146-149, the first period of indentation for molybdenum and tungsten is finished after 5-10 min of loading, moreover most sharply prolonged hardness is changed during first 20-30 s (see Figs. 116, 117).

According to V. D. Kuznetsov [138], in the first period of indentation occurs the shearing strain, and second - diffusion creep of metal.

The third period of the indentation, during which the velocity grows/rises in the course of time, is observed very rarely. V. P. Shishkin [148] he reveal/detected its or testing of tellurium and its alloys with bismuth with 220°C.

AD-A066 482 FOREIGN TECHNOLOGY DIV WRIGHT-PATTERSON AFB OHIO
STRENGTH OF REFRactory METALS. PART I, (U)
OCT 78 G S PISARENKO, V A BORISENKO
UNCLASSIFIED FTD-ID(RS)T-1330-78-PT-1

F/G 11/6

NL

5 OF 5
AD
A066482

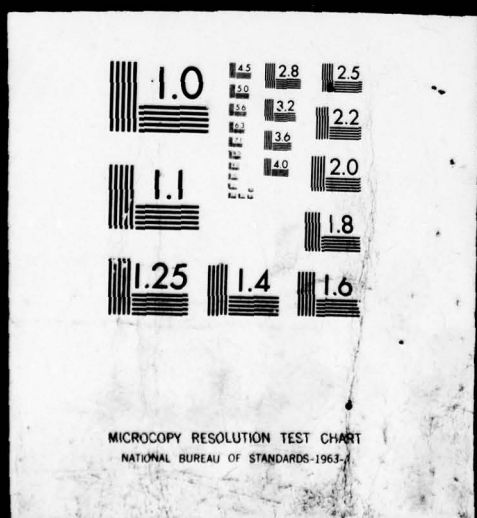


END
DATE
FILMED

5--79
DDC

5 OF 5

AD
A066482



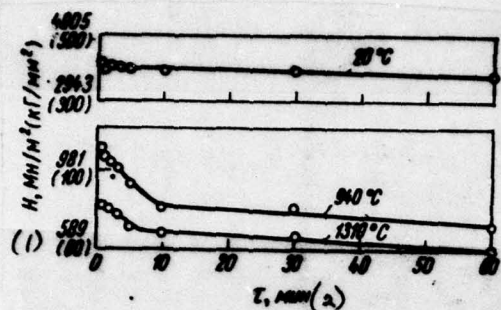


Fig. 149. Prolonged hardness of tungsten.

Key: (1). H , MN/m² (kg/mm²). (2). min.

Page 190.

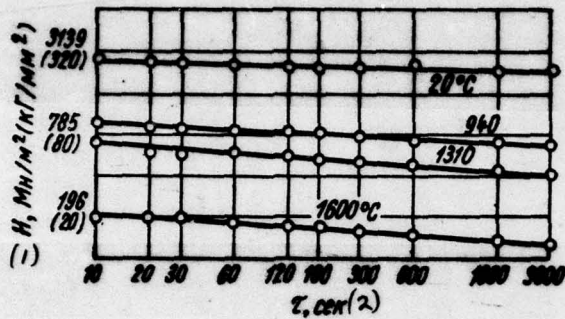


Fig. 150.

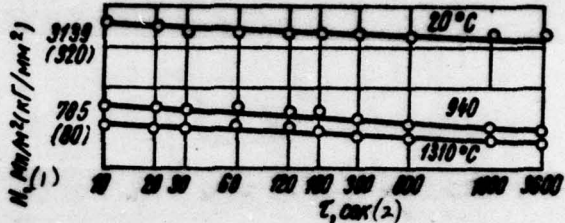


Fig. 151.

Fig. 150. Graphs of the prolonged hardness of molybdenum in logarithmic coordinates.

Key: (1). H, MN/m² (kg/mm²). (2). t, s.

Fig. 151. Graphs of prolonged hardness of tungsten in logarithmic coordinates.

Key: (1). H, MN/m² (kg/mm²). (2). t, s.

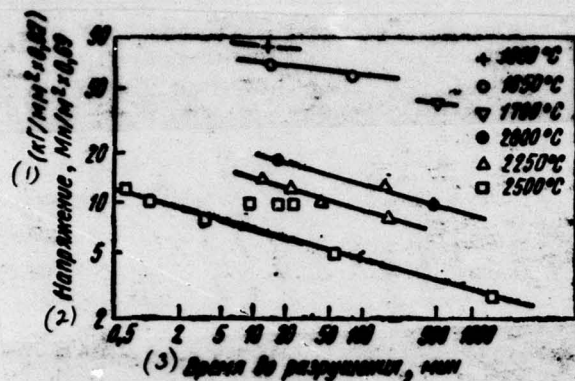


Fig. 152. The stress-rupture strength of molybdenum [150].

Key: (1). Stress, $\text{MN}/\text{m}^2 = 0.69$ ($\text{kg}/\text{mm}^2 = 0.07$) - (2). Time to failure, min.

Page 191.

In works [141, 145, 149] is investigated prolonged hardness with holding to 96 h. Is shown, that the dependence between diameter d (or diagonal b) of impression or the hardness number H and the duration of load τ is determined by the formulas:

$$b = a'\tau^m \quad \text{and} \quad H = a\tau^n. \quad (4.17)$$

where a' , a , m and n - constants, that depend on nature material, moreover $n=-2m$. Coefficient n is called high-speed/velocity index of hardness.

DQC = 78133007

PAGE -47- 384

In the logarithmic coordinates $\log b - \log r$ and $\log H - \log r$ dependences $b-r$ and $H-r$ they must be depicted as straight lines.

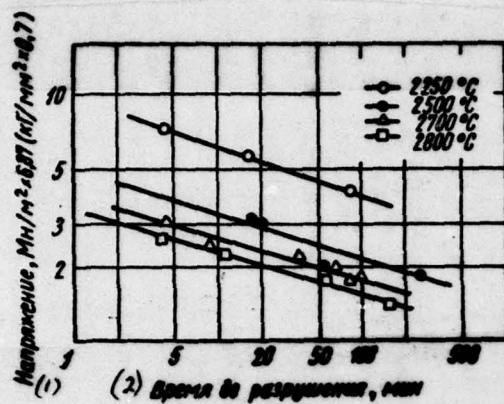


Fig. 153. Prolonged strength of tungsten [150].

Key: (1). Stress, MN/m²*6.87 (kg/mm²*0.7).

Table 23. High-speed/velocity hardness number of tungsten and molybdenum.

(1) Температура, °C	—	
	(2) вольфрам МРН	(3) молибден МРН
20	0,0298	0,0245
940	0,0621	0,0514
1310	0,0627	0,0630
1600	—	-0,0910

Key: (1). Temperature, °C. (2). tungsten VHN. (3). molybdenum MRN.

Page 192.

As it follows from Figs. 150 and 151, the values of the

prolonged hardness of molybdenum and tungsten lie down well on straight lines and, therefore, are subordinated to the equations of V. P. Shishokin; therefore for obtaining of the characteristics of the prolonged hardness of molybdenum and tungsten the sufficiently three hot tests of hardness with a tenfold increase in the duration of loading during each subsequent testing (30 s, 5 and 50 min).

The values of high-speed/velocity hardness number n for molybdenum and tungsten at different temperatures are calculated according to the method of least squares and are given in Table 23.

For a comparison to Figs. 152 and 153, given data on the stress-rupture strength of molybdenum and tungsten at high temperatures [150]. Graphs are constructed in the logarithmic coordinates $\log \sigma - \log \tau$.